

POLITECNICO DI MILANO

School of Civil, Environmental and Land Management Engineering

Master of Science in Civil Engineering for Risk Mitigation



**Flood Damage Assessment in Support of the
Definition of Risk Mitigation Strategies:
The Case of Lodi**

Supervisor: Dr. Daniela Molinari

Co-supervisors: Dr. Alessio Radice

Dr. Giulia Pesaro

MSc Thesis of
Edoardo Gattai
Matr. 873870

Academic Year 2017/2018

"Page intentionally blank"

Acknowledgements

I would like to express my sincerest gratitude to my thesis advisor Dr. Daniela Molinari of the Department of Civil and Environmental Engineering at Politecnico di Milano for the support, advices and valuable comments during the development of this thesis, always provided with great enthusiasm and enviable charisma. Further thanks for the opportunity of working within the project Flood-IMPAT+, developing skills and acquiring knowledge on a topic that I hope can be a strong component of my future work.

Heartfelt thanks go to the co-advisor Dr. Alessio Radice of the Department of Civil and Environmental Engineering at Politecnico di Milano for the precious teachings and advices in the first part of this thesis, for which I am gratefully indebted, and for the kindness and calm way with which he has always addressed to me.

Sincere thanks go also to the co-advisor Dr. Giulia Pesaro of the Department of Architecture and Urban Studies at Politecnico di Milano for the valuable teachings and advice on economic aspects of the risk management, of which I will make precious use in the future.

I would like also to acknowledge to Dr. Renato Vacondio and Dr. Susanna Dazzi of the Department of Engineer and Architecture at Università degli Studi di Parma for the fundamental support and patience provided to me in learning the software used in the hydraulic modelling.

Special thanks go to Dr. Scira Menoni of the Department of Architecture and Urban Studies at Politecnico di Milano, for letting me know and appreciate since the first class the topic of risk.

Greatest gratitude goes to my babbo Carlo, my mother Laura, my brother Enrico, my girlfriend Anne and Jack for the unfailing support, encouragement and love shown to me throughout my university career, full of joy but also pitfalls, overcomes thanks to them too.

A dutiful thanks to my colleague Valerio for the great work done together in this adventurous academic journey, always achieving excellent results.

Eventually, i would thank my friends Marcone, Bernardo, Marco and the rowing team mates, who have helped me to relieve moments of stress with a good beer and sincere laughs.

Abstract

Riverine floods are natural phenomena that affect many people living in floodplain areas and cause serious damages to the built environment, urban services and natural ecosystem. In this regard, the EU Flood Directive 2007/60/EC requires member States to establish flood risk management plans, in order to reduce the potential adverse consequences caused by flooding.

This thesis has been developed within the research project Flood-IMPAT+ (an Integrated Meso and micro-scale Procedure to Assess Territorial flood risk), undertaken by the Politecnico di Milano in collaboration with the Po River District and the partnership of several other stakeholders. The project aims at improving the quality of flood hazard maps and at developing tools for quantitative damage assessment to residential buildings, agricultural sectors and other important assets, to be implemented in Flood Risk Management Plans (FRMP). The province of Lodi has been selected as a case study for the research work, because it was hit by a large flood in 2002 and several data are available for this event.

After such event, several protective structures (banks) were designed, part of which are now in place while others are to be built in the future. The thesis assesses the effectiveness of the structural mitigation measures built on the hydraulic right of the Adda river, with tools developed by Flood-IMPAT+. Five return periods have been considered and, for each of them, hazard maps were produced for a condition before the bank construction and a condition with the new structures in place. The hazard maps were produced by two-dimensional river modelling, taking advantage of a preliminary calibration of the model with reference to the flood of 2002. For all the ten scenarios (corresponding to five return periods for two conditions), a monetary estimation of damages to residential buildings and agricultural activities has been obtained with the INSYDE and AGRIDE-c models, respectively. The yearly benefits of flood protection, quantified as the avoided damages, have been compared to the annual costs of the mitigation measures in a cost-benefit analysis. A positive result of the benefit-cost ratio (B/C) shows the usefulness of the structural defences. In order to supply a more comprehensive appraisal of benefits brought by the structure, damages to other assets, such as economic activities, important facilities and services, have been estimated in terms of exposure to flood; the results of the assessment should be also considered and included in a multi-criteria analysis. These non-quantifiable benefits would enrich the result obtained from the B/C, remarking the importance of a wider analysis in order to assess the efficiency of flood risk mitigation measures.

Keywords: flood risk, urban flood modelling, flood damage assessment, CBA for flood risk mitigation, MCA for flood risk mitigation

Abstract (Italian version)

Le alluvioni fluviali sono fenomeni naturali che colpiscono un elevato numero di persone residenti in zone a rischio alluvionale e causano gravi danni all'ambiente costruito, ai servizi urbani e all'ecosistema naturale. A tale riguardo, la direttiva europea sulle alluvioni 2007/60 / CE impone agli Stati membri di definire piani di gestione del rischio di alluvione, al fine di ridurre le potenziali conseguenze negative provocate da questo tipo di eventi.

Questa tesi è stata sviluppata nell'ambito del progetto di ricerca Flood-IMPAT + (una procedura integrata alla piccola e medio scala per valutare il rischio alluvionale territoriale), intrapresa dal Politecnico di Milano in collaborazione con l'Autorità di Distretto del Fiume Po e con la partecipazione di altri stakeholders. Il progetto ha come obiettivo quello di migliorare la qualità delle mappe di pericolosità alluvionale e di sviluppare procedure per la valutazione quantitativa dei danni agli edifici residenziali, ai settori agricoli e ad altri importanti settori, da utilizzare come base per i Piani di Gestione Rischio Alluvioni (PGRA). La provincia di Lodi è stata selezionata come caso di studio per il lavoro di ricerca, poiché colpita da una grave alluvione nel 2002 e perché diversi dati sono stati resi disponibili per questo evento.

Dopo tale evento, sono state progettate diverse strutture di difesa (muri arginali e argini in terra), parti delle quali sono già state costruite mentre altre verranno aggiunte in futuro. La tesi valuta l'efficacia delle misure di mitigazione costruite in destra idraulica del fiume Adda, con modelli sviluppati da Flood-IMPAT+. Sono stati considerati eventi con cinque tempi di ritorno diversi e, per ciascuno di essi, sono state prodotte mappe di allagamento per una condizione antecedente la costruzione degli argini di difesa e per una con le nuove strutture in atto. Le mappe di allagamento sono state prodotte con una modellizzazione fluviale bidimensionale, a seguito di una calibrazione del modello eseguita con riferimento all'alluvione del 2002. Per tutti i dieci scenari (corrispondenti ai cinque tempi di ritorno per due condizioni), una stima dei danni in termini monetari per gli edifici residenziali e per le attività agricole è stata ottenuta utilizzando, rispettivamente, i modelli INSYDE e AGRIDE-c. I benefici annuali ottenuti dalla protezione delle alluvioni, in termini di danni evitati, sono stati confrontati con i costi annuali delle misure di mitigazione, all'interno di un'analisi costi-benefici. Un risultato positivo del rapporto costi-benefici (B/C) dimostra l'efficacia delle difese strutturali. Al fine di fornire una valutazione più completa dei benefici apportati dalla struttura, i danni ad altre attività, come le attività economiche e le strutture con servizi importanti, sono stati stimati in termini di esposizione alle alluvioni; questi risultati dovrebbero essere poi considerati e inclusi in un'analisi multi-criteri. I benefici non quantificabili in termini economici andrebbero certamente ad arricchire il risultato ottenuto dal B/C, rimarcando l'importanza di un'analisi più completa nella valutazione dell'efficacia delle misure di mitigazione del rischio alluvionale.

Parole chiave: rischio alluvionale, modellazione di alluvioni urbane, valutazione del danno alluvionale, CBA per la mitigazione del rischio alluvionale, MCA per la mitigazione del rischio alluvionale

INDEX

1	Introduction	1
1.1	Aim of the work	1
1.2	Case study localisation	4
1.3	River Adda	5
1.4	The November 2002 flood event	7
1.5	Works performed after the November 2002 flood event	10
1.5.1	Structural defences typologies for each stretch	10
2	Workflow and theoretical basis of the work	20
2.1	Flood modelling in urban areas	22
2.2	Uncertainties in flood modelling	26
2.3	Calibration of a hydraulic model	27
2.4	Software used for the hydraulic modelling	30
2.4.1	Surfer software	30
2.4.2	Parflood calculation code	32
2.5	Multi-criteria analysis (MCA)	36
2.5.1	Cost Benefit Analysis (CBA)	39
2.5.2	Non-quantifiable damage assessment	42
2.6	Simplified INSYDE model	44
2.7	AGRIDE-c model	48
2.8	Sensitivity analysis: climate change impact on flood occurrence and levee effect	52
3	Case study	54
3.1	Flood modelling	54
3.1.1	Available data for flood modelling	54
3.1.1.1	Flooded area of the November 2002 event	55
3.1.1.2	Observed water surface elevations in control points post flood event	55
3.1.1.3	Hydrometer levels and hydrograph of the November 2002 flood event	56
3.1.1.4	River Adda's cross-sections	57
3.1.1.5	DSM, BC and IC files, computational domain file, multi-resolution file and orthophoto	57
3.1.1.6	Altimetric survey on the structural defences	58
3.1.1.7	Past reports	59
3.1.2	Geometry	60
3.1.3	Unsteady modelling	64
3.1.4	Calibration procedure	66
3.1.4.1	Parameters used for the model calibration	68

3.1.4.2	Operations and modifications on input files during the model calibration	71
3.1.4.3	Results of the calibration and choice of the model.....	79
3.1.4.4	Results of the quantitative indicators for the goodness of the simulations	87
3.2	Hazard assessment for some reference scenarios	90
3.2.1	Available data for hazard assessment	90
3.2.1.1	Relationship between return period (T) and discharge (Q) of the Adda in Lodi	90
3.2.2	Synthetic boundary conditions for reference scenarios	91
3.2.3	Flood Hazard Maps	94
3.3	Multi Criteria Analysis (MCA)	105
3.3.1	Available data for MCA.....	106
3.3.2	Cost of structural defences and annual maintenance.....	107
3.3.3	Quantifiable damage assessment.....	108
3.3.3.1	Direct damage to residential buildings.....	108
3.3.3.2	Direct damage to agriculture sector.....	115
3.3.4	Benefit assessment.....	120
3.3.5	Non – quantifiable damage assessment.....	123
3.3.5.1	Direct damage to economic activities	123
3.3.5.2	Systemic indirect damage to economic activities	128
3.3.5.3	Exposed population	132
3.3.5.4	Exposed road network.....	140
3.3.5.5	Exposed important facilities	143
3.3.5.6	Exposed cultural heritage	148
3.3.5.7	Other non-quantifiable damages to be considered in MCA.....	151
3.3.6	Conclusions of the MCA.....	152
3.3.7	Sensitivity analysis.....	153
3.3.7.1	Levee effect	153
3.3.7.2	Flood in May as consequence of climate change.....	157
4	Conclusions	167

LIST OF FIGURES

Figure 1-1 – Italian population density distribution map (ISTAT, 2011) on the left and Italian hazard distribution for flood event with return period between 100 and 200 years (ISPRA, 2018) on the right	1
Figure 1-2 Location of Lodi (on the left) and drone view of the municipality (on the right)	4
Figure 1-3 - The Adda catchment (Castelletti et al., 2011).....	5
Figure 1-4 Profile of the last 140 km of the Adda river from the Olginate sluice gate (Lecco) to the entrance in the Po river (Lodi)	6
Figure 1-5 - The river Adda in Lodi during peacetime	6
Figure 1-6 - Weather forecast of the 25th of November (MeteoSwiss) and estimated hydrograph after the confluence Adda-Brembo (Rossetti & Cella, 2010)	7
Figure 1-7 - Water level at the historical bridge before the overflow	8
Figure 1-8 - Hydrometer levels registered at the Napoleone Bonaparte bridge in Lodi.....	8
Figure 1-9 Rescue team (on the left) and Viale Dalmazia (on the right) during the flood	9
Figure 1-10 Piarda Ferrari (on the left) and a top view of Lodi (on the right) during the flood	9
Figure 1-11 - Planimetry of the works performed on the hydraulic right of the river “Adda”. Soil embankments in yellow polyline, defence walls and connection walls in red polyline, sluice gates in light blue polylines, openings in green polylines.....	10
Figure 1-12 - Section of the designed soil embankment (A1 typology)	11
Figure 1-13 - Particular of the sluice gate without pumping plant	11
Figure 1-14 - Particular of the “Via Napoli” opening.....	12
Figure 1-15 Montage procedure of the vertical support	13
Figure 1-16 Section of the designed defence wall (B1 typology)	14
Figure 1-17 Particular of the designed defence wall (B1 typology)	14
Figure 1-18 Particular of the soil embankments (A1 typology).....	15
Figure 1-19 Particular of the sluice gate with pumping plant	15
Figure 1-20 Particular of the connecting defence wall in reinforced concrete (B3 typology)	16
Figure 1-21 Particular of the “Piarda Ferrari” opening	16
Figure 1-22 Section of the designed defence wall (B2 typology)	17
Figure 1-23 Particulars of the defence wall upstream of the "Napoleone Bonaparte" bridge.....	17
Figure 1-24 Particulars of the defence wall and opening downstream of the “Napoleone Bonaparte” bridge	18
Figure 1-25 Particular of the brick and r.c. wall downstream of the historical bridge.....	18
Figure 1-26 Particular of the junction between defence wall and soil embankment	19
Figure 1-27 Particular of the interruption and openings	19
Figure 2-1 Workflow of the methodologies in order to create a MCA, where: the circular polygons regard input topic and output results; the rectangles are processes; the parallelograms are intermediate results	21
Figure 2-2 Representation of the Manning’s roughness embedded in a larger computational domain (on the left) and simply disposition of quadrangular buildings with local bed friction (on the right) (Alcrudo, 2004)	24
Figure 2-3 Examples of bottom elevation techniques on a coarse mesh (on the left) and on a finer mesh (on the right) (Alcrudo, 2004)	24
Figure 2-4 Representation of vertical walls technique (Alcrudo, 2004).....	25
Figure 2-5 Example of the grid math procedure	31
Figure 2-6 Example of the grid mosaic procedure	31
Figure 2-7 Extract of the bathymetry file representing the municipality of Lodi.....	32
Figure 2-8 Example of .BLN file.....	34
Figure 2-9 Example of .BCC file.....	34

Figure 2-10 Representation of the annual yearly damages considering event with return period equal to 5, 20, 100 and 200 years (Meyer et al., 2009).....	41
Figure 2-11 Scheme of the conceptual model AGRIDE-c	49
Figure 2-12 Physical damage to maize as a function of vegetative stage, flood depth and duration (adapted from Agenais et al., 2013)	51
Figure 2-13 Relative damage to maize crops (in case of conventional tillage) for the different combinations of times of occurrence of the flood (i.e. month), flood intensities (i.e. water depth and flood duration) and damage alleviation strategies ("c"=continuation; "r"=reseeding; "a"=abandoning)	52
Figure 3-1 Extension of the estimated flooded area in Lodi	55
Figure 3-2 Representation of control points in Lodi.....	55
Figure 3-3 Hydrometer levels of the November 2002 flood event (Natale, 2003)	56
Figure 3-4 Discharge hydrograph of the November 2002 flood event (Natale, 2003)	56
Figure 3-5 Cross section of the river in correspondence of the Napoleone Bonaparte bridge	57
Figure 3-6 Cross section of the river at the tip of Achilli islet in Lodi	57
Figure 3-7 Extract of the digital surface model of the municipality of Lodi	58
Figure 3-8 Location of the altimetric survey.....	59
Figure 3-9 Measurements of the elevation of structural wall belonging to the opening of Via Napoli	59
Figure 3-10 Extract of the bathymetry file representing the irrigation ditches on the left and a top view from Google Earth on the right	60
Figure 3-11 Insertion of the underpass under the historical bridge and field survey picture	60
Figure 3-12 Added paths along the "Tangenziale sud" road overpass.....	61
Figure 3-13 Added pillars of the "Tangenziale sud" road viaduct.....	61
Figure 3-14 Example of the added soil embankments downstream of the City of Lodi	62
Figure 3-15 River bed between historical bridge and dike and added concrete reinforcements.....	63
Figure 3-16 Snapshots of water depth in relevant time step of a simulation.....	66
Figure 3-17 Calibration process flow diagram where: the circular polygons regard input data and output results; the rectangles are processes; the intermediate polygon is an intermediate result; the rhombus is a decision.....	67
Figure 3-18 Location of the hydrometric station along the Napoleone Bonaparte bridge in Lodi	69
Figure 3-19 Cluster grouping representation	70
Figure 3-20 Comparison observed - obtained WSE of Simulation 17	70
Figure 3-21 Location of points for the creation of the profiles over a google earth base map	71
Figure 3-22 Values of Manning's coefficients for floodplains (Chow, 1959).....	73
Figure 3-23 Top view of Lodi and extract of the .MAN file representing the urban area	74
Figure 3-24 Top view and extract of the .MAN file representing an area with medium to dense brush and forest	74
Figure 3-25 Hydrographs used for the model calibration	77
Figure 3-26 Representation of computational domain Original BLN (red polygon), New BLN (blue polygon), upstream boundary condition (green ellipse) and downstream boundary conditions (yellow ellipse)	78
Figure 3-27 Results of the simulation n°29	81
Figure 3-28 Results of the simulation n°34	82
Figure 3-29 Results of the simulation n°44	83
Figure 3-30 Results of the simulation n°50	84
Figure 3-31 MAXWSE on the entire domain of simulation n°50	85
Figure 3-32 MAXVEL on the entire domain of the simulation n°50	86
Figure 3-33 Results of the Average of Difference indicator	87
Figure 3-34 Results of the Average Absolute Difference indicator	87
Figure 3-35 Nash-Sutcliffe Efficiency indicator.....	87

Figure 3-36 Sub-division of the cluster E	88
Figure 3-37 Relationship $T - Q_p$ in Lodi according to different studies, where: 1) $Q(T)$ from past study by Rossetti & Cella in 2005; 2) $Q(T)$ based on Gumbel function by Rossetti in 2005; 3) $Q(T)$ from several studies by Paoletti in 2005; 4) $Q(T)$ upstream of Lodi from past report "Sottoprogetto SP1" by AdbPo; 5) $Q(T)$ downstream of Lodi from past report "Sottoprogetto SP1" by AdbPo; 6) Estimation of the return period of the November 2002 flood event	91
Figure 3-38 Adimensionalised representation of the 17 chosen events.....	92
Figure 3-39 Representation of the average curve.....	92
Figure 3-40 Estimated synthetic hydrographs for different return periods T	93
Figure 3-41 Flood Hazard Map for $T=50$ years without structural defences	95
Figure 3-42 Flood Hazard Map for $T=50$ years with structural defences	96
Figure 3-43 Flood Hazard Map for $T=100$ years without structural defences	97
Figure 3-44 Flood Hazard Map for $T=100$ years with structural defences.....	98
Figure 3-45 Flood Hazard Map for $T=120$ years, corresponding to the November 2002 flood event, without structural defences.....	99
Figure 3-46 Flood Hazard Map for $T=120$ years, corresponding to the November 2002 flood event, with structural defences.....	100
Figure 3-47 Flood Hazard Map for $T=200$ years without structural defences	101
Figure 3-48 Flood Hazard Map for $T=200$ years with structural defences.....	102
Figure 3-49 Flood Hazard Map for $T=500$ years without structural defences	103
Figure 3-50 Flood Hazard Map for $T=500$ years with structural defences.....	104
Figure 3-51 Procedure to assign h value E to buildings inside impervious blocks: 1) representation of two buildings as impervious blocks; 2) conversion of the water depth raster into points; 3) interpolation procedure; 4) interpolated values inside impervious blocks	109
Figure 3-52 Total damage to residential buildings for reference scenarios, without structural defences ...	111
Figure 3-53 Total damage to residential buildings for reference scenarios, with structural defences	112
Figure 3-54 Relationship $T - \text{Damage}$ for residential buildings with and without structural defences.....	113
Figure 3-55 Two extracts of the simulator excel file	115
Figure 3-56 Damages to agricultural sector in November, without structural defences.....	117
Figure 3-57 Damages to agricultural sector in November, with structural defences	118
Figure 3-58 Relationship $T - \text{Damage}$ to agricultural sector in November with and without structural defences	119
Figure 3-59 Relationship probability of occurrence – damage to residential buildings.....	120
Figure 3-60 Relationship probability of occurrence – damage to agricultural sector.....	121
Figure 3-61 Exposed economical activities for reference scenarios, without structural defences.....	125
Figure 3-62 Exposed economical activities for reference scenarios, with structural defences	126
Figure 3-63 Indirect systemic damage for reference scenarios, without structural defences	129
Figure 3-64 Indirect systemic damage for reference scenarios, with structural defences	130
Figure 3-65 Total exposed population for reference scenarios, without structural defences.....	133
Figure 3-66 Total exposed population for reference scenarios, with structural defences	134
Figure 3-67 Exposed vulnerable population for reference scenarios, without structural defences.....	135
Figure 3-68 Exposed vulnerable population for reference scenarios, with structural defences	136
Figure 3-69 Exposed foreign population for reference scenarios, without structural defences	137
Figure 3-70 Exposed foreign population for reference scenarios, with structural defences.....	138
Figure 3-71 Exposed road network with and without structural defences for reference scenarios	140
Figure 3-72 Exposed road network (red links) for reference scenarios, without structural defences.....	141
Figure 3-73 Exposed road network (yellow links) for reference scenarios, with structural defences.....	142
Figure 3-74 Exposed important facilities for reference scenarios, without structural defences.....	145

Figure 3-75 Exposed important facilities for reference scenarios, with structural defences	146
Figure 3-76 Exposed cultural heritage for reference scenarios, without structural defences.....	149
Figure 3-77 Exposed cultural heritage for reference scenarios, with structural defences	150
Figure 3-78 Representation of the new potential building area (red polygon) and of the structural defences in the hydraulic right (yellow polyline).....	153
Figure 3-79 Hydrometer levels over the last twenty years	157
Figure 3-80 Damage to agriculture with the combination May - 3 days, without structural defences.....	159
Figure 3-81 Damage to agriculture with the combination May - 3 days with structural defences	160
Figure 3-82 Comparison of damage trend curves for the scenarios “May – 3 days”	161
Figure 3-83 Damage to agriculture with combination the May - 15 days, without structural defences.....	163
Figure 3-84 Damage to agriculture with combination the May - 15 days with structural defences	164
Figure 3-85 Comparison of damage trend curves for the scenarios “May – 15 days”	165
Figure 3-86 Relationship probability of occurrence – damage to agricultural sector for the combination “May – 3 days”	166
Figure 3-87 Relationship probability of occurrence – damage to agricultural sector for the combination “May – 15 days”	166

LIST OF TABLES

Table 2-1 Characteristics of different multi-criteria methods (FHRC/RPA, 2002)	38
Table 2-2 Event parameters and building characteristic features considered in the simplified version of INSYDE	46
Table 2-3 Replacement values for residential building (Cineas – Cresme – Ania, 2018)	47
Table 3-1 Available data for flood modelling	54
Table 3-2 Simulations performed during calibration procedure of the flood model (G=green area characterized by medium to dense brush and forest; U=urban environment; D=area downstream of the city of Lodi; A=portion of terrain downstream of “Tre Cascine”)	72
Table 3-3 Available data for hazard assessment	90
Table 3-4 Relationship Q – T for reference scenarios according to Rossetti & Cella (2005)	91
Table 3-5 Available data for Multi Criteria Approach	106
Table 3-6 Summary of the costs for typologies of structural defences	107
Table 3-7 Summary of the costs for the annual ordinary maintenance of structural defences	107
Table 3-8 Summary of damages with and without structural defences and % damage reduction	113
Table 3-9 Damage to crops in November: no damage (green), slight damage (yellow), total damage (red)	116
Table 3-10 Summary results of the damages to agricultural sector in November without and with structural defences	119
Table 3-11 Exposed economic activities for reference scenarios	124
Table 3-12 Summary table of exposed population for reference scenarios without structural defences	139
Table 3-13 Summary table of exposed population for reference scenarios with structural defences	139
Table 3-14 Summary table of reduction of exposed population for reference scenarios	139
Table 3-15 Summary table of exposed road network for reference scenarios	140
Table 3-16 Summary table of exposed facilities without structural defences	144
Table 3-17 Summary table of exposed facilities with structural defences	144
Table 3-18 Reduction of exposed facilities with structural defences	144
Table 3-19 Summary table of exposed cultural heritage without structural defences	148
Table 3-20 Summary table of exposed cultural heritage with structural defences	148
Table 3-21 Reduction of exposed cultural heritage with structural defences	148
Table 3-22 Summary table of the damage assessment	152
Table 3-23 Summary table of estimated direct damages of the new residential buildings, considering the “levee effect” scenario	154
Table 3-24 Damage to crops in May: no damage (green), slight damage (yellow), medium damage (orange), total damage (red)	158
Table 3-25 Summary results of the damages with and without structural defences and damage reduction for the combination “May – 3 days of water permanence”	161
Table 3-26 Summary results of the damages with and without structural defences and damage reduction for the combination “May – 15 days of water permanence”	165

“A model should be composed as simply as possible, but as complex as necessary” (Popper, 1982).

1 Introduction

1.1 Aim of the work

Floods are natural phenomena that involve river basins around the world, affecting a large number of people every year, with severe social and economic impacts (Poljanšek et al., 2017). Population over the planet is not evenly distributed, with some areas characterised by a high population density, usually located within flood plains. Therefore, floods have a great impact on human settlements and natural ecosystems. Alfieri et al. (2016) estimate flood impact at the European Union level to be \approx € 6 billion per year, affecting annually 250 000 people. Moreover, during the last century observed urban flood events have been increasing in frequency, due to climate change and dense urbanisation, and in severity as a consequence of population growth in cities located in flood prone areas. Due to these factors, urban risk will increase in the future. As a result, improved modelling of urban flooding has been identified as a research priority (Poljanšek et al., 2017), as well as damage assessment and benefit evaluation of mitigation measures.

Italy reflects the aforementioned conditions of population density and location in floodplains, as shown in Figure 1-1, which reports the number of residents per km², on the left, and, on the right, the Italian hazard distribution for flood events with return period between 100 and 200 years. According to ISPRA (Istituto Superiore per la Protezione e la Ricerca Ambientale) 6 million Italians live in areas at risk of flood, that correspond to almost 10% of the entire population. Emilia Romagna, Toscana, Veneto, Lombardia and Liguria are the regions with the highest population values in the medium-high hydraulic hazard scenario.

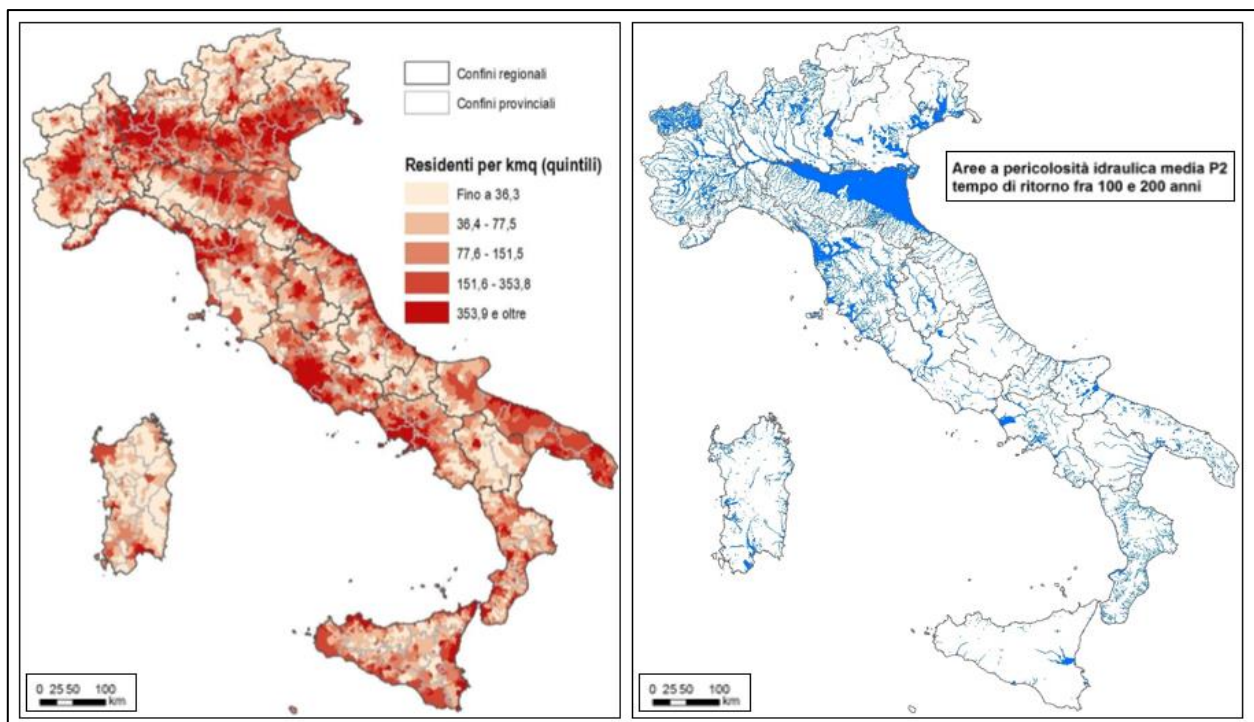


Figure 1-1 – Italian population density distribution map (ISTAT, 2011) on the left and Italian hazard distribution for flood event with return period between 100 and 200 years (ISPRA, 2018) on the right

To cope with flood risk, Italian legislation has implemented, with the Legislative Decree 49/2010, the European Directive 2007/60/EC, called Floods Directive, the reference for the flood risk assessment and management in European countries. According to the aforementioned Directive, floods are defined as temporary inundation of areas, even with mobilisation of sediments, that are usually not covered with water. This include floods caused by lakes, rivers, streams, artificial drainage networks, marine flooding of coastal areas and excludes flooding not directly caused by weather events. Flood hazards is defined as the probability of occurrence of a flood event in a certain area and in a determined time interval, while flood risk as the combination of the probability of occurrence of an event and the potential negative consequences for human health, the environment, the assets, the economic and social activities and the cultural heritage, deriving from the flood event. The commonly adopted definition of flood risk is defined as the expected losses for exposed elements having a specific vulnerability and affected by a given hazard (Menoni & Margottini, 2011).

The Floods Directive is a prime example of radical change in the risk assessment and management, in which a significant shift from a hazard-centred perspective to a wider understanding of risk is proposed, which also comprises concepts of exposure, vulnerability, resilience, and the coping capacity of systems and societies (Molinari et al., 2014). Therefore, risk analysis is composed essentially by two phases: hazard assessment and potential damage quantification. The determination of flood hazard scenarios with different return periods, consists in describing the flooded area extents, the water depths and the velocities, as key variables to be implemented into damage models. The potential damage assessment relates the hazard parameters of flood scenarios to the vulnerability and exposure of different assets, in order to quantify the expected potential damage (Scorzini et al., 2018). Vulnerability is defined as the propensity of an element to suffer damages as result of stresses induced by a natural or technological event. Exposure is the number unit elements (people, buildings, economic activities, infrastructures, etc.) and their value (if quantifiable) potentially at-risk present in a given area. Eventually, a distinction between direct and indirect damage, which may be tangible or intangible according to the possibility of quantifying the loss in monetary terms, must be done. Direct damage refers to physical destruction of assets, objects and infrastructures, as well as victims in terms of injuries and fatalities. Indirect damage can be referred to as “higher order damage” (Rose, 2004), as the consequences generated by the direct physical damages, such as business interruption, lifelines failure, impact on the environmental and other systemic damages generated in a cascade effect.

Damage assessment can be carried out ex-ante, in order to establish which mitigation measures better reduces potential losses for future events, or ex-post to quantify and inform decision-makers about the incurred losses or to assess the efficiency and goodness of already built structural and non-structural flood protections. Moreover, ex-post damage assessment can help to improve emergency plans, to define priorities for future interventions and reconstructions, and it would also provide support to insurance companies in estimating premiums (Meyer et al., 2013; Molinari et al., 2014). The choice of the measures to be implemented to reduce flood risk needs a multi-disciplinary evaluation of different flood protections through a Multi-Criteria Analysis (which can include also a

Cost-Benefit Analysis) to demonstrate their potential benefits, namely the reduction of direct damages, as well as indirect damages to economic activities, cultural heritage, living society and natural ecosystem. Flood risk management requires a rational assessment of mitigation strategies, which involves a complex decision-making process and many uncertainties, such as sparse and short datasets, assumptions in statistical analysis of extreme flood events and depth-damage functions and models. Moreover, it involves challenges in defining damages for different elements at risk (e.g. houses, public spaces, industries), and transferring solutions in space (from one region to another) and in time (from one flood event to another) (Poljanšek et al., 2017).

This thesis work has been performed within the research project conducted by Politecnico di Milano with the collaboration with the Po River District, denominated Flood-IMPAT+ (Integrated Meso-scale Procedure to Assess Territorial flood risk). The project has the main objective of exploiting all existing modelling capacity, and developing new ones, to overcome limits of hydrogeological risk maps developed in Italian River Districts, especially as regards risk quantification (Molinari et al., 2016). Therefore, Flood-IMPAT+ aims to develop tools in order to provide a quantitative assessment of flood risk (in monetary terms, where possible) from the meso and micro-scale, applicable to the Italian territory and in line with the requirements of the Floods Directive. In particular, the project wants to develop and implement up and down-scaling methods for determining the distribution of hazard, vulnerability and exposure variables at different spatial scales, as well as models for assessing the potential expected damage to residential buildings, agricultural sector and other important assets. Eventually, with the use of the aforementioned developed tools and models, the project wants to evaluate the effectiveness of the structural mitigation measures built after the occurrence of the November 2002 flood event in Lodi, which has been selected as case study for the application of the aforesaid objectives.

This thesis work is focused on the last goal of the project and aims at assessing the potential benefits, in terms of both quantifiable and non-quantifiable avoided damages, arisen from the construction of flood protections on the hydraulic right of the river Adda in Lodi, after the severe event occurred in 2002. It is worth to specify that non-quantifiable damages are defined as those damages that cannot be evaluated in monetary terms with tools developed within Flood-IMPAT+ and validated in the Po Plain context, and not as those priceless and intangible losses. Damages to residential buildings and agricultural sector have been monetarily evaluated and included in a Cost-Benefit Analysis (CBA), while non-quantifiable losses to other assets have been analysed in terms of exposure, to be included eventually in a Multi-Criteria Analysis (MCA) for a more comprehensive assessment of the flood protection effectiveness. In order to perform such analysis, ten flood hazard maps have been created, simulating five floods scenarios with different severities, without and with the presence of the build structural mitigation measures. These maps are the result of a hydraulic flood modelling, calibrated with data and observations of the November 2002 flood event in Lodi. In order, the thesis is composed by a brief introduction of the case study, the river Adda, the November 2002 flood in Lodi and the work performed after the occurrence of the latter event that are presented in chapter 1. Chapter 2 reports the theoretical basis of the work inherent to flood modelling and damage assessment procedures and models as support of CBA and MCA. The third

chapter regards their application to the case study of Lodi, in which the first part is devoted to the urban flood modelling and its calibration, followed by the creation of the ten hazard maps and the flood damage assessment to evaluate the effectiveness of the built structural mitigation measures. The latter is subdivided into an estimation of quantifiable losses to residential buildings and agricultural sector, which a CBA has been performed, and a qualitative assessment of maximum potential damage, in terms of exposure, for other important assets to be included in a more comprehensive MCA. Eventually, at the end of chapter 3, a sensitivity analysis of the CBA results has been proposed, considering, separately, a “levee effect” scenario and the occurrence of the flood in a different period of the year as potential consequence of the climate change. Chapter 4 containing the discussion of the results and the conclusion.

1.2 Case study localisation

Lodi is an Italian town, located in Lombardia region (Northern Italy). The municipality covers an area of 41.38 km² of the biggest Italian alluvial plain called Pianura Padana, the number of inhabitants is 45.252 (ISTAT, 2018) and the population density is about 1.095 people per km². Lodi is located in the Adda watershed, about 40 km downstream the Brembo river confluence, upstream of the Serio river confluence and 60 km upstream of the confluence into the Po river. Being located nearby the aforementioned rivers, Lodi is exposed to a significant hydraulic risk. Moreover, six irrigation ditches (Squintana, Rio, Negrina, Sorgino, Ramello e Mozzanica) on the hydraulic left and one (Roggione) on the hydraulic right flow into the river Adda, as well as minor channels built for irrigation purposes. The historical upper part of the municipality has its origin on the Eghezzone hill, located on the hydraulic right of the river Adda. The urban development of Lodi has brought to construction of neighbourhoods and industrial zones in flood prone areas, nearby the aforementioned river. The province of Lodi covers lowland and hilly territory, dedicated mainly to agriculture and handicraft activities. In recent years, a strong development of tourism has been observed, as well as the development of the service industry.



Figure 1-2 Location of Lodi (on the left) and drone view of the municipality (on the right)

1.3 River Adda

The river Adda, whose name comes from the Celtic word “Abdua” meaning "flowing water", is the fourth longest main river (after Po, Adige and Tevere) in Italy and it is the longest tributary of the Po river. The source of the Adda is the mountain Pizzo del Ferro (2150 m a.s.l.) and it flows into the Po river in the province of Lodi. With a length of 313 km and 7927 km² of catchment (11% of the total Po basin’s surface), the river passes through the provinces of Sondrio, Como, Lecco, Bergamo, Monza e Brianza, Milano, Cremona and Lodi.

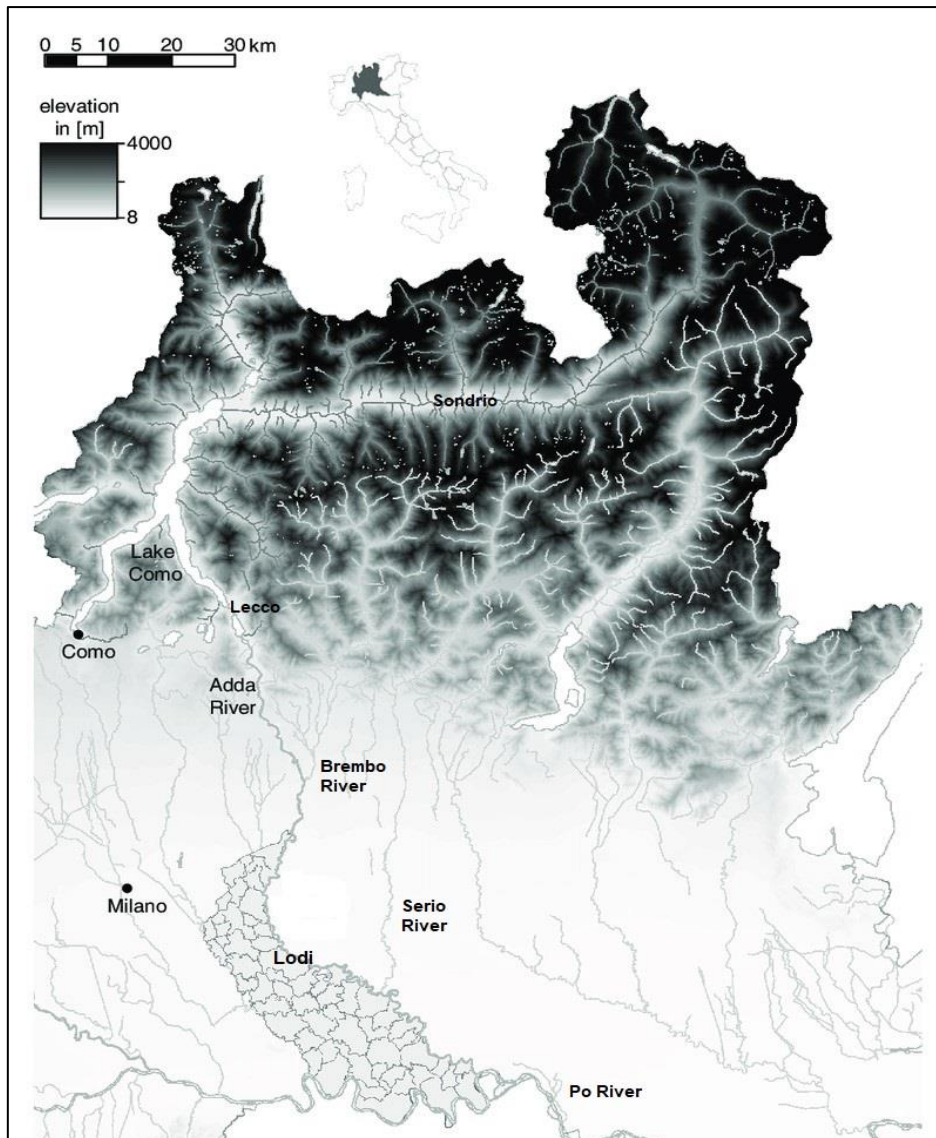


Figure 1-3 - The Adda catchment (Castelletti et al., 2011)

The flow regime of the river is alpine and it is naturally controlled by the Lake of Como, where the Adda is the main tributary and the only emissary. Along its 313 km, some dams and gates, located in the mountain area (Ardenno, San Giacomo di Fraele, Cancano) and in the downstream part of the river (Olginate, Trezzo sull’Adda), influence the flow regime of the river. The maximum discharge can be greater than 1000 m³/s as happened in 1987 and in 2002 (1840 m³/s) (Natale, 2003). Indeed, historically, the river Adda has been subject to floods along its entire course and it has changed its

river bed several times. Despite human interventions, which have gradually reduced the flood risk, exceptional events have been occurred. The November 2002 flood caused serious damages to the lower part of the municipality, with water level above 2 m in some neighbourhoods.

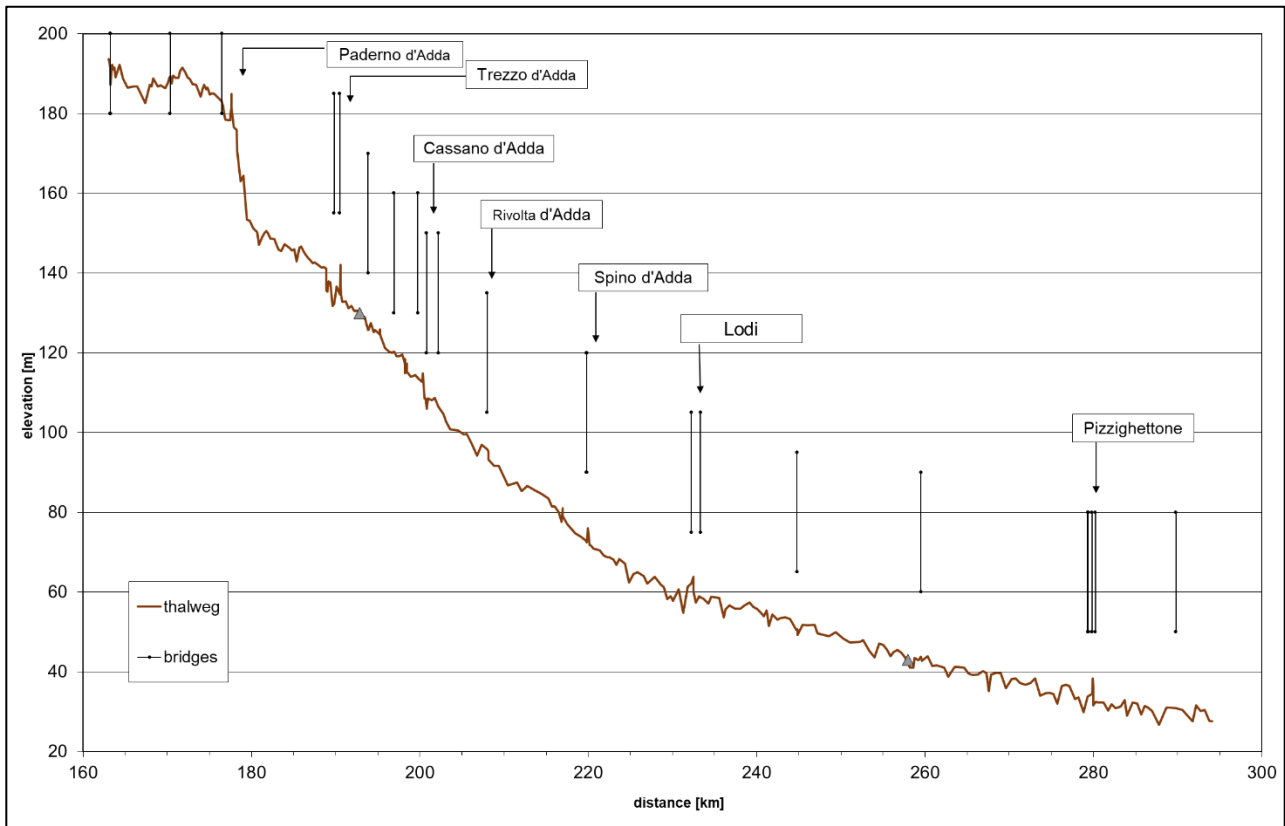


Figure 1-4 Profile of the last 140 km of the Adda river from the Olginate sluice gate (Lecco) to the entrance in the Po river (Lodi)



Figure 1-5 - The river Adda in Lodi during peacetime

1.4 The November 2002 flood event

During the flood event of the river Adda in Lodi in November 2002, serious inundations interested the municipality of Lodi. The most critical condition for the lower part of the Adda occurred, namely the contemporaneous increase of discharge of the tributary Brembo and the maximum outflow from the Como lake.

From the 14th to 16th of November 2002, intense rainfall had been registered in Piemonte and Lombardia, that involved the entire watershed of the river Adda (257 mm measured by the pluviometer located in Fuentes and 355.8 mm by the station in Valtorta). Rainfall continued until the 24th of November, when a shorter period of rainfall with a violent and concentrated peak occurred.

Such events led to the conditions of saturation of the soil and to a sudden increase of the discharge of the affluent Brembo that overlapped with the flood wave coming from the Como lake, already with high levels when the second perturbation began. The following picture reports the weather forecast of intense rainfall of the 25th of November (Lodi is located nearby the red dots) and the estimated hydrograph after the confluence Adda-Brembo, due to the overlapping of the flood waves coming from the Brembo and from the Como lake.

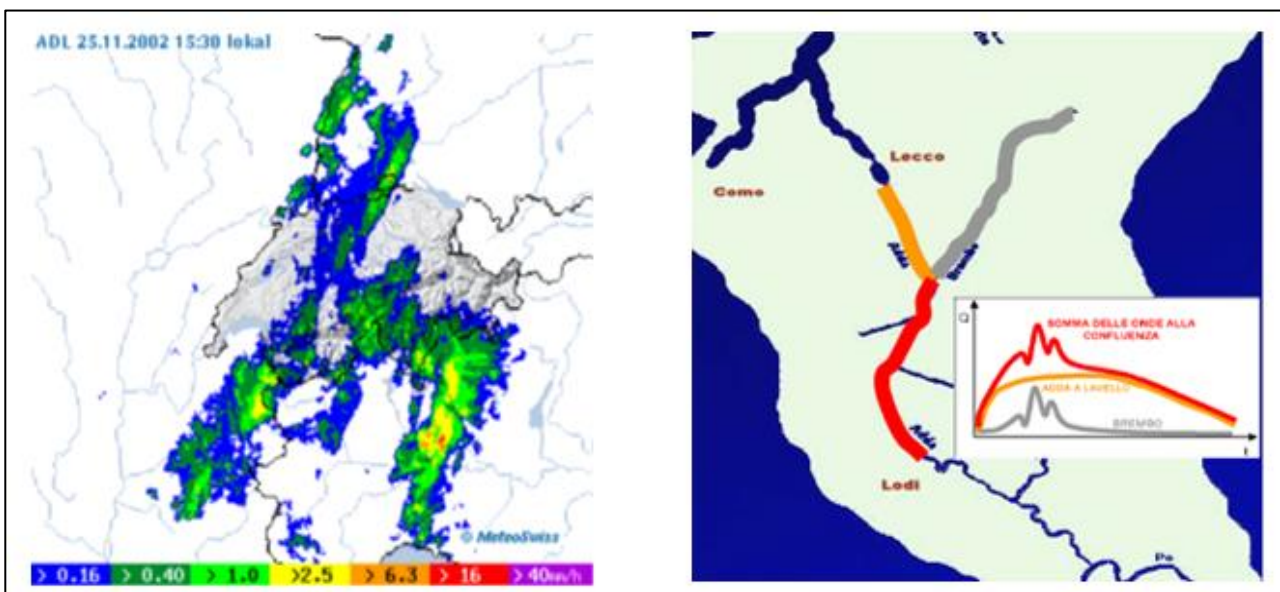


Figure 1-6 - Weather forecast of the 25th of November (MeteoSwiss) and estimated hydrograph after the confluence Adda-Brembo (Rossetti & Cella, 2010)

The entire event from the 18th to the 26th of November, that involved the Adda watershed and the Municipality of Lodi, can be summarised by the following scheme:

- 18 November 2002: after the intense rainfall between the 16th and 17th November, some farmlands in the province of Lodi were flooded. The water level, which had increased until 1.5 meters under the Napoleone Bonaparte bridge, started to decrease and the emergency seemed to be over. However, weather forecast announced that another and less strong perturbation could arrive within 3/4 days.

- 25 November 2002 (point 1 in the Figure 1-8): after other intense rainfall events, areas near the Cascina Ciribina, Dordona and on the depression near the courthouse were flooded by the water coming from the ditches system. Water levels increased up to 1.7 m, still far from 2.7 m, namely the estimated hydrometer height at the historical bridge for the overflow. Few hours later, at 6 pm, the water level decreased until 123 cm (point 2 in the Figure 1-8). However, the discharge of the Adda in correspondence to the dam of Olginate increased up to 1100 m³/s and additional discharge 360 m³/s was flowing from the affluent Brembo. At the end of the day, National Civil Protection stopped the alarm, due to the decrease of the water level. In the meantime, weather forecast predicted 60/70 mm of rain in the following hours.



Figure 1-7 - Water level at the historical bridge before the overflow

- During the night between 25th and 26th the Adda reached the record height of 3.43 m above the hydrometric 0 level (68.28m a.s.l.). The flood has been estimated as an event with return period between 100 and 200 years. It was known that the overpass of 3 m at the bridge corresponded to a discharge between 1800 and 2000 m³/s. The record hydrometer level of 343 cm was reached (point 3 in the Figure 11) around 01.30 am of the 26th of November.

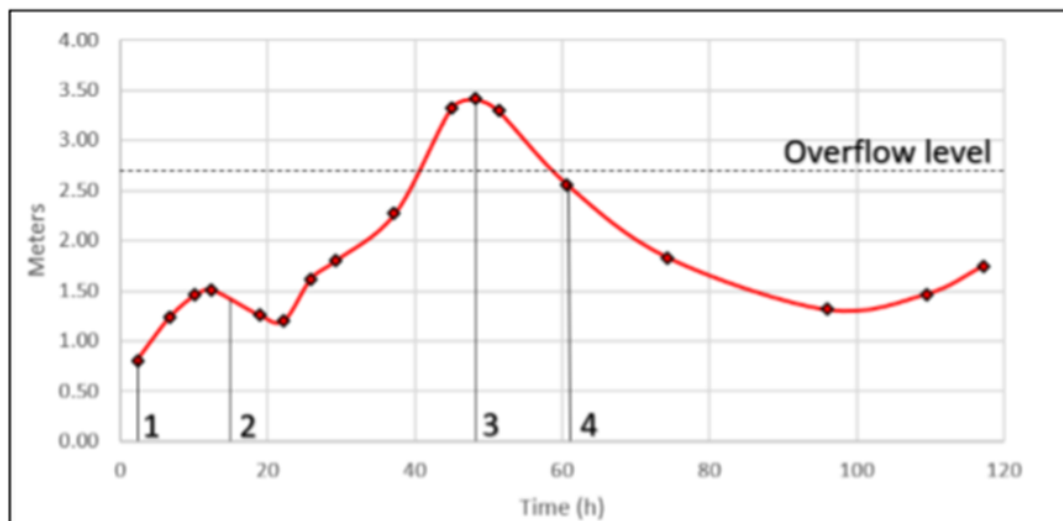


Figure 1-8 - Hydrometer levels registered at the Napoleone Bonaparte bridge in Lodi

- 26 November 2002: part of the city adjacent to the river was underwater. In details, the flood was caused by the overcoming of the river banks and by the flooding of ditches and canals connected to the river Adda. On the left bank, the Revellino and Campo Marte neighbourhoods were flooded. On the right bank, the districts of Borgo Adda and Martinetta were inundated, while the south east area, protected by the Tangenziale sud state road, suffered flooding due to the regurgitation of the arches crossing the ring road itself. About 500 people were evacuated and some of these were accommodated in shelters since their houses were full of mud and water. Houses, farms, and offices were flooded. National Civil Protection, Firefighters, Red Cross and Police helped people with boats, helicopters and others rescue vehicles. At 13.30 pm, water level decreased under the 2.5 m (point 4 in the Figure 11) and, few hours later, the state of emergency ended.



Figure 1-9 Rescue team (on the left) and Viale Dalmazia (on the right) during the flood



Figure 1-10 Piarda Ferrari (on the left) and a top view of Lodi (on the right) during the flood

1.5 Works performed after the November 2022 flood event

After the November 2022 flood event, for the hydraulic safety of the Municipality of Lodi, several works have been performed. In particular, structural mitigation measures have been designed both on the hydraulic left and right of the Adda river by AIPO (*Agenzia Interregionale per il fiume Po*) and Regione Lombardia. However, in this thesis, only the defences on the hydraulic right have been considered for a Multi Criteria Analysis (MCA). The aforementioned measures start from the S.P. 202 (Lodi-Montanaso Lombardo) to the historical bridge (Napoleone Bonaparte bridge), for approximately 2350 m, and continue until the “Tangenziale Sud” state road for about 1150 m.

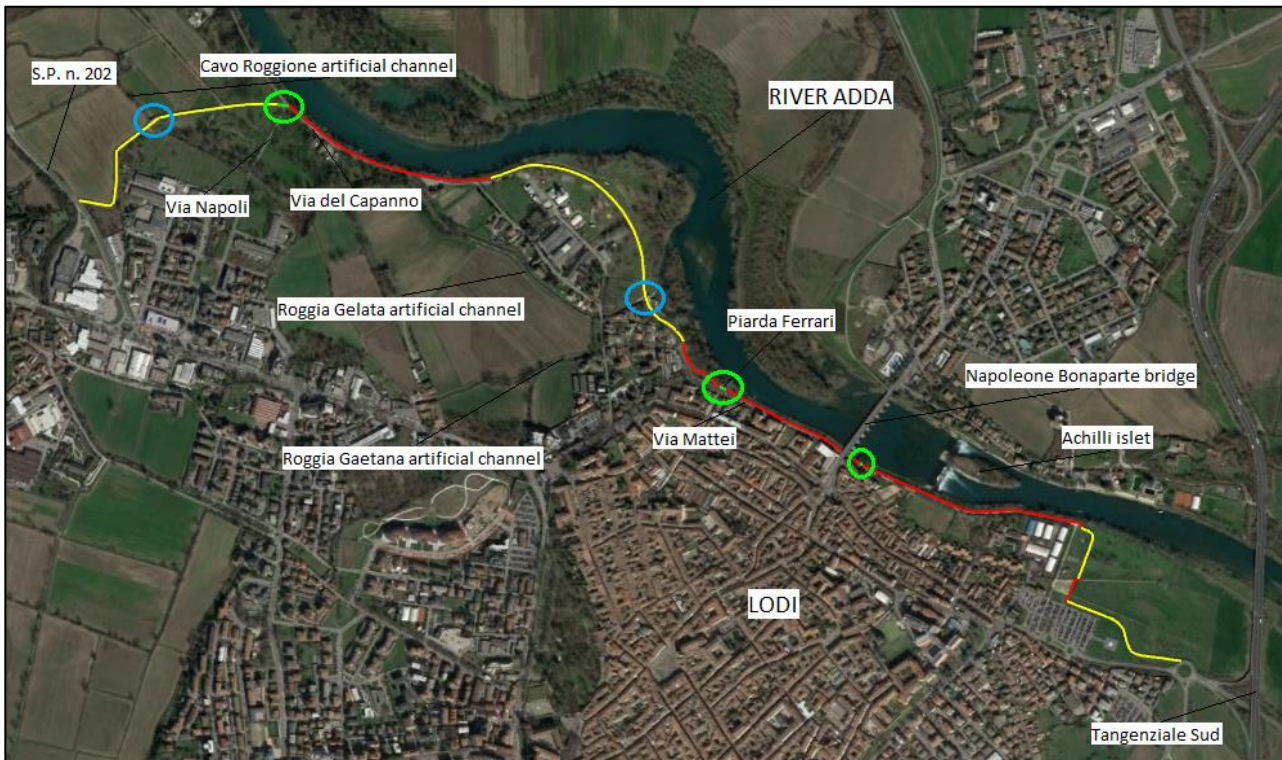


Figure 1-11 - Planimetry of the works performed on the hydraulic right of the river “Adda”. Soil embankments in yellow polyline, defence walls and connection walls in red polyline, sluice gates in light blue polylines, openings in green polylines

1.5.1 Structural defences typologies for each stretch

In this chapter, a description of the structural mitigation measures built after the November 2022 flood event will be proposed. In details, starting from the S.P. n.202 (Lodi-Montanaso Lombardo) until the “Tangenziale Sud” state road, the following structural elements have been realized.

Soil embankment with a traditional trapezoidal section (A1 typology) extends between the intersection “Via Napoli” – “Via del Capanno” and the provincial road “S.P. 202 (Lodi – Montanaso Lombardo)”, with a 596.70 m length. Soil embankments have been realized in the stretches where the structural defence recedes from the river moving towards the city. The top of the embankments reaches the designed elevation (water level of T=200 years flood event + margin of safety) and it is 4 m wide, in order to ease the surveillance during a flood warning and an ordinary maintenance of the slopes or reinforcements after a flood event. Moreover, in peace time, this space can be used

In correspondence of the crossing between “Via del Capanno” and “Via Napoli”, a 15 m opening along the structural wall has been designed. Other two gates of 1.5 m each are positioned between “Via del Capanno” and the crossing with “Via Napoli”, in order to ease the access to the riverbank. The closure of the aforementioned gates will be carried out in case of flood warning, by inserting metal barriers in appropriate junctions.



Figure 1-14 - Particular of the “Via Napoli” opening

Reinforced concrete defence wall (B1 typology) in the stretch between “Via del Capanno” and “Via Napoli”, for a 548.59 m length has been constructed. The basement and the external coating of the structural element is the same one used for the defence wall already present downstream of the historical bridge. Below the sidewalk, a storage space for placing the metal barriers during peacetime have been created. The structural defences have been realized taking, as reference water level, an event with a return period of 200 years. Moreover, a margin of safety of 80 cm has been adopted and, in order to make the structure reaches such a level and to provide the same height of the soil embankments realized between the mentioned walls, a system of metal barriers has been designed. This decision not to build a wall of such a height to reach the level of safety compared to the maximum water levels of 200 years has been taken to reach the compromise between the necessary protection of the town against flood events, and the need to ensure adequate standards of landscape-recreational usability of the river environment in peacetime. Indeed, the system of metal barrier allows the realization of two accesses to the flood plain area, respectively in Piarda Ferrari and in the crossroad between Via del Capanno and Via Napoli, without interfering with the current environment.

Metal barrier will be assembled and mounted over specific basement already present on field if a flood warning is issued. The system of floating barriers is essentially composed by the following elements:

- stackable aluminium panels;
- stainless steel vertical supports, equipped with gaskets along the lateral faces that act as guide to the metal barrier, to be inserted in appropriate bore on the crowning of the walls.



Figure 1-15 Montage procedure of the vertical support

The sizes of each slab are 15 cm of height, 5 m of length and 90 mm of thickness. The total weight is about 37 kg per element.

The vertical support is composed by a cylindrical lower part with a diameter of 154 mm and a height of 50 cm. The upper portion has an H section with a variable height according to the number of barriers to be mounted in different portions of the structural measures in the hydraulic right of the river.

The support elements at the ends of a stretch or in correspondence of intermediate structure (i.e. r.c. pillars or lighting poles) are permanently installed on the defense wall.

The total amount of material to be installed during the assembly phases of the floating barrier is made up of 100 vertical supports and 781 metal barriers.

Some peculiarities related to the storage and montage of these elements must be remarked:

- The elements to be used for the assembly (metal barriers and vertical support) are stored in special compartments in correspondence with the defense walls over which they must be mounted. The latter are placed below the sidewalk along “Via del Capanno” and inside the new flowerpot along “Via Mattei”. This solution involves the total elimination of the supplying times of the elements from the place of storage to the assembly site. Moreover, the immediate availability of each element in situ eliminates all risks related to the mismanagement of a further storage area, like exchange between objects and lack of elements.
- Vertical supports are inserted into the wall through special holes, using a quick and easy "bayonet" system. Moreover, some of the vertical supports have been permanently fixed to still structures (i.e. lampposts placed on the embankment along “Via Mattei” stretch and pillars along “Via del Capanno”) and it will not be necessary to mount them during emergencies. This brings to a considerable reduction in the time necessary for the installation of the vertical supports.

In order to assembly 6 metal barrier and 1 vertical support (the other one is already present, or because it is fixed, or because the adjacent element is already installed), the total amount of time is approximately 5 minutes. Moreover, for the assembly of each of these elements, 2 operators are necessary. Based on simulations and past experiences, considering to use at least 6 teams (3 for the stretch along “Via del Capanno” and 3 along “via Mattei”), the estimated total time for the assembly of the entire mobile flooding barrier is equal to 2.5 hours. Eventually, the number of workers necessary for the mounting of the floating barriers is therefore 12.

A section of the designed structure and particulars taken during a field survey are reported in Figure 1-16 and Figure 1-17.

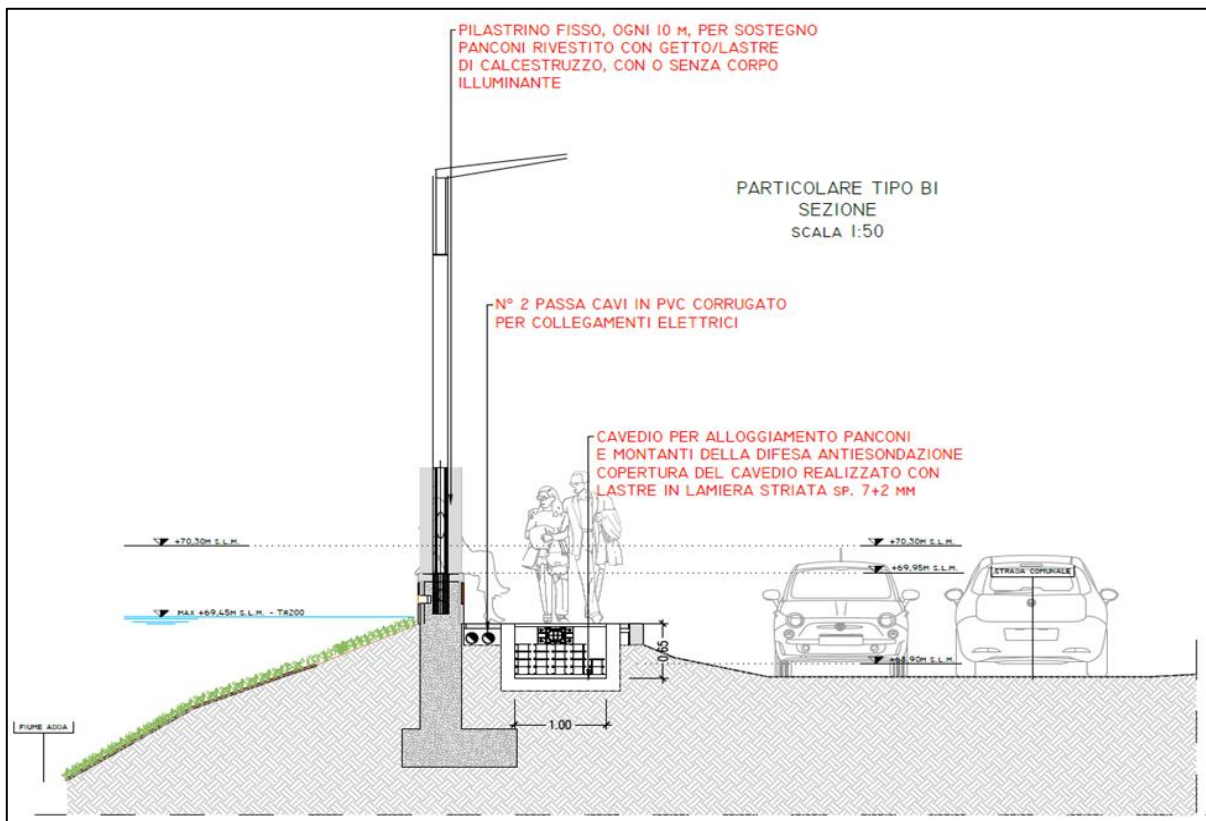


Figure 1-16 Section of the designed defence wall (B1 typology)



Figure 1-17 Particular of the designed defence wall (B1 typology)

Soil embankment with a traditional trapezoidal section (A1 typology) has been realised in the stretch between the previously mentioned defence wall and “Via del Capanno”, with a 769.83 m length, as represented in the Figure 1-18.



Figure 1-18 Particular of the soil embankments (A1 typology)

Sluice gates with four pumping plants, in order to dispose the upstream flows coming from “Gelata” and “Gaetana” artificial channels, is located in correspondence of the confluence between “cavo Roggione” artificial channel and the river “Adda” has been built along the soil embankment (A1 typology). From an architectural point of view, this sluice gate is externally identical to the aforementioned one.



Figure 1-19 Particular of the sluice gate with pumping plant

Upstream of the “Piarda Ferrari” opening, a connecting defence wall in reinforced concrete extends up to the connection with the following soil embankment (A1 typology). In details, the proposed solution includes the development of a path that slowly increases its elevation up to reach the designed quote of the soil embankments (70.40 m a.s.l.).



Figure 1-20 Particular of the connecting defence wall in reinforced concrete (B3 typology)

In order to ease the access to the river Adda, a 15 m length opening along the wall in correspondence of “Piarda Ferrari” has been designed. Moreover, other two gates of 1.5 m length have been localised along the defense structure between “Piarda Ferrari” and the “Napoleone Bonaparte” bridge. The closure of the aforementioned gates will be carried out in case of flood warning, by inserting metal barriers in appropriate junctions, as previously mentioned.



Figure 1-21 Particular of the “Piarda Ferrari” opening

A defence wall in reinforced concrete (B2 typology) has been realized in the stretch between the historical bridge and Piarda Ferrari, for a 422.37 m length. The difference of this wall typology with respect to the B1 is the presence of the flowerpot under which the metal barriers are stored. The section and pictures of particulars of the mitigation measure taken during a field survey are reported in the following.

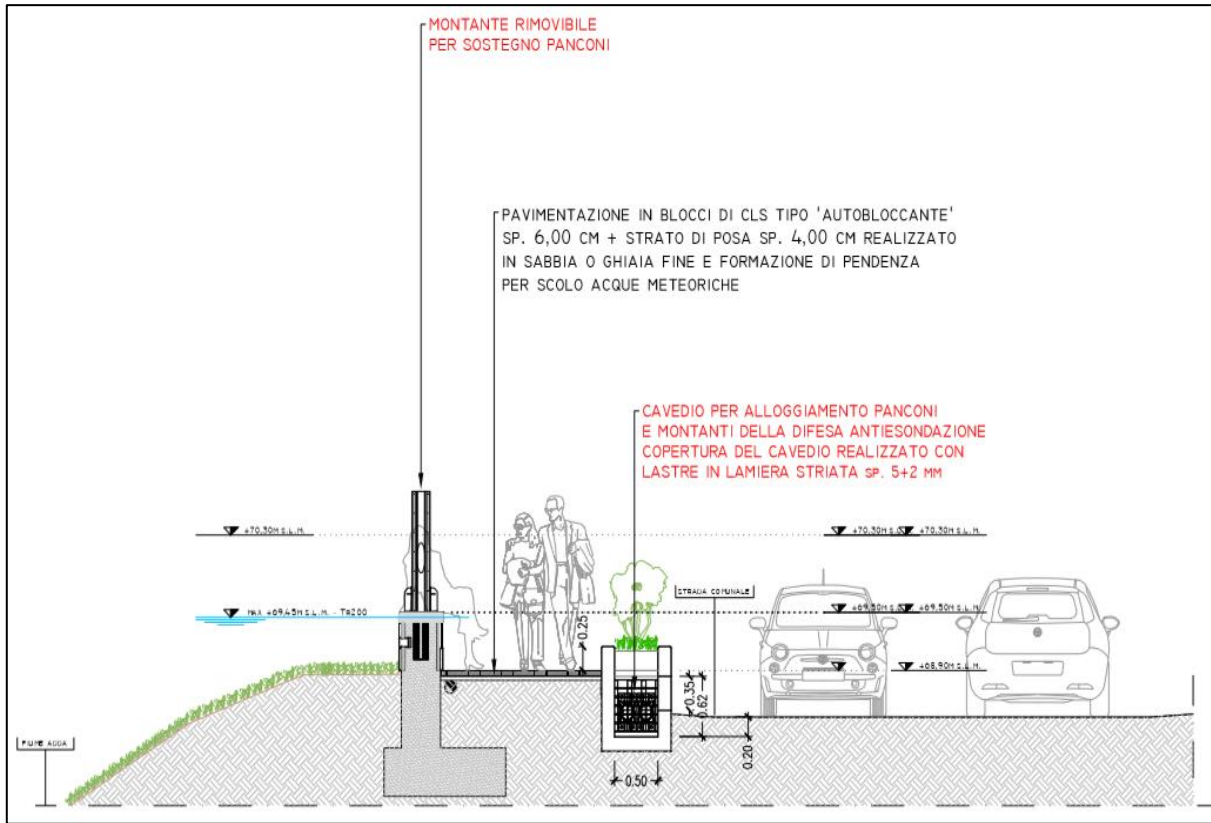


Figure 1-22 Section of the designed defence wall (B2 typology)



Figure 1-23 Particulars of the defence wall upstream of the "Napoleone Bonaparte" bridge

After the “Napoleone Bonaparte” bridge, a reinforced concrete wall extends for approximately 35 m until an opening that connects the following lower defense wall.



Figure 1-24 Particulars of the defence wall and opening downstream of the “Napoleone Bonaparte” bridge

The defence wall that starts after the previous opening is made of bricks and reinforced concrete. The representation of a stretch of this wall is reported in Figure 1-25, taken during a field survey. As it is possible to observe, the upper part of the structural defence doesn't present vertical supports for the positioning of the metal slab system. This is due to the fact that the height of the wall is enough to contain the water level reached by 200 years return period flood event.



Figure 1-25 Particular of the brick and r.c. wall downstream of the historical bridge

The previously mentioned defense wall continues for approximately 560 m before reaching the soil embankments reported in Figure 1-26. The characteristics of the latter are the same of the A1 typology structural mitigation measures previously discussed.



Figure 1-26 Particular of the junction between defence wall and soil embankment

The soil embankment covers about 540 m before reaching the roundabout at the entrance of the “Tangenziale sud” state road. Moreover, in this last portion of structural protection, two orthogonal brick walls of approximately 2 m of height with two openings have been built. Figure 1-27 shows the aforementioned interruption and the accesses to the flood plain in peace time.



Figure 1-27 Particular of the interruption and openings

2 Workflow and theoretical basis of the work

The workflow in Figure 2-1 describes the entire procedure adopted for the achievements of the objectives of this thesis work. Starting from urban flood models, after several numerical simulations that include the calibration of the model, ten hazard maps, reporting five different event severities without and with structural defences, have been created. These maps represent the input for the estimation of the exposed element to flood and, together with an independent vulnerability assessment, for the determination of the expected damages. These losses have been computed for the five investigated scenarios, using both the terrain geometry of the 2002 and the configuration with flood protections. The expected benefits arisen from the construction of flood protections, in terms of avoided damages, have been assessed comparing the scenarios without and with banks, with the same return period event. The expected losses have been sub-divided into quantifiable and non-quantifiable damages, being the firsts involved into the computation of the benefit-cost ratio (B/C) within a cost-benefit analysis (CBA), while the latter have been estimated in order to be included, with the results of the CBA, in a more comprehensive multi-criteria analysis (MCA). The MCA is a procedure that allows the evaluation of the effectiveness of built mitigation measures or as a tool for the determination of the best flood mitigation strategies to be implemented. It has to be remarked that the multi-criteria analysis has not been applied in the case study reported in chapter 3. Indeed, this process requires an evaluation from the delegate decision maker and the participation of different stakeholders involved into the assessment. However, this thesis wants to provide part of the material needed for a comprehensive MCA, as proposed in the chapter 3.3. Eventually, a sensitivity analysis of the CBA results has been performed assuming a different month for occurrence of the flood, as potential consequence of climate change, and a future urbanisation in flood prone area caused by the levee effect. These assumptions influence the exposure of the expected losses and therefore the entire second part of the risk assessment reported in the workflow.

The following sections regard the theoretical basis of the methodologies and approaches that have been analysed and considered for the purpose of this thesis. The consulted material concerns mainly two topics: hydraulic flood modelling and flood damage assessment as support of a multi-criteria analysis.

In regards of the hydraulic modelling, the analysed topics include:

- Flood modelling in urban areas;
- Uncertainties in flood modelling;
- Calibration of a hydraulic model;
- Software used for the hydraulic modelling.

For what concerns the damage assessment as support of a Multi Criteria Analysis, the following topics have been analysed:

- Multi-Criteria Analysis (MCA);
- Cost-Benefit Analysis (CBA);

- Non-quantifiable damage assessment;
- Simplified INSYDE model;
- AGRIDE-c model;
- Sensitivity analysis: climate change impact on flood occurrence and levee effect.

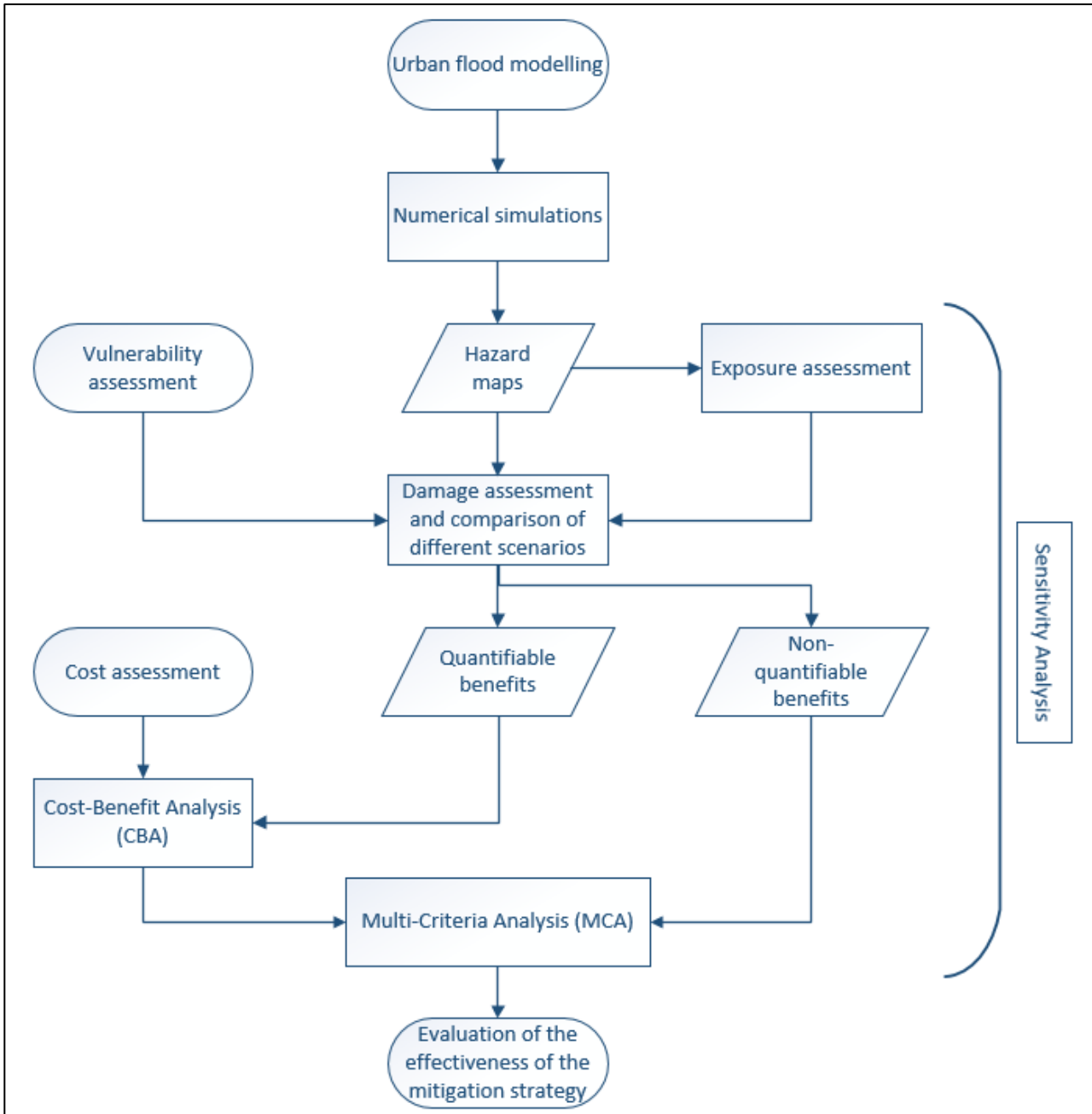


Figure 2-1 Workflow of the methodologies in order to create a MCA, where: the circular polygons regard input topic and output results; the rectangles are processes; the parallelograms are intermediate results

2.1 Flood modelling in urban areas

The following theoretical description has been reviewed taking as reference the document “Mathematical modelling techniques for flood propagation in urban areas”, presented by Alcrudo (2004).

The flood propagation over the earth surface is a 3D time dependent, incompressible, fluid dynamics problem. The Navier-Stokes (NS) equations describe the dynamics of the flood propagation but the turbulent flow, the large computational domain and the length of the time duration domain can compromise any attempt to determine their solution. In order to overcome the problem of the turbulent flow, the NS equations can be averaged in time (Spurk, 1997), leading to the Reynold Averaged Navier-Stokes (RANS) equations, which describe the mean flow. The RANS are widely used in industrial fluid mechanics and aerodynamics but still to complex to describe a flood propagation. In order to simplify the mathematical description, the NS equations are averaged over depth, obtaining the Shallow Water equations (SWE) model (Benqué et al., 1982). The latter can also be derived from the momentum conservation and the continuity equation in the plane of motion (Cunge et al., 1980).

The expression of the shallow Water Equation (SWE) is reported below:

$$\begin{array}{c}
 \begin{array}{ccccc}
 \text{Acceleration} & & \text{Pressure} & \text{Weight} & & \text{Bed Friction} & & \text{Lateral Stress} \\
 \hline
 \end{array} \\
 \left\{ \begin{array}{l}
 \frac{\delta u d}{\delta t} + \frac{\delta u^2 d}{\delta x} + \frac{\delta u v d}{\delta y} + g d \left(\frac{\delta d}{\delta x} - S_{0x} \right) = -g d S_{fx} + \frac{1}{\rho} \frac{\delta}{\delta x} (dT_{xx}) + \frac{1}{\rho} \frac{\delta}{\delta y} (dT_{xy}) \\
 \frac{\delta v d}{\delta t} + \frac{\delta u v d}{\delta x} + \frac{\delta v^2 d}{\delta y} + g d \left(\frac{\delta d}{\delta y} - S_{0y} \right) = -g d S_{fy} + \frac{1}{\rho} \frac{\delta}{\delta x} (dT_{yx}) + \frac{1}{\rho} \frac{\delta}{\delta y} (dT_{yy}) \\
 \frac{\delta u d}{\delta x} + \frac{\delta v d}{\delta y} + \frac{\delta d}{\delta t} = 0
 \end{array} \right. \\
 \begin{array}{cc}
 \hline
 \text{Fluxes} & \text{Storage}
 \end{array}
 \end{array}$$

where:

- d is the water depth;
- u and v are the depth averaged velocity components along x and y axis;
- g is the acceleration of gravity;
- S_{0x} and S_{0y} are the bed slopes along the x and y components;
- S_{fx} and S_{fy} are the friction slopes along the x and y components, computed based on Manning's coefficient for roughness;
- ρ is the kinematic viscosity;
- T_{ij} are the friction forces that consider the lateral stresses.

However, the SWE are not a true mathematical representation of the flood propagation over the earth surface and the following shortcomings and approximation stand:

- Vertical velocities are neglected;
- A hydrostatic pressure is considered;
- The slope of the river bed is assumed small enough to consider the sine of the slope angle, the angle itself;
- Uniform horizontal velocity field is assumed across the water layer;
- Friction formulae are taken from the condition of uniform flow.

The numerical solution of differential equations, like the SWE, is defined by the space discretisation strategy, the used mesh configuration and the numerical scheme performed. The SWE represents an evolutionary problem in the form of propagation waves. A space discretisation is initially achieved with the method of lines, resulting in Ordinary Differential Equations (ODE), to be solved, then, in time. The spatial discretisation can be performed with the Finite Differences, the Finite Volume and the Finite Element Method. The latter is progressively less used being geometrically less flexible than the others. The Finite Volume formulation has a flexible geometrical treatment and it is conceptually simple method, that makes of it the most widespread flood modelling strategy. Moreover, this procedure assures the conservation of the mass and momentum. The studied domain is divided into non overlapping finite volumes over which the integral form of the SWE is applied. This method can be applied to both structured and non-structured grid meshes and any geometrical shape of the single volumes can be used. Furthermore, the non-structured mesh approach allows a mesh refining in parts of the domain where higher flow resolution is required.

In case of urban context, several modelling techniques can be used to deal with the representation of buildings and other obstacles in urban flood propagation, whose choice depends on the scale of the analysis and on the required accuracy (modelling the indoor flooding processes or road crossings and sidewalks, that certainly affect the wave propagation, could be computationally inconvenient if an entire city must be modelled). Four methods are proposed:

- One dimensional (1D) treatment of the city as a channel network representation (Tanguy et al., 2001), capable of providing local flow information with low computational costs. However, this method can suffer from problems at the junction nodes or in wide areas where the flow could be predominantly 2D. In this case, the expression of the SWE is reduced to 1D:

$$\left\{ \begin{array}{l} \frac{\delta V}{\delta t} + v \frac{\delta V}{\delta s} + g \frac{\delta d}{\delta s} = g(S_0 - S_f) \\ \frac{\delta Q}{\delta s} + \frac{\delta A}{\delta t} = 0 \end{array} \right.$$

The differential equations are solved numerically with the aforementioned described methods if boundary and initial conditions are provided. If more detailed descriptions of the flood propagation are envisaged, as well as precise assessment of the flood effects, the physical representation of buildings must be introduced into the model.

- Local friction-based representation of buildings in a 2D approach, in which obstacles are considered as areas with increased friction coefficient, in order to capture flow effects with little additional costs. If only a rough estimation of water depth and velocity is required, without a detailed local description of the physical effect of buildings, this method can be implemented. Local friction is treated as another field variable and one of the difficulties of this method is the determination of the correct roughness coefficient to be assigned. Several tables provide Manning's values according to different land uses but every case must be treated singularly because friction coefficients may depend on building density, scale of the flooded area and ratio of flow depth to buildings height. Another issue is that buildings are considered as storage tanks.

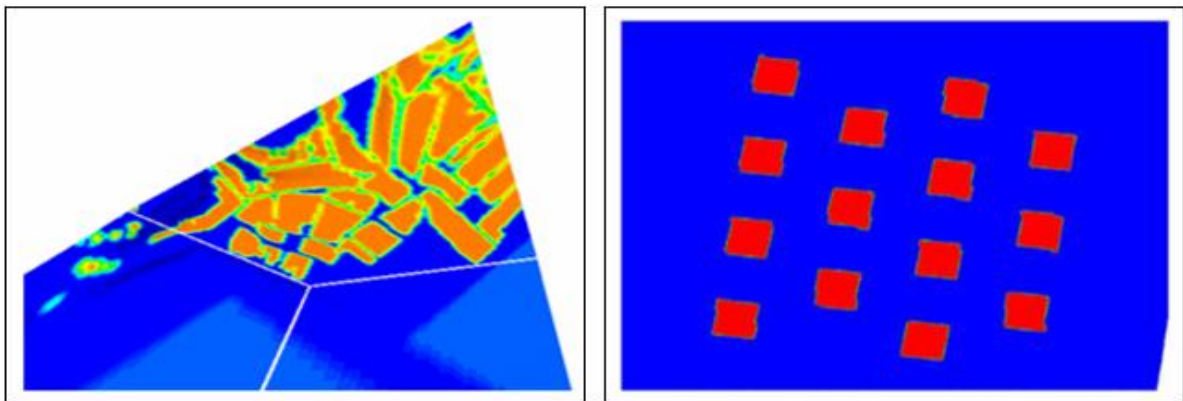


Figure 2-2 Representation of the Manning's roughness embedded in a larger computational domain (on the left) and simply disposition of quadrangular buildings with local bed friction (on the right) (Alcrudo, 2004)

- 2D building representation with bottom elevation technique, increasing the grid points that fall within a building area. The main problem of this method is the representation of the slope between the higher point and the ground point, which can be of the order 1 if the discretisation is coarse (mesh size similar to building elevation) or reach several orders of magnitude if the discretisation is fine (mesh size much smaller than building elevation). This fact violates the aforementioned mild slope assumption of the SWE. However, the model does not fail because buildings acts as internal boundaries causing water stagnation and water around buildings is still considered shallow.

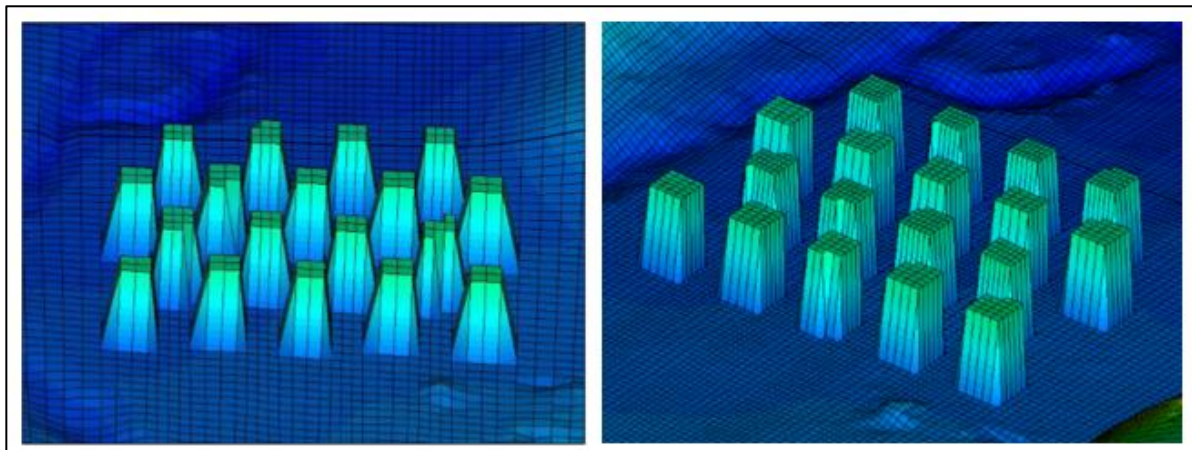


Figure 2-3 Examples of bottom elevation techniques on a coarse mesh (on the left) and on a finer mesh (on the right) (Alcrudo, 2004)

- 2D vertical wall representation of buildings, excluding obstacles from the computational domain. This method is the most accurate technique to reproduce a city, in which the 2D flood model is run in the void areas only. However, the meshing procedure can be difficult in urban areas in which a heavy stretching of the mesh is required to represent the complex street patterns, increasing the computational effort.

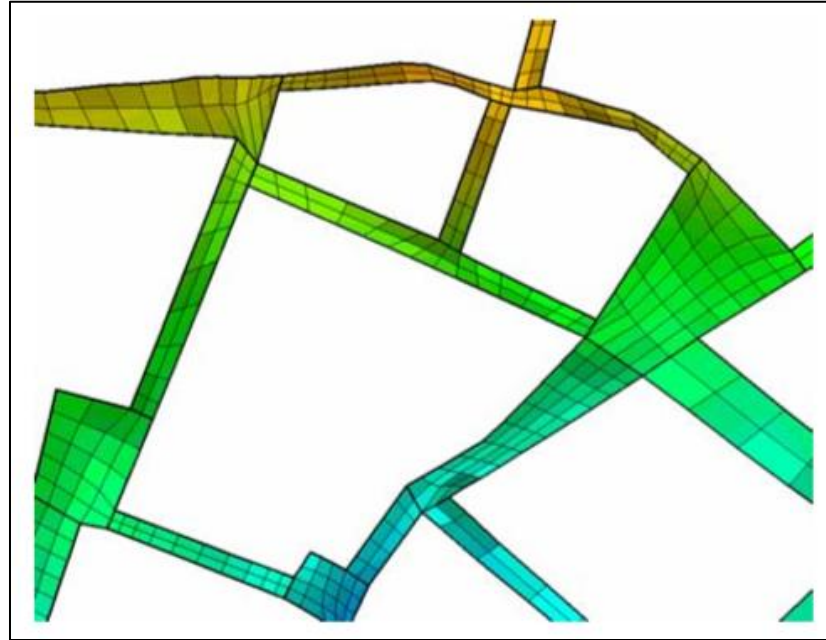


Figure 2-4 Representation of vertical walls technique (Alcrudo, 2004)

2.2 Uncertainties in flood modelling

A number of important issues must be taken into account by users when dealing with flood modelling. In addition to difficulties in evaluation of model results due to false confidence of high-resolution outputs and lack of observed data, some uncertainty sources in flood modelling regards the available input data (Dottori et al., 2013), which may influence the simulated dynamics of the flow (Romanowicz and Beven, 2003). Some of the possible sources of input data uncertainties in flood modelling regard:

- Topographic data from ordinary survey techniques used as geometrical input (Dottori et al., 2013);
- Digital Terrain Models (DTM) errors;
- Imprecision on the magnitude and position of the inflow boundary conditions (Brandimarte and Di Baldassarre, 2012), such as the difficulties in reconstruct flood hydrographs which can affect all the resulting simulations (Romanowicz and Beven, 2003; Bates, 2004; Mignot et al., 2006; Masoero et al., 2012);
- Reproduction of complex interactions between surface flow and subsurface drainage system in urban floods. Moreover, in case of inundation events, drainage system may be affected by unpredictable local breaks and obstructions, adding further uncertainties in order to represent flooding mechanisms (Dottori et al., 2013);
- Interactions of water flows with several small-scale features. The latter can be fixed structures such as small embankments, ditches, walls and fences (Wright et al., 2008; Bates et al., 2006; Hailemariam et al., 2013; Yu and Lane, 2006) and moving elements like cars, other vehicles, bus-stops, trees and garbage bins that can partially obstruct streets and contribute in forming debris accumulation (Mignot et al., 2006), as well as modify the flow pattern (Bazin et al., 2017). Fixed features can be included in the geometry if high resolution data is available (Yu and Lane, 2006b; Fewtrell et al., 2011), while the location of minor moving obstacles are more difficult to reproduce during the flood, leading usually to their exclusion from model grids (Bazin et al., 2017). However, in case of floods characterised by high energy flow, like the November 2011 flood event in Genova, Italy (Cavallo et al., 2012), these minor moving elements can affect the overall flow processes;
- The complex interactions of the built environment with flow processes. Treating buildings as impervious blocks excludes the indoor dynamic flows that are normally verified during floods (Dottori et al., 2013);
- Soil and build-ups debris transport and erosion processes can modify the configuration of the area and consequently affect the dynamic of the flow, especially with floods characterised by high energy flow (Mignot et al., 2006; Gallegos et al., 2009).

The aforementioned sources of uncertainties must be taken into consideration and quantified if possible (and if necessary) or at least mentioned during the flood model showing potential limitations of the simulation. Moreover, the extreme precision of models and data sets may induce non-expert users to become overconfident in obtained results, ignoring some issues important to perform reliable flood analysis (Dottori et al., 2013). The analysis of multiple flood scenarios, performing a sensitivity analysis on input data and modelling techniques, before and after running the simulations, could help in understanding the impact of each model and data uncertainty on the final result.

2.3 Calibration of a hydraulic model

The model calibration is a procedure of adjustment of the model input parameters in order to obtain a model representation of the interested processes that satisfies pre-establish evaluating criteria (Coastalwiki, 2007). Cunge (2003) defines the calibration as an iterative process consisting in executing several simulations of past observed events, varying the parameters of the model, until an acceptable (to the modeller) match between observations and computations is obtained, compensating for model insufficiencies and errors. Despite the evolution and improvement of modelling technology, the model calibration remains a critical and time-consuming operation within the modelling process. According to Dung et al. (2001), the lack of appropriate data is a weak point for the model calibration. The data requirements for a calibration process depend on the used model type (i.e. for a lumped rainfall-runoff model, runoff data of the catchment are needed (Madsen, 2000), while for highly distributed hydrodynamic models, spatial data such as satellite-derived flood extents maps are strongly recommended as calibration dataset (Bates, 2004)).

The choice of the best calibration run can be based on objective functions, in order to evaluate the effectiveness of the model in predicting the flooded area extent and water depths in observed points (Scorzini et al., 2018). The latter can be:

- The Average of the Differences (AD) between simulated and observed water surface elevation for each cluster (grouping of observed water elevations, taking into account their spatial distribution and the presence of discontinuities in the terrain). The goal value of this indicator is equal to 0, namely a perfect match between observed and obtained water surface elevation. A value of AD greater than zero means abundance of water in the model, while a negative result means an underestimation of the water depth compared to the measured one;
- The Average absolute of the differences (AAD) between the modelled and observed water surface elevation for each cluster. It is obtained computing the absolute value of the AD results. Also, in this case, the goal value for this indicator is 0;
- Nash-Sutcliffe Efficiency (NSE) (Nash et al., 1970), defined as:

$$NSE = 1 - \frac{\sum_{i=1}^n (O_i - P_i)^2}{\sum_{i=1}^n (O_i - \bar{O})^2}$$

where:

- O_i indicates the observed value in the location i ;
- P_i indicates the quantity obtained by the model simulation in the location i ;
- \bar{O} stands for the average of the observed quantities.

The value of NSE ranges from $-\infty$ to the goal value of 1, with higher value indicating better agreement. The largest disadvantage of the NSE is the fact that the differences between the observed and predicted values are calculated as squared values (Krause et al., 2005).

Therefore, larger results in a simulation contribute more to overestimate the results of NSE, while lower values are neglected, highlighting that NSE is very sensitive to extreme numbers. A value of zero for the coefficient of efficiency indicates that the observed mean \bar{O} is a good predictor as the model, while negative values indicate that the observed mean is a better predictor than the model (Wilcox et al., 1990);

- The Flood Area Index (FAI) (Dung et al., 2011), through the formula:

$$FAI = \frac{A^{11}}{A^{11} + A^{01} + A^{10}}$$

where:

- A^{11} is the number of pixels for which both obtained and observed results indicate presence of water;
- A^{01} is the number of pixels for which the simulated results indicate presence of water and observed ones report absence of water;
- A^{10} is the number of pixels for which the simulated results indicate absence of water and the observed ones report presence of water;

The FAI may range between 0 and 1, which represent the goal.

Despite the limitations of this measure, for example bias towards large inundation extent, are known and reported, due to lack of better indicators up to date, the FAI is still the basic measure used and recommended for deterministic calibration (Dung et al., 2011).

Model performance is often evaluated with other tools, to assess the degree of collinearity between observed and model-simulated variates. However, the latter suffer from limitations that reduce their use in evaluating model performances (Legates & McCabe Jr., 1999). Some basic methods for model evaluation (among which there is the NSE) are:

- Coefficient of determination (R^2), that is the square of the Pearson's product-moment correlation coefficient, describes the proportion of the total variance in the observed data that can be analysed by the model (Legates & McCabe Jr., 1999) and it is given by the formula:

$$R^2 = \left\{ \frac{\sum_{i=1}^N (O_i - \bar{O}) * (P_i - \bar{P})}{[\sum_{i=1}^N (O_i - \bar{O})^2]^{0.5} * [\sum_{i=1}^N (P_i - \bar{P})^2]^{0.5}} \right\}$$

where:

- O_i are the observed values;
- \bar{O} is the mean of the observed values;
- P_i are the simulated values;
- \bar{P} is the mean of the predicted values;
- N is the total number of values.

The coefficient of determination (R^2) ranges from 0 to 1, where higher values indicates a better agreement. A limitation of this coefficient is that it standardises differences between the observed and predicted averages and variances because it assesses linear relationship

between variables only (Legates & McCabe Jr., 1999). If $P_i = (AO_i + B)$, for any non-zero value A and any B , then $R^2=1$, making this coefficient insensitive to additive and proportional differences between observations and simulations (Willmott, 1984). Large values of R^2 can be achieved even with model-simulated values different in terms of variability and magnitude. Moreover, correlation-based measures are more sensitive to outliers with respect to observations near the mean (Legates and Davis, 1997), leading to a bias toward the extreme events if correlation measures are used to evaluate models (Legates & McCabe Jr., 1999).

- Index of agreement (d), that overcomes the insensitivity of correlation-based measures to differences in observed and simulated means and variances (Willmott, 1981), is given by:

$$d = 1 - \frac{\sum_{i=1}^N (O_i - P_i)^2}{\sum_{i=1}^N (|P_i - \bar{O}| + |O_i - \bar{O}|)^2} = 1 - N \frac{MSE}{PE}$$

where the O_i , P_i and \bar{O} represent the same values previously described for R^2 .

The index of agreement (d) ranges from 0 to 1, with higher values indicating better match between observed values and modelled ones. This index represents also the ratio between the mean square error (MSE) and the potential error (PE), represented by the denominator of the first proposed fraction, multiplied by the total number of values and then subtracted from unity (Willmott, 1984). Together with the NSE coefficient, the index of agreement is considered an improvement of the coefficient of determination, but it is sensitive to extreme values as well.

2.4 Software used for the hydraulic modelling

The flood modelling of this thesis has been carried out using the calculation code Parflood, developed by the Università degli Studi di Parma (UNIPR), and the software Surfer 13, belonging to the Golden Software LLC company. In the following sections, the most important characteristics and properties of these tools will be explained, in relation to the performed operations in this thesis work. All the operations with Parflood have been run with Cygwin software, which allows to run the model using LINUX language, by remote computer using the UNIPR servers, through the use of WinSCP software.

2.4.1 Surfer software

Surfer 13 has been used both to create/modify the input files needed by the calculation code Parflood and to display/analyse the output of flood model simulations. In the next sections, a detailed explanation of the used commands in Surfer, as well as the modifications performed on the model input files, are proposed. In order to modify, add and delete elements on the geometry file, as well as for the roughness file, the map command “digitize” and the grid commands “blank”, “math” and “mosaic” have been used.

The map digitize command allows to write map coordinates to a data file. Selected points are written into the Digitized Coordinates window, containing the x, y and z coordinates of the point. This command has been used to create computational domains over which boundary conditions are applied and to select portions of geometry file to be modified.

The grid blank command is used to remove grid node data from a grid file. Once defined the boundaries of the interested area with the map digitize command, it is possible to blank internal or external nodes. Blanking assigns a blanking value ($1.70141e+038$) to specified groups of grid nodes in a blanked grid file, containing the same number of grid nodes and the same grid limits as the original grid file. This operation has been performed in order to extract portions of geometry file (blanking the external nodes) and to modify the latter using the grid math command.

The grid math command allows to transform the z values of a single grid file or to combine z values from different grid files. An example of the use of the grid math command is reported in the Figure 2-5, in which the variable A is referred to the Manning’s coefficient of the input grid selected. In the function dialog box, the required operation is written, in which all the elements of the A matrix that are equal to 0.028 will be changed in 0.06, while all the others will remain with the original value of the A matrix. In addition to roughness grid file modifications, as previously described, this command has been used to add the structural defences on the hydraulic right, modifying portion of terrain over which the flood protections have been located.

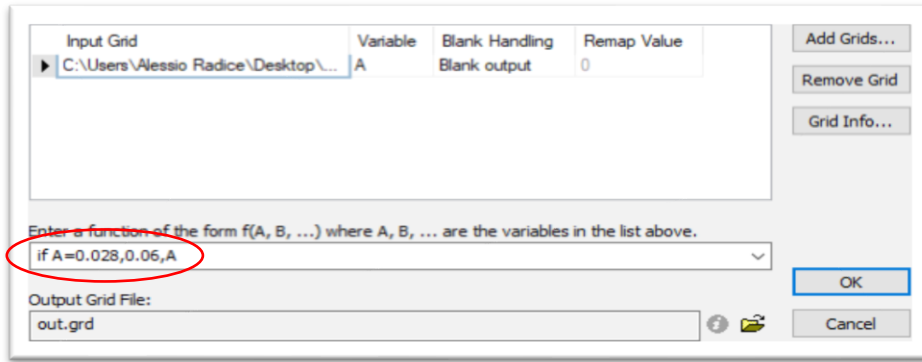


Figure 2-5 Example of the grid math procedure

The grid mosaic command combines two or more grids files into a single output grid file. In Figure 2-6, an example of the application of the grid mosaic command is shown. In the input grid files dialog box, the two selected files involved in the computation are reported. Then the resample method must be chosen between the proposed ones. An important operation regards the choice of the overlap method. In this case, the software will overlap the two grids files and will take, as final value in the new grid file, the one coming from the second (last) file. It has to be remarked that the input grid files involved in the calculation must have the same coordinate system. This operation has been used to overlap the modified portion of terrain with the structural defences on the geometry file without flood protections.

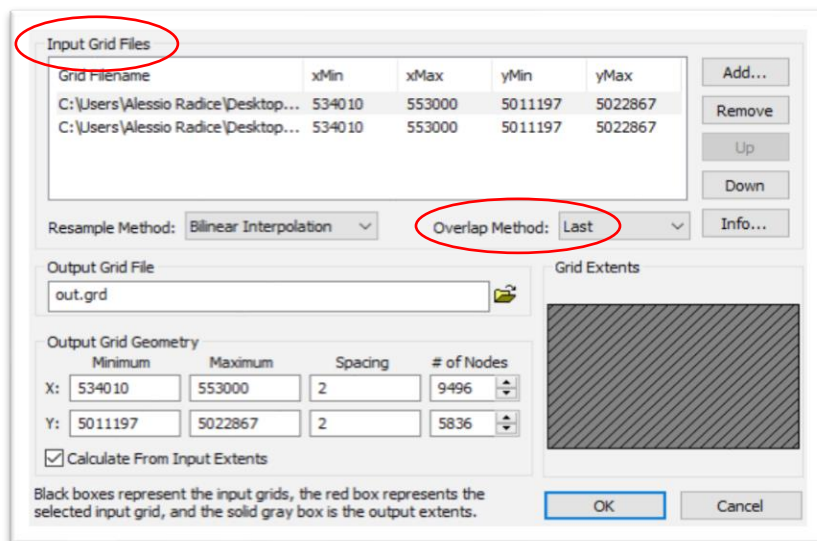


Figure 2-6 Example of the grid mosaic procedure

2.4.2 Parflood calculation code

In order to solve the shallow water equations, Parflood code needs information regarding the bathymetry and the roughness of the studied area, as well as the computational domain and boundary conditions, requiring the following input files:

- .BTM file, namely the bathymetry or geometry file;
- .MAN file, that is the roughness expressed with the Manning's coefficient;
- .BLN file and .BCC file, respectively the computational domain and the boundary conditions files;

Additional optional files regard the initial velocity along x and y directions (set to zero by default), the initial condition file (dry bed is set by default) and multi-resolution grid file.

In the following, an explanation of the main features regarding the aforementioned four input files is reported and, eventually, the available Parflood's output files described. The modifications and operations performed on the input files, in order to create the inputs for the flood model, as well as for model calibration purposes, are described in the chapter 3.1.4.2.

The .BTM input file, related to the bathymetry, contains the geometry of the area under investigation. In Figure 2-7, an extract of the used .BTM file for the flood model is reported. The ancient part of the City of Lodi is on the hydraulic right of the river Adda, while the Revellino district, one of the most flooded areas after the November 2002 event, is located on the hydraulic left of the river. Different colours mean different terrain heights, highlighting how the Revellino district is located in an area more prone to flood with respect to the historical part of Lodi.

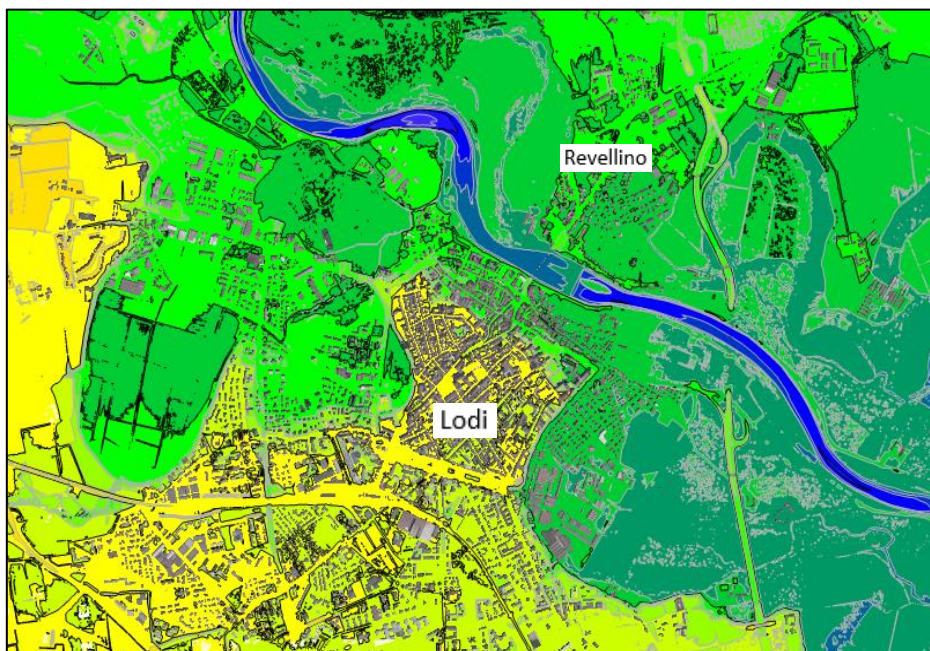


Figure 2-7 Extract of the bathymetry file representing the municipality of Lodi

The .MAN input file contains all the information regarding the roughness, expressed with the Manning's coefficient. Both the .BTM and .MAN grid files, having the same grid size, are constituted by points with x, y, z coordinates. The third value differs only, representing the altimetry of the terrain in the .BTM file, and the corresponding Manning's coefficient value in the .MAN one. This analogy permits to obtain the .MAN file just by changing the z coordinate of the .BTM, using the grid math command in surfer.

During the model calibration, different values of Manning's coefficients have been used, in order to represent different areas, i.e. urban environment, forests and cultivated lands. In order to pursue these modifications, the digitize map command (to select the interested area), the grid blank command (to blank external nodes), the grid math command (to change the current roughness with a new one) and the mosaic grid command (to overlap the new grid file on the original one) have been used in surfer. Examples of .MAN grid files are presented in chapter 3.1.4.2, describing the model calibration.

In Parflood calculation code, boundary conditions are introduced with the use of two types of files: .BLN file and .BCC file. The first one represents the computational domain and is built using the digitize grid command on the Surfer software, in which a polygon, that delimitates the area over which the boundary condition will be applied, is traced in counter-clockwise direction. It has to be remarked that these points must be inside the limits of the bathymetry file, to avoid problems of numerical instability during the simulation.

The .BLN file is structured as follow:

- Number of points;
- x and y coordinate values for each point, including the boundary condition;
- Indicator of the boundary condition to be applied at the segment between the selected point and the following one, in counter-clockwise direction.

The third value, that specifies which kind of boundary condition is applied for each point of the .BLN file, can assume one of the following values:

- 21: discharge (initial hydrograph along the following finite segment);
- 1: wall, meaning that the water cannot flow forward as if it encounters an impermeable obstacle;
- 2: specific discharge;
- 3: set water level;
- 4: "farfield", meaning that the water can flow away without disturbance, as if it would move on a planar and obstacle-free undefined field;
- 5: rating curve, meaning that on the selected section the relation regarding the discharge trend as function of the water level is known.

An example of the .BLN file used in one of the flood model simulation has been reported in the Figure 2-8:

1	29		
2	538127.25573483	5021551.2410428	21
3	537966.78784281	5021561.9389023	1
4	537865.15817786	5021577.9856915	1
5	537480.035237	5021339.9583183	1
6	537239.33339896	5020981.5800261	1
7	536603.57230517	5021198.9881861	1
8	536185.73725452	5020992.7151864	1
9	535514.0277427	5020463.810059	1
10	535889.7777429	5018528.7513308	1
11	536289.74845716	5016399.1775279	1
12	538884.1530902	5014885.7748253	1
13	541846.09837959	5014096.6434161	1
14	545897.63191698	5012778.3059222	1
15	548097.06901612	5012484.0668454	1
16	548431.94075789	5014119.3872305	1
17	547801.36851805	5014796.6685251	1
18	547071.53953676	5015252.0818094	1
19	548106.05106732	5015863.2980298	5
20	548267.90941587	5015872.8191091	1
21	548734.44230285	5015887.1007281	1
22	548953.42712735	5016006.1142197	1
23	549970.41429782	5017373.6132352	1
24	550664.09637982	5019271.6139527	1
25	548616.21224773	5019875.2008548	1
26	546230.60687281	5020119.509839	1
27	543629.43474713	5020579.3855739	1
28	541509.69503146	5021657.2193276	1
29	540180.33065953	5021885.1458365	1
30	539645.34029474	5021795.8338826	1

Figure 2-8 Example of .BLN file

The aforementioned file is composed by 29 points. In the first one, condition 21 is applied, meaning that the upstream boundary condition, in the form of flood hydrograph, is linked to the segment between the point 2 and the following point 3. Condition 5, in terms of rating curve is applied on segment 19-20, while all the other points of the BLN. file act as impermeable walls.

If one of the conditions 21, 2, 3 and 5 is assigned, the .BCC file, as a specification of the .BLN file, must be added in the input files. The used .BCC file, containing the flood hydrograph as upstream b.c. and the rating curve as downstream b.c., is a txt file structured as follow:

1	2			124	18	99	
2	1	121		125	0.000000	0.000000	-0.000000
3	0	0	801.35215	0	126	48.6633605	0.000000
4	3600	0	808.83435	0	127	48.5683605	0.000000
5	7200	0	803.2227	0	128	48.6633605	0.000000
6	10800	0	814.446	0	129	48.7583605	0.000000
7	14400	0	821.9282	0	130	48.8533605	0.000000
8	18000	0	823.79875	0	131	48.9483605	0.000000
9	21600	0	836.8926	0	132	49.0433605	0.000000
10	25200	0	840.6337	0	133	49.1383605	0.000000
11	28800	0	846.24535	0	134	49.2333605	0.000000
12	32400	0	857.46865	0	135	49.3283605	0.000000
13	36000	0	861.20975	0	136	49.4233605	0.000000
14	39600	0	855.5981	0	137	50.3733605	1.118539
15	43200	0	864.95085	0	138	50.4683605	1.262167
16	46800	0	864.95085	0	139	50.5633605	1.419485
17	50400	0	863.0803	0	140	50.6583605	1.589429
18	54000	0	876.17415	0	141	50.7533605	1.77127
19	57600	0	881.7858	0	142	50.8483605	1.964454
20	61200	0	889.268	0	143	50.9433605	2.168536
21	64800	0	900.4913	0	144	51.0383605	2.384748
22	68400	0	921.06735	0	145	51.1333605	2.618412
23	72000	0	950.99615	0	146	51.2283605	2.870962
24	75600	0	973.44275	0	147	51.3233605	3.14471
25	79200	0	1038.912	0	148	51.4183605	3.436964
26	82800	0	1055.74695	0	149	51.5133605	3.746464
27	86400	0	1104.38125	0	150	51.6083605	4.072358
28	90000	0	1126.82785	0	151	51.7033605	4.413994
29	93600	0	1117.4751	0	152	51.7983605	4.770845
30	97200	0	1149.27445	0	153	51.8933605	5.14683
31	100800	0	1132.4395	0	154	51.9883605	5.54398

Figure 2-9 Example of .BCC file

The value 2 means that the boundary conditions to be specified are two, the first of which is composed by 121 elements. It is worth notice that the number 1 is also the first listed coordinate on which the boundary condition "21" is applied in the .BLN file. This is exactly how these two files are linked. The reported example of .BCC file is cut, indeed the first condition ends at the 123rd row, after which the second boundary condition is specified. Being a boundary condition "21", the first column represents the time, the second reports the water levels (that are not read in this case and zeros are present, like the fourth column), while the third column specifies the discharge at each assumed time of the flood simulation.

The second boundary condition is reported on the right-hand side of the Figure 2-9. It specifies that downstream boundary condition is applied to the 18th coordinate (until the following one) of the .BLN file and contains 99 elements, from the 125th to the 223rd row (in this case the file is cut until the 154th one). The first column reports the water level [m a.s.], the second and the third columns contain, respectively, the discharge along the x component (Q_x [m³/s]) and on the y component (Q_y [m³/s]).

Parflood calculation code provides, as available outputs, the following files:

- .WSE file, namely the water surface elevation;
- .DEP file, that is the water depth;
- .VVX and .VVY file, or rather the component of the velocity along x and y axis;
- [name of the simulation] output.txt file, that contains n-rows corresponding to n-temporal instant and reports calculation and saving times;
- Output_[name of the simulation].txt file, that describes the whole procedure of the model calculation; moreover, from this txt file, it is possible to read possible mistakes occurred during the calculus that bring to an unexpected stop of the simulation.

The time discretization starts from 0 and ends up with LAST file, containing the last results before the end of the simulation. For instance, if the entire simulation lasts 120h, the output files will be with a 0000.DEP file, 0001.DEP file, ..., until 0119.DEP file, a time step before the LAST.DEP file. The same output structure is obtained also for the other types of output files. Among the LAST files, another important and useful output is the .MAXWSE file. It contains the envelope of the highest water level values reached by the individual cells during the entire simulation.

Once the simulation is completed, the obtained output files are written in binary code and, in order to be visualized on Surfer, a decode procedure must be run, using the Cygwin software and Win SCP software.

2.5 Multi-criteria analysis (MCA)

The current practise of flood risk assessment focuses mainly on damages that can be measured in monetary terms, leading to processes that manage only a certain portion of the flood risk (Meyer et al., 2009). Multi-Criteria Analysis (MCA) includes techniques potentially able to consider a wide range of flood impacts and diverse attributes that don't need to be expressed in monetary terms, resulting in a fundamental tool for decision-makers. Beyond direct damages to quantifiable assets such as residential buildings, agricultural sector, etc, MCA usually is able to include non-quantifiable expected damages (and therefore benefits) referred to social, economic and environmental impacts that are often neglected (Meyer et al., 2009). Moreover, MCA is able to include, in the risk evaluation, priceless values like cultural heritage and human life, whose ethical issues has always limited its involvement in decision-making processes. Information on vulnerable groups should be integrated in the population criterion, while greater effort is required to define economic criteria, calculated both at meso and micro-scale. In other words, MCA is able to address also the qualitative costs and benefits with the internalisation of intangible consequences, while CBA is used to address only the quantitative costs and benefit. Decision makers may choose the most cost-effective strategy (largest risk reduction with smallest resources implementation) if only monetary aspects are accounted, while alternative solutions could be selected, considering also ecological, social and intangible values, even if the latter would not be the most economically favourable (Brinkhuis-Jak et al., n.a.). The choice to use CBA and MCA in an integrated assessment, rare so far (Brouwer and van Ek, 2004), would result in a more comprehensive and efficient evaluation of possible impacts of hazards on the different assets.

MCA methods are able to screen out "worse" option and possibly to identify the "best" option, merging results coming from different attributes into a single indicator or relative performance (RPA,2004). The approach consists in evaluating criteria for different risk dimensions, then to identify methods in order to assess and weight these criteria (considered as the core of the MCA) and, eventually apply different multi-criteria decision rules in order to get an overall risk assessment, ranking, if necessary, possible alternatives according to the final score (Mechler, 2016). The evaluation of criteria should be the more complete as possible to ensure that the entire problem is encompassed but, on the other hand, the number of criteria should be kept as minimal as possible to reduce the complexity of the evaluation process (Keeney and Raiffa, 1993). The determination of threshold values and weights is a crucial part of the overall assessment, strongly influencing the final result (Munda 2006, Proctor and Drechsler 2006). Sometimes, a sensitivity analysis on criteria and weights can support decision makers, in order to understand the influence of the latter on the overall assessment. Moreover, stakeholders' involvement in projects to develop tools and methods jointly, and not only interviewing them to obtain feedbacks, has been an increasing requirement of many project calls by the European Commission for FP7 (Molinari et al., 2014).

MCA approaches could play an important role demonstrating longer-terms implications of Disaster Risk Reduction (Shreve and Kelman, 2014). Indeed, according to Brouwer and van Ek's (2004), integrated MCA and CBA in flood risk management in the Netherlands demonstrated that while structural mitigation measures were most cost-effective in a short-term analysis according to CBA

only, floodplain restoration can be justified in a long-term analysis using both the CBA and MCA, involving socio-economic and ecological impacts. The latter would have not been clear with the use of a CBA only.

Geographical Information System (GIS) are considered as appropriate tools to be implemented in the MCA, thanks to their ability to handle spatial data and to represent vulnerability and exposure of both monetary and non-monetary assets. Moreover, it is expected that such integrated mapping techniques will be more frequently used thanks to the new European “directive on the assessment and management of flood risk” (EU 2006/C 311 E/02), that requires, in article 6, a risk mapping of social, economic and environmental flood risk (Meyer et al., 2009). GIS-based integrated risk assessment provides, as results, mapping of economic, environmental and social flood risk.

In the following, some of the advantages and disadvantages in using a Multi-Criteria Analysis are reported.

Advantages of MCA consist in:

- allowing the participation of a wider number of stakeholders with respect to CBA;
- allowing the comparison of different potential options;
- allowing a greater range of awareness and involvement across scales, thanks to its flexibility;
- enabling different non-quantifiable objectives to be considered;
- ensuring relative transparency to decisions taken at all levels of the appraisal, easing the visualisation of consequence of giving different importance to different objectives;
- promoting the identification of the best option by consensus of a panel of experts, through democratic voting.

On the contrary, limitations of MCA can be identified in the following points:

- the score can be influenced by the stakeholders’ subjectivity;
- the inclusion or exclusion of criteria can greatly influence the evaluation and then process’ result (Meyer et al., 2009);
- the assessment can be performed with a limited number of judges, potentially increasing the subjectivity of results;
- stakeholder’s participation to the MCA process is legitimised by other decision-makers;
- weighting the criteria involved or multiplying the obtained scores of each option can bring to an overall score that can be seriously misled in a decision-making process.

According to FHRC/RPA (2002) and among the enormous array of possible techniques, MCA methods can be classified in terms of three main characteristics:

- The set of alternatives, differentiating discrete versus continuous problems. Discrete problems involve a finite set of options, such as the selection of possible measures (i.e. storage reservoir, structural defences, channel improvement) inside a flood management strategy, while continuous decisions are characterized by an infinite number of alternatives (i.e. the determination of the design height of a flood protection or the storage capacity of an additional reservoir);

- The measurement scale, separating quantitative and qualitative attributes scales. However, decisions results may involve a mixture of qualitative and quantitative information, with the addition of graphical evaluation as integration of the decision-making processes;
- The valuation function, strictly related to quantitative scores. Indeed, the latter can be measured in different ways and, to make them comparable, they have to be transformed into common dimension or dimensionless units, through the use of linear standardisation function or utility functions.

Table 2-1 lists some of the MCA methods according to the level of information required, the proposed result, the level of transparency and, eventually, the computational and utilisation costs.

Table 2-1 Characteristics of different multi-criteria methods (FHRC/RPA, 2002)

MCA METHOD	REQUIRED INFORMATION	PROPOSED RESULT	LEVEL OF TRANSPARENCY	COMPUTATIONAL EFFORT	UTILISATION COSTS
Weighted summation	Quantitative	Performance scores/ranking	High	Simple	Low
Ideal point method	Quantitative	Distance to target/ranking	Medium	Simple	Low
Evaluation by graphics	Quantitative, Qualitative and Mixed	Visual presentation	High	Simple	Low
Outranking methods	Quantitative	Ranking / incomplete ranking	Low	Very complex	Medium
Analytical hierarchy process (AHP)	Qualitative	Performance scores/ranking	Low	Complex	Medium
Regime method	Quantitative, Qualitative and Mixed	Ranking / probability	Low	Very complex	Low
Perturbation method	Qualitative	Ranking	Low	Very complex	Medium
Evamix method	Mixed	Ranking	Low	Simple	Low

The level of the required information determines which method can be implemented in the analysis. According to the Table 2-1, the weighted summation can provide relative performances of alternatives, in addition to a ranking result used by most of the quantitative methods. Results in terms of final aggregated ranking can over-simplify the whole process, without prioritising decisions and needs. Graphic and visual representations take an intermediate position between weighed performances and final ranking. In regards of transparency, low value means that few stakeholders are involved in the decision-making process. Computational effort is complex in some MCA methods but this issue is overcome thanks to new powerful IT tools and software. Utilisation costs are

generally higher for those methods that require the participation of several experts in decision-making procedures (FHRC/RPA, 2002). Weighted summation technique, dealing with quantitative information, seems to be the most appropriate due to the high level of transparency, simple computational effort and low utilisation costs. In regards to qualitative information, evaluation by graphics looks the best options thanks to the high level of transparency and limited costs. The strength of the AHP method, using only qualitative information, provides results both in ranking and performance scores, but the low level of transparency and the complex computational efforts limit its applications.

In light of what has been said so far, the selected MCA technique to be integrated with a CBA in flood risk management has to be simple to apply, able to deal with quantitative and qualitative data and information, must have a high transparency in the appraisal process and low utilisation costs.

In the following considerations about quantifiable damages (to be included in the CBA) and non-quantifiable damages (to be included in the MCA, as additional important assessment to the CBA) will be reported. These losses can be computed among an ex-ante assessment in order to quantify the potential benefits (in terms of avoided damages) of designed structural and non-structural mitigation measures, or in a post-event assessment to evaluate the total amount of losses. Damage estimation must be precise and concrete and results must be accessible as precious information sources to assess future potential impacts of hazards (IDEA, 2014).

2.5.1 Cost Benefit Analysis (CBA)

As mentioned in chapter 2.4, quantifiable benefits in terms of avoided damages can be compare with the costs of the structural or non-structural measure and evaluated with a Cost Benefit Analysis (CBA). The Cost-Benefit Analysis (CBA) is defined as an “analytical tool in decision-making procedures and provides an overview of economic advantages or disadvantages of a decision” (E.C., 2014). CBA is defined also as a systematic procedure for assessing, ex-ante or post-event, all the potential benefit of a given project or activity with the costs of employed resources in a comparable unit of measure, money. This analysis can be implemented for the evaluation of different intervention options of hazard and damage management, comparing the arisen benefits with the corresponding costs of the strategy, to establish the effectiveness of the involved operation, as the degree to which a measure achieves specific targets. This analysis considers only values expressed in monetary terms (Romijn and Renes, 2013), highlighting its limitation in evaluating of non-market goods.

Costs are defined as the amount of investments needed to develop mitigation measures and regard all the procedure related to a risk assessment and to the realisation of structural or non-structural interventions to mitigate hazard occurrence and severity. Among the construction works amount, other additional costs must be considered, such as maintenance and management of the structure, design support activities, activities related to expropriation procedures and compensation, design charges, work management and safety coordination in the planning phase and execution costs, charges for upgrading existing services, contingency costs and VAT (Value Added Tax) charges, etc.

Benefits are defined as the potential avoided damages to assets quantifiable in monetary terms, such as physical damage to built environment, agricultural sector, physical infrastructure, lifelines and economic activities (mainly related to contents and systems linked to the structure), as well as potential economic growth, less emergency costs and time to recover from disaster impacts. The procedure of damage assessment involves information on land use and exposed assets, the estimation of hazard parameters (water depth, velocity, etc. in case of floods) and the implementation of models or damage curves. Damage to residential buildings regard mainly reconstruction costs of the structures and losses to contents, involving though both vulnerability and exposure parameters. In order to assess these damages, a simplified version of the INSYDE model, developed by Politecnico di Milano, will be presented in details in chapter 2.5. Damages to agricultural sector is related to the loss of production and direct damages to soil and fields. The presentation of AGRIDE-c model, developed by Politecnico di Milano, will be proposed in chapter 2.6, in which all the parameters and agricultural aspects involved into the damage computation will be described.

Literature strongly underline that CBA deals with uncertainties, due to the presence of assumed values adopted in the analysis that potentially increase with the scale of the event (Handmer, 2003). These uncertainties regard the estimation of costs and benefits, discount rates or externalities evaluation (IDEA, 2014), making the outcome of a CBA highly sensitive to the made assumptions (Brouwer and van Ek, 2004).

In order to evaluate the economical effectiveness of a designed or built measure, there are several key metrics of economic efficiency within CBA: the Effective measure (E), the Cost-Effectiveness (CE), the Economic Rate of Return (ERR), the Net Present Value (NPV), the Present Value Ratio (PVR), the Internal Rate of Return (IRR) and the Benefit Cost ratio (B/C). The latter seems to be the most intuitive criterion due to its relative metric (benefits per costs), for assessing the effectiveness of a designed or built measure. B/C is frequently used in context of DRR and to communicate with decision makers (Shreve and Kelman, 2014). US Federal Emergency Management Agency (FEMA), among an investments' review of 4000 mitigation programs in the US, has found an average B/C ratio of 4, underling the goodness of the mitigation measures (Shreve et Kelman, 2014).

B/C is defined as the ratio between the arisen benefits from a project or a proposal and the overall costs employed for its realisation. The B/C is described by the following formula:

$$B/C \text{ ratio} = \frac{\sum_{t=1}^T \frac{B_t}{(1+r)^t}}{\frac{C}{(1+r)^{T_s}}}$$

Where:

- B_t are the arisen benefits, in terms of avoided expected damage, for an event with return period t ;
- C are the cost of the designed or realised mitigation measure;
- r is the discount rate;
- T_s is the year of the realisation of the structure.

The procedure for the computation of the B/C, in order to evaluate the effectiveness of flood structural mitigation measures, is described in the following:

- 1) the costs of the flood mitigation measure are assessed;
- 2) The total cost is contextualised at the moment of the analysis and evaluated over the lifetime of the flood mitigation measure, considering also potential different future costs through the discount rate;
- 3) Quantifiable damages without the construction of the flood mitigation measure are computed for different return period events T;
- 4) A plot containing the exceedance probability ($1/T$) on the x axis and the quantifiable damages without mitigation measure on the y axis is created, as represented in Figure 2-10;

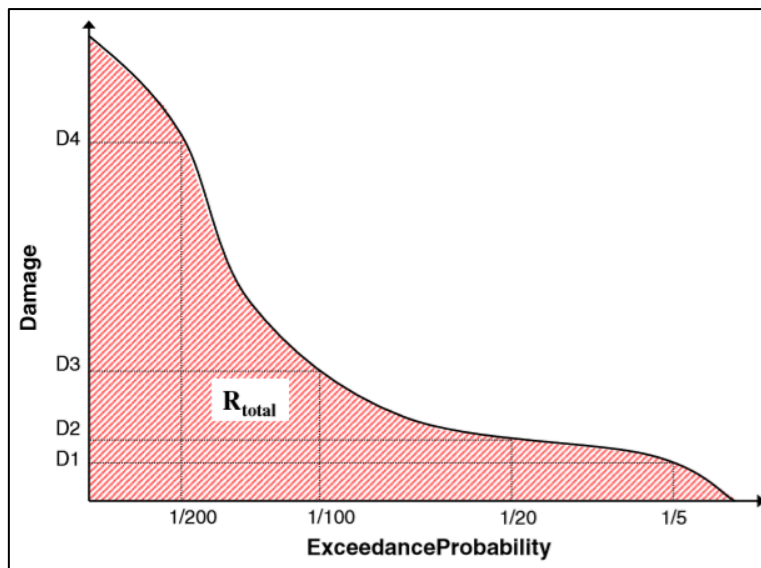


Figure 2-10 Representation of the annual yearly damages considering event with return period equal to 5, 20, 100 and 200 years (Meyer et al., 2009)

- 5) The risk (or the annual average damage) is shown by the area or the integral under the obtained curve. However, being known only few points of the curve, the exact computation is not possible and assumptions must be done (Meyer et al., 2009).
- 6) Points 3, 4 and 5 are repeated for the scenarios with the addition of the flood mitigation measures;
- 7) The area between the obtained curves represent the yearly benefits (B) arisen from the flood mitigation measure;
- 8) B/C ratio is obtained dividing the estimated yearly benefits with the computed annual costs of the flood mitigation measure.

If $B/C > 1$ means that the benefits generated by the flood protection measure exceed the cost and therefore the structure represents a good investment for the society. The higher the benefit-cost ratio, the better the investment.

2.5.2 Non-quantifiable damage assessment

Flood disasters affect a large number of urban settlements in the world, with severe potential adverse consequences for human health, the environment, cultural heritage, social and economic activities (Molinari et al., 2014). According to literature, there is less evidence of damage assessments to economic sectors and territorial resources, such as natural environment, cultural heritage and social models, with respect to the built environment (IDEA, 2014). This is due to the incidence of indirect and systemic damages (Cochrane 2003 and 2004), which most of the times is neglected or underestimated (Shreve and Kelman, 2014). Sometimes, the exclusion of such non-quantifiable potential damages could bring to results of CBA in which benefits do not exceed the costs for the realisation of the measure. It has to be remarked also that assessing environmental impact, as well as social and economic damages, requires a complex analysis at different spatial and temporal scales to qualify and quantify potential damages, involving the participation of experts in such fields (Molinari et al., 2014).

Since the end of the past century, attention on economic aspects related to natural disaster has increased, leading to a greater contribution of economists in multidisciplinary risk assessment (IDEA, 2014). Direct losses to economic activities regard damages to structures and their contents, expressed in monetary unit, if possible, and regard replacement of the lost material, such as machinery, inventories, raw materials and stored objects. The latter can trigger indirect and systemic damages in a “loss chain” effect, which quantitative assessment require complex and long-time procedures by means of meso-scale approaches. Such damages are business interruption (it can be caused also by failure of important lifelines, which require a complete vulnerability, exposure and damage assessment), bankruptcies, rebuilding investments, loss of customers, loss of competitive power and reduction of market shares, sometimes so high to pull economic subjects to stop their activities (IDEA, 2014). Assessing the macroeconomic impact requires an estimation of aggregate economic variables like the gross domestic product (GDP). Indirect and systemic damages to economic sectors may be huge and the time needed for restoration or reconstruction might considerably weight in terms of capability of the whole territorial system to bounce back to the “everyday life” (IDEA, 2014).

Some examples of environmental negative externalities are pollution, soil contamination, ecosystem service degradation, landscape deterioration and effects on biodiversity and natural habitats. According to literature, environmental cost and benefits can be assessed considering the Total Economic Value (TEV), as the sum of use values and non-use values. Use values regards benefits gained from actual use and consumption of the environment, as well as secure the potential use of resources in future. Use values include private sector uses (agriculture, industry, etc...), education and scientific benefits, recreational and general amenity benefits. Non-use values or passive values are generally related to the individual’s willingness to secure the environment so that future generation may use the asset (RPA, 2004). Brouwer and van Ek (2004) evaluated the ecological effects of mitigation measures in terms of changes in the vegetation, in the relative wealth of species of different “ecotopes”, as spatial units, homogeneous from an ecological point of view. Meyer et al. (2009) evaluate the impact on the environment assigning scores to criteria of

erosion potential, accumulation of pollutants, destruction of biotopes. However, most of the times, environmental and social costs (and benefits) fall outside the marketplace, leading to an impossibility of a CBA to take into consideration these assets and requiring the implementation of MCA approaches.

Social impact evaluation can be based on qualitative judgment, assigning qualitative scores for the most important social criteria identified by experts (Brouwer and van Ek, 2004). Meyer et al. (2009) evaluate the social impact of flood in terms of affected population and probability of hot spots to be damaged, such as hospitals, schools, old people's and children's homes. Direct social effects are loss of life and people injured, while indirect effects regard unemployment, population distress, increased of health conditions, team demotivation, lower social cohesion, decreasing public safety and community destruction (IDEA, 2014). Human life is usually not evaluated in monetary terms, due to its complexity (each person should be assessed singularly) and, most important, for ethical issues. However, if it would be quantified, the B/C ratio will definitely report much higher results. In the Kunreuther and Michel-Kerjan study, the potential benefit of structural retrofitting of schools in seismic areas does not exceed the costs until the value of human life is added or, at least, considered (Shreve and Kelman, 2014). Therefore, the inclusion of the exposed population in a MCA, without assigning monetary values to human life, would increase the goodness and effectiveness of the mitigation measure and would guarantee a more comprehensive and complete flood impact assessment. The assessment of the population at risk is normally done overlaying potential hazard maps with exposed population in that specific area; however, a larger community may be affected, according to the severity of the event and the systemic importance of the damage assets (Molinari et al., 2014). Particular attention should be paid also to potential damages to non-renewable, non-repeatable resources and non-refundable important memorabilia like cultural heritage and historical places which can be damaged or lost in case of severe floods, like the one in Florence in 1966 (IDEA, 2014). Even though such externalities are easy to be identified, their assessment and inclusion in decision-making processes can be difficult due to absence of market values (EC, 2014).

2.6 Simplified INSYDE model

According to Molinari et al. 2016, nowadays, in Italy, involved public agencies and authorities use qualitative approach to evaluate flood damage, preventing the assessment of expected potential damage in monetary terms. The latter should be included into CBA or MCA to assess the effectiveness of mitigation measures, as required by the European Flood Directive 2007/60/EC.

Direct and tangible quantifiable damages are estimated with standard damage curves or functions (FLOODsite, 2007), combining hazard maps with element exposed at risk. In Italy, the aforementioned tools are not frequently used, due to not consolidated approaches, the scarcity of available damage data for calibrating and validating the model and because foreign damage models are strongly context related, which could be different from the Italian territory (Merz et al., 2010, Molinari et al., 2012, Scorzini and Frank, 2015). Empirical damage models are strongly dependent on the collected data (Wagenaar et al., 2013), while synthetic damage models result to be more complex because more parameters and variables (Schrotel et al., 2014) are involved in the computation of damages. The optimal solution would be a model that is simple, as the empirical ones, but that include quantitative and qualitative explicative parameters in damage assessment, as the synthetic ones. A relevant obstacle in developing such models is represented by the absence of appropriate data able to guarantee a complete damage assessment of flood impacts (Ballio et al., 2015).

The chosen method, in order to calculate the damage to residential buildings, represents a simplified version of the INSYDE (IN-depth SYNthetic Model for Flood Damage Estimation) model, which complete description is reported in Dottori et al., 2016. The latter is a synthetic micro-scale multi-variable model based on a component-by-component analysis of the physical damage (Scorzini et al., 2018), that allows to reproduce damage mechanisms to residential buildings for different flood scenario. Indeed, it simulates damages caused by floods with different values of water level, velocity and duration, and the related damage considering different vulnerability levels. Moreover, INSYDE has been validated on Italian flood events and it consider the Italian price list for computing damages.

The proposed model considers several explicative variables, both related to the hazard and to the vulnerability of the affected buildings. The overall damage D is obtained summing up all the mathematical function describing the damage mechanisms C_i , as follow: $D = \sum_{i=1}^n C_i$. In the following, the procedure of the aforementioned method is described, focusing on each damage component involved in the computation of the damage D .

The total absolute damage D [€] is obtained using the following formula:

$$D = d * RV * A$$

where:

- d is the relative damage, considered as the ratio between the damage and the replacement cost of the exposed element;

- RV [€/m²] is the replacement value, obtained as function of different parameters, such as building typologies, structures and finishing levels (*Cineas – Cresme – Ania, 2014*);
- A is the footprint area of the building, considered as the sum of the areas of the storeys exposed to the flood in a building, included the basement storey (it is assumed that the basement and the upper floors have the same replacement values but not the same damage mechanism);

An important step in the damage assessment is the definition of the exposed elements. The latter are composed by the storey directly affected by the flood and not the entire buildings to which they belong. The overall damage to buildings is determined by summing the damages of the storeys affected by the flood. Moreover, the total absolute damage D is divided in four damage components obtained through four different functions. Indeed, the aforementioned formula can be expressed as:

$$D = d_{basem} * RV * A_{basem} + \sum d_{storey-i} * n * RV * A + d_{pavem} * RV * A + d_{boiler} * RV * A$$

where:

- d_{basem} is the damage to basement that is assumed totally inundated in case of flood and therefore it doesn't depend on the water level;
- n is the number of flooded storeys;
- d_{storey} is the damage to the storey that represent the greater component of the damage and it depends on the water level;
- d_{pavem} is the damage to pavements that is considered as a constant value if the water level is greater than zero;
- d_{boiler} is the damage to boiler that depends on the water level if the basement is present only, otherwise it is considered located in the basement and therefore entirely inundated.

In the following, for each of the previously listed damage components, the used formulae and the parameters, involved into the computation of damage to residential buildings will be reported.

A crucial step for the damage assessment is the identification of the variables which the damage depends on, or define criteria in order to determine which variable can be neglected from the damage computation. These criteria have been used to reduce the number of involved parameters of the INSYDE model and regard:

- Variables that, due to the small variability in the analysed context, is assumed as constant;
- Variables not available in open database and which determination is complex;
- Variables that can be assumed as function of others;
- Variables whose variation, in a local sensitivity analysis, don't imply significantly changes in the final damage.

Among the six event parameters and the eighteen building characteristics features considered by INSYDE model, the following reported in the Table 2-2 have been selected in the simplified version:

Table 2-2 Event parameters and building characteristic features considered in the simplified version of INSYDE

Variable	Description	Unit of measurement	Range of values	Default values
h	Water depth outside the building	m	≥ 0	Incremental step: 0,01 m
du	Duration of the water inside the building	hours	> 0	24
q	Presence of pollutants in the water	-	0: No 1: Yes	1
FA	Footprint area	m ²	> 0	100
BA	Basement area	m ²	> 0	% FA
NF	Number of floors	-	≥ 1	2
BT	Building type	-	1: detached house 2: semi-detached house 3: Apartment house	1
BS	Building structure	-	1: reinforced concrete 2: masonry	2
FL	Finishing level	-	0,8: low 1: medium 1,2: high	1,2
LM	Level of maintenance	-	0,9: low 1: medium 1,1: high	1,1

The basement damage depends on the basement area BA , the level of maintenance LM of the building and the duration of the water inside the construction du , and it is obtained with the following formula:

$$d_{basem} = f(BA) * f(LM, du)$$

where:

$$f(BA) = (0.02 + \frac{0.35}{\sqrt{BA}})$$

$$f(LM, du) = \begin{cases} (1 + 0.09 * (\arctan(du - 36))), & \text{if } LM \text{ is low} \\ (0.7 + 0.3 * (\arctan(du - 36))), & \text{if } LM \text{ is high} \end{cases}$$

The storey damage depends on water level h , footprint area FA , duration of the water inside the building du , level of maintenance LM , building structure BS , finishing level FL , presence of pollutants q and it can be computed using the following formula:

$$d_{storey} = f(h) * f(FA) * f(LM, du) * f(BS) * f(FL) * f(q)$$

where:

$$f(h) = (0.17 * h - 0.02 * h^2)$$

$$f(FA) = (0.2 + \frac{7}{\sqrt{FA}})$$

$$f(LM, du) = \begin{cases} (1 + 0.15 * (\arctan(du - 36))), & \text{if LM is low} \\ (0.8 + 0.2 * (\arctan(du - 36))), & \text{if LM is high} \end{cases}$$

$$f(BS) = \begin{cases} 1.35, & \text{if BS is masonry} \\ 1, & \text{else} \end{cases}$$

$$f(FL) = \begin{cases} 1.5, & \text{if FL is high} \\ 1, & \text{else} \end{cases}$$

$$f(q) = \begin{cases} 1.2, & \text{if presence of pollutants} \\ 1, & \text{else} \end{cases}$$

The pavement damage depends on the finishing level *FL* only. In particular, the pavement is assumed to be damaged if made of wood only, therefore for high finishing level and it is calculated as:

$$d_{pavement} = f(h, FL) = \begin{cases} 0.04, & \text{if } h > 0 \text{ and } FL \text{ is high} \\ 0, & \text{else} \end{cases}$$

The damage to the boiler depends on the presence of the basement and on the water level. Indeed, it is assumed that the boiler is located in the lower level, if present, otherwise the boiler is supposed to be placed at more than 1.60 m from the pavement level (*Dottori et al., 2016*). Therefore, this component of the total damage can be computed using the following formula:

$$d_{boiler} = f(h, BA) = \begin{cases} 0.015, & \text{if } BA \neq 0 \text{ or } BA = 0 \text{ and } h > 1.6 \text{ m} \\ 0, & \text{else} \end{cases}$$

For what concerns the replacement value *RV* [€/m²] of residential buildings, involved in the calculation of the total absolute damage, the values (*Cineas – Cresme – Ania, 2018*) reported in Table 2-3 has been taken as reference:

Table 2-3 Replacement values for residential building (Cineas – Cresme – Ania, 2018)

Replacement Value [€/m ²]		Building type		
		Detached house	Semi-detached house	Apartment
Building structure	r.c.	1580	1432	1288
	Masonry	1131	1027	1288

2.7 AGRIDE-c model

According to literature, the hazard parameters usually included in damage modelling are water depth, flow velocity, flood duration, sediment and contaminant load. For crops, an important role is played also by the period of the year (generally the month) of the flood event, making the damage strongly dependent on crop calendars (USACE, 1985; Morris and Hess, 1988; Hussain, 1996; RAM, 2000; Citeau, 2003; Dutta et al., 2003; Förster et al., 2008; Agenais et al., 2013; Shrestha et al., 2013; Vozinaki et al., 2015; Klaus et al., 2016). Indeed, the vegetative stage of any crop type, at the occurrence of the flood, is the only vulnerability parameter that strongly affects the damage suffered by the plant. Moreover, the behaviour of the involved farmers, like abandoning the production or to continue at increasing costs, is usually not considered in damage assessments to agricultural sector, despite the clear and strong influence of the latter in the final damage sustained by the farm (Pangapanga et al., 2012; Morris and Brewin, 2014). Expected damage can be expressed as percentage of the gross profit (USACE, 1985; RAM, 2000; Agenais et al., 2013; Shrestha et al., 2013) or of the turnover of the farmer (Citeau, 2003; Dutta et al., 2003; Forster et al., 2008; Vozinaki et al., 2015; Klaus et al., 2016).

The conceptual model AGRIDE-c (AGRIculture DamagE model for Crops) has been developed by adopting an expert-based approach, encapsulating the available knowledge on damage mechanisms triggered by floods, as well as on their implications in terms of income for the farmers, and including opinions of experts like agronomists and economists (Molinari et al., 2019). The structure of AGRIDE-c model is valid in different geographical areas, but the computation of damages requires the definition of the hazard parameters and an exposure assessment of the crops effectively involved at the occurrence of the flood, making the damage model strongly context related. Indeed, damage to crops depends on several local features, related to vulnerability and hazard assessment, that cannot be generalised. The assessment of flood damage to agricultural sector has been performed here using AGRIDE-c and its analytical implementation in the Po valley.

Absolute damage (D) is a function of the time of occurrence of the flood, water depth, flood duration and alleviation strategies, and it is expressed as the difference between the reduction in the turnover (ΔT) and the decrease in production costs (ΔPC) in case of flood. This is equal to consider absolute damage as the change in the gross profit ($GP = T - PC$, where T = turnover and PC = production costs) due to the flood, compared to the case when no flood occurs (Scenario 0):

$$D = GP_{\text{noflood}} - GP_{\text{flood}} = (T_{\text{noflood}} - T_{\text{flood}}) - (PC_{\text{noflood}} - PC_{\text{flood}}) = \Delta T - \Delta PC$$

It has to be remarked that absolute damage always includes costs related to soil restoration, which is required every time a flood occurs.

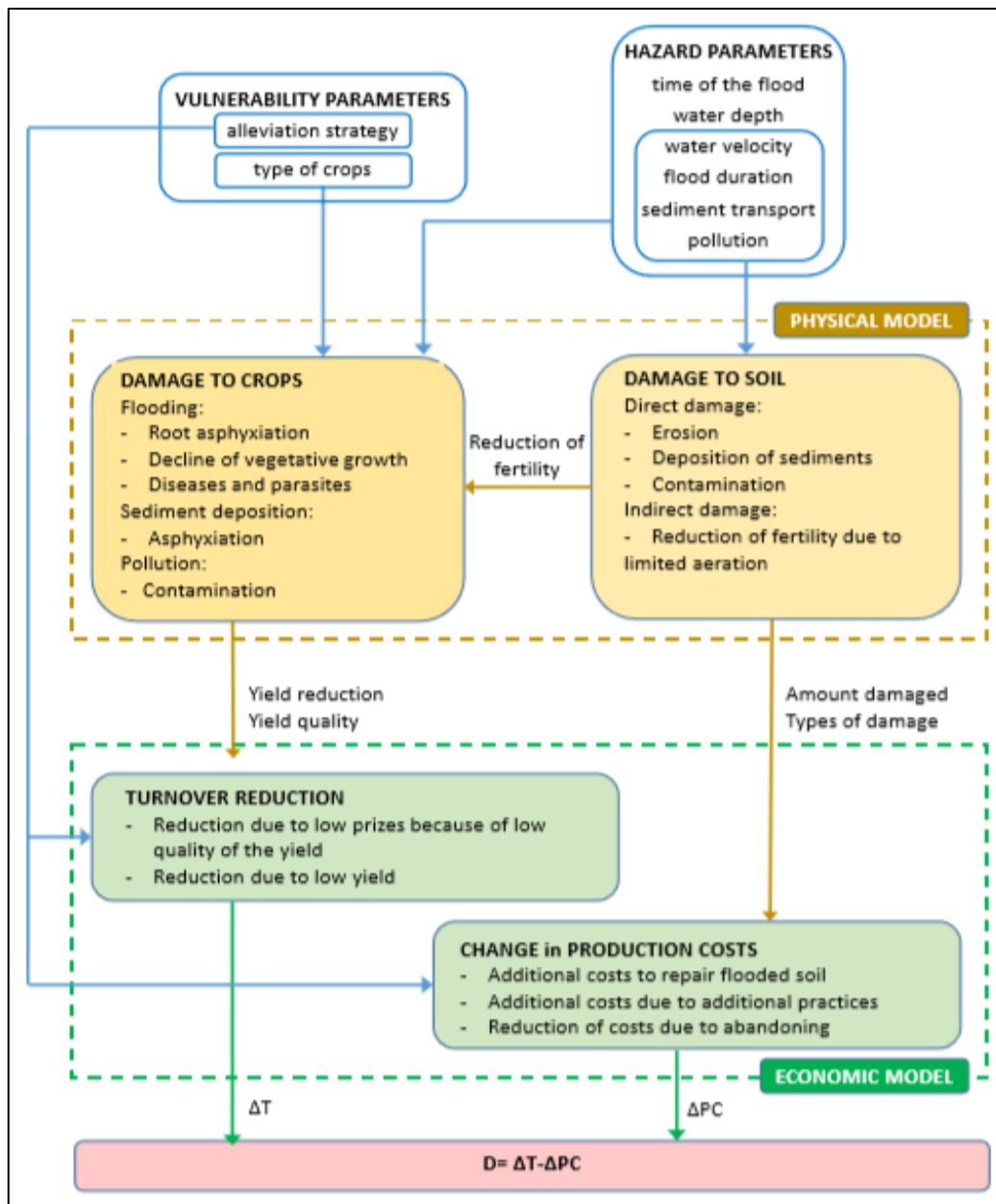


Figure 2-11 Scheme of the conceptual model AGRIDE-c

A physical and an economic model are included in AGRIDE-c in order to evaluate the absolute damage D, as shown in Figure 2-1. The first one provides information on the physical damage, while the second one converts the physical losses due to the flood into monetary terms. The physical model is then composed by two sub-models, for the evaluation of damages to crops and soil, respectively. The economic model of AGRIDE-c is also divided into two sub-models: one for evaluating the reduction in the turnover and the other one for assessing the decreasing in production costs compared to the scenario 0.

Physical damage to crops depends both on the direct contact of the flooding water with the plants and on damages to other components of the farm, such as damage to soil, to machineries and equipment. AGRIDE-c considers only the damage to soil because it is demonstrated that plants and soil are damaged at the same time during the flood occurrence while other components can be affected independently on the damage to plants. Damages to crops are evaluated in terms of

reduction in the amount and quality of the harvest, considering hazard features (water depth and permanence of the flood) and type of affected crops, because cultures resist flood impacts differently according to their physical condition and vegetative stage at the occurrence of the flood (Rao and Li, 2003; Setter and Waters, 2003; Zaidi et al., 2004; Araki et al., 2012; Ren et al., 2016). The assessment of physical damage to soil considers the kind of damage suffered (i.e. erosion, contamination) and the consequent reduction in fertility (influencing the quality and the quantity of the harvest), as function of the flood hazard parameters.

For what concerns the economic model of AGRIDE-c, the first sub-model calculates the ΔT as the reduction in the turnover due to the yield reduction and to the decreasing price of the of the harvest caused by the lower quality of the latter. The second sub-model evaluated ΔPC as the costs to restore the flooded soil and additional costs for adopted strategies by the farmers. These can be the continuation of the flooded crops when damages are relatively low, reseeding a new late crop depending on the period of flood occurrence, and abandon the production when the yield loss is severe.

The implementation of the model in the Po Plain requires first the identification of the typical parameters of floods occurring in the analysed area and the main crops cultivated in the region to be considered. Secondly, after the characterisation of the scenario 0, an analytical expression of the process described in Figure 2-1 is derived and then flood damages to crops are evaluated for different flood severities, time of occurrence and damage alleviation strategies adopted by farmers.

As regard the hazard, riverine long-lasting floods (like the November 2002 event in Lodi) are characterised by medium to high water depths, low flow velocities and low sediment transport. Therefore, in the application of AGRIDE-c model to the case of Lodi, water depth, flood duration and time of flood occurrence have been considered only. For what concerns the main cultivation in the analysed area, according to cadastral data supplied by the Regional Authority, the most common crops are grain maize, wheat, barley, grassland and soy.

Scenario 0 is characterised as the annual gross profit per hectare for the farmer, in case of no flood, implying the estimation of the annual turnover and the distribution of production costs over the year. Moreover, the annual EU contributions for agriculture as a further income for the farmer has been taken into account. The production and management costs and the prices of the different cultivation practices cannot be generalised and have been identified involving experts and consulting regional price books. According to the aforementioned data, the analysis for the scenario 0 in Lodi results in a gross profit for the farmer equal to 1376 €/ha per year.

Physical damage to crops has been estimated adopting the model developed in France by Agenais et al. (2013). This choice is supported by the fact that the independent flood variables considered in the model are coherent with the flooding characteristics of the Po Plain. Moreover, the model is independent on the crop calendars as they use vegetative stages of the plant as time variable for the flood occurrence. An example of the implemented physical damage model for maize is reported in Figure 2-12. This model consists of functions giving the yield reduction cause by a flood, as percentage of the scenario 0, considering water depth and flood duration, for the seeding, growing, flowering and maturation vegetative stages.

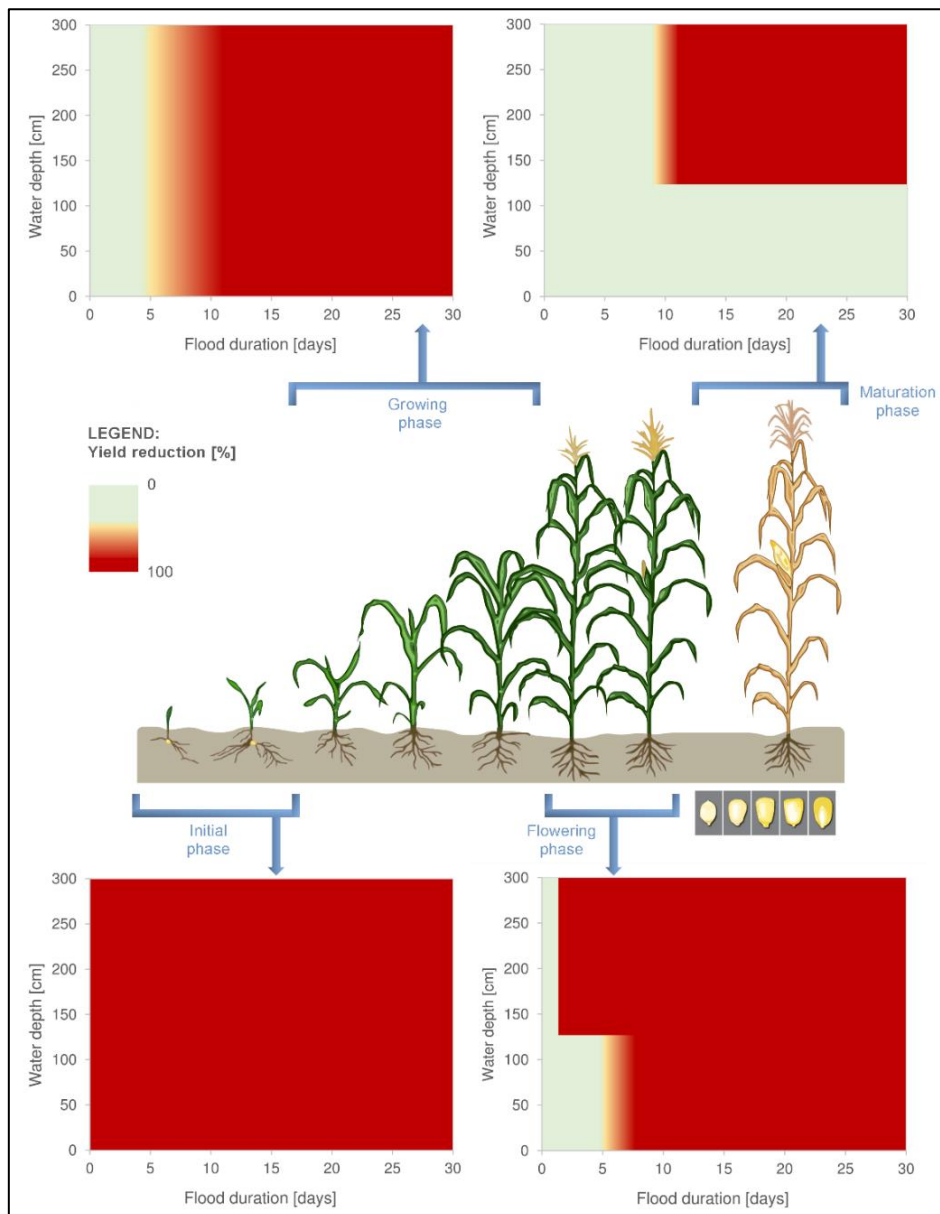


Figure 2-12 Physical damage to maize as a function of vegetative stage, flood depth and duration (adapted from Agenais et al., 2013)

For what concerns the damage to soil, according to the characteristics of floods in plains, the model is based on the assumption that soil requires restoration in case of inundation, consisting in removing of sediment and levelling of the terrain, while no reduction in fertility occurs. The estimated restoration costs have been assumed to be around 500 €/ha.

As regard the alleviation strategies, the model assumes that reseeding does not implies a yield reduction in terms of quality and quantity of the harvest. In terms of production costs, reseeding implies other additional costs such as preparation of the soil, the acquisition of new seed and the seeding process.

An example of the damage functions for maize crops implemented in AGRIDE-c is shown in Figure 2-13. All the damage functions for the aforementioned types of crops are proposed in the Appendix.

Water depth	Strategy	Flood duration [days]										
		<5	5	6	7	8	9	10	11	>11		
Bare field	Jan	c	60%									
		r	-									
		a	-									
	Feb	c	60%									
		r	-									
		a	-									
	Mar	c	60%									
		r	-									
		a	-									
Initial phase	Apr	c	-									
		r	129%									
		a	261%									
	May	c	-									
		r	129%									
		a	261%									
Growing	Jun	c	60%	104%	149%	193%	237%	282%	326%	371%	-	
		r	129%									
		a	308%									
Flowering	Jul	c	60%	149%	237%	326%	-					
		r	-									
		a	314%									
	Aug	c	60%	149%	237%	326%	-					
		r	-									
		a	314%									
Maturation	Sep	c	60%									
		r	-									
		a	-									
	Oct	c	60%									
		r	-									
		a	-									
Bare field	Nov	c	60%									
		r	-									
		a	-									
	Dec	c	60%									
		r	-									
		a	-									

Water depth	Strategy	Flood duration [days]										
		<5	5	6	7	8	9	10	11	>11		
Bare field	Jan	c	60%									
		r	-									
		a	-									
	Feb	c	60%									
		r	-									
		a	-									
	Mar	c	60%									
		r	-									
		a	-									
Initial phase	Apr	c	-									
		r	129%									
		a	261%									
	May	c	-									
		r	129%									
		a	261%									
Growing	Jun	c	60%	104%	149%	193%	237%	282%	326%	371%	-	
		r	129%									
		a	308%									
Flowering	Jul	c	60%	149%	237%	326%	-					
		r	-									
		a	314%									
	Aug	c	60%	149%	237%	326%	-					
		r	-									
		a	314%	314%	314%	314%	314%	314%	314%	314%	314%	
Maturation	Sep	c	60%									
		r	-									
		a	-									
	Oct	c	60%									
		r	-									
		a	-									
Bare field	Nov	c	60%									
		r	-									
		a	-									
	Dec	c	60%									
		r	-									
		a	-									

Figure 2-13 Relative damage to maize crops (in case of conventional tillage) for the different combinations of times of occurrence of the flood (i.e. month), flood intensities (i.e. water depth and flood duration) and damage alleviation strategies ("c"=continuation; "r"=reseeding; "a"=abandoning)

2.8 Sensitivity analysis: climate change impact on flood occurrence and levee effect

Climate change and urban development are primary contributor for the increase of flood damage (Poelmans et al., 2011), therefore, a change in the month of occurrence of the flood and a case of levee effect have been considered within the sensitivity analysis of the results.

According to Beckers et al. (2013) and EEA (2010), climate change will increase the occurrence of floods in many European cities, both in terms of peak discharge intensity and frequency, that combined with land use evolution, will represent a key factor for the future flood risk. Extreme flood frequency is result of an increasing of CO2 concentration in the atmosphere (Milly et al., 2002) and scenarios reported in the IPCC (IPCC 2007) confirm this aspect as consequence of the always greater green-house gases and aerosol concentration (Ballesteros-Cànovas et al., 2013).

Ten of the warmest years since 1800 in Italy are after 1990 and, among these ten, six occurred after the year 2000, demonstrating the upward trend in global temperature. Evidences of climate change are in meteorology, climatology modelling and atmospheric physics, influencing different processes, such as the hydrological cycle and desertification, impacting natural systems like agriculture, forests, mountain, marine system, and affecting population's health, urban planning, transport, energy and economic system (Science on the net, 2013).

Scenarios with climate change have been rarely evaluated into CBA or MCA sensitivity analysis (Shreve and Kelman, 2014). These scenarios would provide a projections of future damage costs (Mechler and Kull) and will help to predict a more comprehensive portrait of the expected future risk (Shreve and Kelman, 2014). However, variability in the accuracy and precision of available climate change data, difficulties in predicting hazard occurrence, challenges in incorporating future social behaviour and policies, as well as uncertainties related to future urban development demand (Mustafa et al., 2018), increase the uncertainty of future climate change impact (Shreve and Kelman, 2014).

The transformation from natural to urban artificial surfaces causes an increase in flooding frequency because of poor infiltration (Huong and Pathirana, 2013). Inadequate land-use policies, related to a major human activity on flood plains, could increase flood risk as result of greater exposure and vulnerability (Ballesteros-Cànovas et al., 2013). Flood damages are increasing because of the growth, in number and values, of territorial assets and exposed activities such as buildings, infrastructures and other physical elements. Avoiding new urban and infrastructures developments in flood-prone zones would enable a strong reduction of expected increases exposure (Mustafa et al., 2018). According to Collenteur et al. (2015), “Many studies have shown that the urbanization of flood-prone areas continues, and puts more and more people, and property, at the risk of flooding, for instance in Africa (Di Baldassarre et al. 2010), the Netherlands (De Moel et al. 2011), USA (Montz and Gruntfest 1986), Bangladesh (Rasid and Paul 1987), UK (Parker 1995) as well as globally (Jongman et al. 2012)”.

In case of realisation of structural mitigation measures, people might gain a false sense of security leading to urban developments of areas “protected” by the flood defences, without taking any further disaster risk reduction measures (Shreve and Kelman, 2014). Indeed, the presence of flood protection, such as soil embankments and walls, might increase the exposition in flood prone area, inducing greater potential damages in case of defense failure. This false sense of safety that brings to development of the areas protected by levees is also called ‘the levee effect’ (Di Baldassarre et al. 2009; Lane and Landstrom 2011). This phenomenon, together with low resilience of population, in terms of bad memories of past severe events and conviction of being safe, might happen after the implementation of mitigation measure. Despite the known “levee effect” and knowing that approximately 33% of flood losses in the United States are due to levee failure or overtopping (Committee on Risk-Based Analysis for Flood Damage Reduction 2000), levees are sometimes used to encourage development (Hutton et al., 2018). The decay rate of the memory increase as structural measures are implemented to ‘eliminate’ the flood risk. Hipple et al. 2005 showed significant post-flood development the areas protected by structural defences around St. Louis (Collenteur et al., 2015). According to Newell and Wasson (2002), most damage and death will occur during severe floods for which the population is unprepared, despite the presence of structural mitigation measure. The city of Olivehurst has experienced high population growth despite a history of flooding, partly due to failure of structural mitigation measures, being a clear example of increased development stemming from a false sense of security associated with mitigation projects (Hutton et al., 2018).

3 Case study

3.1 Flood modelling

In this chapter, first the available data used for the flood modelling will be presented, followed by the modification performed on the geometry in order to reproduce the condition before the bank construction and a condition with the new structures in place. Then, results of the unsteady modelling will be shown, before reporting the procedure of calibration of the model.

3.1.1 Available data for flood modelling

This work has started with the collection of data taken by the advisor of the project and the writer, coming from reports of previous studies and researches, national and local organisations and literature review. In the following, the available data used for the flood modelling are described in details and regard:

Table 3-1 Available data for flood modelling

AVAILABLE DATA	SOURCE	DATE	UTILIZATION
Flooded area on the November 2002 event	<i>Studio idrologico-idraulico del tratto di F. Adda (Rossetti & Cella)</i>	March 2005 – updated on January 2010	Model calibration
Observed water surface elevations in control points post flood event	<i>Damage compensation forms and from reconstruction of post-event photos</i>	2002-2003	Model calibration
Hydrometer levels and hydrograph of the November 2002 flood	<i>Studio di fattibilità della sistemazione idraulica (Po river basin authority (AdbPo))</i>	2003	Model calibration
River Adda's cross sections	<i>Studio di fattibilità della sistemazione idraulica (Po river basin authority (AdbPo))</i>	2004	Modification of the terrain morphology
DSM, BC and IC files, computational domain file, orthophoto	<i>Università degli Studi di Parma (UNIPR)</i>	March 2018	Hydraulic model and model calibration
Altimetric survey on the structural defences	<i>Politecnico di Milano</i>	January 2019	Modification of geometry for the creation of the five hazard maps with structural defences
Past reports	- <i>Delimitazione delle aree inondabili ad assegnati tempi di ritorno (Natale);</i> - <i>Flood Hazard Modelling for the City of Lodi (Agosti & Crippa);</i>	2003 2018	Additional information and comparison of the obtained results

3.1.1.1 Flooded area of the November 2002 event

The estimated extension of the flooded area (Rossetti & Cella, 2010) has been used as reference and compared with the obtained flooded areas of simulations being part of the model calibration.

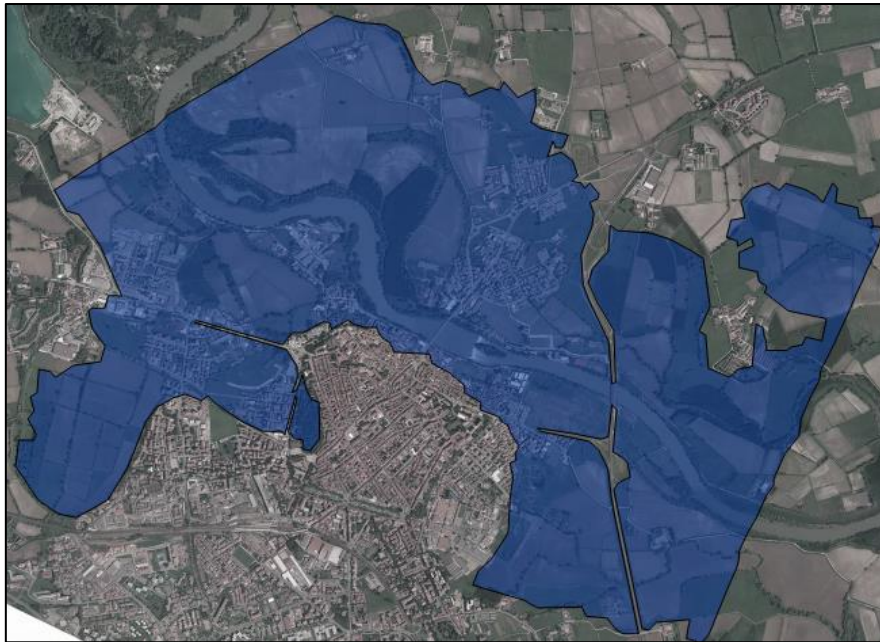


Figure 3-1 Extension of the estimated flooded area in Lodi

3.1.1.2 Observed water surface elevations in control points post flood event

Several measurements of water elevation have been obtained in control points (red dots) after the occurrence of the flood in Lodi. These heights have been obtained from information on water depth available from a total of 121 georeferenced points, described in the damage compensation forms compiled by citizens, and from reconstruction of photos taken mainly post-event. These observed water levels will be used to calibrate the hydraulic model.



Figure 3-2 Representation of control points in Lodi

3.1.1.3 Hydrometer levels and hydrograph of the November 2002 flood event

Hydrometer levels of the November 2002 flood event (Natale, 2003) has been obtained from measurements of the station located in the second arch from the hydraulic right of the Napoleone Bonaparte bridge and reported in the Figure 3-3.

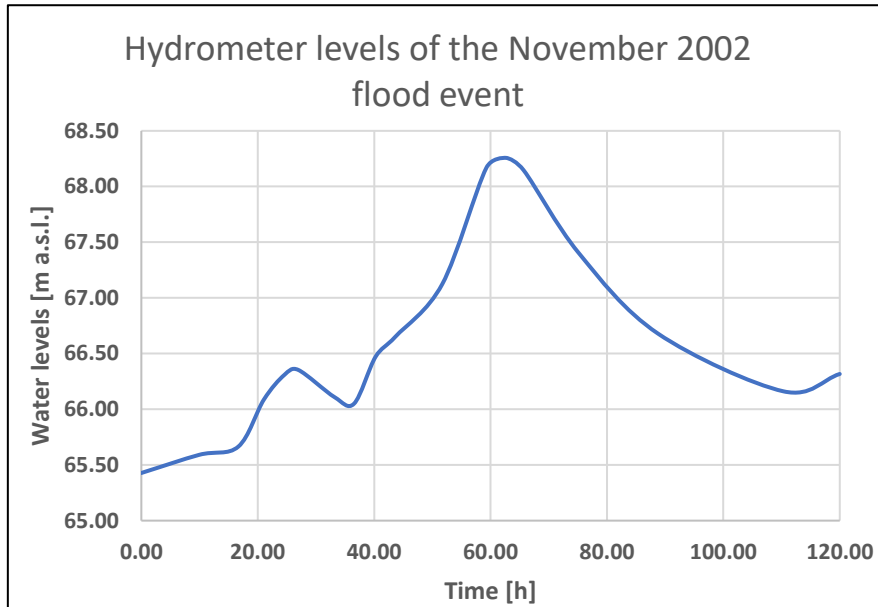


Figure 3-3 Hydrometer levels of the November 2002 flood event (Natale, 2003)

In regards of the estimated hydrograph, representing the November 2002 event, it has been taken from a former study (Natale, 2003). The discharge curve, reported in Figure 3-4, has a duration of 120 hours and a peak flow equal to approximately 1837 m³/s.

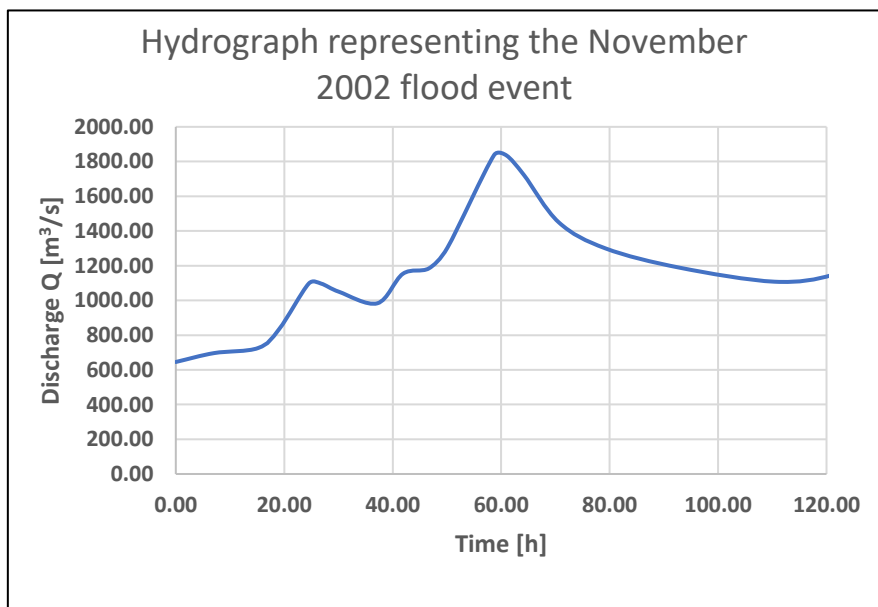


Figure 3-4 Discharge hydrograph of the November 2002 flood event (Natale, 2003)

3.1.1.4 River Adda's cross-sections

A total number of 313 river Adda's cross-sections have been provided by the river Po basin authority (AdbPo) but only 4 have been used in order to reproduce the geometry in the hydraulic model. The latter have been used to modify the geometry used in the flood model, in order to reproduce the bathymetry conditions of November 2002.

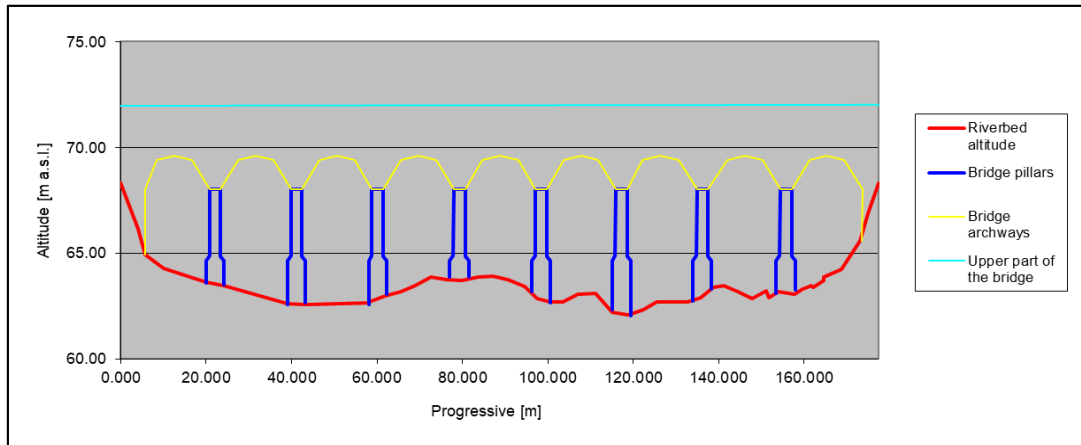


Figure 3-5 Cross section of the river in correspondence of the Napoleone Bonaparte bridge

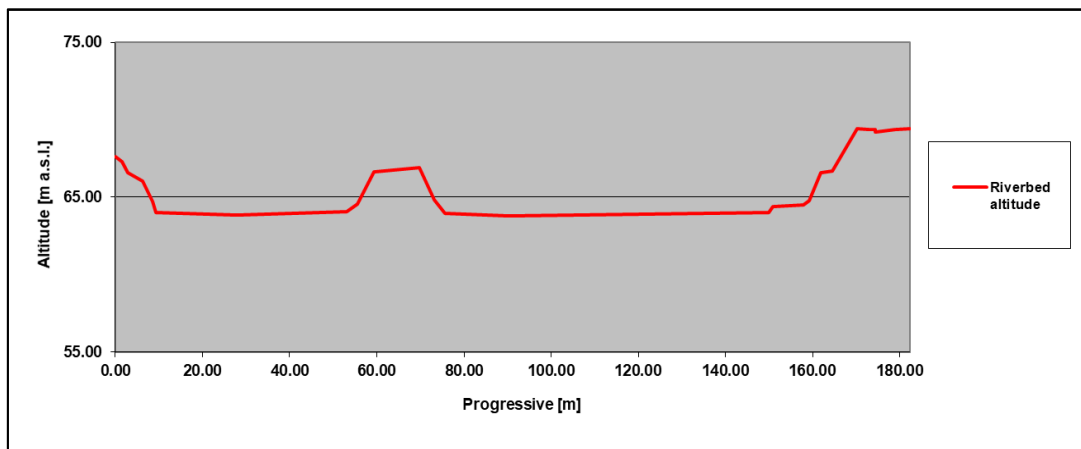


Figure 3-6 Cross section of the river at the tip of Achilli islet in Lodi

3.1.1.5 DSM, BC and IC files, computational domain file, multi-resolution file and orthophoto

The default input files provided by the Università degli Studi di Parma, have been modified and used during the model calibration and the creation of the hazard maps. These files regard:

- digital surface model (DSM) with 1 m resolution, containing a portion of the municipality of Lodi;

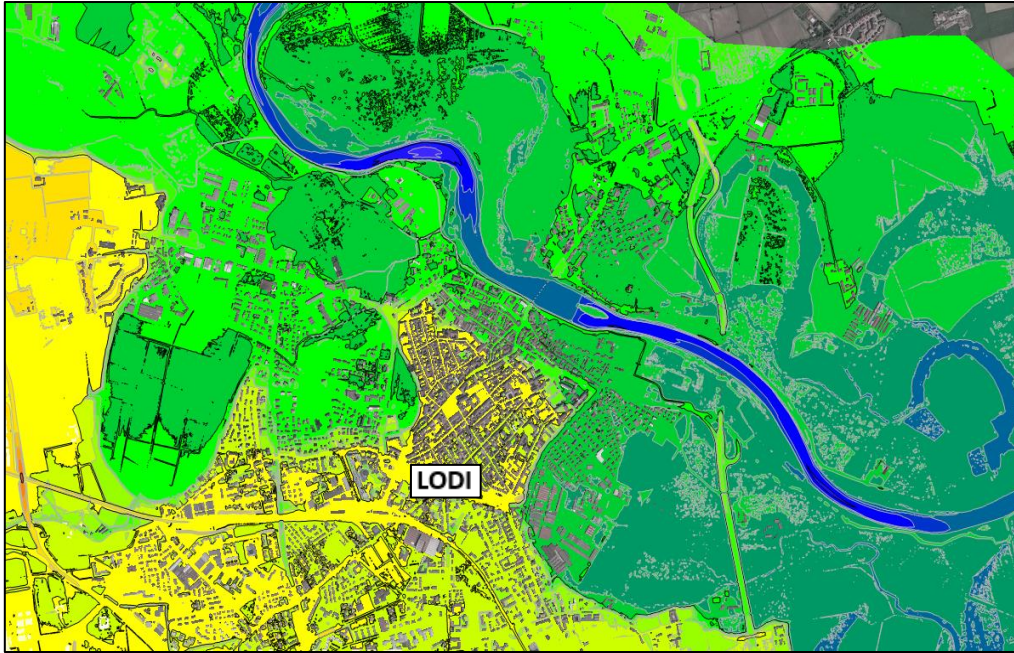


Figure 3-7 Extract of the digital surface model of the municipality of Lodi

- Boundary conditions (BC) file;
- Computational domain file;
- Orthophoto of the area of interest, containing a portion of the Municipality of Lodi.

The BC and the computational domain files have been proposed in the chapter 2.4.2, during the description of Parflood software. Moreover, some of these have been modified during the model calibration, explained in chapter 3.1.3.

3.1.1.6 Altimetric survey on the structural defences

The altimetric survey of the right bank of the Adda river in Lodi has been performed by the geodesy and geomatics laboratory of Politecnico of Milan and by the writer on the 30th of January 2019 with Leica Nova GS14 GPS / GNSS instrumentation in NRTK mode (NTRIP connection to the SpinGNSS regional network). 56 measurements along about 3.5 km of structural defences have been computed. The plan coordinates are UTM / WGS 84. The heights are ellipsoidal and geoidic type (Italgeo National Geoid) and the latter have been transformed with the ConVERGO software (source CISIS). The precision of the orthometric heights (on the geoid) is ± 5 cm (1 sigma).

In Figure 3-8 and Figure 3-9, the location of the 56 measurements and the survey operation on a structural wall have been reported. These measurements have been used to reproduce the geometry, used as input file for the simulation of scenarios with structural defences.

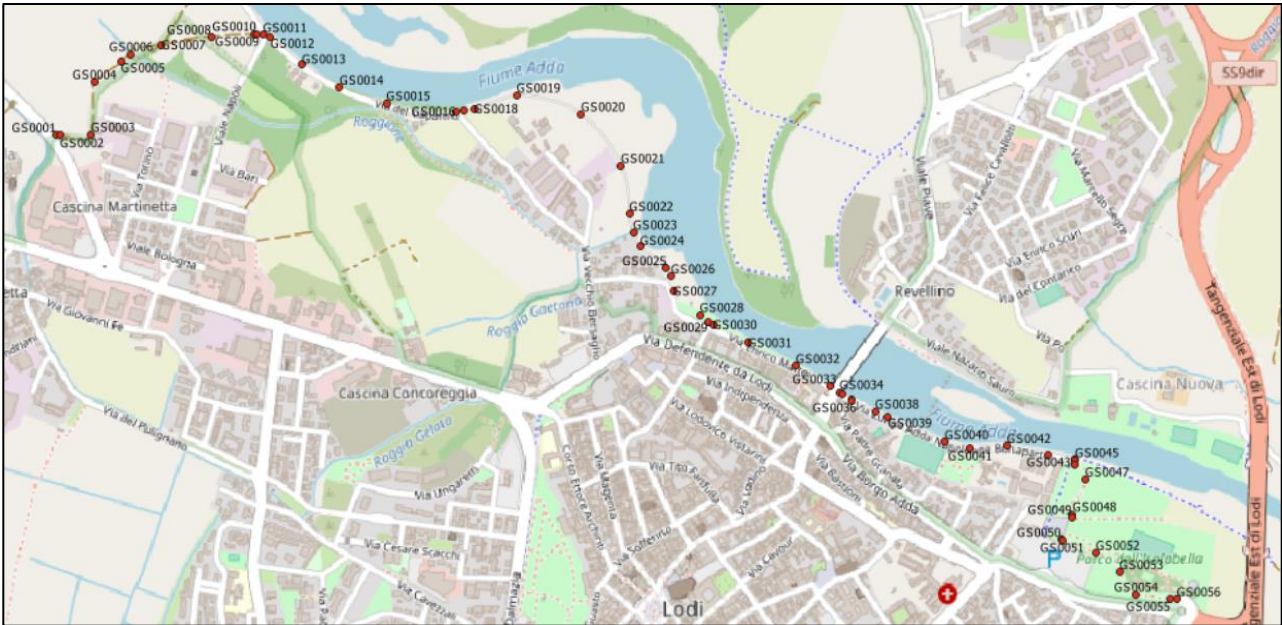


Figure 3-8 Location of the altimetric survey



Figure 3-9 Measurements of the elevation of structural wall belonging to the opening of Via Napoli

3.1.1.7 Past reports

Some reports about previous researches on the river Adda and the November 2002 flood event have been consulted. The latter have been used to collect additional information and to enrich data for the flood model calibration. The most important studies are:

- *Studio idrologico-Idraulico del tratto di F. Adda* (Rossetti & Cella, 2010a);
- *Studio di fattibilità della sistemazione idraulica* (Autorità di bacino fiume Po, 2003);
- *Delimitazione delle aree inondabili ad assegnati tempi di ritorno* (Natale, 2003);
- *Flood Hazard Modelling for the City of Lodi* (Agosti e Crippa, 2018);

3.1.2 Geometry

Two different geometry files, respectively without and with structural defences have been created, starting from a bathymetry file representing the Municipality of Lodi after the flood event, provided by the “Università degli Studi di Parma”.

In the geometry file without structural defences (levees, protective walls, sluice gates, embankments reinforcements), several operations have been performed in order to reproduce, as closely as possible, the environment of the interested area hit by the November 2002 flood event. Irrigation ditches have been added upstream of the historical municipality, using bathymetry of previous studies (like was done by Agosti & Crippa, 2018), pictures taken during field surveys, google earth and google street view. An extract of the bathymetry file, representing the irrigation ditches just upstream of the historical bridge on the hydraulic right and a top view of the channels nearby a sluice gates from google earth are reported in Figure 3-10.



Figure 3-10 Extract of the bathymetry file representing the irrigation ditches on the left and a top view from Google Earth on the right

The underpass below the “Napoleone Bonaparte” bridge on the hydraulic right of the Adda river has been added to the original bathymetry file, as shown in Figure 3-11, taken from Surfer and field survey pictures.

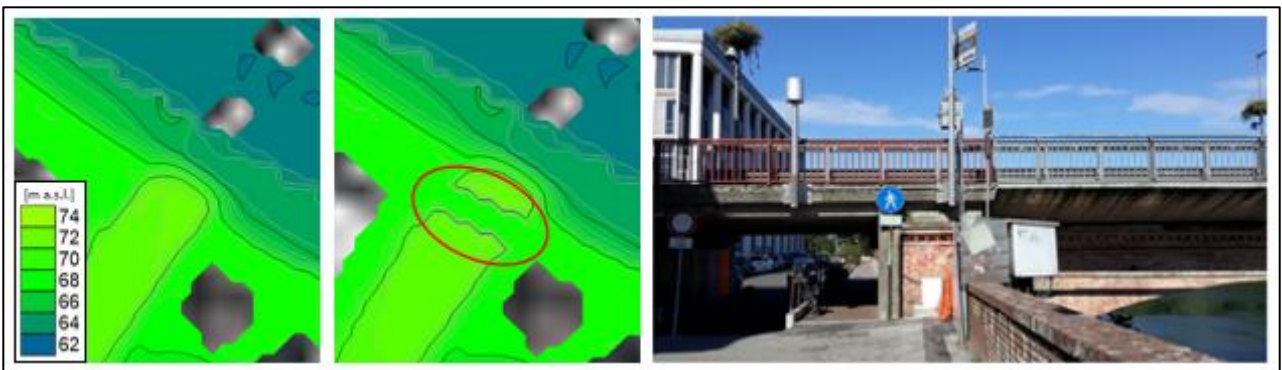


Figure 3-11 Insertion of the underpass under the historical bridge and field survey picture

Seven different paths, mostly irrigation ditches and tunnels, along the “Tangenziale sud” road overpass downstream of the historical bridge have been added to the original bathymetry file, in order to reproduce, in details, the possible paths that the water can follow after the occurrence of a flood.

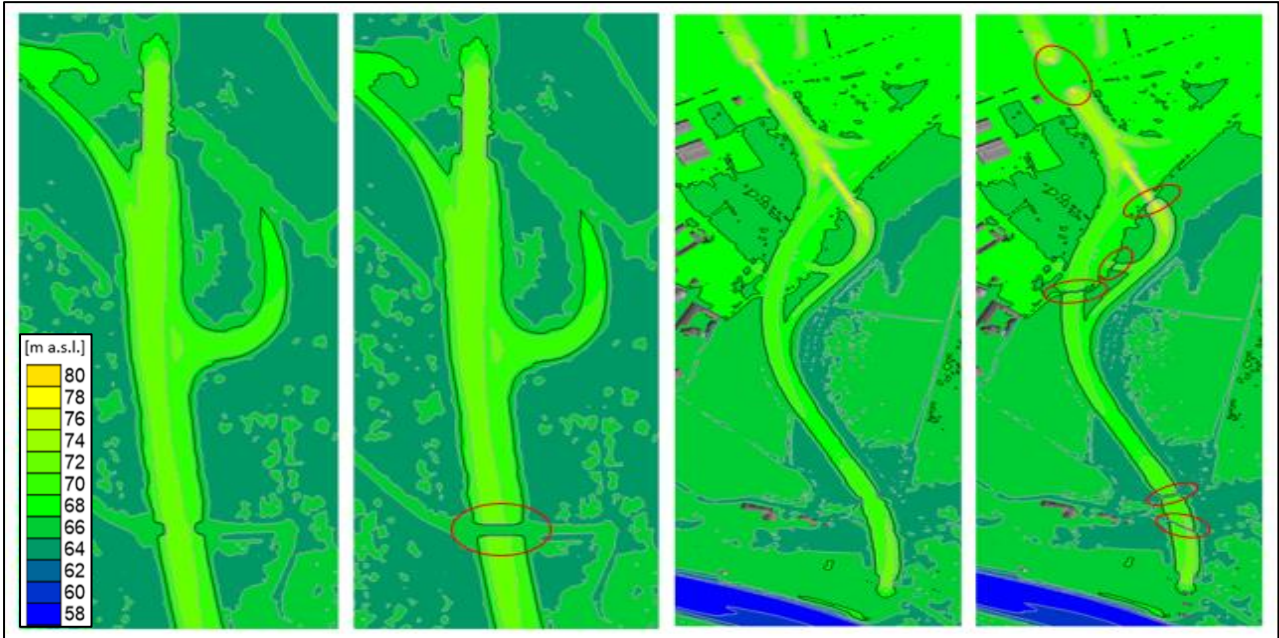


Figure 3-12 Added paths along the “Tangenziale sud” road overpass

Moreover, the pillars of the aforementioned road viaduct downstream of the historical bridge have been added, as shown in Figure 3-13.

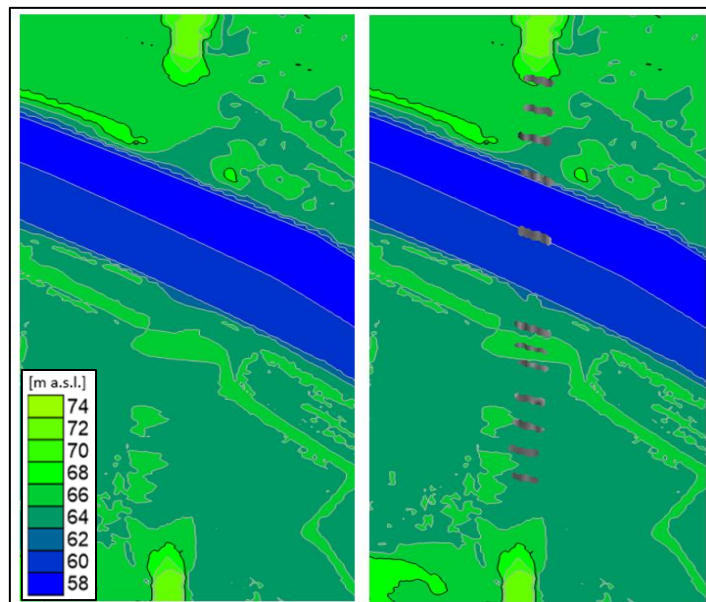


Figure 3-13 Added pillars of the “Tangenziale sud” road viaduct

The built environment of the City of Lodi in 2002 has been reproduced and used for all the simulations, both without structural defences, as during the November 2002 flood, and with structural defences, built after the occurrence of the event. The choice to keep the same built environment has been dictated by the cost benefit analysis purpose of the structural mitigation measures. As consequence, the same potential damage to residential buildings, economic activities and agriculture, as well as the number of exposed people, has been taken into account.

Regarding the used input bathymetry file with structural defences, all the aforementioned modifications of the terrain related to irrigation ditches, paths, tunnels, added pillars and the 2002 built environment have been represented. In addition to the previous geometry file, the structural mitigation measures (soil embankments, walls and sluice gates) have been added, according to the final design of the works drafted by AIPO (*Agenzia Interregionale per il fiume Po*) and Regione Lombardia. In Figure 3-14, two examples of the added defences are shown. In particular, part of the soil embankments (A1 typology) from the intersection between “via Napoli” and “via del Capanno” to the S.P. n.202 and the stretch of soil embankments downstream of the city of Lodi, linked to the “Tangenziale sud” road, are proposed.

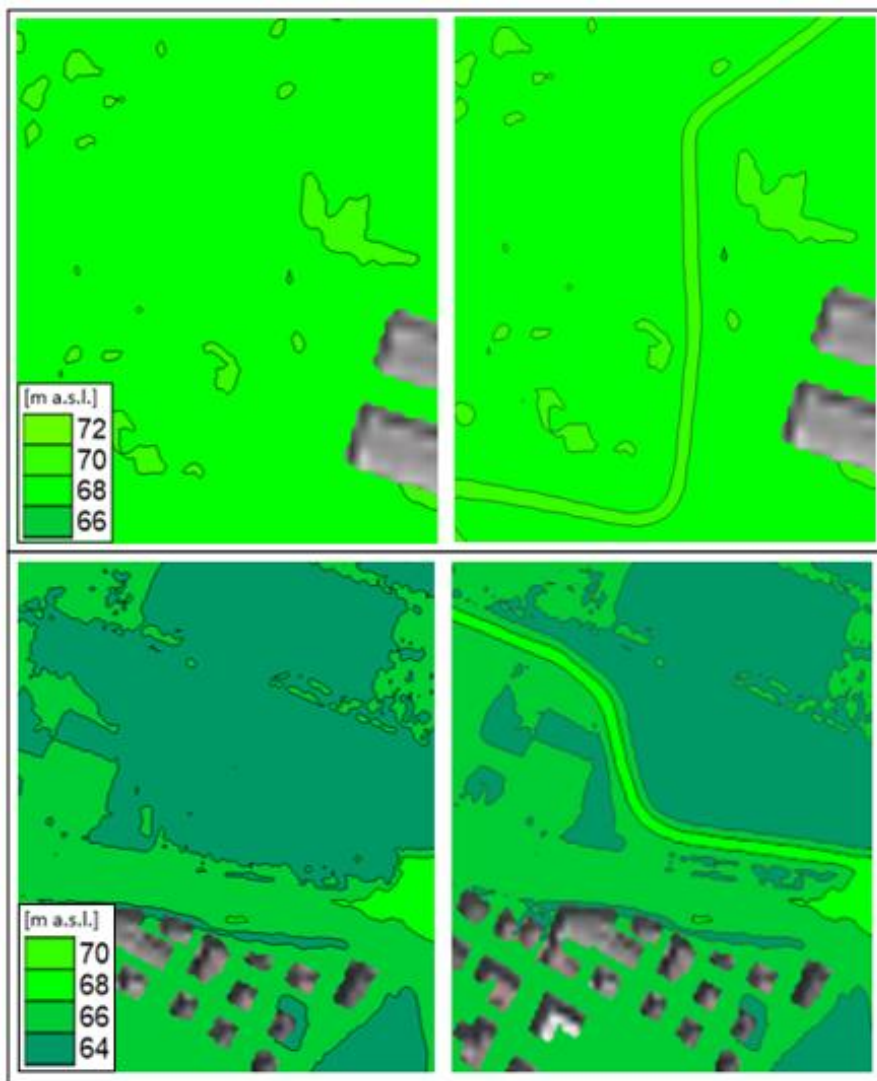


Figure 3-14 Example of the added soil embankments downstream of the City of Lodi

Another modification of the original geometry file regards the addition of a dike downstream of the historical bridge, according to the final design of the works. Moreover, a stretch of approximately 200 m of the river bed between the historical bridge and the aforementioned dike has been modified, decreasing the height of the river bed. In order to do so, nine rectangular “patches” with constant values and with 5cm increments, have been replaced over the previous terrain, leading to an almost linear river bed surface between the approximately 63 m below the historical bridge and the 62.5 m of the designed dike. Eventually, structural concrete reinforcements in the upstream tip of the island and on both sides of the river, in correspondence of the island itself, have been added.

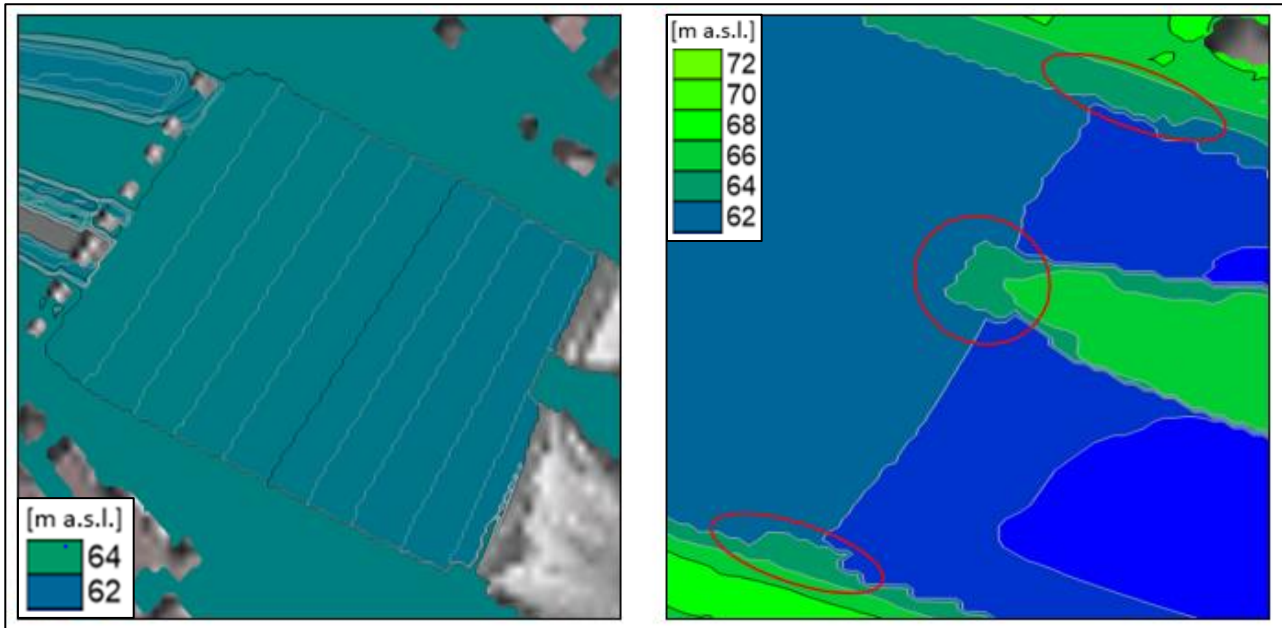


Figure 3-15 River bed between historical bridge and dike and added concrete reinforcements

3.1.3 Unsteady modelling

With the unsteady modelling, it is possible to obtain the flood event evolution, in terms of flooded area, water levels, flow path and permanence of the flood water.

For the purpose of this case study, first the bathymetry without structural defences has been used in order to calibrate the model and to obtain the hazard maps without flood protections. Then, the previously described structural defences have been added to the same bathymetry file, in order to obtain the hazard maps with flood protection and to compare them with the corresponding ones without defences in a benefit cost ratio, inside a Multi Criteria Analysis.

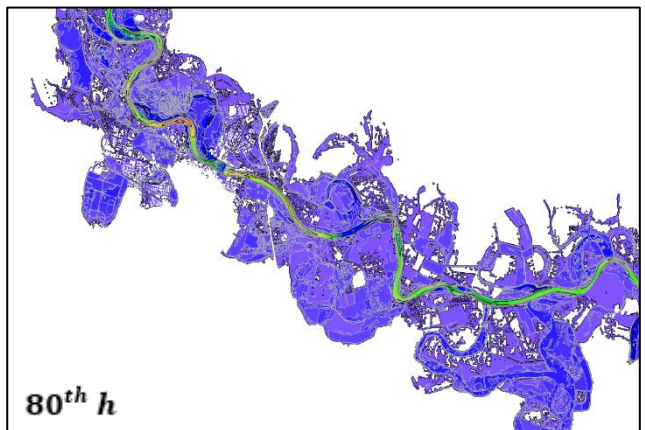
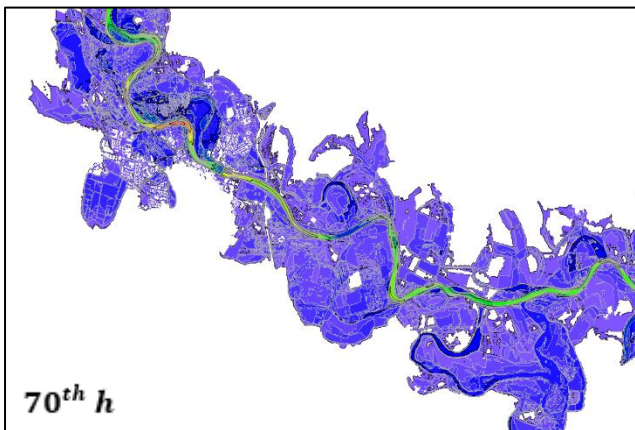
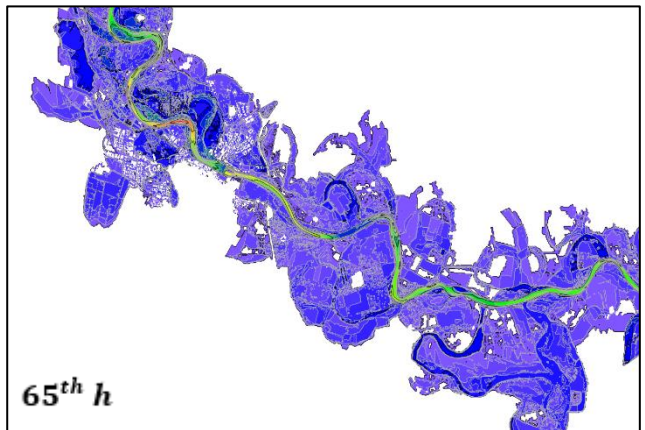
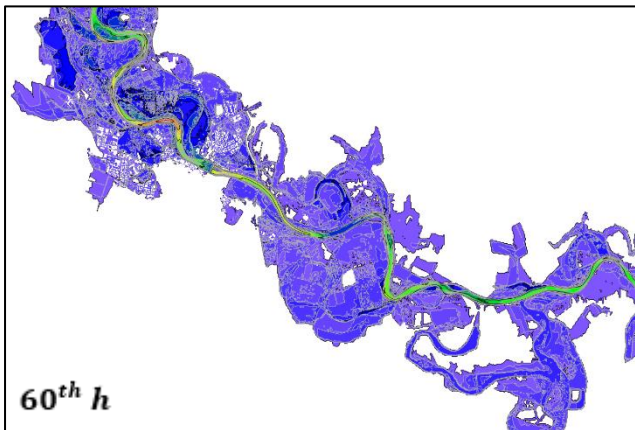
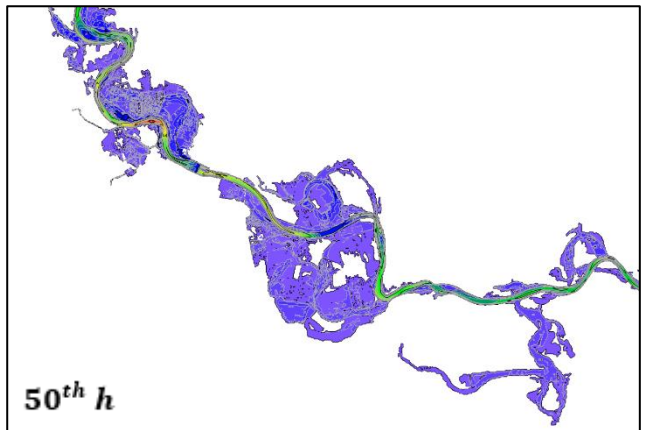
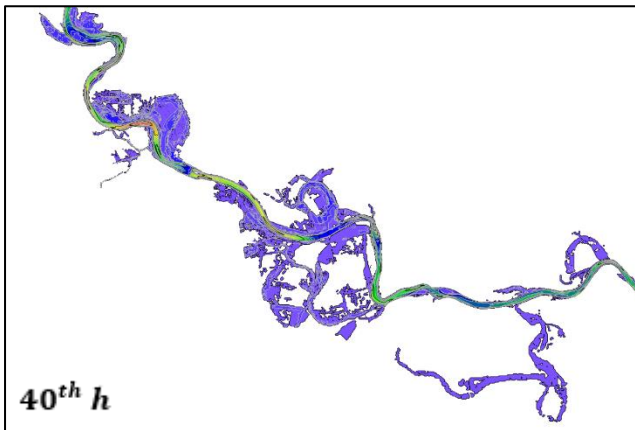
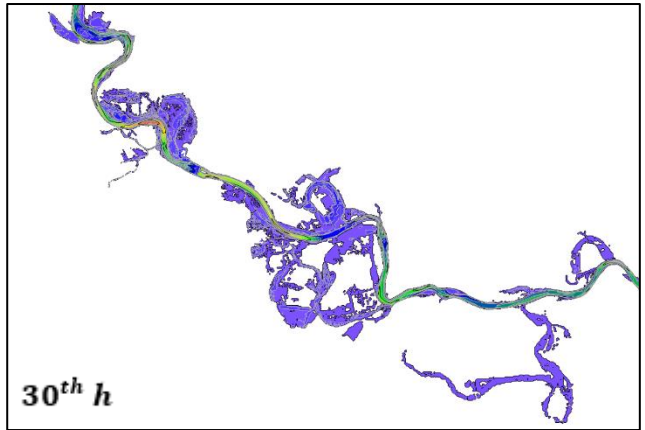
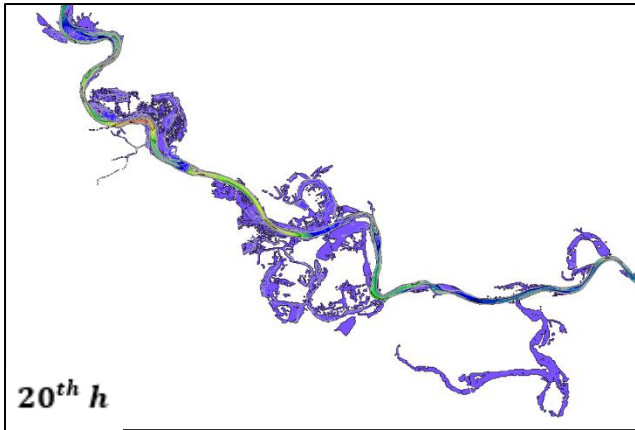
For what concerns the boundary conditions (BC), a discharge hydrograph has been input as upstream one and a rating curve as downstream one. The features of these boundary conditions will be specified in the section dedicated to the model calibration. The two BCs are applied on segments belonging to the simulation domain, whose characteristics have been mentioned in chapter 2.4.2.

The initial time of the simulation has been set equal to 0, as the beginning of the flood hydrograph. The duration of the simulated event has been chosen equal to 120 hours, namely five days.

The flood simulations have been computed with the calculation code “Parflood” provided by the “Università degli Studi di Parma” (UNIPR), while modifications on maps and representation of the latter have been done using the “Surfer” software. Several outputs are available, such as water surface elevation, water depth and velocity in x and y directions, at each time step, and the envelopment of the highest water level and maximum velocity reached by the individual grid cell during the entire simulation. Some other output files can be obtained from “Parflood” code but the latter have not been considered relevant for this thesis work.

The computational time for completing the unsteady simulations with “Parflood” is about 8-10 hours, considering that all the calculations have been done remotely, using the UNIPR servers.

Figure 3-16 reports some results of water depth in the most interesting time steps, in order to show the evolution of the flooded area and the water depth in each cell of the grid domain. In details, the 20th hour of the simulation, the condition at the peak (t = 65 h), the last time step of the computation (t = 120 h) and some other relevant intermediate snapshots are displayed. It has to be remarked that the snapshots in Figure 3-16 are cut out, showing an area containing inside the Municipality of Lodi and that the latter are demonstration results only, with no reference in terms of represented parameters and chromatic scale.



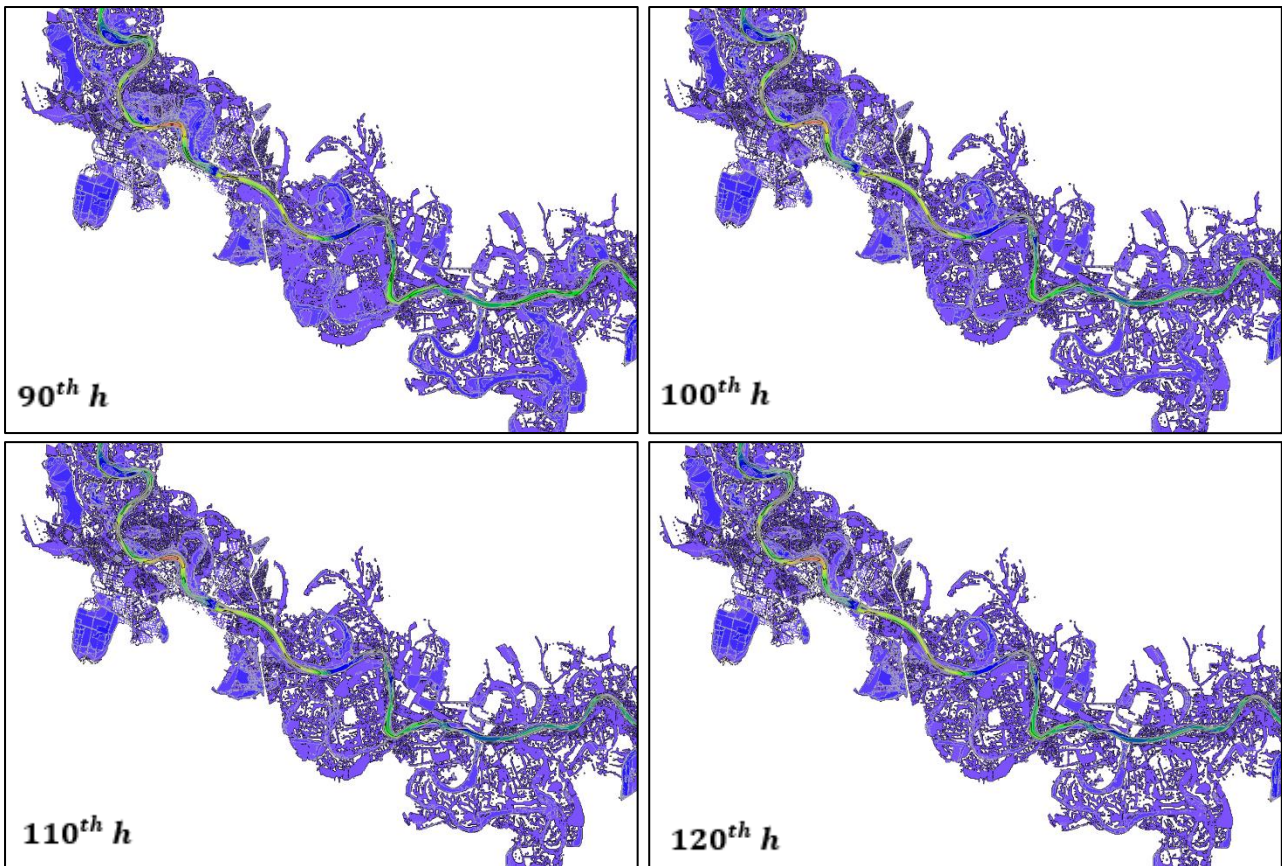


Figure 3-16 Snapshots of water depth in relevant time step of a simulation

3.1.4 Calibration procedure

The model calibration is a recursive process in which the first simulation is performed with reasonable values, for the studied area, of roughness coefficients and boundary conditions. Once the flood simulation is complete, a post processing of the results is carried out based on the match with reference values of specific parameters, such as flooded area, hydrometer levels and measurements in correspondence of control points. If the obtained results satisfy the imposed goal conditions, the model calibration is stopped, otherwise a new simulation is performed with different Manning's values and boundary conditions. In the following flow diagram, the aforementioned recursive process is reported.

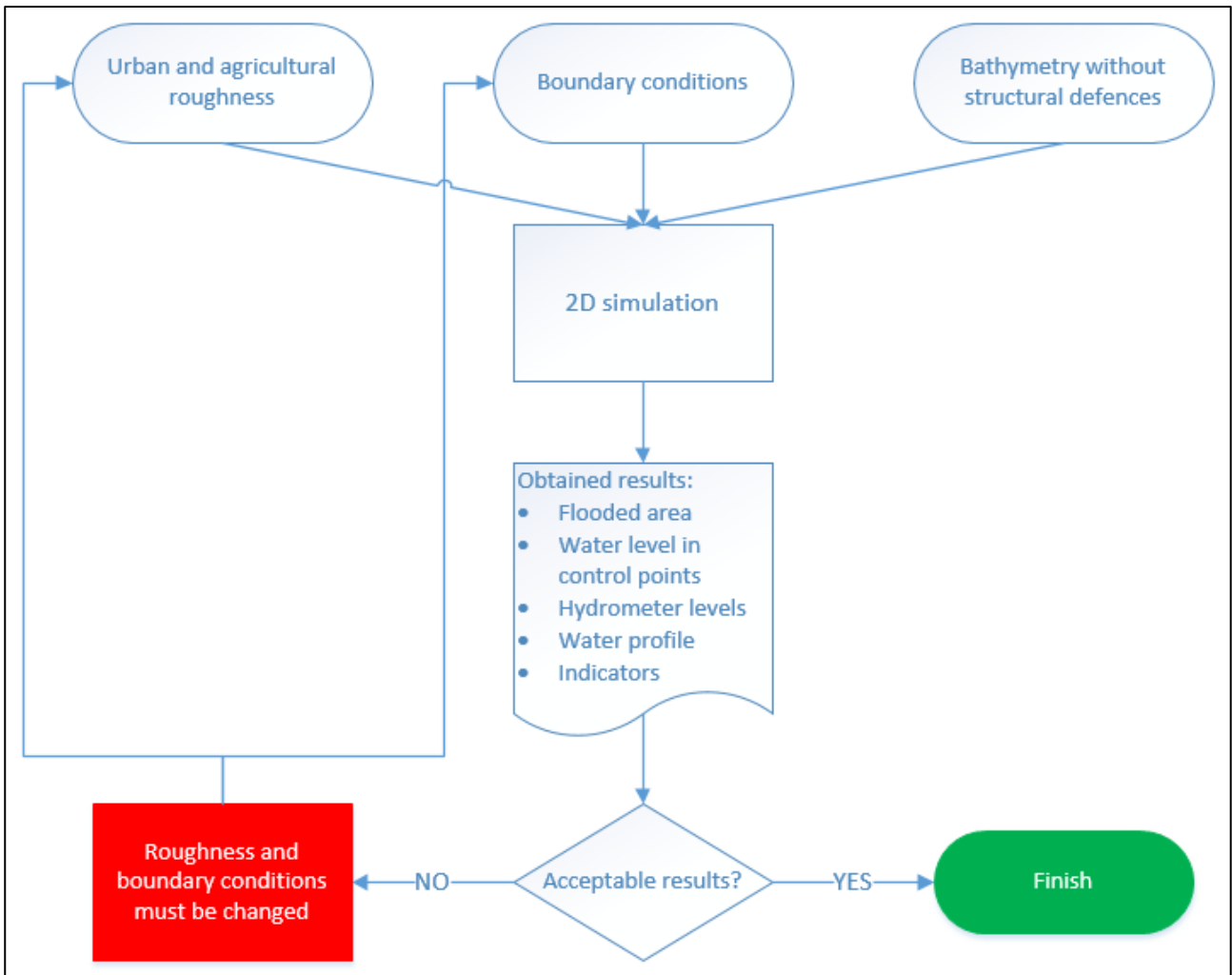


Figure 3-17 Calibration process flow diagram where: the circular polygons regard input data and output results; the rectangles are processes; the intermediate polygon is an intermediate result; the rhombus is a decision

The first simulation performed within the calibration procedure contains as input files the following:

- .BTM file (bathymetry) of the Municipality of Lodi without structural defences, in order to reproduce the November 2002 flood scenario and then calibrate the model with the latter;
- .MAN file (roughness) covering the same area of the bathymetry file with a constant value equal to 0.0333, representing grass and cultivated lands;
- .BNL file representing the limitation of the simulation domain and containing the two sections over which the boundary conditions are applied;
- .BCC file (boundary conditions) listing first the upstream boundary condition, applied approximately 5km upstream of the historical bridge, and then the downstream boundary condition, imposed in correspondence of the SP169 provincial road, around 8km downstream of Lodi.

These files have been modified several times, with the exception of the bathymetry file. Indeed, the scope of the calibration is to obtain results from the flood simulation as close as possible to those for the November 2002 flood event. The features and parameters compared are the flooded area, the levels in correspondence of the hydrometer station, the water levels in control points distributed within the municipality, some indicators and the water profile from the upstream to the downstream boundary conditions.

In the following sections of this paragraph, the aforementioned compared features and parameters are described in detail. Furthermore, all the modification and changes in the “Parflood” input files during the calibration procedure are proposed, before the last section containing the result of the calibration.

3.1.4.1 Parameters used for the model calibration

During the procedure of calibration, results coming from the flood simulations have been compared with the corresponding observed ones after the November 2002 flood event occurrence. In particular, the following features and parameters have been analysed:

- Flooded area;
- Water levels in correspondence of the hydrometer;
- Water levels in control points;
- Quantitative indicators of the goodness of the result;
- Water profile.

Flooded area

Considering the previous parameters, the obtained flooded area represents a parameter that has been strongly taken into consideration to calibrate the model. The latter has been compared with the observed flooded area in Lodi taken from past reports (*Rossetti & Cella, 2010b*), reported in the Figure 3-1.

Water levels in correspondence of the hydrometer

Obtained water levels in correspondence of the hydrometer have been compared with the values measured and reported in previous studies (*Rossetti & Cella, 2010b*). This parameter has been considered relevant for calibration purposes, with a particular attention to the trend and the peak of the hydrometer levels. The position of the mentioned station is currently in correspondence of the second vault from the hydraulic right of the Napoleone Bonaparte bridge and is shown in the Figure 3-18.



Figure 3-18 Location of the hydrometric station along the Napoleone Bonaparte bridge in Lodi

Water levels in control points

Another important parameter in order to calibrate the model regards the water surface elevation observed in control points in the City of Lodi after the November 2002 flood event. These heights have been obtained from:

- information on water depth available from a total of 121 georeferenced points, described in the damage compensation forms compiled by citizens;
- reconstructions from photos taken mainly post event.

After the first simulation, the obtained maximum water surface elevations (namely the envelopment of the highest water level reached by the individual grid cell during the entire simulation) have been compared with the observed ones. Since several measured points are located inside buildings (mainly those levels used for damage compensation purpose), in order to compare observed and simulated heights, the following procedure has been adopted:

- 1) the previously mentioned 121 points have been subdivided into 8 clusters, named from A to H, reported in the Figure 3-19;
- 2) an average of the observed water levels in these clusters (named in the following as averaged observed WSE) has been computed; from the maximum water surface elevations output file, through the use of the map “digitize” command on Surfer, a polygon containing the points of each cluster within has been traced;
- 3) using the grid “blank” command, the area outside the drawn line is blanked, in order to obtain the maximum water surface elevations output result of the area inside the polygon for each cluster only;
- 4) the average of the values inside the extracted area has been calculated for each cluster;

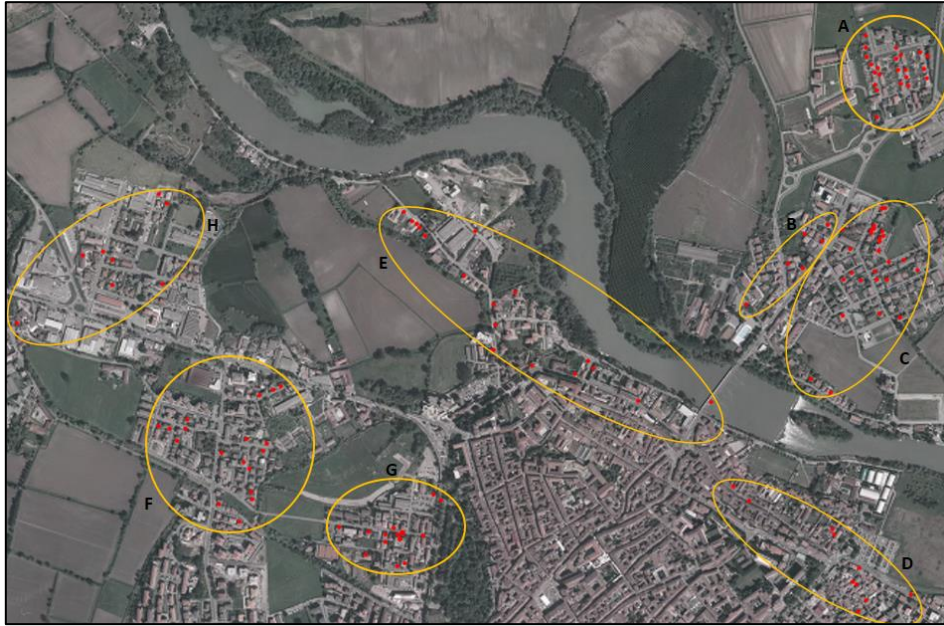


Figure 3-19 Cluster grouping representation

- 5) eventually, in a scatterplot, the averaged observed WSE of each cluster have been compared with the simulated WSE, as reported in the Figure 3-20 (related to the first simulation performed in the procedure of calibration). The more the blue points are closed to the red bisector line, the more the match between observed and obtained water surface elevations.

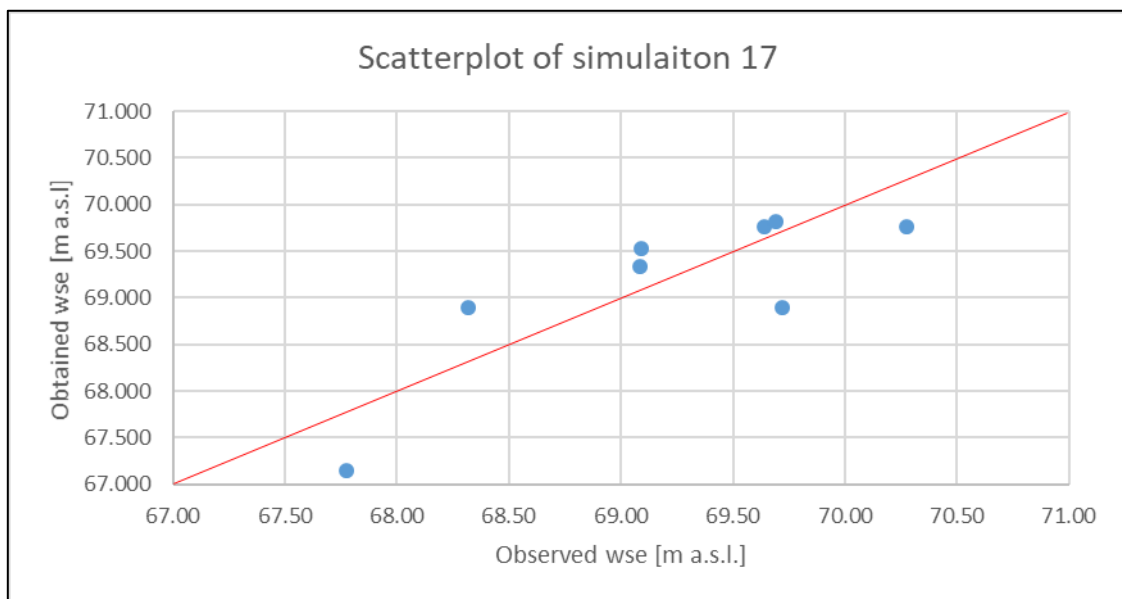


Figure 3-20 Comparison observed - obtained WSE of Simulation 17

Quantitative indicators of the goodness of the result

For what concerns the indicators for the calibration purpose, using the previous observed and obtained WSE values, the average of the differences (AD), the absolute average of the differences (AAD) and the Nash-Sutcliffe Efficiency (NSE) has been computed and reporting in chapter 3.1.4.4.

Water profile

In order to complete the calibration procedure, the water profile for some of the last simulations has been computed. Along the axis of the river Adda, several points have been chosen in the stretch between the upstream and downstream boundary conditions. 14 points have been selected in thirty of the performed simulations and 12 points in two ones only. The different number of selected points is due to a modification of the position of the downstream boundary condition, described in the computational domain file section. With regards to the criteria of choice of the points in which the water level has been measured, a denser selection has been adopted nearby the historical bridge of Lodi. Moving both forwards and backwards with respect to the Napoleone Bonaparte bridge, the aforementioned points have been chosen with a constant distance between them. The location of the aforementioned points over a google earth base map is reported in Figure 3-21.



Figure 3-21 Location of points for the creation of the profiles over a google earth base map

3.1.4.2 Operations and modifications on input files during the model calibration

After the first simulation (Sim 17) with the “Parflood” calculation code, some modifications on the input files for model calibration purposes have been done. In particular, such changes regard:

- Areas with different roughness, expressed through the Manning’s coefficient;
- Choice of the hydrograph as upstream boundary condition in the BCs file;
- Values of the rating curve applied to the downstream boundary condition;
- Position of the segment over which the downstream boundary condition is applied, belonging to the computational domain file.

In Table 3-2, all the simulations performed for calibration purpose are reported, with the addition of the choices regarding the input files. Moreover, all the different features of the input files will be analysed in detail in the continuation of this chapter and the reasons behind these choices explained.

Table 3-2 Simulations performed during calibration procedure of the flood model (G=green area characterized by medium to dense brush and forest; U=urban environment; D=area downstream of the city of Lodi; A=portion of terrain downstream of “Tre Cascine”)

n° Sim	Roughness values	Hydrograph in .BCC file	Rating curve in .BCC file	Boundary domain in .BLN file
17	0.033	Obtained 1	Provided	Original BLN
18	G=0.08 U=0.02	Obtained 1	Provided	Original BLN
20	0.033	Obtained 1	Provided -10%	Original BLN
21	G=0.08 U=0.02	Obtained 1	Provided -10%	Original BLN
22	0.033	Obtained 1	Provided +10%	Original BLN
23	G=0.08 U=0.02	Obtained 1	Provided +10%	Original BLN
24	0.033	Obtained 1	Provided -5%	Original BLN
25	G=0.08 U=0.02	Obtained 1	Provided -5%	Original BLN
26	0.033	Obtained 1	Provided +5%	Original BLN
27	G=0.08 U=0.02	Obtained 1	Provided +5%	Original BLN
28	G=0.08 U=0.02	Obtained 1	Provided -4%	Original BLN
29	G=0.08 U=0.02	Obtained 1	Provided +15%	Original BLN
30	G=0.16 U=0.04 D=0.0015	Obtained 1	Provided +10%	Original BLN
31	G=0.08 U=0.02 D=0.0015	Obtained 1	Provided +10%	Original BLN
32	G=0.08 U=0.02 D=0.015	Obtained 1	Provided +10%	Original BLN
33	G=0.06 U=0.015 D=0.022	Obtained 1	Provided +10%	Original BLN
34	G=0.06 U=0.015 D=0.028	Obtained 1	Provided +10%	Original BLN
35	G=0.06 U=0.015 D=0.028	Obtained 1	Provided +10%	Original BLN
36	G=0.06 U=0.015 D=0.028	Obtained 1	Provided +10%	New BLN
37	G=0.06 U=0.015 D=0.028	Obtained 1	Provided +5%	New BLN
38	G=0.06 U=0.015 D=0.028	Obtained 1	Provided +3%	New BLN
39	G=0.06 U=0.015	Obtained 1	Provided +3%	New BLN
40	G=0.05 U=0.01	Obtained 1	Provided +3%	New BLN
41	G=0.05 U=0.015	Provided 1	Provided	Original BLN
42	G=0.05 U=0.015 A=0.06	Provided 1	Provided	Original BLN
43	G=0.05 U=0.015	Provided 2	Provided	Original BLN
44	G=0.05 U=0.015	Obtained 2	Provided	Original BLN
45	G=0.05 U=0.015	Obtained 3	Provided	Original BLN
46	G=0.05 U=0.015 D=0.022	Obtained 2	Provided	Original BLN
47	G=0.06 U=0.015 D=0.022	Obtained 3	Provided	Original BLN
48	G=0.06 U=0.015 D=0.028	Obtained 3	Provided	Original BLN
50	G=0.06 U=0.015 D=0.022	Obtained 4	Provided	Original BLN

Some of the listed simulations have unexpectedly stopped and the reason may be related to a particular combination of roughness values and downstream boundary condition that have brought the level of the water profile to a critical one.

Roughness coefficients

The first flood simulation contained a constant value equal to 0.033 of Manning’s coefficient in the roughness file, representing grass and cultivated lands, over the entire grid model. During the calibration procedure, the previously mentioned roughness file has been initially changed, adding areas with different Manning’s. In particular, values of 0.01, 0.015, 0.02 and 0.04 have been assigned to the urban area representing the Municipality of Lodi and values of 0.05, 0.06, 0.08 and 0.16 have been attributed to a portion of terrain characterized by medium to dense brush and forests. Going forward in the calibration procedure, another area with smoother roughness has been adopted. In particular, for a considerable area between the historical bridge to nearby the SP169, over which the downstream boundary condition is applied, values from 0.015 to 0.028 have been used. This adjustment has been dictated by results obtained during the calibration, regarding the flooded area, hydrometer levels and water levels in control points.

3. Floodplains			
a. Pasture, no brush			
1. short grass	0.025	0.030	0.035
2. high grass	0.030	0.035	0.050
b. Cultivated areas			
1. no crop	0.020	0.030	0.040
2. mature row crops	0.025	0.035	0.045
3. mature field crops	0.030	0.040	0.050
c. Brush			
1. scattered brush, heavy weeds	0.035	0.050	0.070
2. light brush and trees, in winter	0.035	0.050	0.060
3. light brush and trees, in summer	0.040	0.060	0.080
4. medium to dense brush, in winter	0.045	0.070	0.110
5. medium to dense brush, in summer	0.070	0.100	0.160
d. Trees			
1. dense willows, summer, straight	0.110	0.150	0.200
2. cleared land with tree stumps, no sprouts	0.030	0.040	0.050
3. same as above, but with heavy growth of sprouts	0.050	0.060	0.080
4. heavy stand of timber, a few down trees, little undergrowth, flood stage below branches	0.080	0.100	0.120
5. same as 4. with flood stage reaching branches	0.100	0.120	0.160

Figure 3-22 Values of Manning’s coefficients for floodplains (Chow, 1959)

Looking at the second column of the previous summary Table 3-2, green areas characterized by medium to dense brush and forest have been attributed to the letter “G”, urban environment to “U”, the previously mentioned area downstream of the City of Lodi to “D” and, eventually, a small portion of terrain downstream of “Tre Cascine” to “A”. The latter has been added in the simulation number 42 in order to increase the flooded area in a zone located on the south-east of Lodi. However, this modification has not brought to an improvement in the goal result and, therefore,

abandoned in the following simulations. Eventually, changing the Manning's values, different flooded area, hydrometer levels, water surface elevations in control points in Lodi and values of indicators have been obtained. The latter have been compared then to the ones observed in the previous reports and studies, selected for calibration purposes.

Two examples of the aforementioned areas with different roughness value are reported in Figure 3-23 and Figure 3-24, showing a top view representation of the base map used as reference and an extract of the roughness grid file.



Figure 3-23 Top view of Lodi and extract of the .MAN file representing the urban area



Figure 3-24 Top view and extract of the .MAN file representing an area with medium to dense brush and forest

For what concerns the flood modelling in urban areas, buildings have been treated as solid walls. In other words, inside the area subject to flooding, built environment has been excluded from the grid computation domain. In details, very high values ($1.70141E+038$) have been attributed to points of the bathymetry file over which the buildings are located. It is worth to remark that the roughness values of the roughness file in these points have been left as 0.033, considering that the treatment

of buildings as impervious blocks makes the value 0.033 not relevant in the simulation, being impossible for the flood to cover these grid cells.

In order to reproduce the November 2002 flood that occurred in the City of Lodi, a hydrograph representing the trend of the discharge observed during the event has to be input in the calculation code. Indeed, in the aforementioned BCs file, through the use of a txt file, the discharge corresponding to a specified time discretization has been added, in addition to the rating curves in the downstream boundary condition. Both conditions have been changed several times during the procedure of calibration. In particular, the upstream boundary condition has been modified using six different hydrographs, while the downstream one has been increased or decreased in the water levels of the rating curve, computed in steady flow and based on the geometry, slope and roughness.

Upstream boundary condition

Regarding the choice of the hydrographs in the boundary conditions input file, the first used curve (named obtained 1 in Table 3-2) representing the event has been obtained from an elaboration of the hydrometer levels detected during the occurrence of the flood in 2002. The station is set in correspondence of the second archway of the historical bridge from the right side of the city. Then, considering a relation between hydrometer levels and discharge, obtained from estimations by the Municipality of Lodi, the first hydrograph of the November 2002 flood event has been computed. Curve 1, reported in the Figure 3-25, has been compared with the one used in past reports by Rossetti and Cella and a good match has been observed. This curve has been used for more than half of the simulations in the model calibration, in which manning's coefficients have been modified, in order to find good results in terms of flooded area, water levels in control points and measurements in correspondence of the hydrometer. Curve 1 has a duration of 120 hours, laps of time in which the peak discharge ($1860 \text{ m}^3/\text{s}$) is approximately located in the middle of the time band, at the 65th hour.

However, using this hydrograph, a backwater nearby the downstream boundary condition has been observed, both looking at the obtained MAXWSE maps and during the computation of the water profile of the simulation. Therefore, other hydrographs have been computed and used in the model calibration.

A second hydrograph representing the 2002 flood event has been taken from the input files proposed by the "Università degli Studi di Parma" (UNIPR). As it can be noticed, this curve (named provided 1 in the summary Table 3-2 and curve 2 in Figure 3-25) has a shape similar to the first hydrograph mentioned before (curve 1). Moreover, the peak of the given curve has increased from the original discharge of $1540 \text{ m}^3/\text{s}$ until $1860 \text{ m}^3/\text{s}$, in order to have a comparable maximum discharge with the first mentioned hydrograph. Furthermore, the laps of time of the second curve is exactly the same of the first one, as well as the time position of the peak discharge (65th hour). However, comparing the curves 1 and 2, reported in the Figure 3-25, different volumes of water can be noticed, considering that the hydrograph "provided 1" has been computed with a different rating curve.

The curve “provided 1” has been slightly changed reducing the peak discharge from 1860 m³/s to 1837 m³/s but keeping the same shape. The latter has been named as “provided 2” in the summary Table 3-2 and used as third input curve for one simulation only.

These two proposed hydrographs (provided 1 and provided 2) have been used in order to find a good match between observed and obtained hydrometer levels and to reduce the backwater nearby the downstream boundary condition, as well as to improve the results of the other parameters involved in the calibration procedure. However, not all the previous goals have been achieved using these curves and some other hydrographs have been computed. Therefore, other curves have been constructed after the following hydraulic analysis and tried as upstream boundary condition. The observed levels described in the reports of Natale, in agreement with the study performed by Rossetti, has been converted in discharge hydrographs, using different rating curves.

A fourth and fifth curve (named respectively as obtained 2 and obtained 3 in the summary Table 3-2 and curve 4 and curve 5 in Figure 3-25) have been input in the upstream boundary condition. As it can be noticed from the Figure 3-25, the duration of the simulated event is 120 hours, the position of the peak discharge at the 62th hour, while maximum discharge is 1560 m³/s for the curve 4 and 1786 m³/s for the curve 5. The fifth hydrograph has been computed with the rating curve described by the following formula, which has been obtained from an elaboration of the curve proposed by UNIPR:

$$Q = 4.8068 * d^{3.2557}$$

where:

- Q is the discharge expressed in m³/s;
- d is the depth obtained with the difference between z and 62.1 (height of the river bed in correspondence of the hydrometer);
- z is the water surface elevation obtained summing up the hydrometric zero and the registered measured by the fixed station.

Taking this last rating curve and considering the maximum water level observed by Natale ($z = 68.26$ m), the peak discharge is about 1786 m³/s, as it can be seen in the curve representing hydrograph 5.

Concerning the discharge – water stage relationship used to determine the curve 4, the formula is slightly different from the previous one and it is:

$$Q = 4.8068 * \left(\frac{1560}{1786}\right) * d^{3.2557} = 4.1985 * d^{3.2557}$$

Using the two aforementioned hydrographs, improvements in the results of the parameters assessed for the model calibration have been observed, especially for the curve 5.

Eventually, a sixth hydrograph (named as obtained 4 in Table 3-2 and curve 6 in Figure 3-25) has been used and computed with the formula using the previous rating curve, adapted in order to obtain a match between simulated and observed hydrometer levels:

$$Q = 4.8068 * \left(\frac{1840}{1786}\right) * d^{3.2557} = 4.9521 * d^{3.2557}$$

The curve 6, with a duration of 120 hours and a peak discharge of about 1840 m³/s, has been used in the simulation n°50, the one that gives the best parameter results among all the trials in the procedure of calibration.

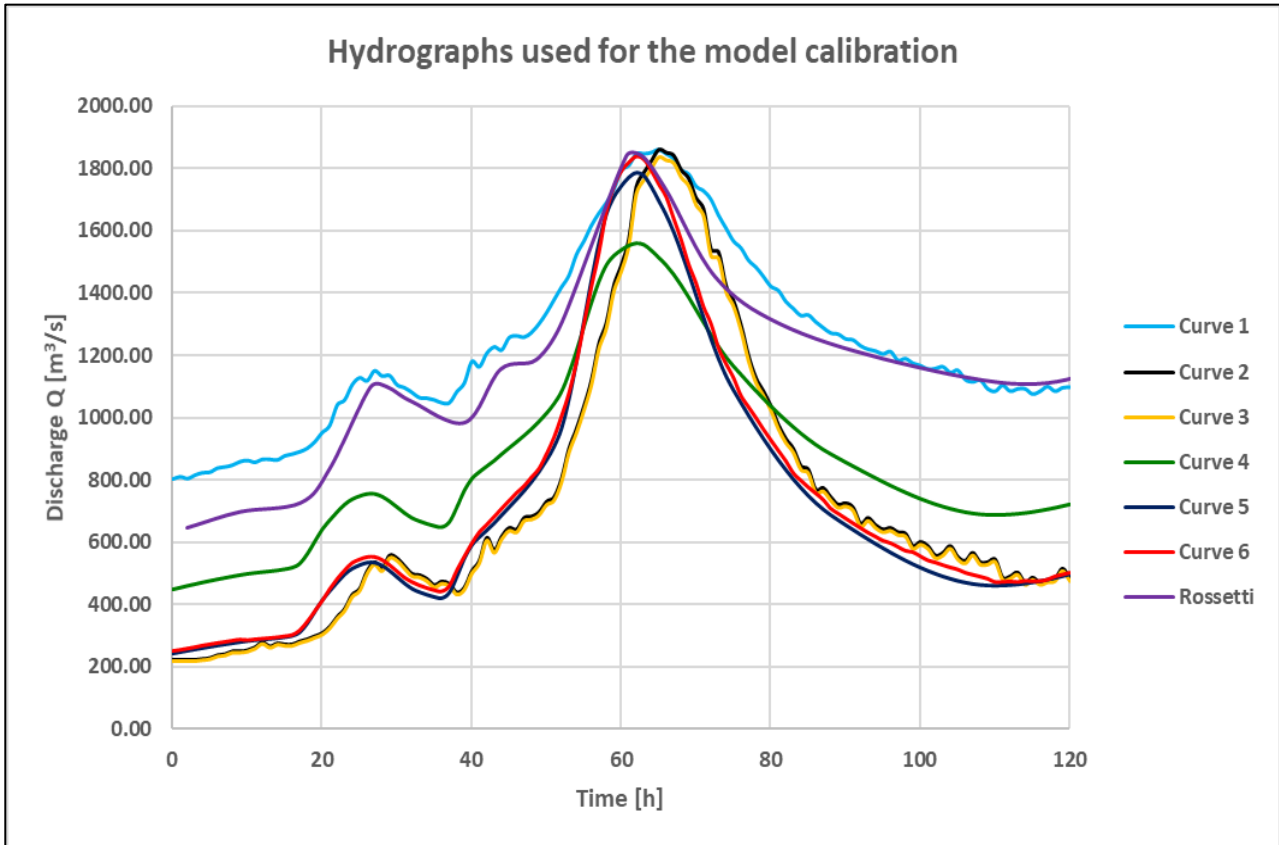


Figure 3-25 Hydrographs used for the model calibration

Downstream boundary condition

The fourth column of the summary Table 3-2 reports the values of the used rating curves, namely the relationship between discharge and water stage in a specific point. For all the simulation performed, the original values, computed in steady flow and based on the geometry, slope and roughness, have been used and sometimes slightly modified, increasing or decreasing the levels with a constant value. However, it has been noticed that this modification was creating backwater in the zone nearby the downstream boundary condition or, anyway, it was not improving the results of the parameters taken as reference for the calibration. Therefore, as it is possible to notice from the summary Table 3-2, from the simulation number 41 until the ones eventually chosen, the original rating curve has been assumed again.

Computational domain

Regarding the computational domain file, the file proposed by UNIPR (named Original BLN in the summary Table 3-2) has been used for most of the calibration. A new domain (New BLN) has been adopted in five simulations only, in order to solve a backwater problem nearby the downstream boundary condition. However, these wrong high-water depths downstream of the historical bridge were caused by an excessive volume of water using the hydrograph “obtained 1”, whose characteristics have been previously discussed. Therefore, as illustrated in the summary Table 3-2, the last simulations have been run again with the first mentioned computational domain.



Figure 3-26 Representation of computational domain Original BLN (red polygon), New BLN (blue polygon), upstream boundary condition (green ellipse) and downstream boundary conditions (yellow ellipse)

3.1.4.3 Results of the calibration and choice of the model

Among all the simulations performed, number 50 has shown the best results for what concerns the reference calibration features and it has been chosen in order to reproduce the November 2002 flood event. In the following, the results of the parameters related to four simulations will be proposed. In particular, the trial number 29, 34, 44 and 50 have been selected, each of them to highlight improvement of the obtained results and to remark encountered problems and wrong values. Therefore, for each of the aforementioned simulations, the flooded area, the hydrometer levels, the scatterplot of the control points and the water profile will be proposed, all of these compared with the observed values used for the model calibration.

As far as the flooded area is concerned, the obtained one has been compared with the one observed in previous studies (*Rossetti & Cella, 2010b*). In Figure 3-27, Figure 3-28, Figure 3-29 and Figure 3-30, the obtained MAXWSE maps, namely the envelopment of the highest water level reached by the individual grid cell during the entire simulation, have been overlapped to the red polyline representing the observed flooded area by Rossetti and Cella.

The second parameter taken into consideration for the model calibration is the level registered at the hydrometer station, located in the second archway of the “Napoleone Bonaparte” bridge. The plots below show the comparison between the obtained hydrometer levels during the simulations and the observed ones by past studies (*Rossetti & Cella, 2010b*).

In order to compare the averaged observed WSE of each cluster and the WSE obtained in control points, a scatterplot has been created and reported below. It has to be remarked that the more the points are closed to the red bisector line, the more the match between observed and obtained WSE. Eventually, the water profiles obtained through the measures of selected points along the river Adda in between the boundary condition have been reported. In particular, the water level at the 65th and the 120th hours of the simulation, namely respectively the peak and the final time intervals of the input hydrograph, have been overlapped.

Looking at the results of the simulation number 29, a wider flooded area with respect to the observed one in 2002 has been obtained, due to the increased water levels in the downstream boundary condition (+10% of the original values), assumed in this trial. Regarding the hydrometer level, neither the peak nor the trend of the obtained levels matches the observed ones by past studies. The scatterplot of the simulation number 29 shows that half of the obtained WSE in clusters are far from the match bisector line, with some values more than 1m higher than the corresponding observed. The water profile of this trial is in line with the expected results and no backwater nearby the downstream boundary condition has been registered. As consequence of the wrong results in the first three assessed parameters, the simulation number 29 has been discarded.

Moving to the trial number 34, a good match between the flooded areas has been obtained, as well as the compared levels in control points shown in the scatterplot. However, both the peak and the trend of the obtained hydrometer levels are far from the observed ones in 2002. Moreover, the water profile highlights the presence of backwater in correspondence of the downstream boundary condition, in which there is not an expected decreasing of the levels at the 120th hour of the simulation. These wrong water levels increase the ones nearby the municipality, improving the results for what concerns the flooded area. However, after the computation of the hydrometer

levels, it has been noticed that the good match in the flooded area was due to the backwater and not to the correct calibration of the model. Therefore, simulation number 34 has been abandoned too.

Figure 3-29, related to simulation number 44, shows an improvement in the obtained results of the analysed parameters. In particular, the flooded area covers almost the same perimeter of the observed one by Rossetti & Cella, with the exception of the fields located on the East side of Lodi. In particular, looking at the hydraulic left downstream of the “Tangenziale sud” state road, some agricultural areas, observed as flooded, have not been inundated by the model simulation. However, analysing the bathymetry file, the aforementioned zones have higher altitude than the closed flooded and so very difficult to be inundated. This mismatch could be due to an envelopment selection of the wet area after the simulation performed in past studies. Moreover, other reasons may be the not completely reliable water levels, described in the damage compensation forms and compiled by the involved citizens as well as reconstructions from photos taken after the event. Regarding the comparison between obtained and observed hydrometer levels, an improvement in the results has been noticed. This is due to the different hydrograph (curve 4), used as upstream boundary condition in the BCs input file. On the contrary, the scatterplot shows lower levels with respect to the ones of simulation number 34 and this result is in agreement with the missing flooded area described before. The water profile of trial number 44 is in line with the expectation and no backwater has been observed. In order to improve the results of the hydrometer and of the flooded area, other simulations have followed.

Eventually, simulation number 50 has shown the best results for all the assessed parameters and has been selected as final result of the model calibration. As it can be seen in the Figure 3-30, the obtained flooded area matches the observed perimeter with the exception of a wider area on the West side of Lodi and missing ones downstream of the “Tangenziale sud” state road. For what concerns the comparison of the hydrometer levels, the trends of the two curves are almost the same over the entire simulation and the peak values very similar, being the obtained one at 68.32 m a.s.l. and the observed one at 68.26 m a.s.l.. It has to be remarked that for this simulation, the hydrograph named as “curve 6” has been used as upstream boundary condition. Looking at the scatterplot of simulation number 50, one point representing clusters E is almost 1 m apart from the match line. This is due to the fact that the average values of this cluster have been obtained taking control points covering a wide area. It is worth to remark also that the reference observed WSE values come from not fully reliable sources and this limitation has been taken into account. However, the obtained results in control points show a good match with the observed ones. The water profile of this trial does not show problems related to backwater of water nearby the downstream boundary condition. This brings to reliable water levels obtained at the hydrometer station and in several control points in Lodi, being the latter not influenced by downstream backwater. Moreover, these results have been obtained simulating the November 2002 flood scenario, that approximately can be referred to 120 years return period. Therefore, increasing the severity of the event (i.e. $T=200$ and $T=500$), the aforementioned backwater would have a greater influence to the modelled water levels observed, also being able to influence the values obtained in the city of Lodi.

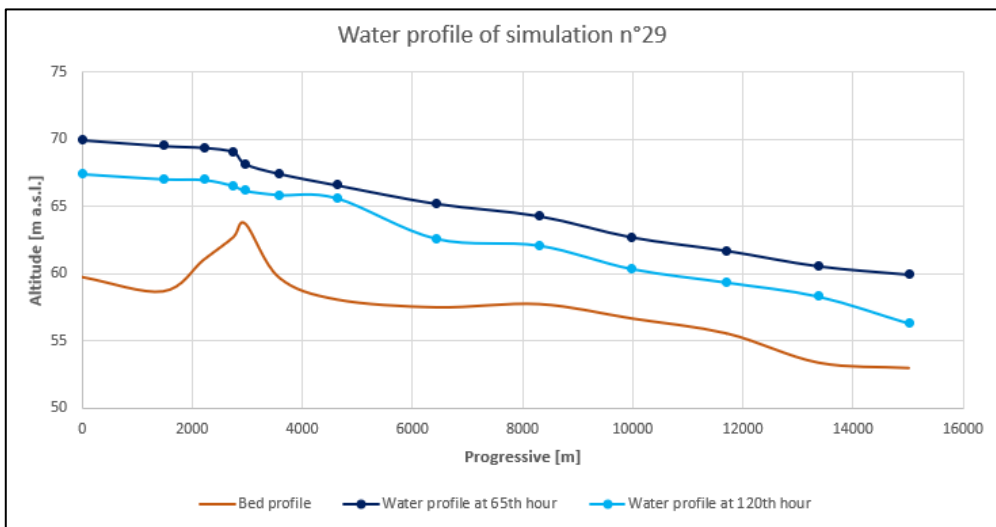
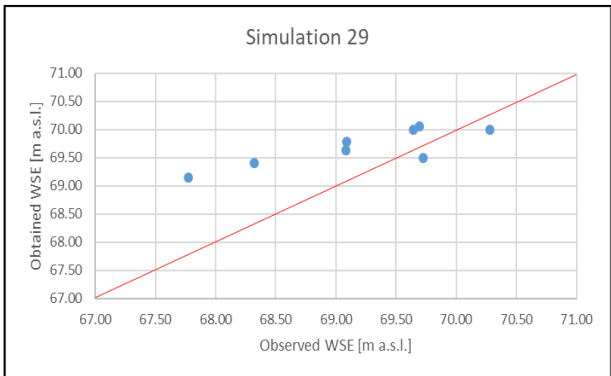
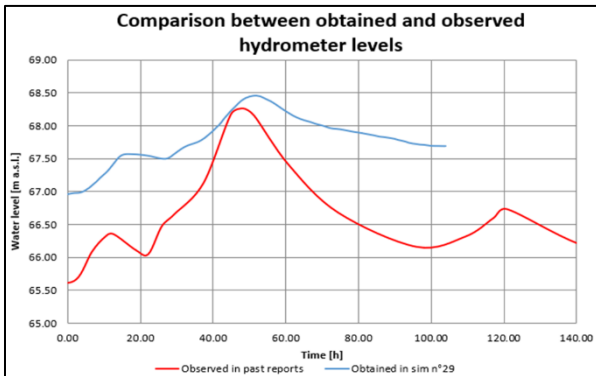
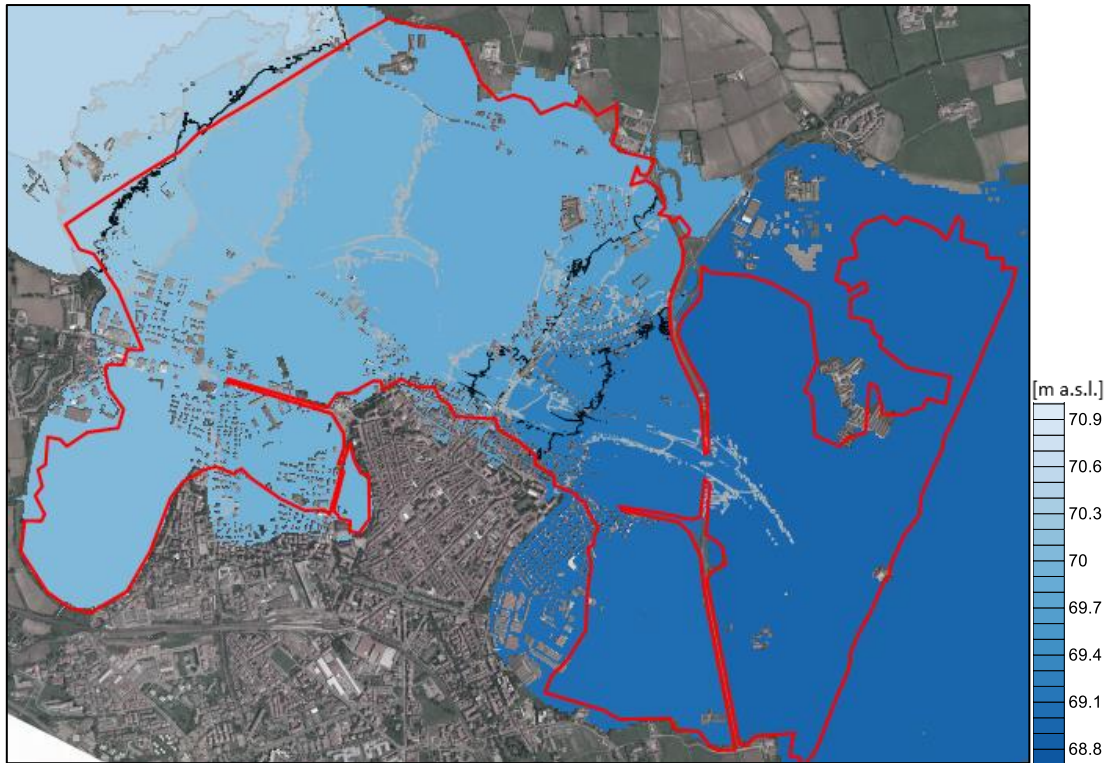


Figure 3-27 Results of the simulation n°29

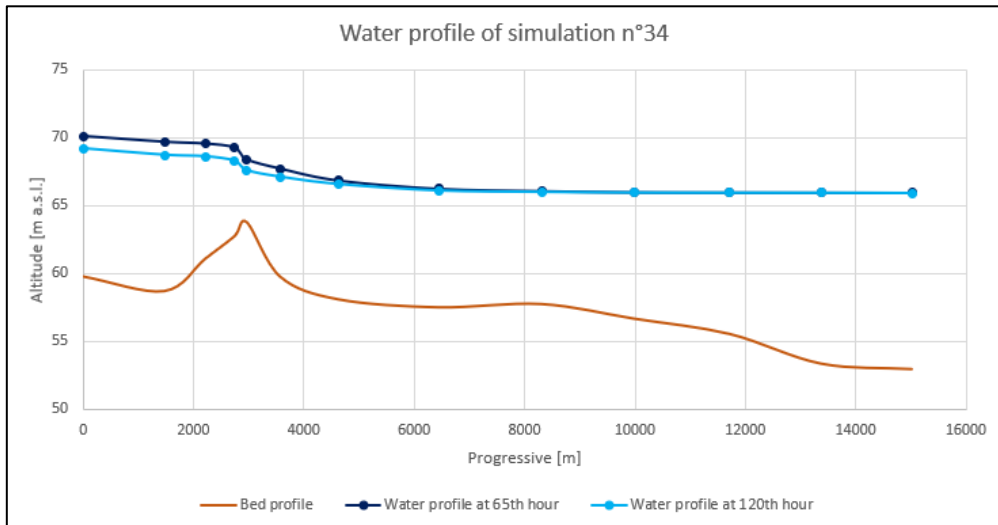
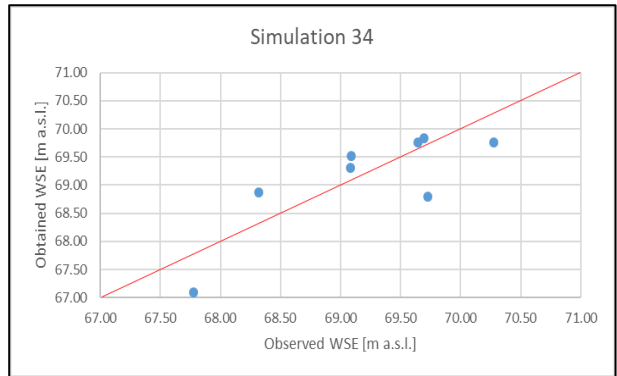
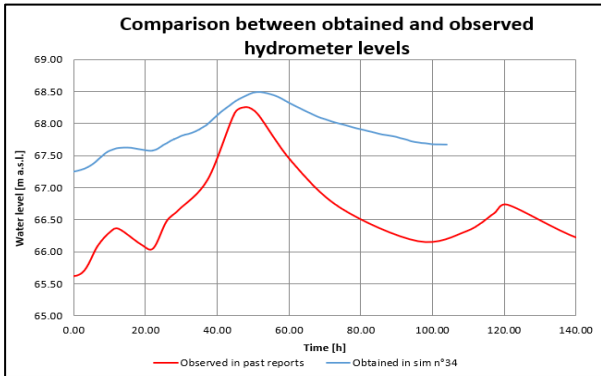
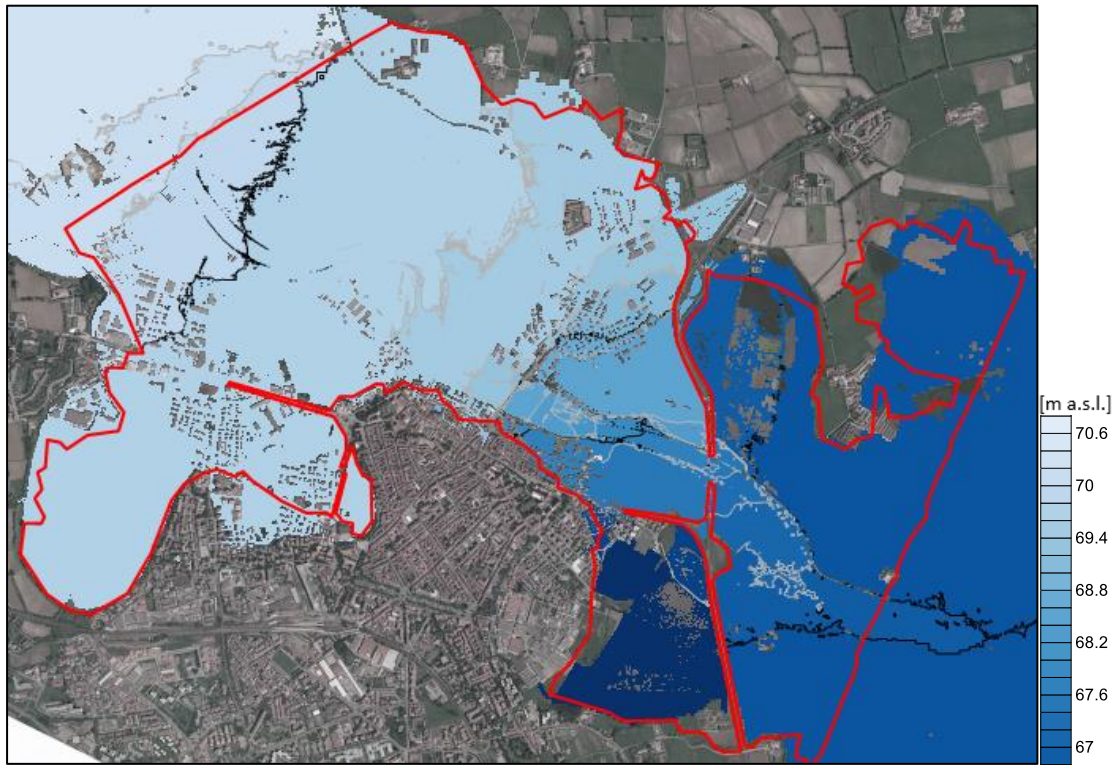


Figure 3-28 Results of the simulation n°34

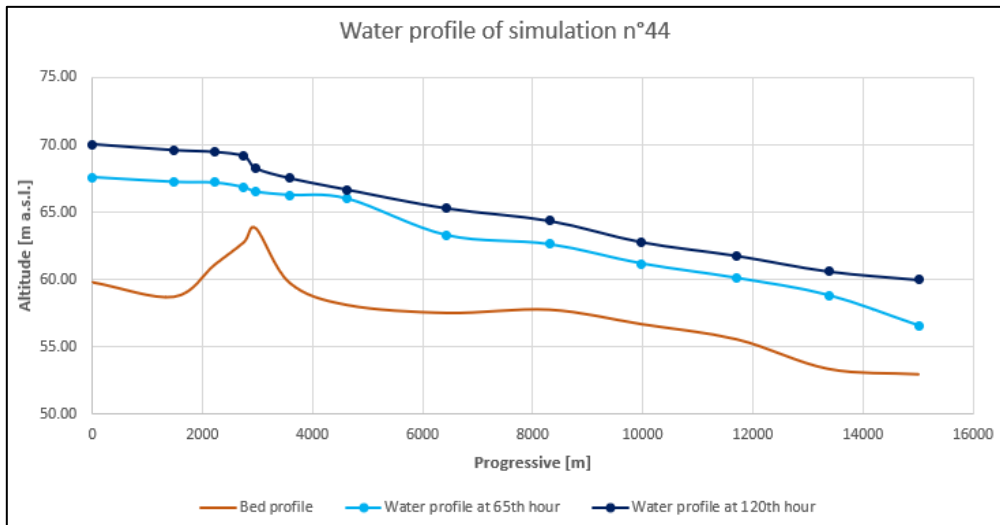
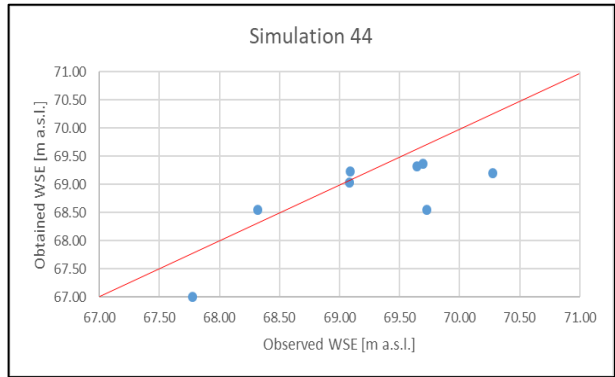
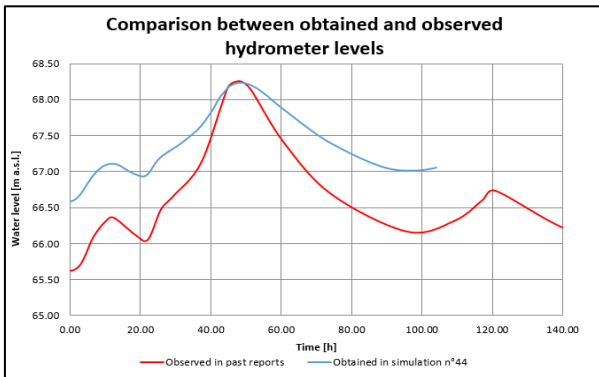
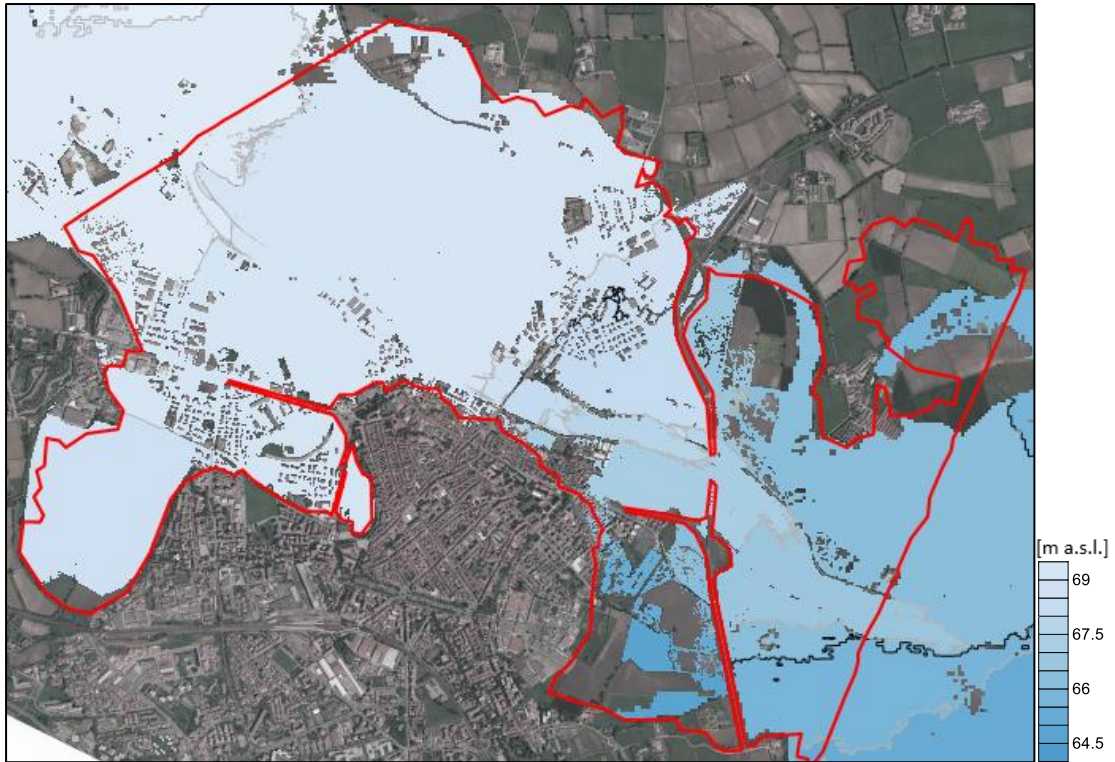


Figure 3-29 Results of the simulation n°44

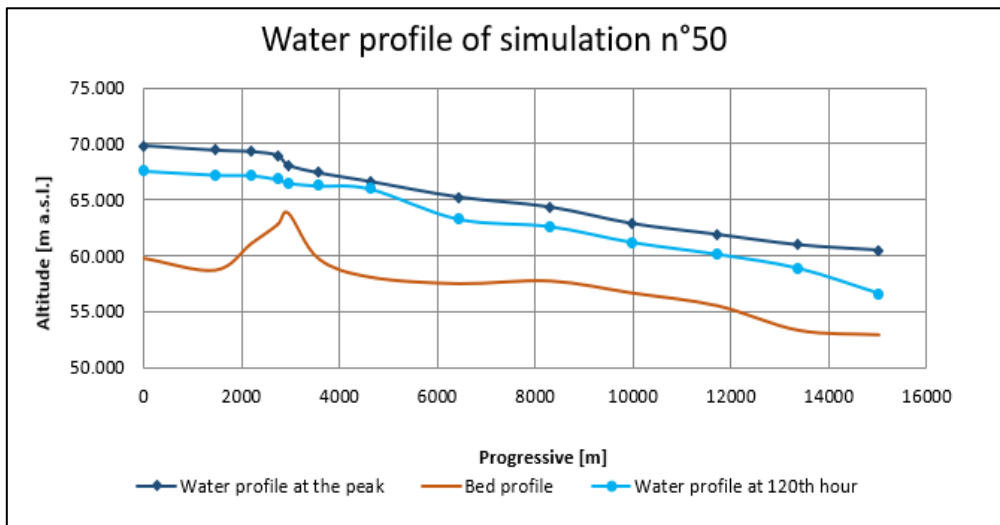
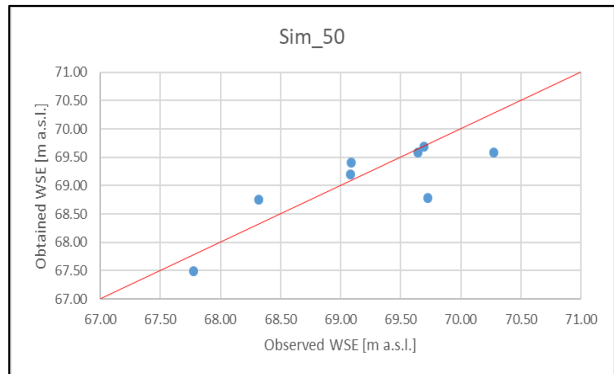
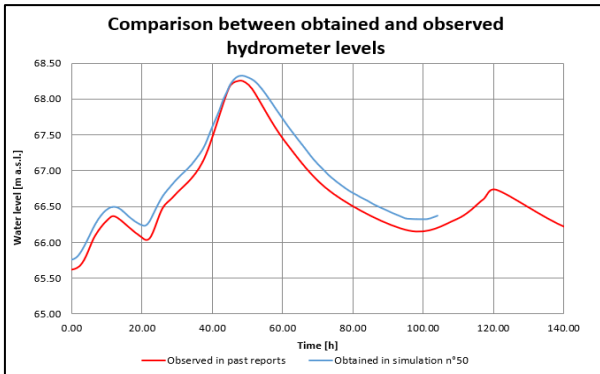
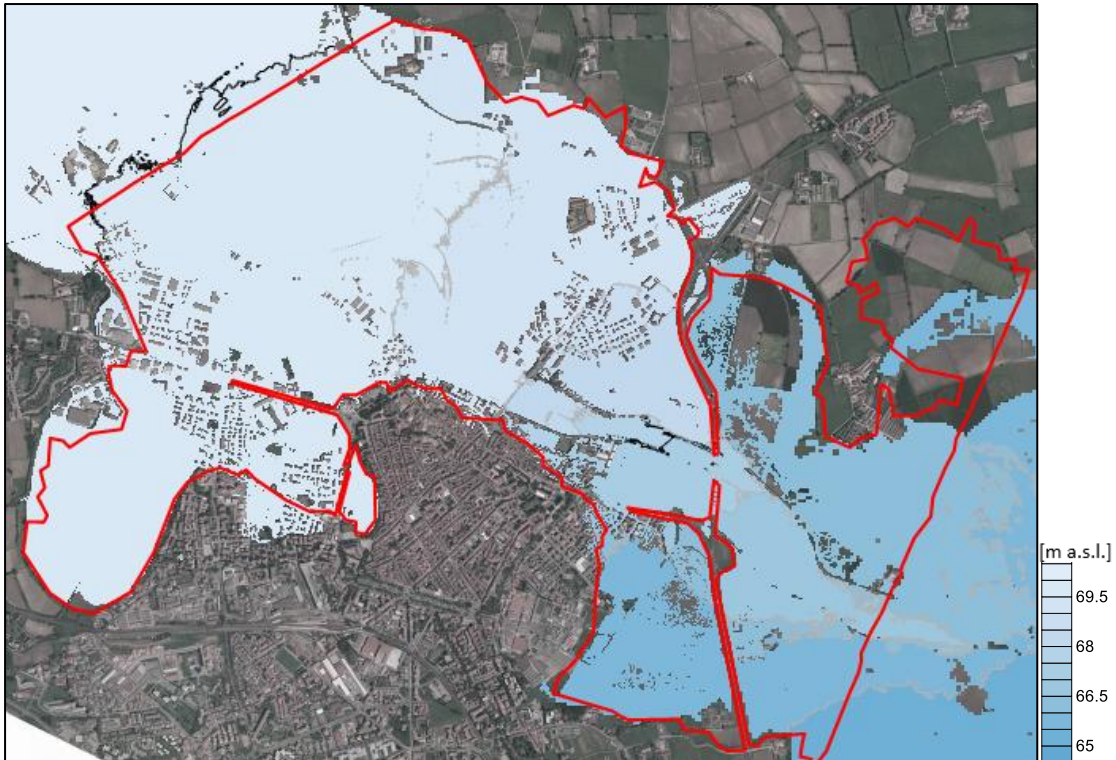


Figure 3-30 Results of the simulation n°50

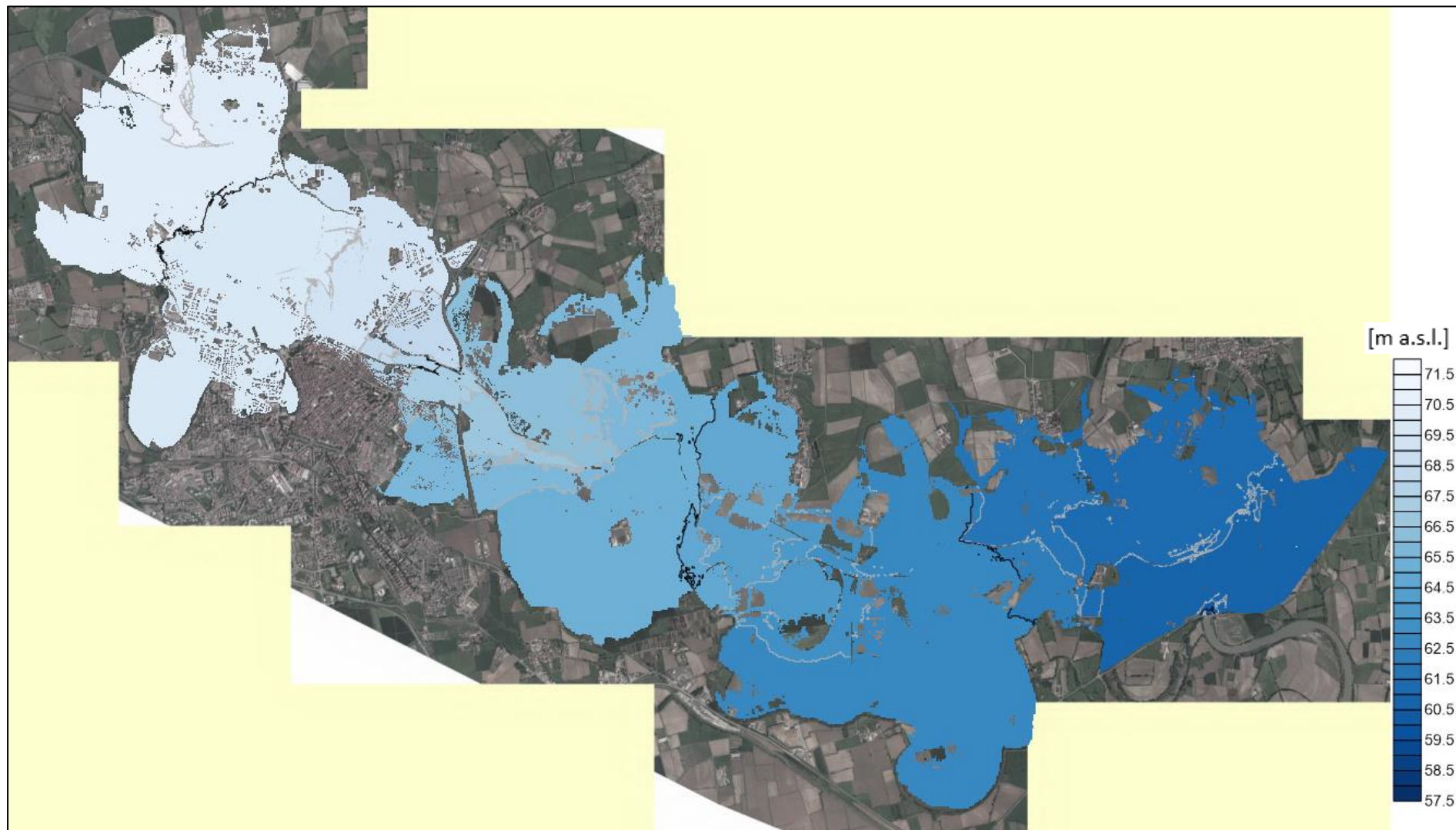


Figure 3-31 MAXWSE on the entire domain of simulation n°50

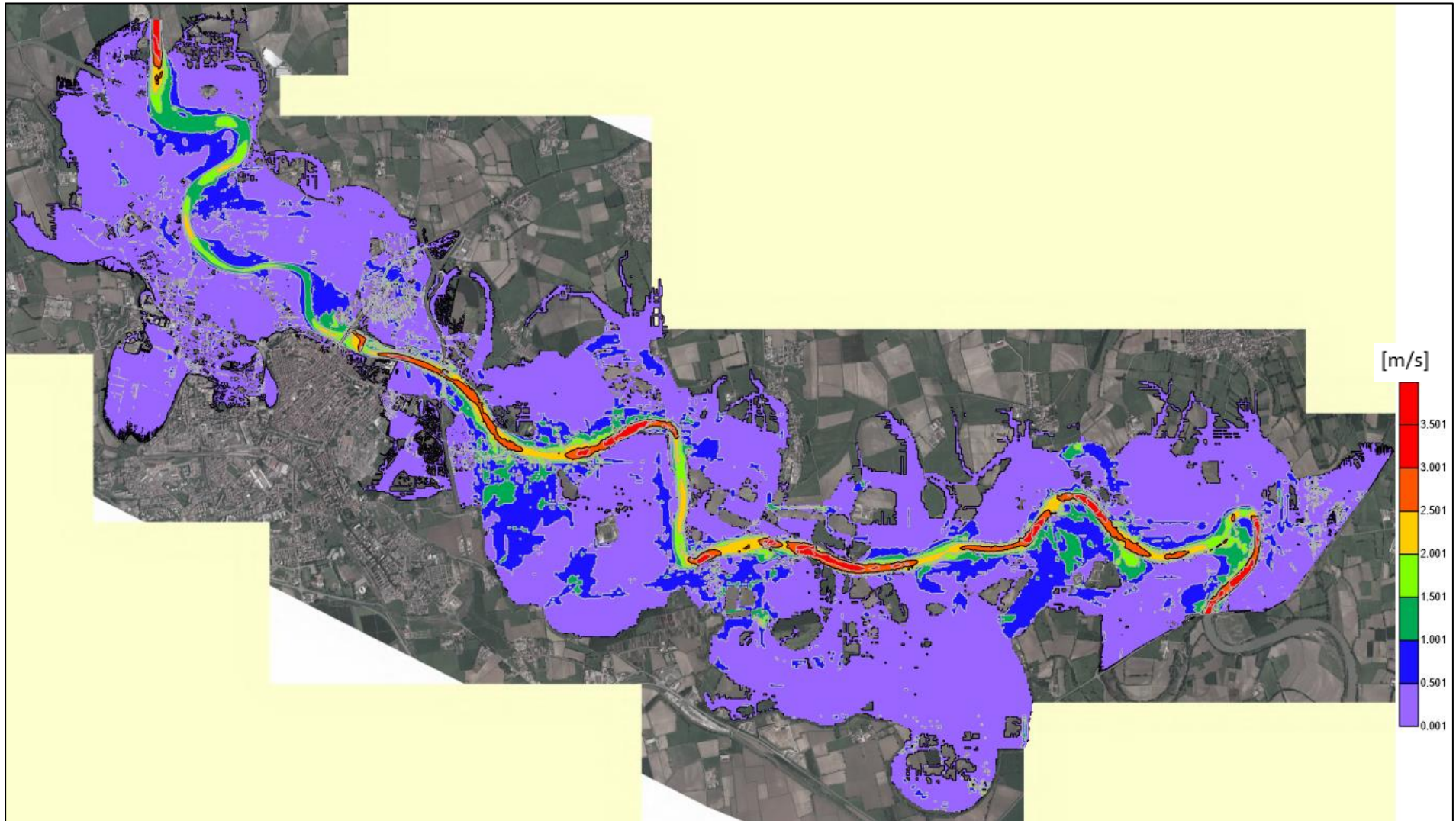


Figure 3-32 MAXVEL on the entire domain of the simulation n°50

3.1.4.4 Results of the quantitative indicators for the goodness of the simulations

In addition to the four aforementioned parameters, the following indicators have been computed in order to identify the best simulation performed or, at least, to check if the selected one (simulation number 50) has a result close to the best one. The observed and obtained values for the computation of the indicators are the same ones used for the previous scatterplot.

In order, results of the Average Difference (AD), of the Absolute Average Difference (AAD) and of the Nash-Sutcliffe Efficiency (E) are reported in Figure 3-33, Figure 3-34 and Figure 3-35. It has to be remarked that the simulations number 20, 21 and 25 don't show results due to an unexpected shutting down of the "Parflood" calculation code. The reason behind the uncomplete simulation could be due to the reach of the critical level of water along the considered stretch of the river Adda.

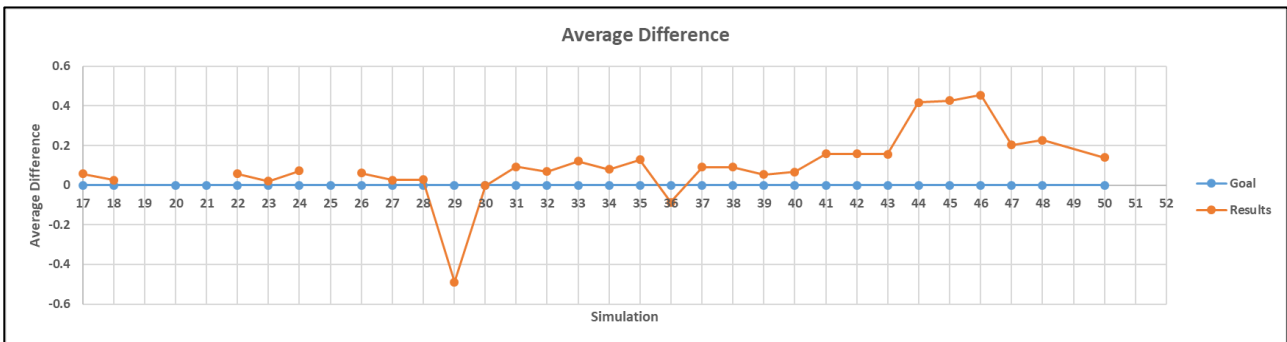


Figure 3-33 Results of the Average of Difference indicator

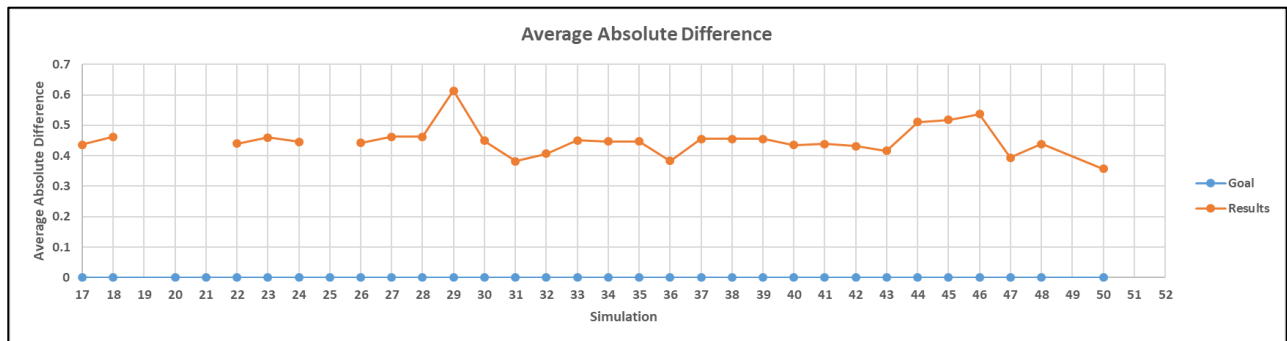


Figure 3-34 Results of the Average Absolute Difference indicator

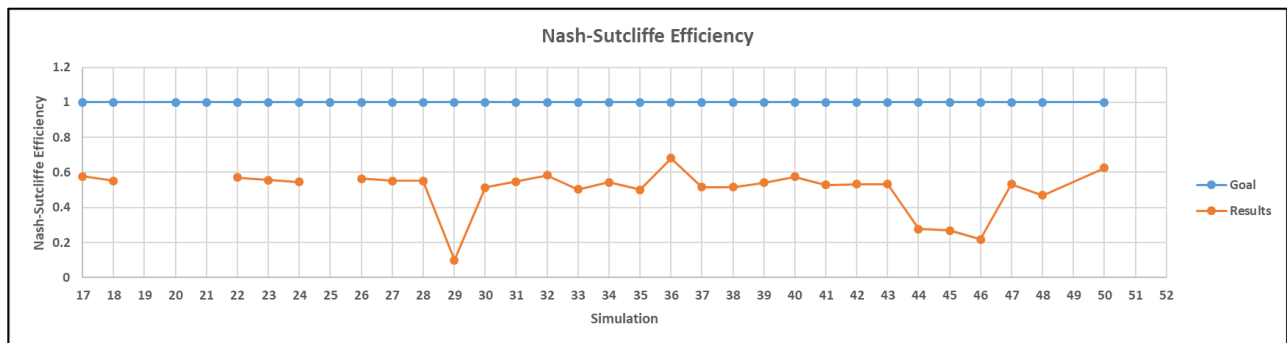


Figure 3-35 Nash-Sutcliffe Efficiency indicator

The average difference indicator results show that for the entire simulation, with the exception of the number 29 and 36, there is abundance of water in the model. The value of simulation 50 is not far from the best result of this indicator. For what concerns the average absolute indicator, the last simulation, namely the chosen one, provides the best results among the other trials, which confirms also the good quality of the other parameters assessed in the model calibration. Nash-Sutcliffe efficiency result of the last simulation is very close to the best one, obtained with the trial number 36. Therefore, as quantitative indicator of the goodness of the result for the model calibration, the obtained values for simulation number 50 are among the bests and the latter confirm the choice of assuming this trial as representative for the November 2002 flood event.

During the computation of these indicators, a remarkable difference has been noticed between obtained and observed average values for the cluster E. Therefore, it has been assumed that the latter has a greater influence with respect to the other clusters. Indeed, as it is possible to observe from the Figure 3-36, the most upstream and the further downstream points are almost 1 km apart and an average value over the entire area could bring to some uncertainties in the result. In order to highlight this fact, the Average Difference, the Average Absolute Difference and the Nash-Sutcliffe Efficiency indicators have been calculated again, considering the cluster E split in two separate groupages (Figure 3-36). The results show an improvement in the values of the three indicators. In detail, focusing on simulation number 50, namely the one chosen as calibrated flood model, the AD goes from 0.139 to 0.110, the AAD from 0.357 to 0.304 and the E from 0.63 to 0.74. Therefore, it can be asserted that the cluster E has a strong influence in the calculation of the three indicators and underline a potential limitation regarding the use of wide zonal clusters for control points in the calibration procedure.



Figure 3-36 Sub-division of the cluster E

“Page intentionally blank”

3.2 Hazard assessment for some reference scenarios

In order to create the flood hazard maps necessary to estimate potential damages, synthetic hydrographs, to be used as input in Parflood model, have to be computed. In particular, for what concerns the November 2002 flood event, the hydrograph to be used as upstream boundary condition has already been found, as result of the model calibration. For the other four reference scenarios (T=50, 100, 200 and 500 years), different hydrographs have to be computed starting from the same synthetic curve. The whole procedure to find the latter will be explained in detail in the continuation of this chapter, after the description of the available data for this assessment. At the end of this chapter, the flood hazard maps will be presented, both without and with structural defences, for the five reference scenario.

3.2.1 Available data for hazard assessment

The available data for the hazard assessment is summarised in Table 3-3, reporting the typology of data, the source, the date and the utilization in this thesis work.

Table 3-3 Available data for hazard assessment

AVAILABLE DATA	SOURCE	DATE	UTILIZATION
Hydrometer levels from July 1998 to June 2018	ARPA Lombardia (<i>"Agenzia Regionale per la Protezione dell'Ambiente"</i>).	2018	Creation of synthetic hydrographs for flood hazard maps
Relationship between return period T and discharge Q in Lodi	<i>Studio idrologico-idraulico del tratto di F. Adda (Rossetti & Cella)</i>	March 2005 – updated on January 2010	Creation of synthetic hydrographs for flood hazard maps

3.2.1.1 Relationship between return period (T) and discharge (Q) of the Adda in Lodi

Figure 3-37, reporting the results of past hydrologic studies, shows the peak discharge for different return periods T. The dashed red curve is the one taken into consideration for the construction of the structural defences in Lodi after the occurrence of the 2002 flood event. Moreover, the discharge corresponding to T= 50, 100, 200 and 500 years of this curve have been assumed as peak values in the four input synthetic hydrographs, used for the creation of the five hazard maps (the hydrograph of the scenario T=120 years, corresponding to the November 2002 flood event, has been obtained during the calibration procedure).

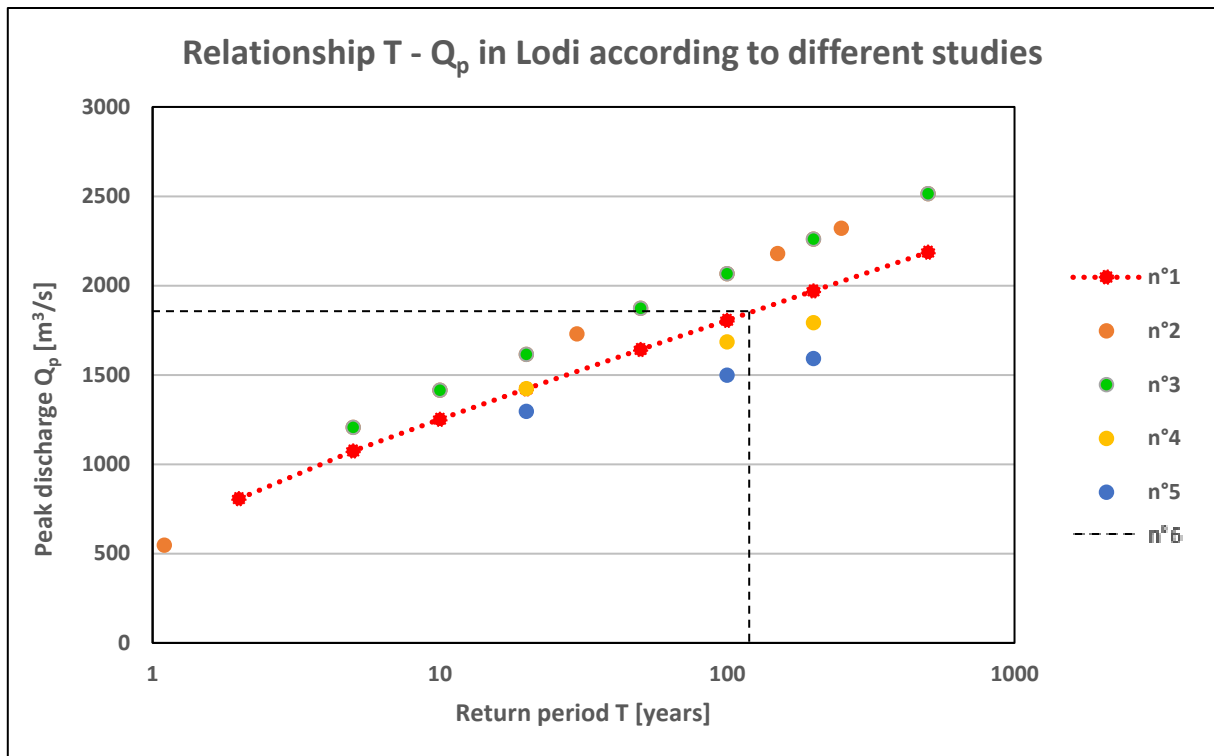


Figure 3-37 Relationship $T - Q_p$ in Lodi according to different studies, where: 1) $Q(T)$ from past study by Rossetti & Cella in 2005; 2) $Q(T)$ based on Gumbel function by Rossetti in 2005; 3) $Q(T)$ from several studies by Paoletti in 2005; 4) $Q(T)$ upstream of Lodi from past report “Sottoprogetto SP1” by AdbPo; 5) $Q(T)$ downstream of Lodi from past report “Sottoprogetto SP1” by AdbPo; 6) Estimation of the return period of the November 2002 flood event

Table 3-4 Relationship $Q - T$ for reference scenarios according to Rossetti & Cella (2005)

T [years]	Q [m³/s]
50	1642
100	1806
200	1971
500	2187

3.2.2 Synthetic boundary conditions for reference scenarios

In order to create hydrographs for different return periods T , a synthetic curve has been created. The latter is the result of an elaboration of different events, identified in the last twenty years. In detail, the hydrometer levels registered from the second half of 1998 until the first half of 2018 have been taken and 17 events with water level higher than 1 m from the hydrometric zero (64.85 m a.s.l.) have been selected. Then for each of the previously mentioned water levels, the corresponding discharge Q has been computed using the rating curve described by the formula:

$$Q = 4.9521 * h^{3.2557}$$

where the variable “ h ” is obtained through the difference between the water surface elevation detected by the hydrometer and the elevation of the river bed in the same position.

After that, the 17 different curves have been overlapped in the Figure 3-38. The latter contains on the x axis the adimensionalisation $[(t - t_p) * Q_p] / d_p^3$, where t_p , Q_p and d_p are respectively the time, the discharge and the water depth in correspondence of the peak of the hydrographs, while on the y axis, the adimensionalised value Q/Q_p has been chosen.

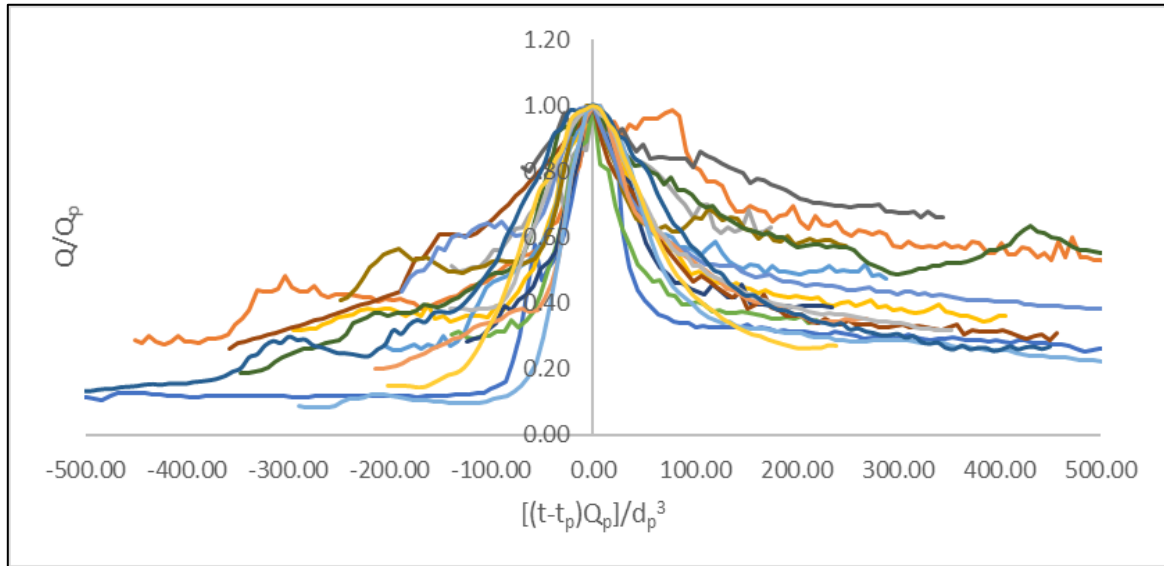


Figure 3-38 Adimensionalised representation of the 17 chosen events

Then, the temporal string of the x axis adimensionalisation between -70 and 175 has been chosen, that represent the largest interval in which all the 17 selected events contain values of Q/Q_p . After that, an interpolation (function interp1 using MATLAB with time step 5) has been computed for all the aforementioned curves. The average value for each time step has been obtained and shown in the Figure 3-39, overlapped with the previous curves, in the selected temporal string between -70 and 175.

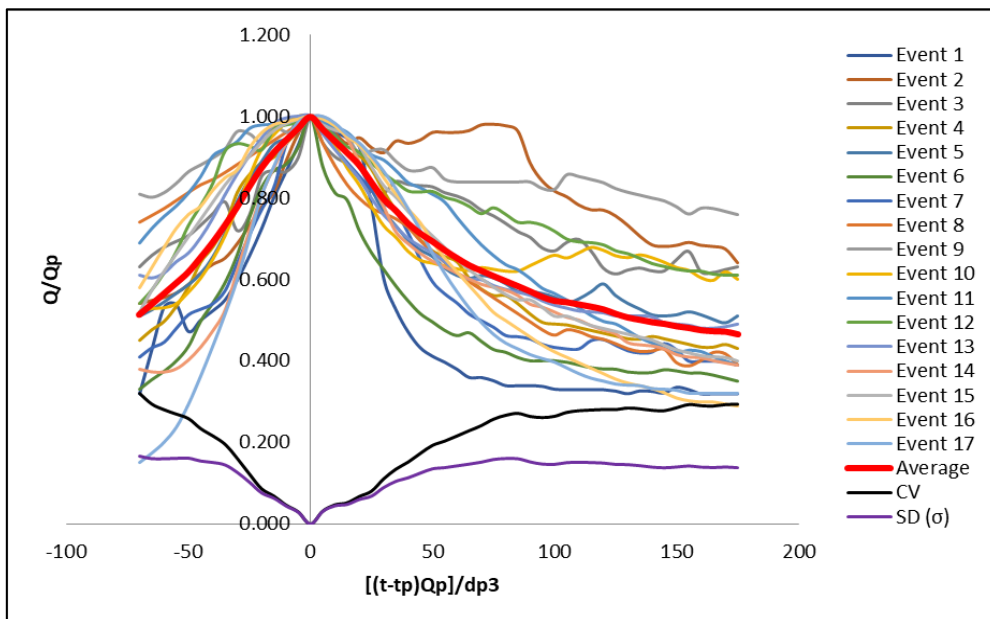


Figure 3-39 Representation of the average curve

The following step concerns the transformation of the adimensionalised average curve into a dimensionalised hydrograph. In order to do so, the value Q/Q_p has been multiplied with the Q_p corresponding to each return period, selected for the creation of scenarios with different severities. For what concerns the x axis, the adimensionalisation $[(t - t_p) * Q_p] / d_p^3$ has been multiplied by the d_p^3 coming from the previous formula of the rating curve and divided by the Q_p . Eventually, imposing t_p equal to zero, the dimensionalised synthetic hydrographs for different return periods T have been obtained. In Figure 3-40, the curves for T equal to 50, 100, 200 and 500 years are reported. It has to be remarked that the original synthetic curves had a duration of 82 hours and, in order to create hydrographs of 120 h like the ones used in the model calibration, more values coming from simple linear interpolations have been added.

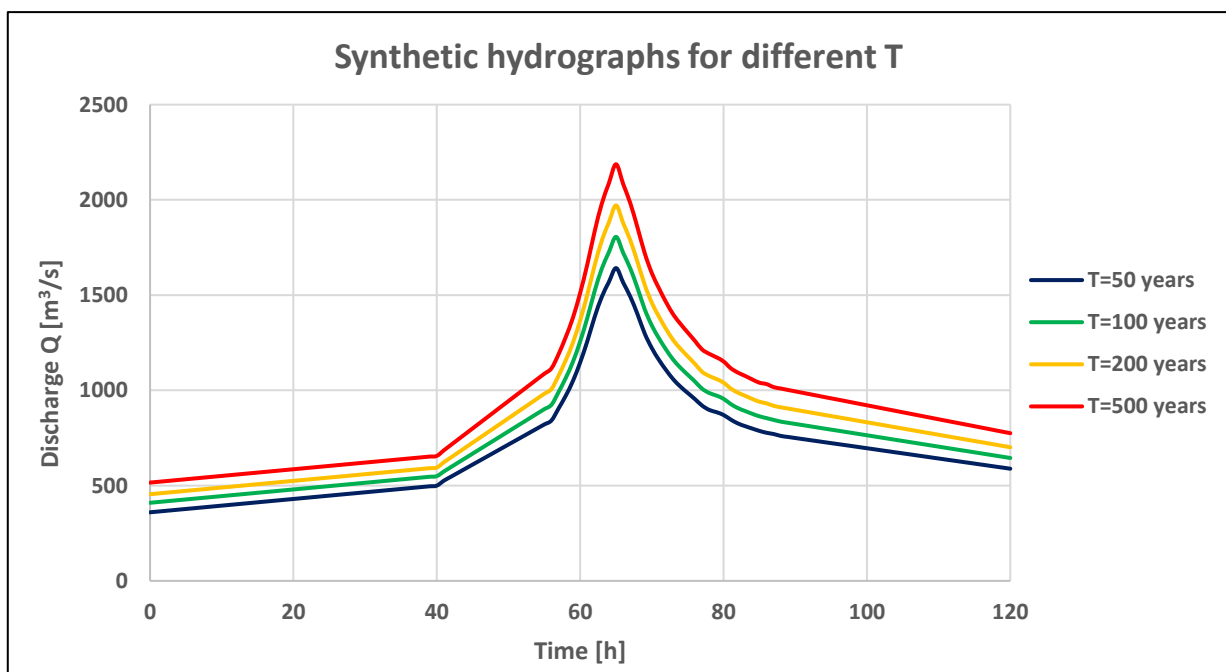


Figure 3-40 Estimated synthetic hydrographs for different return periods T

Through the use of these synthetic hydrographs, the hazard maps for events with 50, 100, 200 and 500 years have been created. The assumed peak discharges for these return periods have been taken from the relationship $Q - T$ the Table 3-4. In addition to the mentioned reference return periods for flood hazard assessment, the event representing the November 2002 flood event in Lodi has been considered too. The latter has been identified as a T=120 years event scenario, taking the peak discharge of the hydrograph used for the last simulation of the calibration. Indeed, the maximum value of water discharge (1840,39 m³/s) has been estimated of an event with a greater severity with respect to the 100 years return period, as shown by the dashed black line in the Figure 3-37.

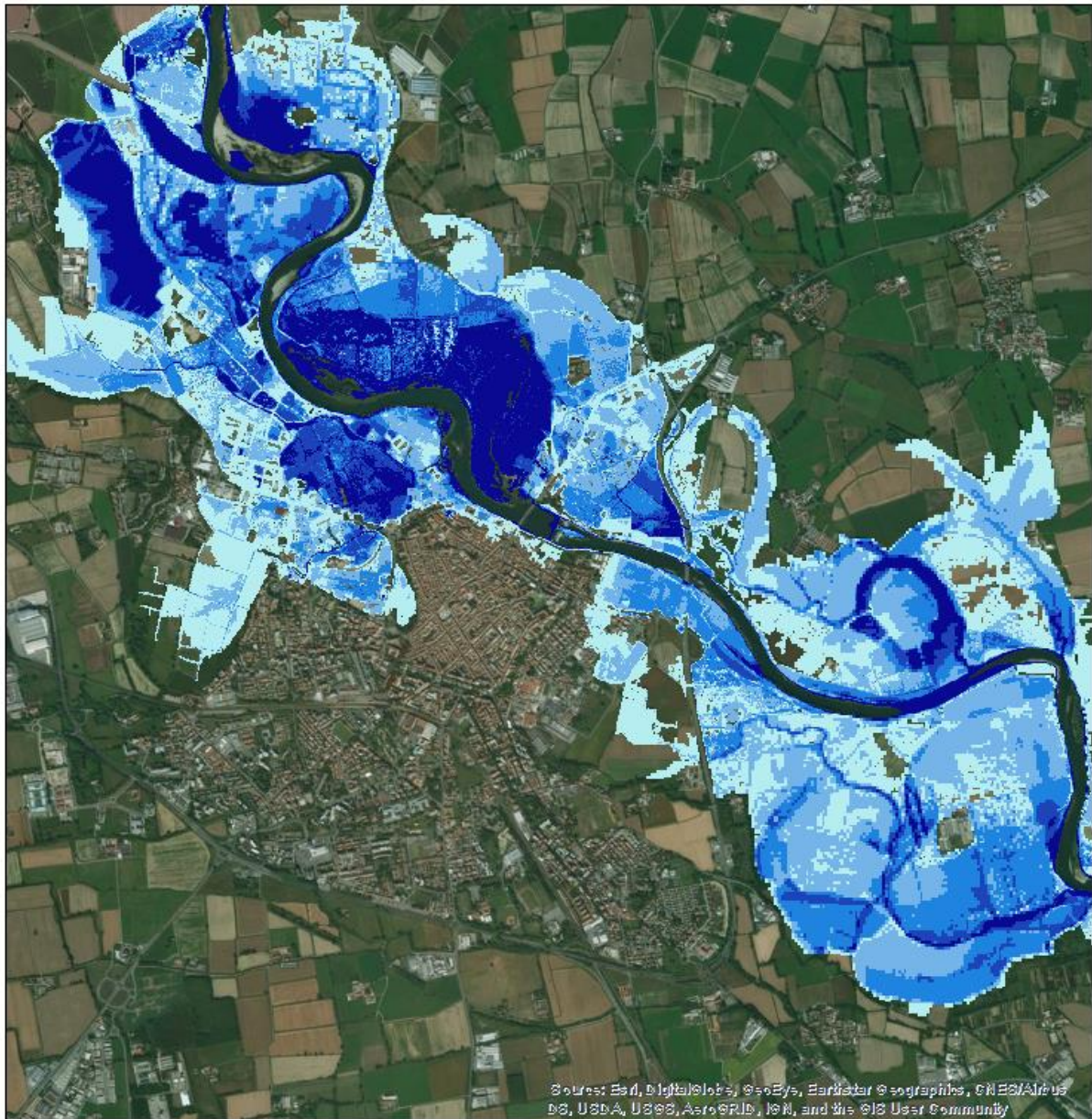
3.2.3 Flood Hazard Maps

In the following, ten hazard maps representing the maximum water depth (MAXDEP) for events with 50, 100, 120, 200 and 500 years of return periods, with and without structural defences are reported. The maps have been obtained through the difference between the MAXWSE grid output file and geometry input file in the two different configurations. Indeed, the water depth has been assumed more relevant with respect to water velocity, considering the floodplain context and so the slope of the river Adda (around 1-2 ‰) in the Municipality of Lodi. Moreover, the water depth is the hazard parameter required by the used model in order to calculate direct damages. However, for the sake of completeness, a map representing the modelled water velocity (MAXVEL grid output file) of the November 2002 flood event (simulation n°50), on the entire computational domain, has been added in Figure 3-32. In order to ease the comparison of the hazard maps with and without structural defences, for each reference scenario, the flood maps in the two different configurations are represented in consecutive pages and in the same page view. It has to be remarked that the following images are extract of the flooded area over the entire computational domain, having a focus on the Municipality of Lodi. Moreover, grid cells with water depth greater than 3,5 m have been excluded from the representation, in order to reduce the range of displayed water depths (levels in the river are up to 15 m) and to have better resolution and distinction of levels in the city.

Results of the hazard maps are in agreement with the expectations, in terms of flooded area and water depth. For what concern the scenario with $T=120$ years, namely the November 2002 flood event, the flooded area and water levels in Lodi are results of the model calibration and, therefore, similar to the observed reference values. In regards the other four reference scenarios without structural defences, increasing the severity of the event from $T=50$ up to $T=500$ years, greater flooded area, as well as the water depths, have been obtained. In particular, the western and eastern areas of the historical town, on the hydraulic right of the river Adda, have shown increments of the flooded area, while slighter ones have been obtained on the left side of the river. Water depths progressively increase, reaching more than 2 m of depth in some areas of the Revellino district and upstream of it (on the hydraulic left) and in two zones upstream the historical town of Lodi (on the hydraulic right).

With the addition of defence walls and soil embankments, up to the 200 years of return period scenario, no flooded areas on the hydraulic right have been observed, highlighting the effectiveness of the built structural defences in terms of hazard reduction. Only two small areas are flooded, nearby the Tangenziale sud state road, downstream of Lodi, and next to the conjunction of the levee with the S.P. 202, upstream of the town, due respectively to the underpass that perpendicularly cross the Tangenziale sud viaduct and the lower level of the bicycle path located in the aforementioned conjunction. Different reasoning has to be done for the 500 years of return period event. Indeed, a considerable area upstream of Lodi is flooded, due to the fact that the structural defences have been designed taking as reference water levels the ones of a 200 years return period scenario with the addition of the safety margin. Therefore, it was expected that some areas would have been flooded due to the overflow of some elements of the structural defences, considering a more severe scenario. For what concerns the water depths, a slight increment of levels on the hydraulic left have been observed, due to the increase of volume of water, generated by the opposition of the structural defences on the hydraulic right.

Flood Hazard Map for T=50 years without structural defences



Legend Maximum water depth [m]

- < 0.5
- 0.5 - 1
- 1 - 1.5
- 1.5 - 2
- > 2

0 0.5 1 2 Kilometers



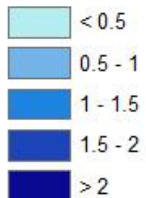
Figure 3-41 Flood Hazard Map for T=50 years without structural defences

Flood Hazard Map for T=50 years with structural defences



Legend

Maximum water depth [m]

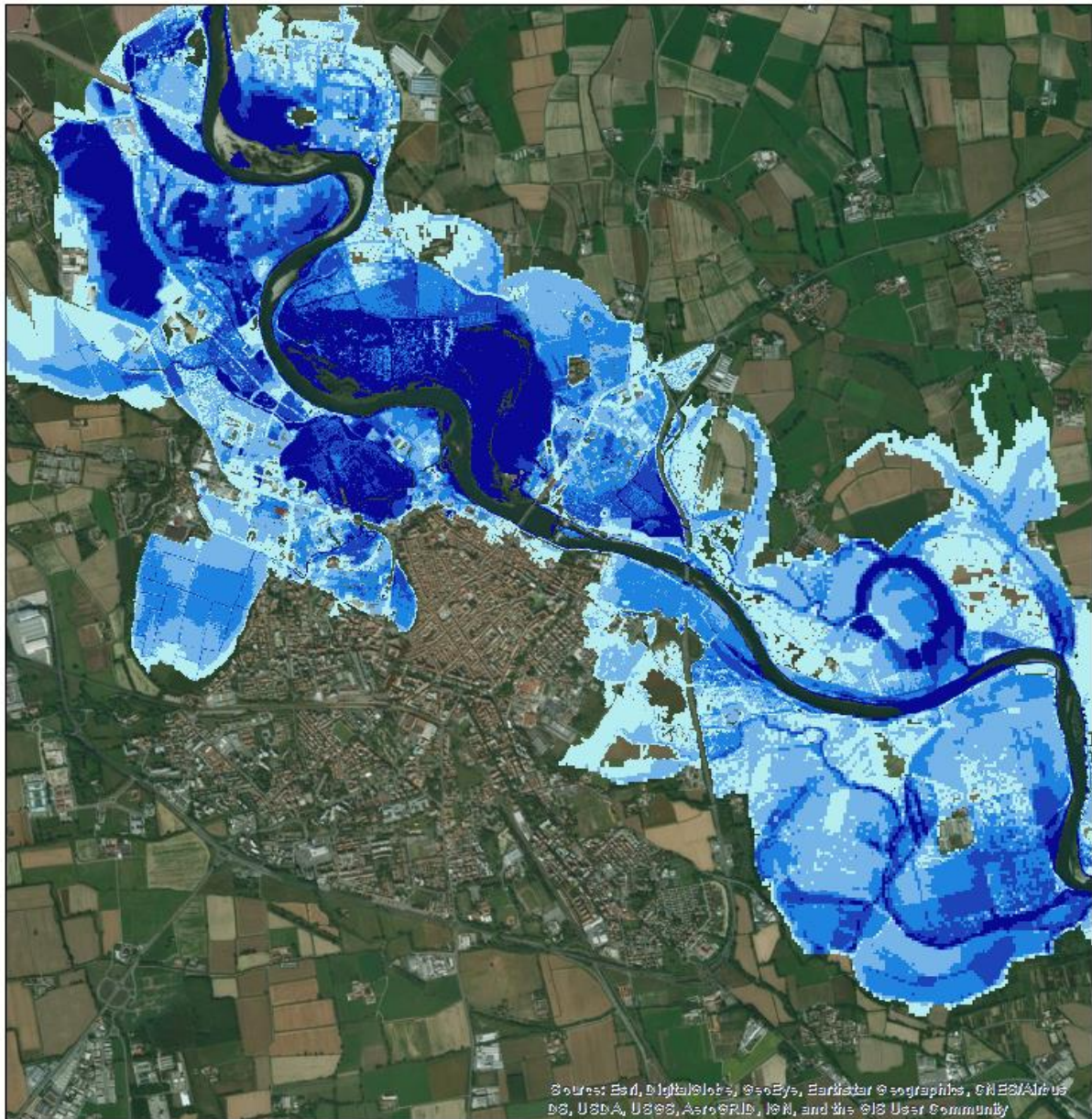


0 0.5 1 2 Kilometers



Figure 3-42 Flood Hazard Map for T=50 years with structural defences

Flood Hazard Map for T=100 years without structural defences



Legend
Maximum water depth [m]

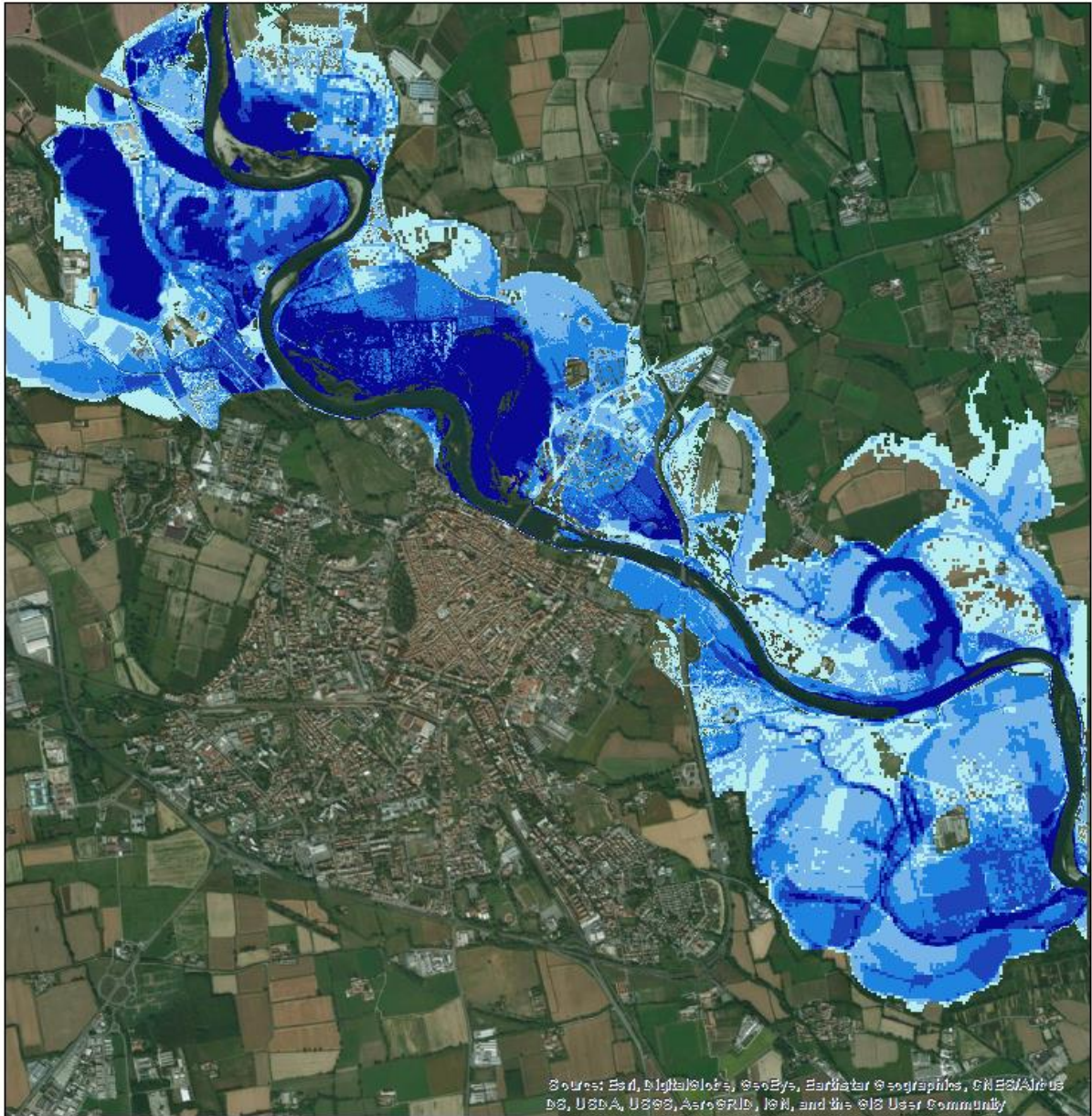
-  < 0.5
-  0.5 - 1
-  1 - 1.5
-  1.5 - 2
-  > 2

0 0.5 1 2 Kilometers



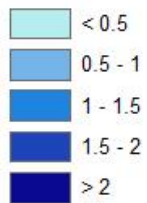
Figure 3-43 Flood Hazard Map for T=100 years without structural defences

Flood Hazard Map for T=100 years with structural defences



Legend

Maximum water depth [m]

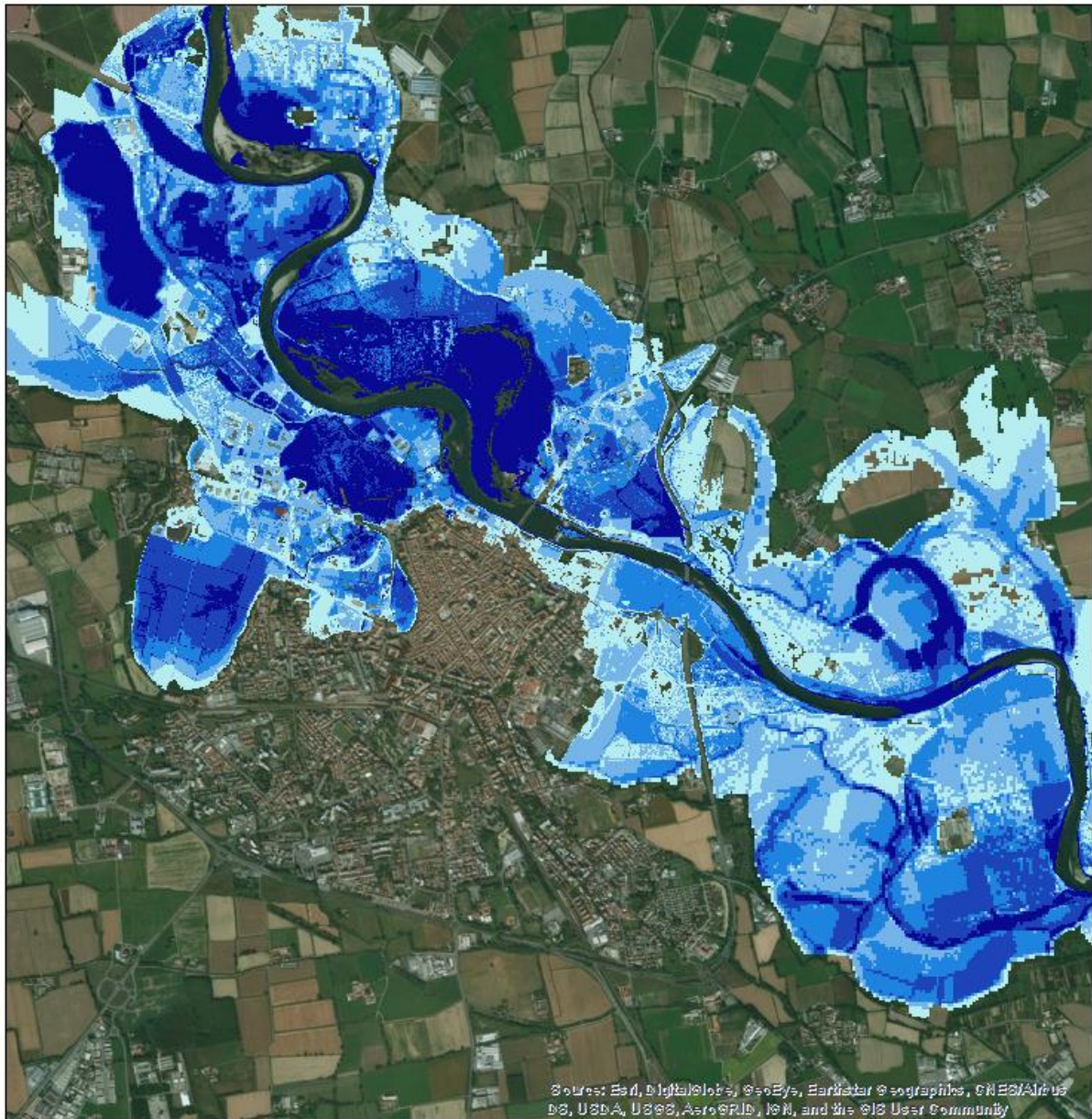


0 0.5 1 2 Kilometers

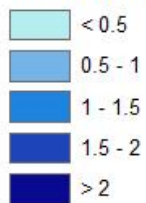


Figure 3-44 Flood Hazard Map for T=100 years with structural defences

Flood Hazard Map for T=120 years without structural defences



Legend Maximum water depth [m]

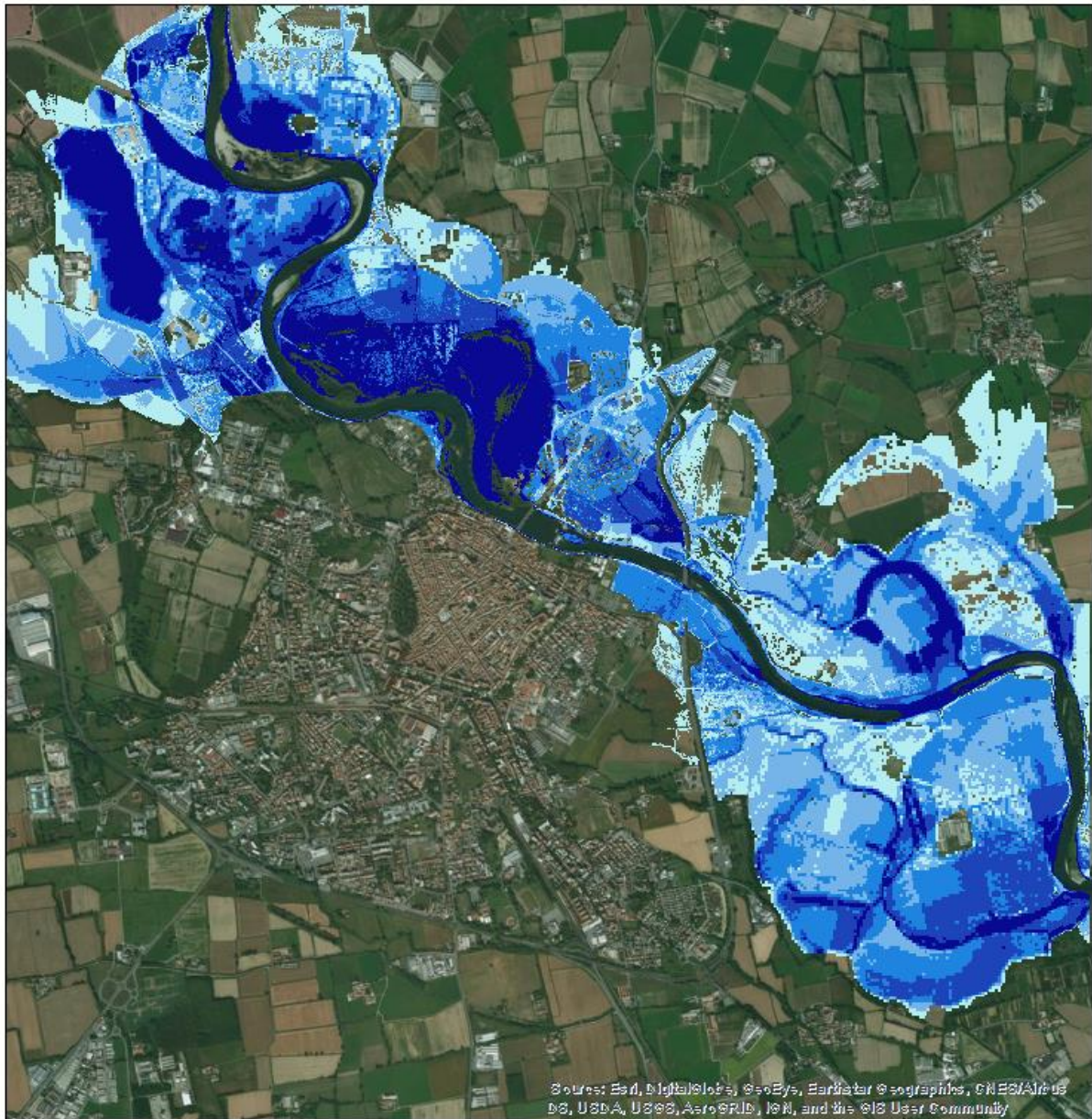


0 0.5 1 2 Kilometers



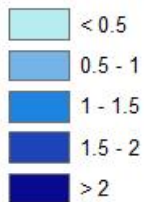
Figure 3-45 Flood Hazard Map for T=120 years, corresponding to the November 2002 flood event, without structural defences

Flood Hazard Map for T=120 years with structural defences



Legend

Maximum water depth [m]

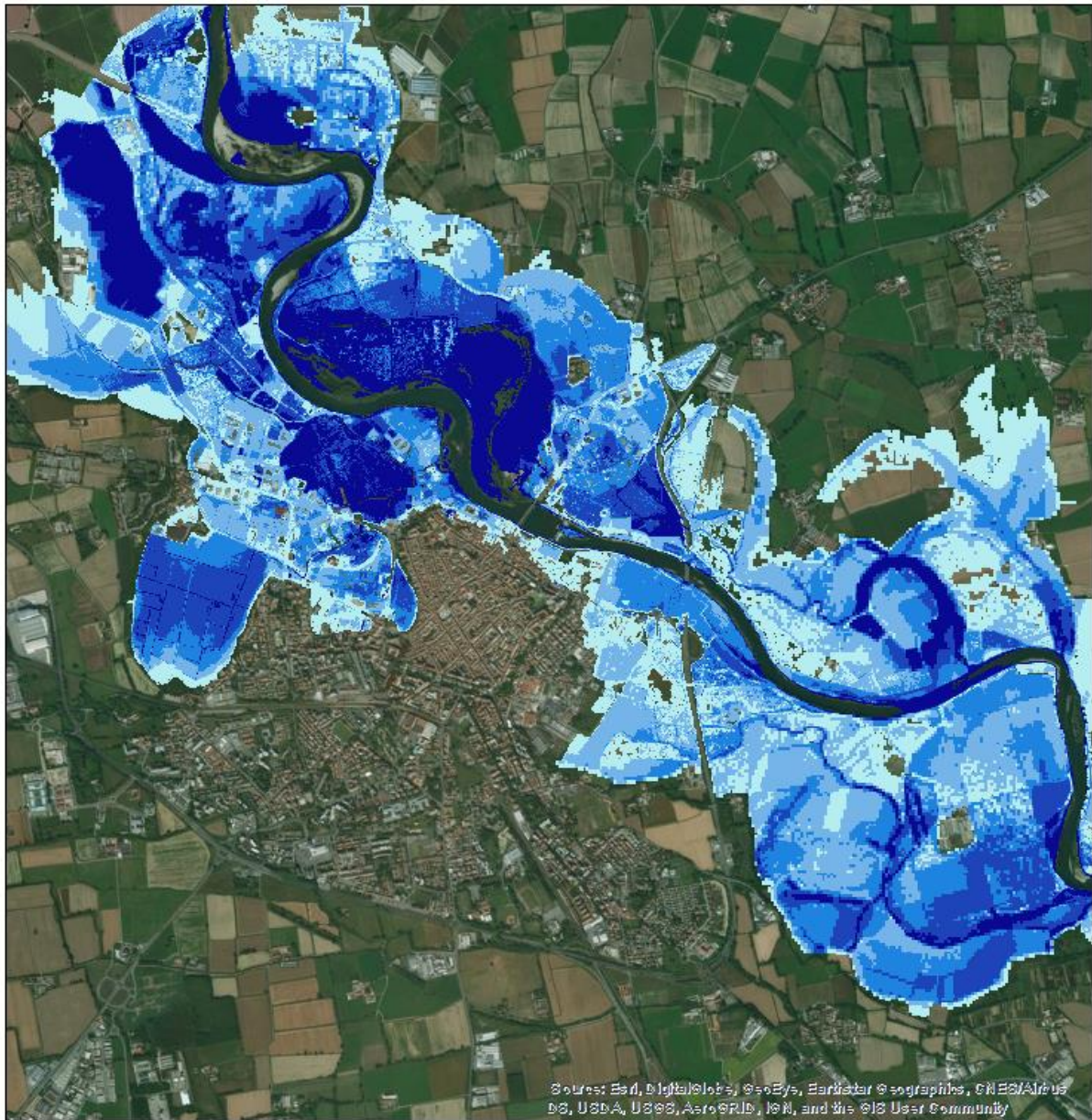


0 0.5 1 2 Kilometers



Figure 3-46 Flood Hazard Map for T=120 years, corresponding to the November 2002 flood event, with structural defences

Flood Hazard Map for T=200 years without structural defences



Legend
Maximum water depth [m]

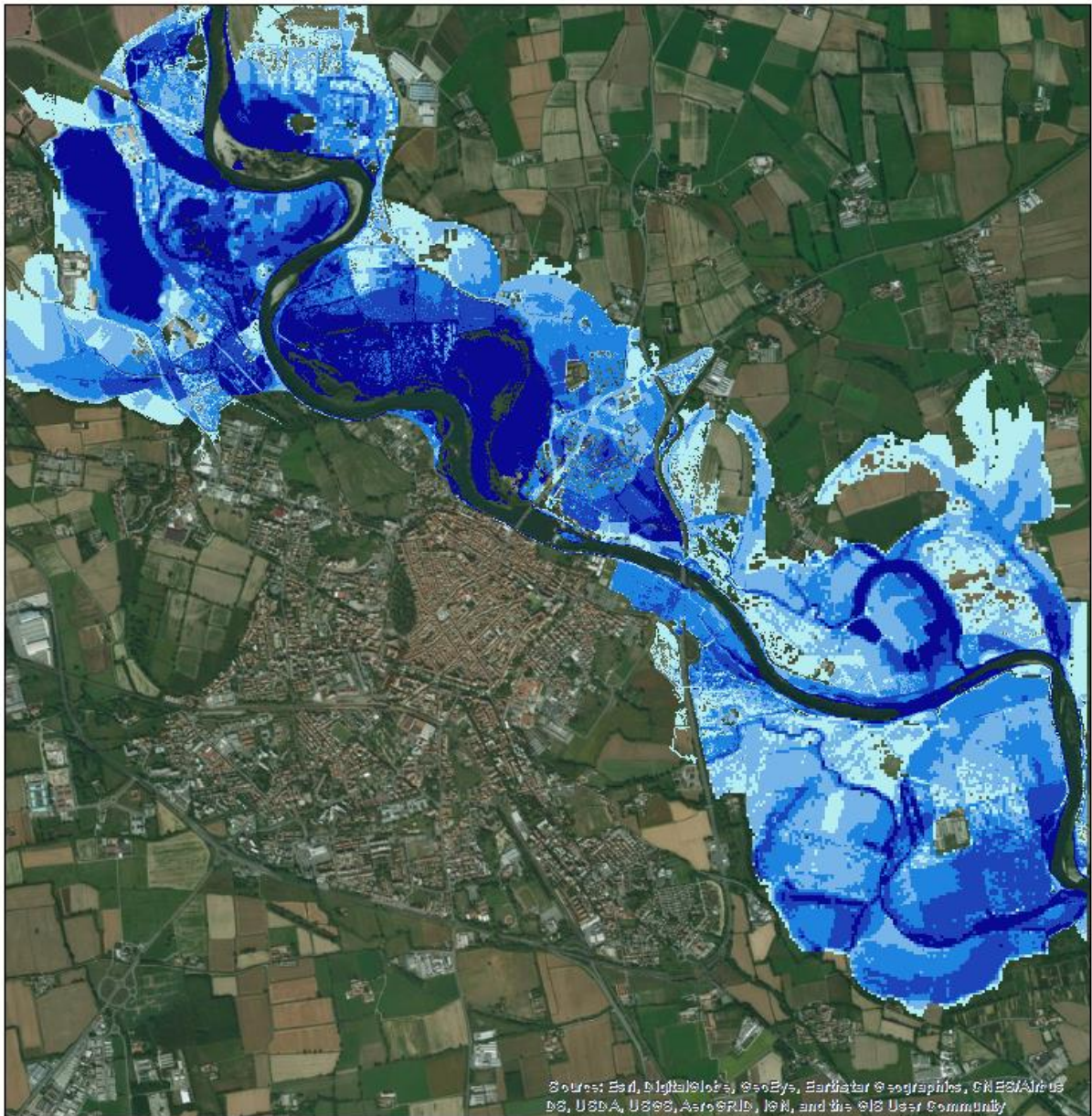
-  < 0.5
-  0.5 - 1
-  1 - 1.5
-  1.5 - 2
-  > 2

0 0.5 1 2 Kilometers



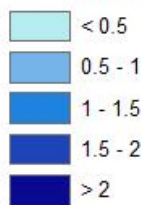
Figure 3-47 Flood Hazard Map for T=200 years without structural defences

Flood Hazard Map for T=200 years with structural defences



Legend

Maximum water depth [m]

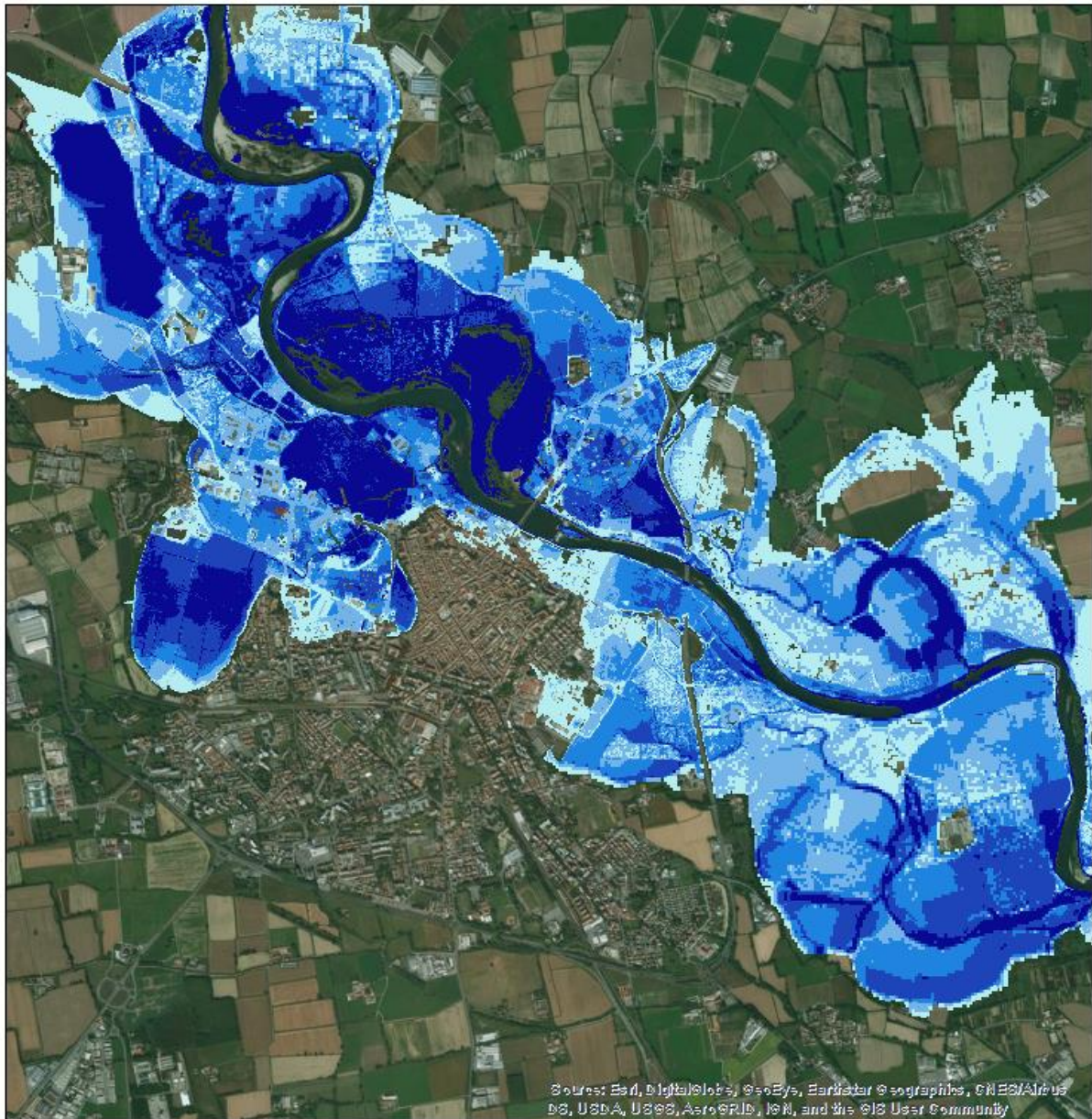


0 0.5 1 2 Kilometers



Figure 3-48 Flood Hazard Map for T=200 years with structural defences

Flood Hazard Map for T=500 years without structural defences



Legend
Maximum water depth [m]

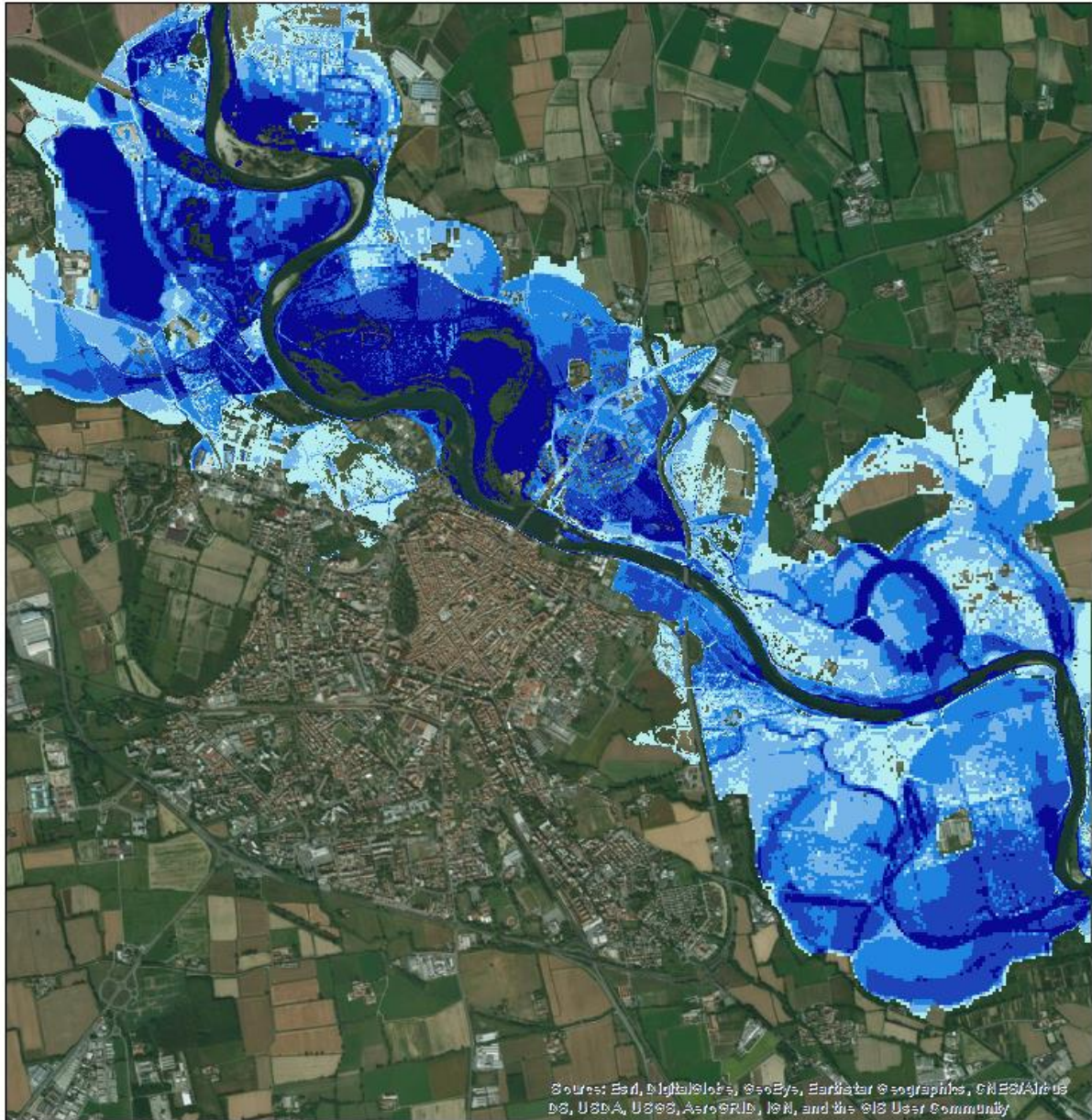
-  < 0.5
-  0.5 - 1
-  1 - 1.5
-  1.5 - 2
-  > 2

0 0.5 1 2 Kilometers



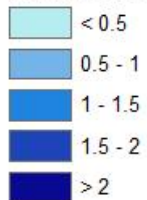
Figure 3-49 Flood Hazard Map for T=500 years without structural defences

Flood Hazard Map for T=500 years with structural defences



Legend

Maximum water depth [m]



0 0.5 1 2 Kilometers



Figure 3-50 Flood Hazard Map for T=500 years with structural defences

3.3 Multi Criteria Analysis (MCA)

This section is dedicated to a Multi Criteria Analysis to evaluate the effectiveness and functionality of the structural mitigation measures against flood, built on the hydraulic right of the Adda river in Lodi, after the November 2002 flood event.

After the collected available data necessary for the MCA, the costs for the construction of the flood protections will be reported, included administrative, legal and management charges and addition costs coming from yearly maintenance and qualifying courses for the montage of metal barriers.

The second step of the MCA regards the definition of the benefits in terms of potential avoided damage due to floods in Lodi. Among these, a distinction between quantifiable and non-quantifiable damages has been made. Indeed, direct damage to residential buildings and agricultural sector belonging to the municipality of Lodi has been monetarily evaluated, for the five reference scenarios, using, respectively, INSYDE and AGRIDE-c models, tools developed within the project flood IMPAT+. Then, using the aforementioned damages, a benefit assessment of the structural mitigation measures has been performed with a CBA and results proposed in terms of benefit cost ratio (B/C).

However, within a complete MCA, all the potential direct and systemic damages must be considered. The remaining non-quantifiable losses have been considered in terms of exposure (maximum potential damage), whose inclusion in the assessment will lead to a certain improvement of the benefits arising from the construction of the mitigation measures. Among these, maximum direct damage to economic activities have been reported, as well as systemic indirect damages generated by the latter. Other potential damages regard the flood exposure of population, road network, important facilities and cultural heritage. Some of these are difficult to be quantified due to lack of validated models while others, such as involved population and cultural heritage, represent priceless values, bringing into question also ethical issues. In case of hazardous event, decision makers have to consider also these non-quantifiable exposed elements, weighted according to the needs and priorities for actions.

Eventually, a sensitivity analysis on the results has been performed, assuming first a levee effect and, separately, the occurrence of a flood in a different month with respect to November, as potential consequence of the climate change. For both the cases, benefit assessment and B/C ratio has been performed and compared with the previously obtained ones. In regards the levee effect, a new residential development has been considered nearby the levee upstream of the historical bridge, due to the beneficial sense of security generated by the structural defence itself.

3.3.1 Available data for MCA

The available data, used for the computation of quantifiable damages and benefits and for the determination of exposed non-quantifiable assets, are reported in the Table 3-5. In the first column the typology of data is reported, followed by the source and date of the latter, before the last column which explain the utilization of the data.

Table 3-5 Available data for Multi Criteria Approach

AVAILABLE DATA	SOURCE	DATE	UTILIZATION
Shapefile of census zones in Lodi	<i>ISTAT (Istituto nazionale di statistica) database</i>	2011	Computation of quantifiable and not-quantifiable damages and benefits
Cadastral shapefile of residential building in Lodi	<i>Provincial database</i>	2011	Computation of damages and benefits to residential buildings
Level of maintenance and buildings construction typologies	<i>ISTAT database</i>	2011	Computation of damages and benefits to residential buildings
Replacement value €/m ² for residential buildings	<i>Cineas – Cresme – Ania</i>	2014	Computation of damages and benefits to residential buildings
Cadastral shapefile of agricultural particles in Lodi	<i>SIARL (Sistema Informativo Agricoltura Regione Lombardia) database</i>	2012	Computation of damages and benefits to agricultural sector
Software implementing AGRIDE-c model	<i>DICA - Politecnico di Milano</i>	2018	Computation of damages and benefits to agricultural sector
Shapefile of geo-localised operational company headquarters in Lodi	<i>DASU - Politecnico di Milano</i>	2018	Computation of exposure and systemic damages of economic activities
ATECO (Attività Economica) codes for economic statistics	<i>ISTAT database</i>	2009	Computation of exposure and systemic damages of economic activities
Net capital values per unit and net capital values per employee for economic activities	<i>ISTAT database</i>	2008	Computation of exposure and systemic damages of economic activities
Information on municipal population sub-divided in different categories	<i>ISTAT database</i>	2011	Determination of the potential exposed population
Shapefiles with localisation of road network, important facilities and cultural heritage	<i>Regional and Provincial database</i>	2017	Determination of the potential exposed road network, important facilities and cultural heritage
Images of November 2002 flood event in Lodi	<i>Civil Protection, Municipality and Police</i>	2002	Additional information in regards flooded areas in Lodi

3.3.2 Cost of structural defences and annual maintenance

The total cost of the intervention is about € 4.394.800,00, of which approximately € 3.148.400,00 of only works (charges for the execution of the security plans included, equal to € 66.100,00) and € 1.246.400,00 for design support activities, activities related to expropriation procedures, design charges, work management and safety coordination in the planning phase and execution costs, publicity of the tender and expropriation procedure, expropriation compensation, charges for compensation / mitigation works, charges for upgrading existing services, costs for price adjustments, contingency costs and VAT (Value Added Tax) charges.

Table 3-6 Summary of the costs for typologies of structural defences

Typologies of structural defences	Costs [€]	Incidence [%]
Culvert at the confluence of "cavo Roggione" into Adda river	710.200,00	21,6
Culvert upstream "cavo Roggione" artificial channel	374.300,00	11,4
Soil embankments	832.500,00	25,3
Displacement of existing irrigation courses	15.700,00	0,5
Defence wall	717.700,00	21,9
Works on river banks of the Adda	84.200,00	2,6
Mobile barriers system	524.300,00	16,0
Embankments nearby Belgiardino neighbourhood	25.700,00	0,8
Discount of 6,16%	202.300,00	
Total amount of interventions	3.082.300,00	

Moreover, annual costs for ordinary maintenance have to be considered, including costs to verify the consistency and integrity of the structural defences and checking for any anomalies.

Table 3-7 Summary of the costs for the annual ordinary maintenance of structural defences

Element of the structural defence	Cost [€/year]
Defence wall on the hydraulic right and connected elements (reinforced concrete works, surrounding areas, mobile barriers system)	22.300,00
Soil embankments on the hydraulic right and connected elements	4.900,00
Culverts on "cavo Roggione" artificial channel and connected elements	4.500,00
Total amount of annual ordinary maintenance	31.700,00

Eventually, annual qualifying courses for the personnel assigned to moutage of the mobile barriers system must be added to the previous costs. The number of workers necessary to assembly the floating barriers is 12 (6 teams with 2 employees per team). The estimated time for the installation of the entire system is about 2,5 hours, from the beginning of the flood warning alarm. The manager in charge must organise qualifying courses in which the procedure of assembly and disassembly of the barriers will be repeated, according to the adopted designed measures. On the basis of experience in similar cases in Italy, it is considered that the training courses have to be conducted on an annual basis. At least 18 people must attend the course, namely 1,5 times the number of employees needed to assemble the barriers in order to have an adequate number of workers in case of sudden unavailability during emergencies. The cost of each qualifying course is estimated to 1.000,00 €, for a total amount of 18.000,00 €/year.

Therefore, the annual costs, which have to be added to the fix costs of the structural mitigation measure, amount to almost 50.700,00 €/year.

3.3.3 Quantifiable damage assessment

Within the Multi Criteria Analysis (MCA), benefit cost ratios (B/C) has been computed in order to evaluate in monetary terms the usefulness and effectiveness of the structural mitigation measures built in Lodi on the hydraulic right of the Adda river. In this case, quantifiable benefits have been considered as the potential avoided damages to residential buildings and agricultural sector. In order to have a monetary evaluation of these benefits, the INSYDE and AGRIDE-c models have been used to quantify first the damages without structural defences and consequently those with structural defences. It has to be remarked that the quantifiable damage assessment has been performed only for those goods that are evaluable with calibrated and validated models. All the other non-quantifiable components of the potential damage caused by the flood will be treated in chapter 3.3.5.

3.3.3.1 Direct damage to residential buildings

Damages to residential buildings have been computed with the simplified version of the flood damage model INSYDE, which characteristics have been explained in chapter 2.6. The first step of the damage assessment is the definition of the flood hazard and its magnitude, in terms of water depth outside the structures, duration of the water inside buildings and contamination of the water.

For what concerns the duration of the flood event, it is assumed that the water inside the buildings is pumped out with modern tools and so presents no more than 24 hours.

As far as the water depth outside the building is concerned, the procedure to assign a water level h to each of the flooded building is described below. The starting point are the flood hazard maps previously proposed, representing the MAXDEP output file, namely the envelopment of the maximum water depth reached by the individual grid cell during the entire simulation. Through the use of ArcMap, the hazard map has been clipped according to the extension of the cadastral zones belonging to the Municipality of Lodi. Then, with the command “zonal statistic as table”, a value of water depth has been attributed to the buildings hit by the flood and attached to the shape file of the cadastre using the command “join and relate”. However, it has to be remembered that during the flood modelling, the built environment has been treated as impervious block, assuming though that inside the area subject to flooding, constructions have been excluded from the grid computation domain. This brought to some difficulties in assigning a water depth to several buildings belonging to the aforementioned shape file. In order to solve this issue, the MAXDEP raster grid file has been converted to points, using the ArcMap conversion tool “from raster to point” and then interpolated with the spatial analyst tool “natural neighbour”. In so doing, the blank values of the MAXDEP raster file, representing buildings as impervious blocks, have been filled with interpolated values and, for all the constructions inside the empty spaces, the maximum interpolated value has been attributed. Eventually, a value of water depth has been assigned to all the residential building affected by the flood. In Figure 3-51, extracts from ArcMap describing the mentioned procedure have been reported, taking as example two residential building located in the “Revellino” neighbourhood, one of the most inundated area during the November 2002 flood event. In the first extract, the representation of two impervious blocks is reported, in the second one the

points containing the value for each grid cell and the result of the interpolation in the third one. The last extract shows the original MAXDEP raster grid file (light blue), overlapped with the interpolated shape file (green).

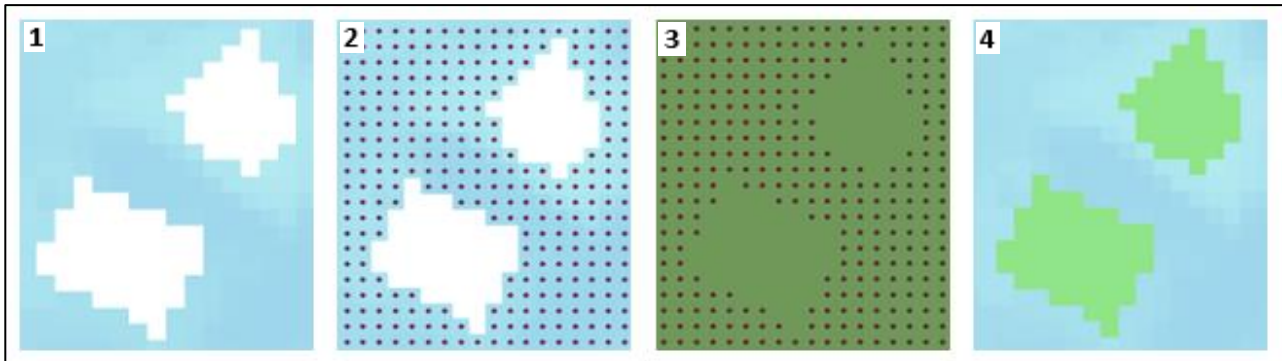


Figure 3-51 Procedure to assign h value to buildings inside impervious blocks: 1) representation of two buildings as impervious blocks; 2) conversion of the water depth raster into points; 3) interpolation procedure; 4) interpolated values inside impervious blocks

Once the water depth has been attributed to all the flooded residential building, the total absolute damage has been computed by means of analytical functions that account for damage mechanisms for the four building components. An expert-based “what-if” approach has been used to implement the damage functions (Scorzini et al., 2018), described in the chapter 2.6.

Vulnerability parameters, such as the level of maintenance (LM), the building type and the building structure (BS), has been taken from the cadastral database and from ISTAT database, while geometric characteristics such as the presence of basement, the number of floors, the footprint area (FA) and the finishing level (FL), linked to the building exposure, has been obtained from the Regione Lombardia geodatabase. Moreover, being the flood in urban area, the potential presence of pollutants in the water has been considered able to increase damages to the built environment as well as to affect people, easing the spread of diseases and intoxications.

Starting from the computation of the damage to basement ($d_{basement}$), the parameters involved in the calculation are the presence of basement, the level of maintenance and the duration of the water inside the building. In order to evaluate the aforementioned damage, the following assumptions have been taken. If the cellar is present, the basement area (BA) has been assumed equal to the footprint area of the construction, otherwise a zero value has been attributed. In cases where the information regarding the presence of the cellar was missing, a different approach was followed. From the total number of buildings, those with information about the presence of cellar has been extracted and among these, the percentage of constructions with basement has been obtained. This value has been multiplied to the footprint area of the buildings without information, leading to a complete assignment of the basement area (BA) to all the involved built environment. For what concern the level of maintenance (LM), a distinction between high and low value has been made, starting from information contained in the ISTAT census section file. In particular, for each section, the number of buildings with optimal and good state of conservation has been summed up, as well as for those with moderate and very bad level of maintenance. If the first amount is greater

than the second one, a high LM is attributed to buildings of that sections, otherwise a low LM is assigned.

As far as the damage to storeys (d_{storey}) is concerned, the considered variables are the water level (h), the duration of the flood (du), the presence of pollutants (q), the footprint area (FA), the finishing level (FL), the level of maintenance (LM) and the building structure (BS). In order, the water depth has been assigned using the hazard map as previously mentioned, the duration of the water assumed to be 24 hours, while for the presence of pollutants a unique value equal to 1,2 has been chosen for $f(q)$, due to the spread location of industries, stables and barns within the Municipality of Lodi. The information regards the footprint area as well as the finishing levels have been taken from the cadastre shapefile, while the level of maintenance from the census section file, as described before. For what concern the building structure, information have been taken from the census too and the following distinction has been done for each section. If the percentage of masonry structure is greater than other types, such as reinforced concrete and wood, the value 1,35 is assigned to $f(BS)$ for all the buildings belonging to the considered census section, otherwise the value 1 is attributed. It has to be remarked that all these considerations and assumptions have been made for each storey of flooded buildings and the damage computed separately. Eventually, all the d_{storey} belonging to the same structure have been summed up and the result used in the formula of the total absolute damage D , as described in the following.

The damage to pavement ($d_{pavement}$), function of the water level (h) coming from the hazard map and of the finishing level (LM), obtained from the census section file, has been computed implementing the formula reported in the chapter 2.6.

Moving to the damage to boiler (d_{boiler}), the latter depends on the presence of basement and on the water level. If the cellar is present, boiler is considered located in the cellar. If absent, boiler is supposed to be placed at more than 1,60 m from the pavement level (*Dottori et al., 2016*).

Eventually, these four components of the damage have been added up in the following formula and the total absolute damage D [€] obtained.

$$D = d_{basem} * RV * A_{basem} + \sum d_{storey-i} * n * RV * A + d_{pavem} * RV * A + d_{boiler} * RV * A$$

In the following, representations of damages to the residential buildings for each of the hazard scenarios considered within the MCA are proposed and overlapped with an imagery base map. In addition to these results, Table 3-8 summarise the damage D for each of the considered event, while the trend of the damage as function of the severity of the flood is reported in Figure 3-54.

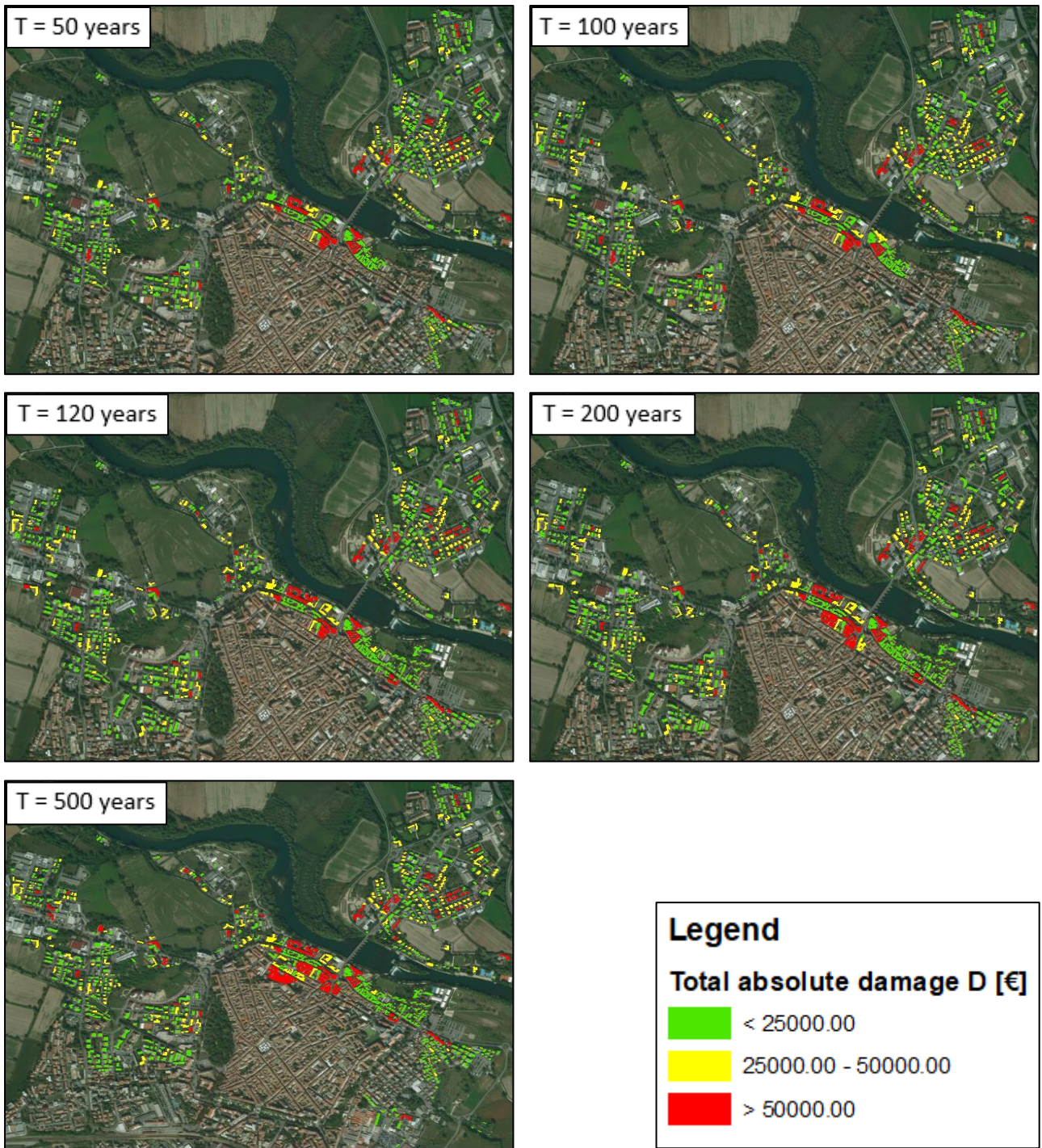


Figure 3-52 Total damage to residential buildings for reference scenarios, without structural defences

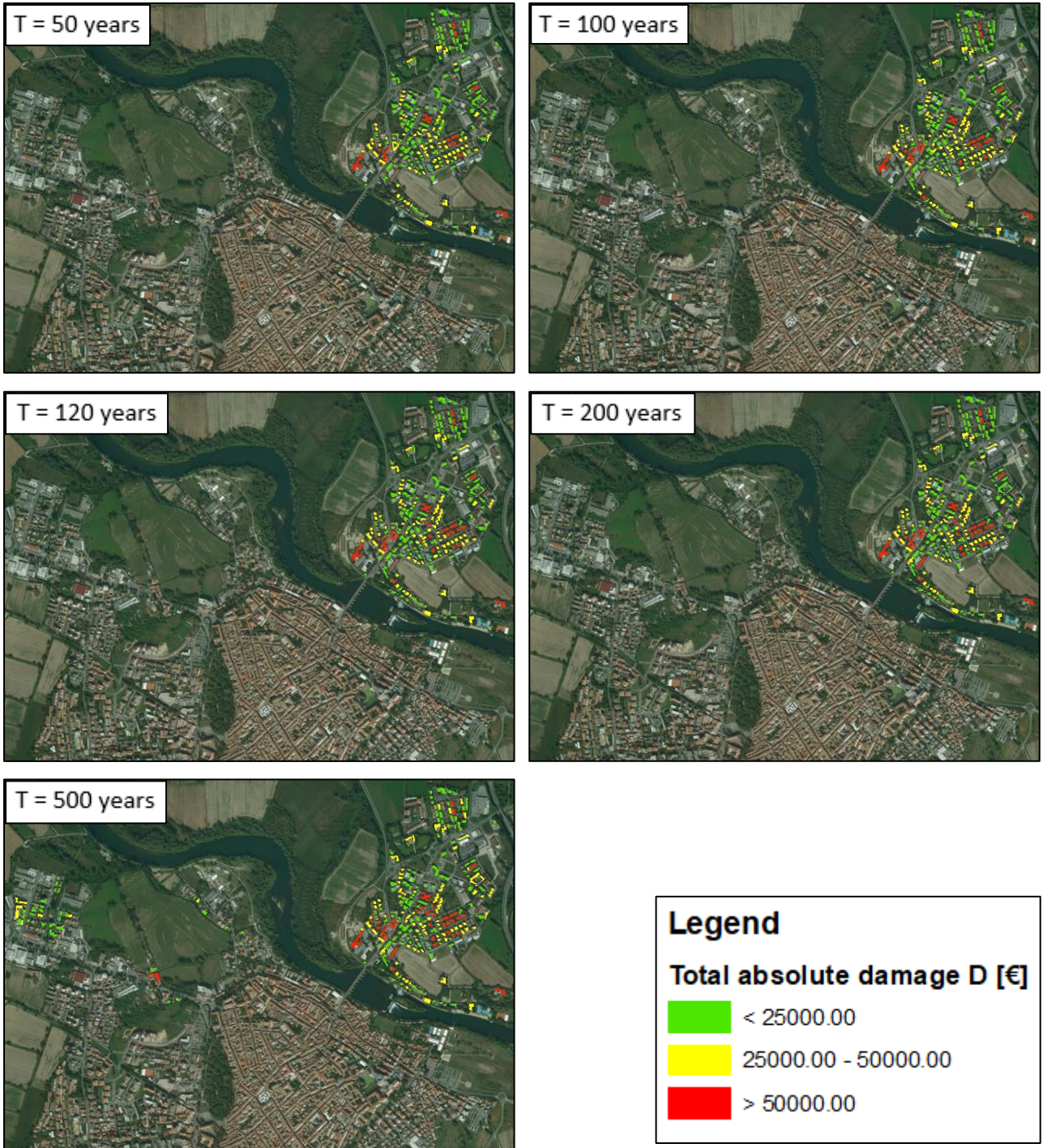


Figure 3-53 Total damage to residential buildings for reference scenarios, with structural defences

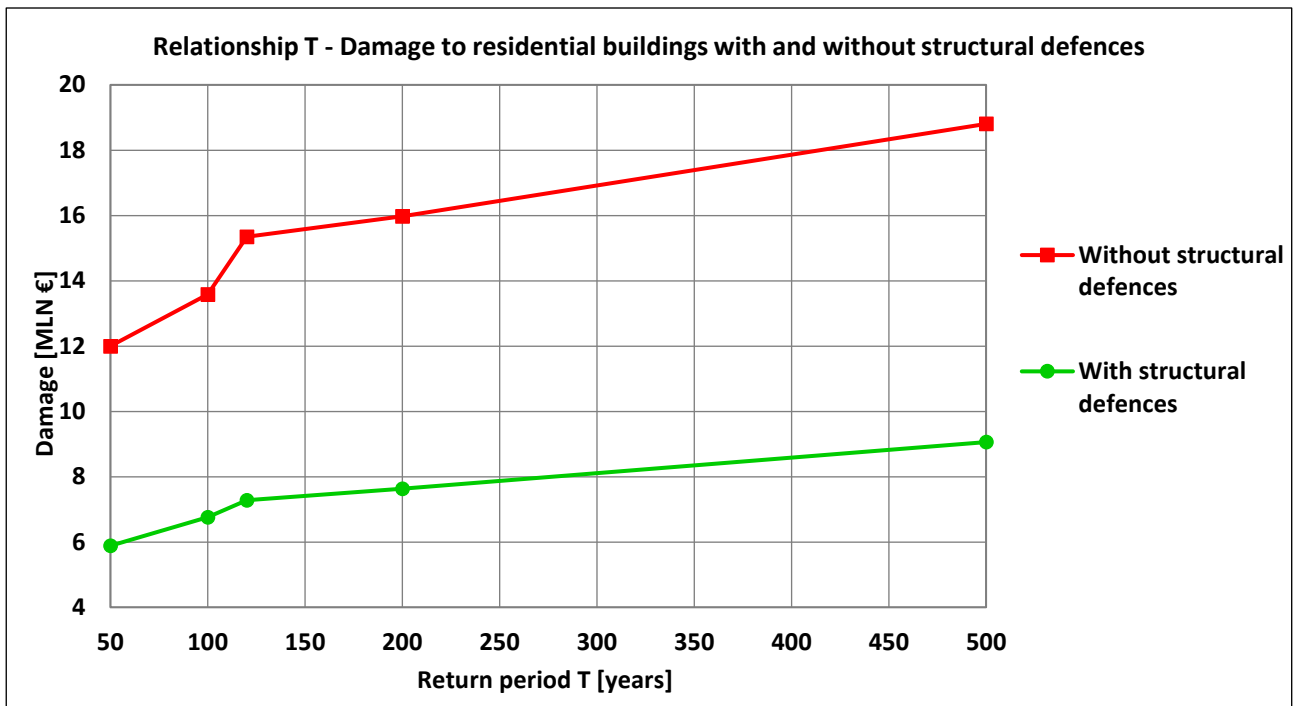


Figure 3-54 Relationship T – Damage for residential buildings with and without structural defences

Table 3-8 Summary of damages with and without structural defences and % damage reduction

T	Damage [MLN €] without structural defences	Damage [MLN €] with structural defences	Damage reduction [%]
50	12,00	5,89	51,0 %
100	13,58	6,76	50,3 %
120	15,34	7,28	52,6 %
200	15,98	7,63	52,2 %
500	18,80	9,06	51,8 %

As it possible to notice from the Figure 3-53, for the scenarios with T=50, 100, 120 and 200 years, damages to residential buildings on the hydraulic right are completely avoided. On the contrary, for the T=500 years one, flood water overtops the soil embankment between S.P. 202 and the first sluice gate, causing some damages to the residential area on the North-West side of the historical municipality.

The trends of the curves of the Figure 3-54 are similar, with the only exception of the higher increment of damage from T=100 years to T=120 years, without structural defences. The latter is due to the fact that, without protection on the hydraulic right of the river, a considerable increase of the flooded area has been estimated for the scenario simulating the November 2002 event with respect to the less severe one (T=100 years). On the contrary, with the addition of the structural defences, the smaller increment of damages is due to an increase of the water depth in the flooded area only.

For what concern the structural defences efficiency, for all the reference scenarios, a damage reduction between 50,3% and 52,6% have been obtained.

“Page intentionally blank”

The computation of damages to agricultural sector has been performed simulating the flood in November, as the event occurred in 2002 in Lodi and used for the calibration of the hydraulic model. Moreover, November represents the month in which high water stages in the river have been registered more frequently, according to the analysed hydrometer levels in the last twenty years in Lodi.

An important parameter involved in the computation of damage to the agricultural sector is the permanence of the flood on the fields. However, in this period of the year, the duration of the water does not influence the potential damage, considering the crop types present in November and their life stages. Indeed, grain maize and soy are absent and an immediate damage is associated to the bare soil only. In regards wheat and barley crops, the latter are in the gemmation phase and, in case of flood, the total damage is obtained immediately, being the crops in the weakest stage of their life. Grassland is in the vegetative rest phase and no damage is observed until the permanence of the water lasts more than 15 days. However, the impact of grassland on the total damage to agriculture is very low with respect to the other types of cultivations. These results are summarized in the Table 3-9.

Table 3-9 Damage to crops in November: no damage (green), slight damage (yellow), total damage (red)

	Permanence of the water [days]																				
	1	2	3	4	5	6	7	8	9	10	11	12	13	14	15	16	17	18	19	20	
Grain Maize	Green	Green	Green	Green	Green	Green	Green	Green	Green	Green	Green	Green	Green	Green	Green	Green	Green	Green	Green	Green	Green
Wheat crop	Red	Red	Red	Red	Red	Red	Red	Red	Red	Red	Red	Red	Red	Red	Red	Red	Red	Red	Red	Red	Red
Barley crop	Red	Red	Red	Red	Red	Red	Red	Red	Red	Red	Red	Red	Red	Red	Red	Red	Red	Red	Red	Red	Red
Grassland	Green	Green	Green	Green	Green	Green	Green	Green	Green	Green	Green	Green	Green	Green	Green	Yellow	Yellow	Yellow	Yellow	Yellow	Yellow
Soy	Green	Green	Green	Green	Green	Green	Green	Green	Green	Green	Green	Green	Green	Green	Green	Green	Green	Green	Green	Green	Green

Results of damage to agricultural sector in November with and without structural defences are graphically represented in Figure 3-56 and Figure 3-57 through the use of the ArcMap software. The trend of the damage is shown in Figure 3-58 and the summary results with the percentages of damage reduction for different T is proposed in Table 3-10.

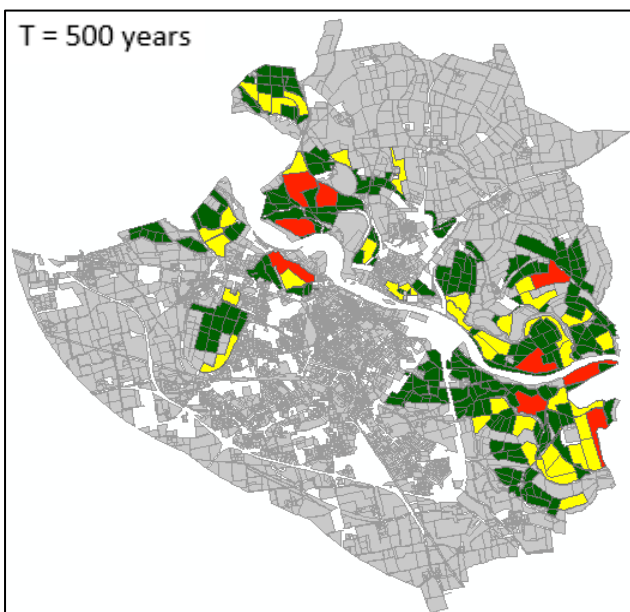
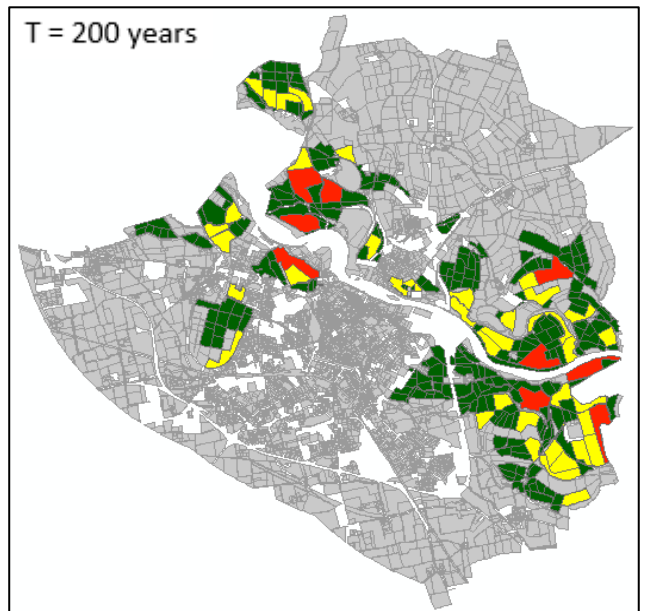
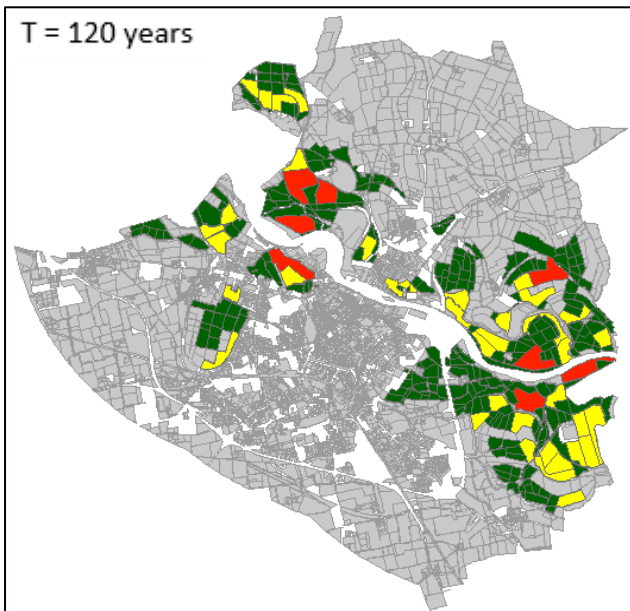
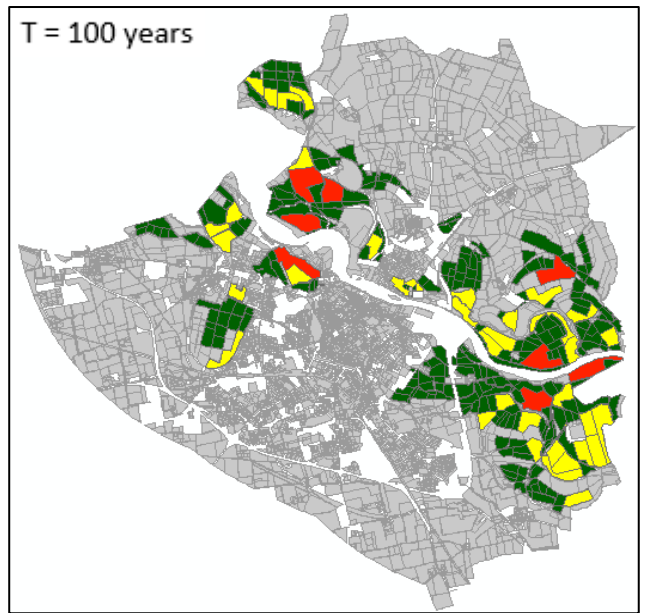
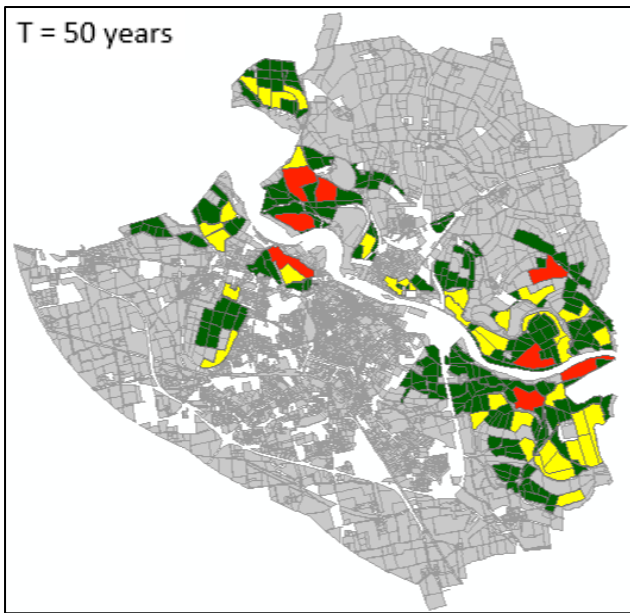


Figure 3-56 Damages to agricultural sector in November, without structural defences

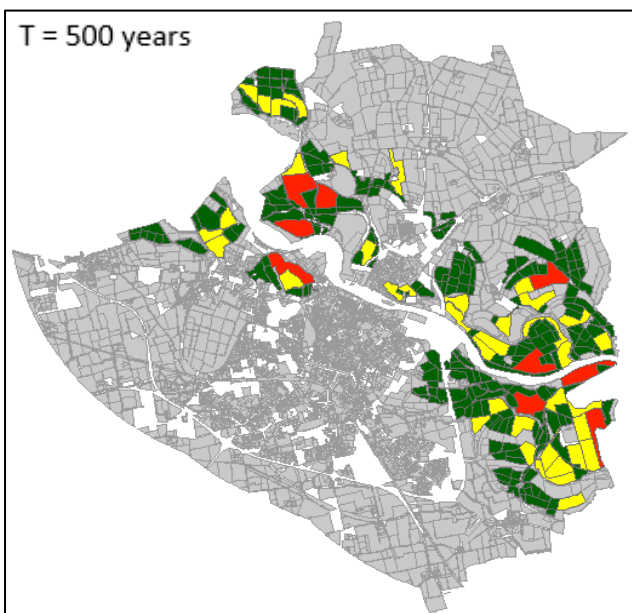
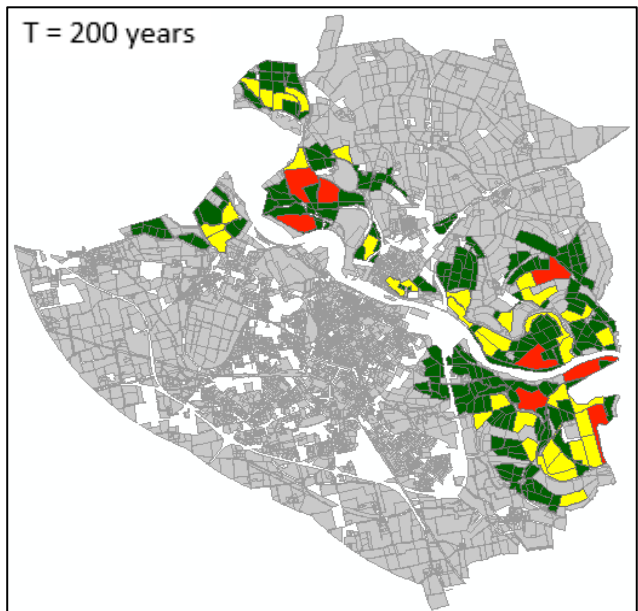
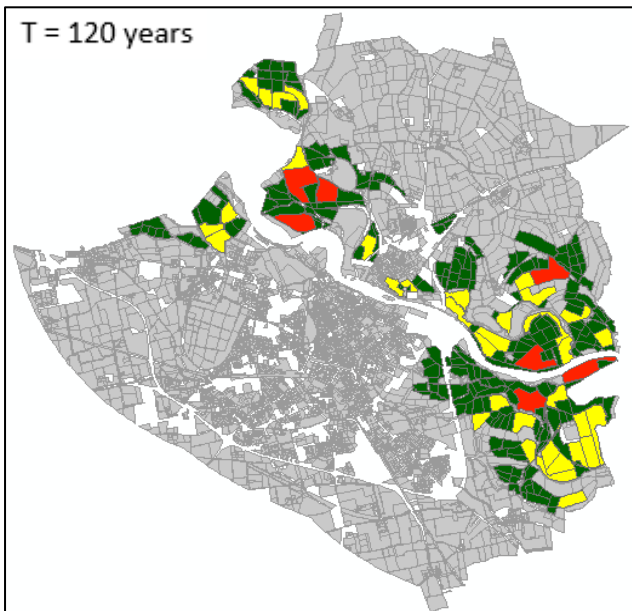
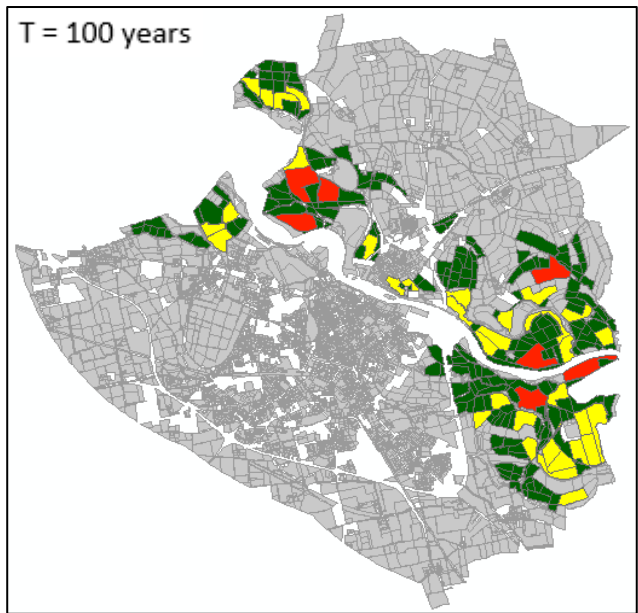
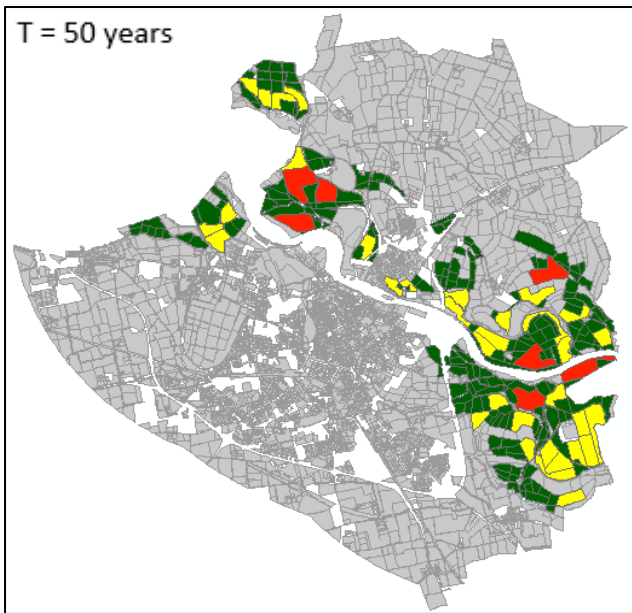


Figure 3-57 Damages to agricultural sector in November, with structural defences

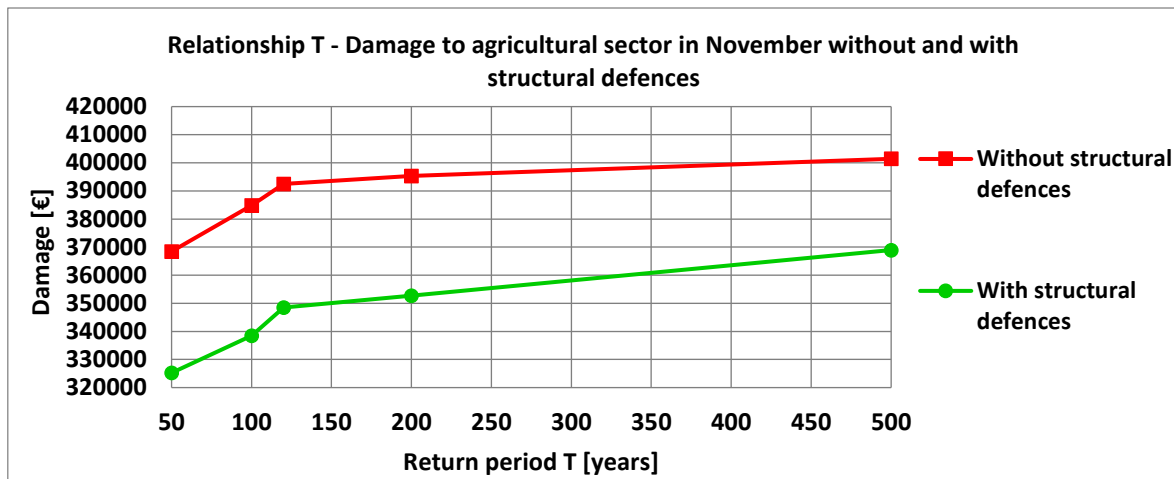


Figure 3-58 Relationship T – Damage to agricultural sector in November with and without structural defences

Table 3-10 Summary results of the damages to agricultural sector in November without and with structural defences

T	Damage without structural defences [€]	Damages with structural defences [€]	Damage reduction with structural defences [%]
50	368.500,00	325.200,00	11,7 %
100	384.800,00	338.500,00	12,0 %
120	392.500,00	348.600,00	11,1 %
200	395.400,00	352.800,00	10,8 %
500	401.400,00	369.000,00	8,1 %

The initial growing trend in Figure 3-58 is due to the increase of the flooded area for different reference scenarios. Indeed, for return periods equal to 50, 100 and 120 years a greater number of cadastral areas, as well as agriculture fields, are hit by the flood. On the contrary, looking at the trend related to events with 120, 200 and 500 years, a slight increase of the damage is observed due to a small increment of the flooded area from the 120 years scenario to the 200 years one. Increasing the severity of the event, namely the 500 years flood scenario, a wider flooded area is obtained but mainly in the urbanised zone nearby the historical part of the city. The latter causes an increment in the damage to residential buildings but not for what concerns the agriculture sector. The only increase in crops damages for the 500 years scenario is due to slightly higher water levels registered with respect to 120 years and 200 years events.

Simulations with structural defences report estimated damage reductions between 11% and 13% for the events with T= 50, 100, 120 and 200 years. These percentages slightly decrease for the 500 years return period event, due to the presence of flood water, overflowed from the soil embankments nearby S.P. 202, in an area on the North-East side of Lodi.

3.3.4 Benefit assessment

Once damages to residential buildings and to agricultural sector have been determined both without and with the structural defences, for the five reference scenarios, benefits, in terms of avoided damages, have been computed as follow. It has to be remarked that in the calculation of the benefit cost ratio, only quantifiable damages have been considered, which have been obtained with validated models. It is assumed that zero damages both for residential buildings and agricultural sector are obtained with flood event estimated with a return period ≤ 20 years. This information comes from flood simulations reported in “Studio di fattibilità della sistemazione idraulica”, performed by AdbPo. Indeed, few agricultural sectors are flooded in the aforementioned scenario and no residential buildings, whose potential damage represent the 96 – 98 % of the total quantifiable losses, would be reached by the water. Therefore, the low amount of damages coming from the agricultural sectors has been neglected and the total quantifiable damage assumed as zero.

In order to compute the potential avoided damages to residential buildings, the area between the red and green curves reported in the Figure 3-59, representing respectively the expected annual damages without and with structural defences, has been calculated. The probability of occurrence, calculated as $1/T$ is assigned to the x axis, while the potential damages to the y axis.

Three important remarks about the mentioned curves must be done. A linear trend has been assumed between obtained damages for the five investigated scenarios. No damages with return periods greater than 500 years have been computed and therefore the final amount of potential avoided quantifiable damages could be underestimated. Moreover, it is not known for sure what will be the costs (and therefore replacement costs and damages) in future years and this aspect should be taken into consideration. However, with the opinion of economists, inflation in recent years has settled near zero and, assuming that it will remain the same in the future, it is reasonable to expect that the estimated damage could remain unchanged.

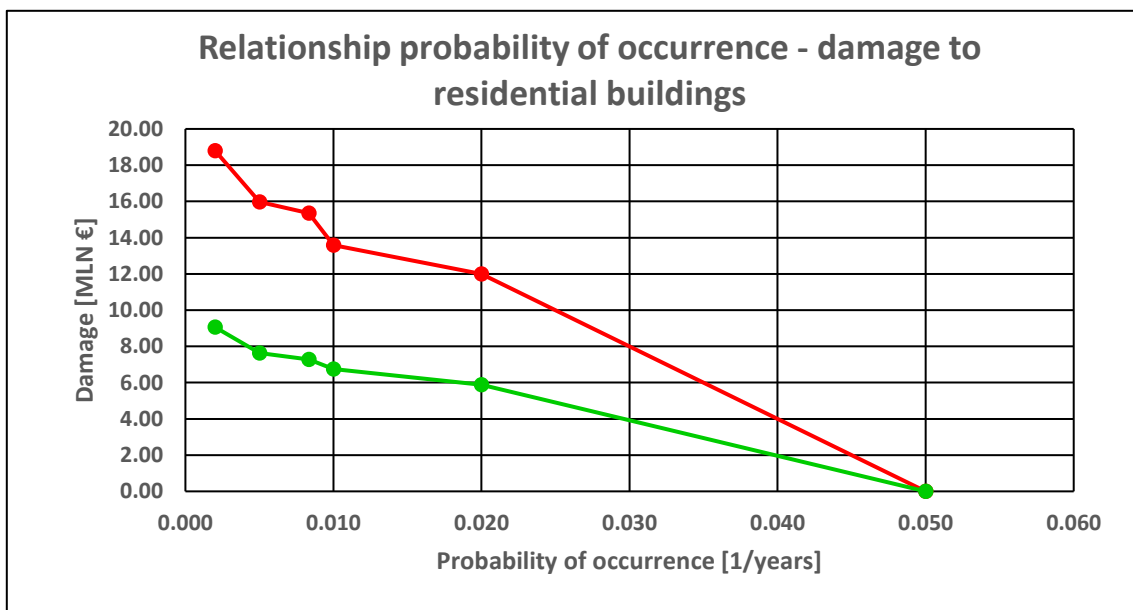


Figure 3-59 Relationship probability of occurrence – damage to residential buildings

The yearly estimated avoided damage to residential buildings is about € 223.300,00.

In regards to the agricultural sector, the same procedure used for the computation of avoided damages to residential buildings has been adopted. Results of the obtained damages without and with structural defences are reported in the Figure 3-60. The final yearly estimated avoided loss for the agricultural sector is around € 1.400,00, two orders of magnitude lower than the residential buildings one.

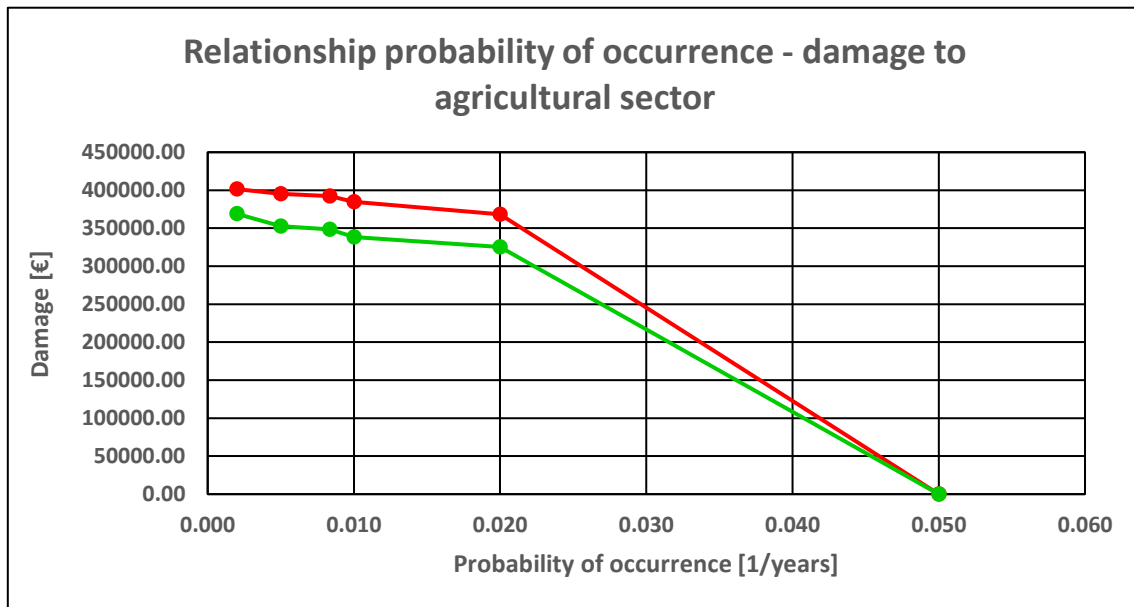


Figure 3-60 Relationship probability of occurrence – damage to agricultural sector

Therefore, summing up the aforementioned yearly avoided damages, the final result is € 224.700,00, representing the annual quantifiable benefit coming from the construction of the structural defences on the hydraulic right of the Adda river.

The total cost of the intervention, as mentioned in chapter 3.3.2, is equal to € 4.394.800,00. Considering the structure's functional duration of 100 years, the cost of the flood protections is € 43.948,00/year. The annual expense for ordinary maintenance is € 31.700,00, to which other € 18.000 /year must be added up for annual qualifying courses of the personnel assigned to mountage of the barriers system. Therefore, the total amount of cost per year is estimated around € 93.648,00.

Therefore, computing the B/C ratio, the obtained result is:

$$B/C = \frac{€ 224.700,00}{€ 93.648,00} = 2,4$$

In other words, the structural defences produce yearly benefits, in terms of avoided damages, 2,4 times greater than the total yearly costs of the flood protections.

However, since the real functional duration of the structures is unknown, especially regarding the r.c. defence walls, it has been computed that 25 are the years of functional duration of the flood protections for which yearly costs equal the estimated arisen yearly benefits (B/C=1). In other words, if the mitigation measure would have been designed to last 24 years, the B/C < 1 and, therefore, the evaluation of its effectiveness would be negative. It has to remarked again that these benefits have been obtained from avoided quantifiable damages to residential buildings and agricultural activities, computed with models developed within the project Flood-IMPAT+.

“Page intentionally blank”

3.3.5 Non – quantifiable damage assessment

In light of the previous results, even considering only quantifiable avoided damages, the yearly benefits of the flood protections exceed the yearly costs of construction and maintenance. However, in a Multi Criteria Analysis, also non-quantifiable avoided damages must be taken into consideration. In so doing, the potential benefits coming from these non-evaluatable assets will certainly improve the previous B/C result.

In the following of this chapter, direct avoided maximum damage to economic activities, as well as the systemic indirect avoided damages induced by the latter have been evaluated in terms of reduction of exposure to flood. Moreover, estimations of the potential exposure of population, road network, important facilities and cultural heritage with and without structural defences have been reported.

3.3.5.1 Direct damage to economic activities

The computation of the damage to economic activities has started with the identification and geo-localisation of the companies belonging to the municipality of Lodi. The latter have been subdivided into operational and legal companies' headquarters. Then, for each ATECO class (the Italian correspondence of the European NACE), the net assets values per economic activity, both for structure and contents, have been taken from the ISTAT database. These two values, coming from an average of the all Italian companies for ATECO class, have been associated to each of the geo-localised companies and then added up. Indeed, contents can be easily damaged in case of flood but also breakage of systems directly linked to the structure (such as electrical, ventilation and heating systems) must be taken into consideration. The obtained value represents the exposure value for each ATECO class company, namely the maximum potential damage that the considered economic activity could face, and not the real damage suffered by the company. In case of flood, it is up to the decision maker to establish the weight to give to this information within the MCA. In order to have a quantifiable value of the potential damage for each flooded company, damage curves should be applied. However, no commonly accepted curves or validated model to assess damages have been developed in Italy. Moreover, each company should be individually analysed, considering its financial status at the occurrence of the flood, as well as the current value of the contents. This approach would require a micro-scale analysis and the intervention of experts in this field.

The total potential damages to flooded economic activities for each scenario have been computed and summarised in Table 3-11, reporting also the estimated reduction with the addition of the flood protections.

Table 3-11 Exposed economic activities for reference scenarios

Maximum potential damage to economic activities			
T	Without structural defences [MLN €]	With structural defences [MLN €]	Damage reduction with structural defences [%]
50	120,79	62,61	48,2%
100	128,12	62,61	51,1%
120	189,51	62,61	66,9%
200	197,58	63,35	67,9%
500	293,89	69,40	76,4%

Results show increasing trend of the estimated reductions of damages from 48,2% for T=50 years scenario to 76,4% for the most severe considered event. It has to be remarked again that the reported damages in MLN of € represent the maximum total potential damages and not the total real damages that flooded economic activities can suffer.

For the five scenarios without structural defences, the amount of damages to contents is between 20% and 26% of the total estimated losses, while for the scenarios with flood protections, these percentages slightly increase, being between 27% and 30%. This means that if the damages to contents only would be considered or weighted more than the damages to structures, the percentages of damage reduction will decrease with respect to the ones proposed in Table 3-11.

In the following pages, extracts of maps with the localisation of the hit economic activities for the reference scenarios are presented, first in the configuration without structural defences and then with the addition of the flood protections.



Figure 3-61 Exposed economical activities for reference scenarios, without structural defences



Figure 3-62 Exposed economical activities for reference scenarios, with structural defences

“Page intentionally blank”

3.3.5.2 Systemic indirect damage to economic activities

Direct damage to economic activities could trigger a series of systemic and indirect damages not only to the companies themselves but also to the municipal and provincial economy. Since the lack of tools and knowledge in order to quantify direct damage to economic activities, also their indirect and systemic damages would be a complex task.

However, in order to represent the potential economic impact that a flooded company may generate in a cascade effect process, the following procedure, based on proxy variables, has been assumed.

Starting from the geolocalised economic activities in Lodi, those flooded in each of the five considered scenarios, have been selected. Then, for each ATECO (ATtività ECONomiche) class, the net assets values of contents per employee, have been taken from the ISTAT database and linked to the geolocalised activities. Eventually, the net assets values have been multiplied by the total number of employees (included the owner of the company) and consequently subdivided by the maximum obtained value, resulting with values between 0 and 1 of a proxy called systemic damage multiplier. This parameter is a way to account for the systemic impact that could derive from the damage to a company, which makes the potential damage much greater than the direct damage to structure and contents only. Values close to zero mean low systemic and indirect damages for the local economy, while higher results indicate a greater potential tendency to generate a cascade effect, involving several sectors in Lodi. Some clarifications have to be done in regards of the systemic damage multiplier. The only workers are not enough to represent the indirect and systemic damage because also the relationship with the potential damages of the involved contents must be highlighted which is strictly linked to the real possibility of restarting the activities. The greater the capital, in fact, the greater will be the investment necessary in the recovery phase. Furthermore, not only the market share is lost but in the meantime competitors which have not faced the flood could have absorbed part of the demand of the flooded companies, resulting in even greater future damages. Eventually, due to the interruption of the activity, employees will lose their job position, involving the society that will have to cover the unemployment's payments, further aggravating the costs to return to normality.

Results for the five reference scenarios both without and with structural defences have been reported in Figure 3-63 and Figure 3-64. As discussed before, there is a considerable reduction of the exposition of economic activities after the construction of the structural defences, resulting in lower systemic damages for the entire Municipality.

The potential systemic impact of the companies, expressed with the systemic damage multiplier, has been differentiated in three categories, low, medium and high, according to the Jenks Natural Breaks algorithm (The features are divided into classes whose boundaries are set where there are relatively big differences in the data values, *ArcGIS Pro Help*).



Figure 3-63 Indirect systemic damage for reference scenarios, without structural defences

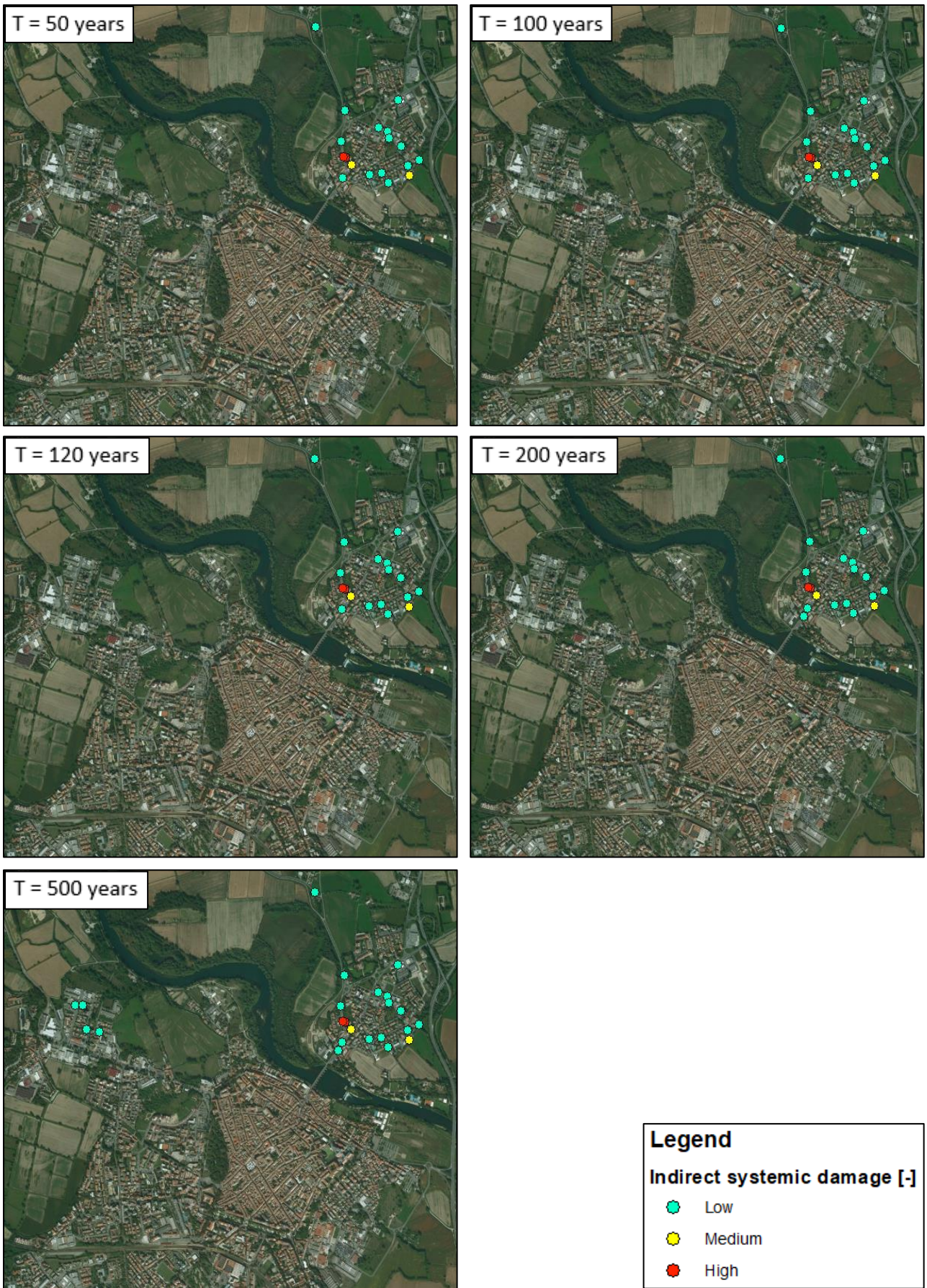


Figure 3-64 Indirect systemic damage for reference scenarios, with structural defences

“Page intentionally blank”

3.3.5.3 Exposed population

For what concerns the damage to the population, an estimated number of people exposed for different scenarios has been computed only. Several damage curves can be implemented in order to obtain potential injuries and fatalities (FHRC and HR Wallingford, 2006) but a lot of variables must be taken into account. Indeed, a distinction between water depth outside and inside buildings should be done, as well as velocity and flow direction of the flood. The latter are not easy to be assessed, due to lack of information or complexity regarding their computation. Moreover, in Italy, it is commonly assumed the non-quantification of the human life, due to the complexity in their estimation and, more important, for ethical issues.

Information about the population for each census area of the Municipality of Lodi have been taken from the census section shape file. Results are proposed in the next pages of this chapter which report the total exposed population, the number of vulnerable individuals and foreign inhabitants, for each census section and for all the ten investigated scenarios. Further considerations should be made regarding the population effectively present in Lodi at the occurrence of the flood, assessing the number of commuters, the location of their work place and the potential night and day population (the peak of the flood in 2002 was during the night between the 25th and 26th of November), which can increase or decrease the total exposure.

As suggested by Xia et al. (2014), instability conditions of people in case of flood include physical attributes such as age, sex, height and weight, and the latter can be specifically adopted to account for particularly weak categories like elderly or sick. Moreover, subjects with larger weight and height are able to resist to higher solicitations (Cox et al., 2010, Russo et al., 2013). Therefore, within the entire affected population, individuals with an age lower than 14 years and greater than 65 years have been assumed as vulnerable. Information on the latter can be relevant for evacuation purposes and emergency management.

It is also important to assess the number of foreign people that could potentially be exposed to risk. Indeed, foreigners could not be aware of the flood history of the city where they live and of any emergency procedures, in case of evacuation, they could have problems of communications with other citizens and local authorities.

In order to obtain these values, the shapefile containing all the census sections of the Municipality of Lodi has been clipped with the extensions of the flooded areas. This operation has been done using the spatial analyst command “clip” of the software ArcMap, for all the ten considered scenarios. Then, for each census section, the percentage of the area effectively flooded has been calculated and the latter multiplied with the total value of exposed population, vulnerable individuals and foreign inhabitants. As results, a greater number of expositions in all the three selected fields is observed increasing the severity of the event, with the exception of the 200 years return period event scenario which has a similar flooded area with respect to the 120 years one. However, as mentioned before, any damage curve, which takes into consideration water depth and velocity as input, has been adopted and so the result of this analysis regards all the population that dwells inside the flooded area.

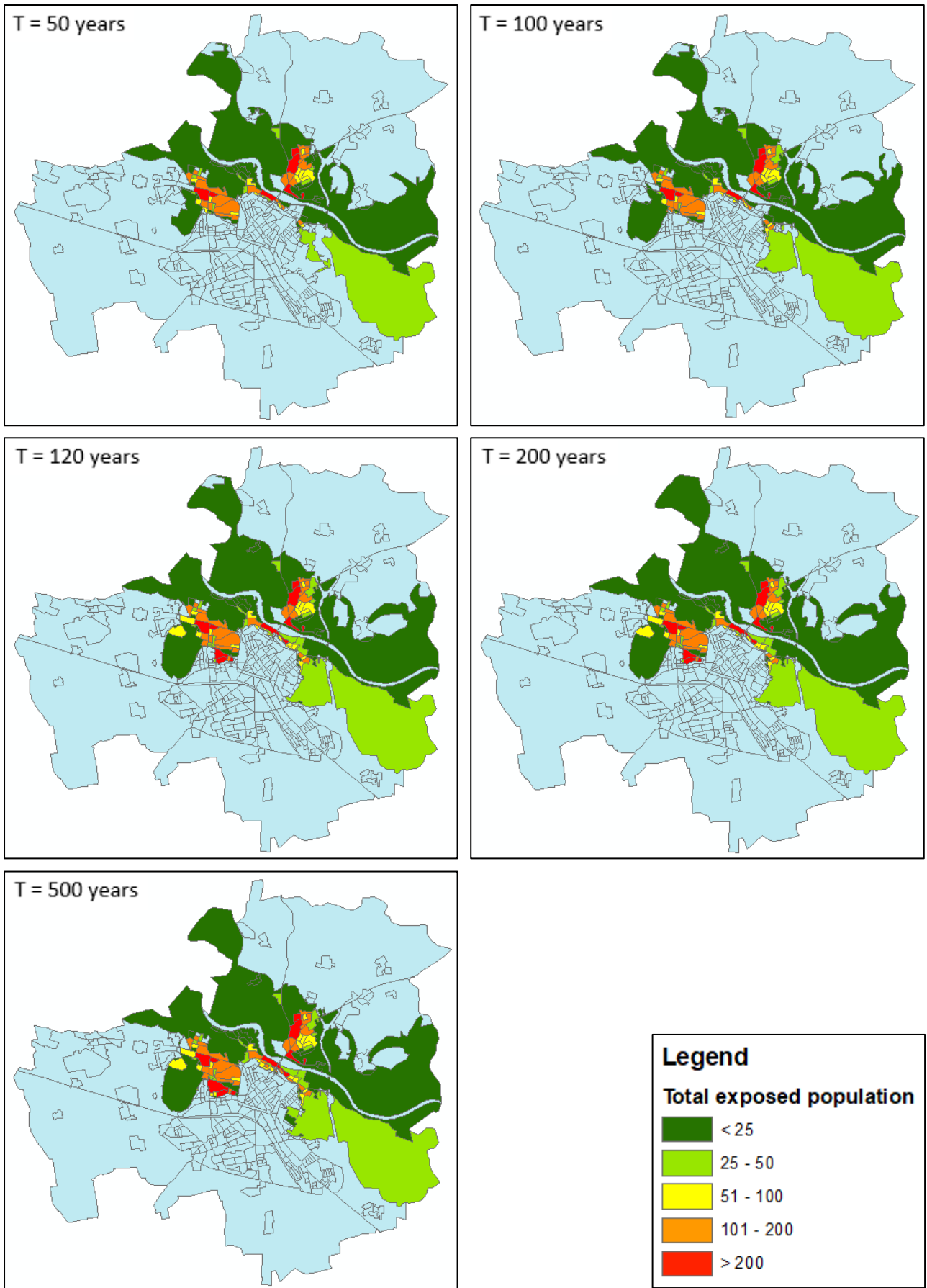


Figure 3-65 Total exposed population for reference scenarios, without structural defences

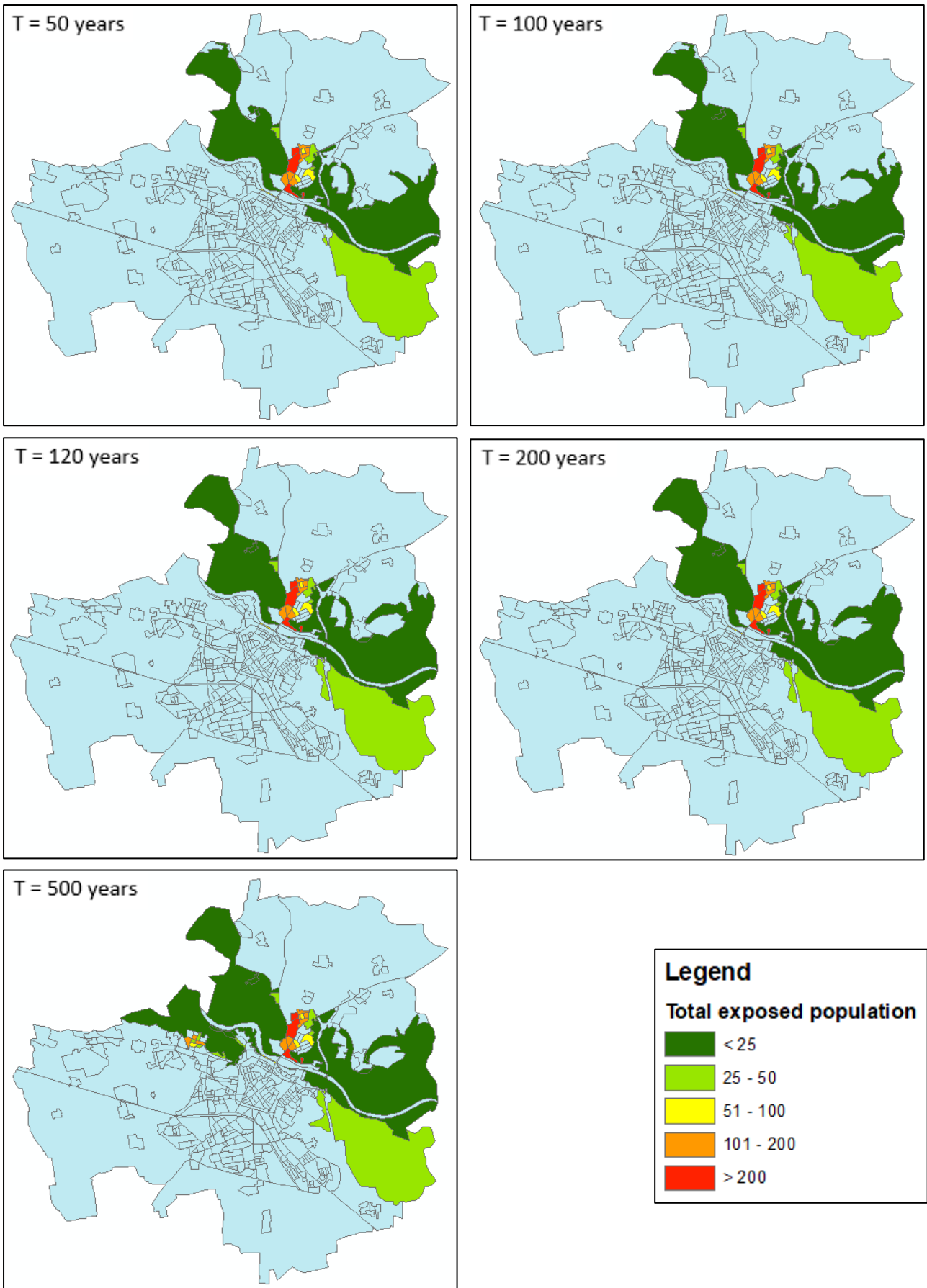


Figure 3-66 Total exposed population for reference scenarios, with structural defences

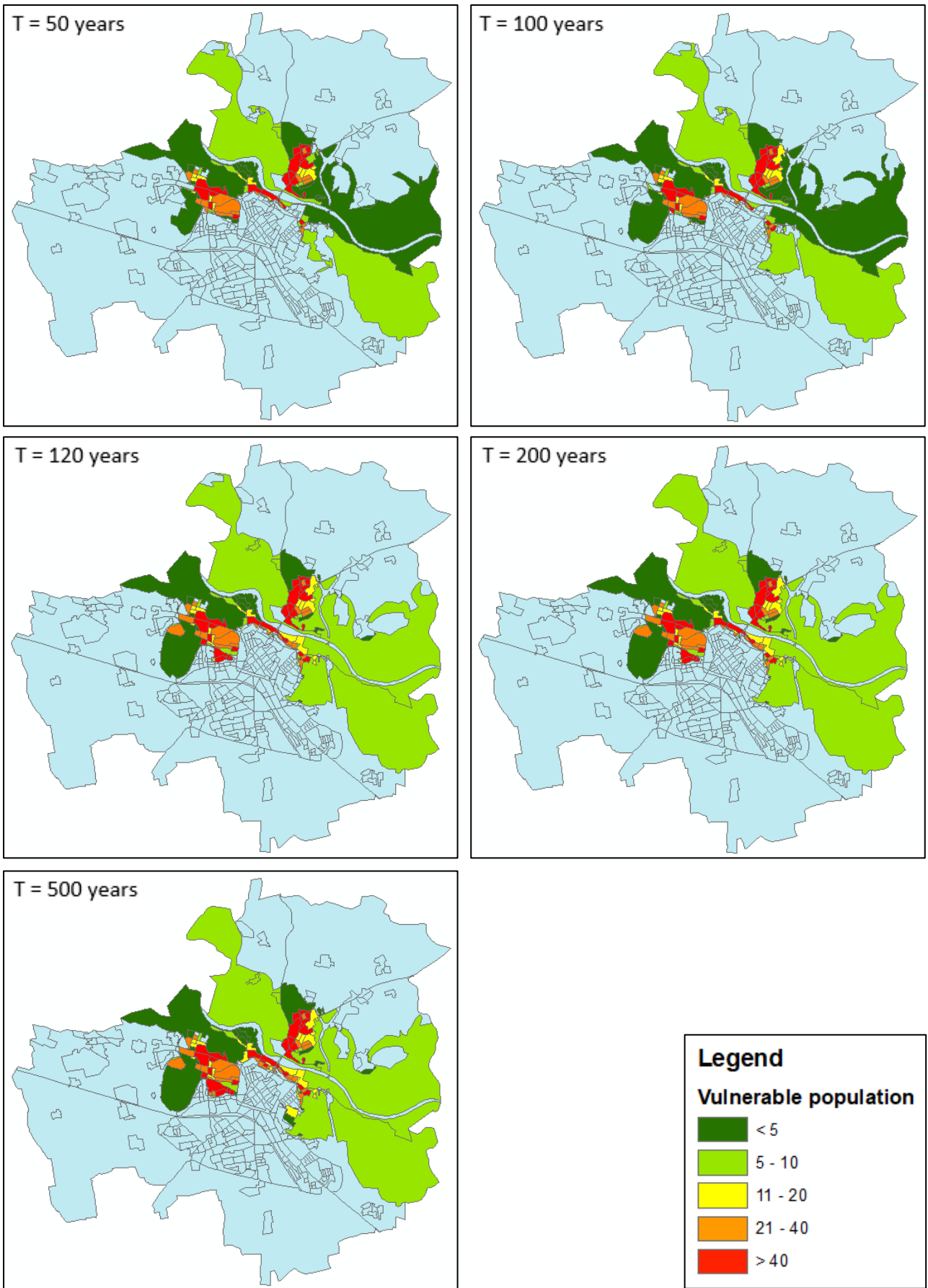


Figure 3-67 Exposed vulnerable population for reference scenarios, without structural defences

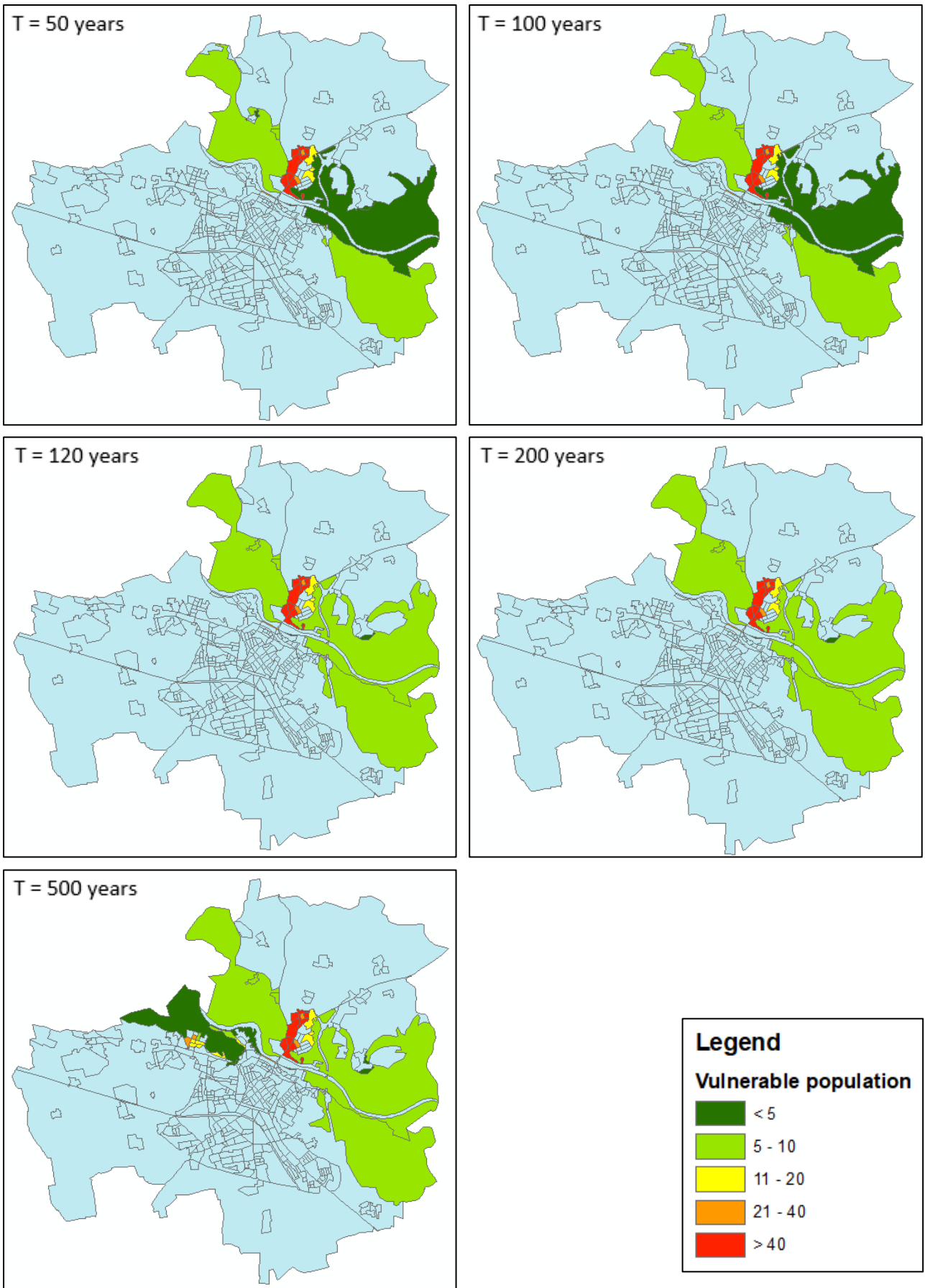


Figure 3-68 Exposed vulnerable population for reference scenarios, with structural defences

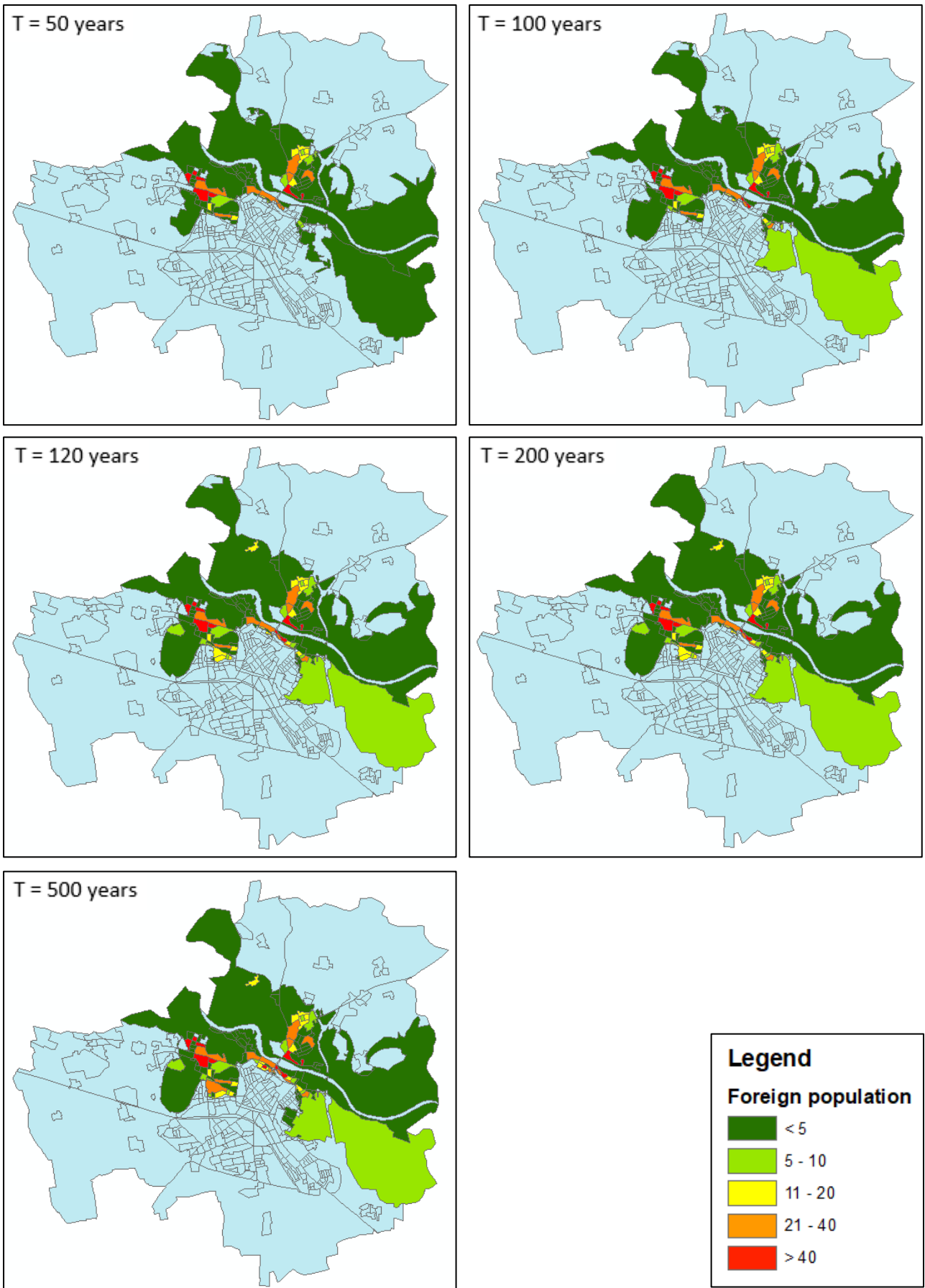


Figure 3-69 Exposed foreign population for reference scenarios, without structural defences

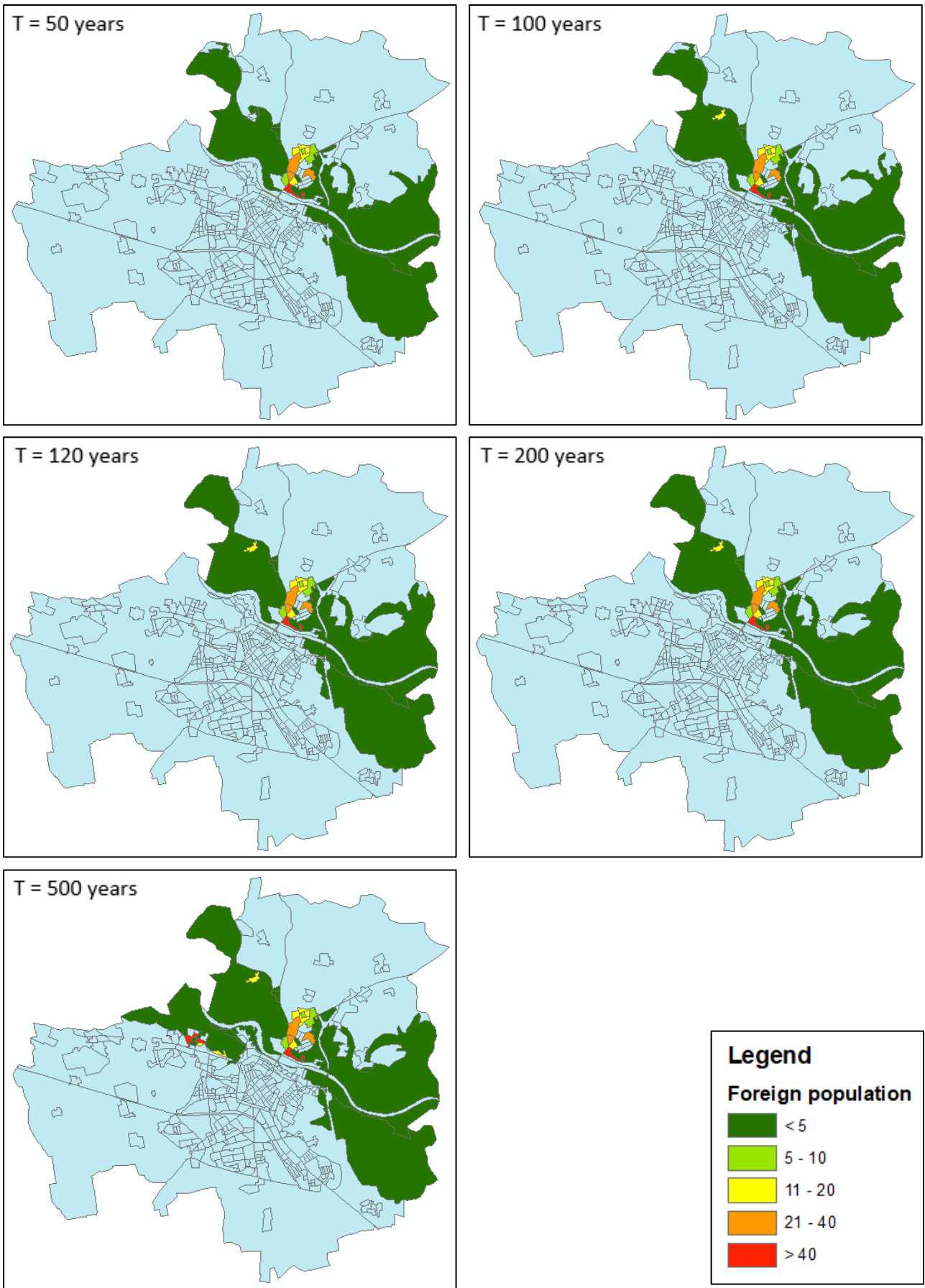


Figure 3-70 Exposed foreign population for reference scenarios, with structural defences

Table 3-12 Summary table of exposed population for reference scenarios without structural defences

Exposed population without structural defences			
T	Total exposed population	Exposed vulnerable population	Exposed foreign population
50	6439	2127	827
100	6858	2307	924
120	8399	2921	1077
200	8399	2922	1077
500	9647	3361	1250

Table 3-13 Summary table of exposed population for reference scenarios with structural defences

Exposed population with structural defences			
T	Total exposed population	Exposed vulnerable population	Exposed foreign population
50	2524	826	287
100	2542	832	295
120	2546	836	296
200	2547	836	297
500	3233	1023	481

Table 3-14 Summary table of reduction of exposed population for reference scenarios

% reduction of exposed population with structural defences			
T	Total exposed population	Exposed vulnerable population	Exposed foreign population
50	60.8%	61.2%	65.3%
100	62.9%	63.9%	68.1%
120	69.7%	71.4%	72.5%
200	69.7%	71.4%	72.4%
500	66.5%	69.6%	61.5%

From Table 3-14, it is possible to notice a reduction of the total exposed population between 60,8% and 69,7%, of the vulnerable individuals between 61,2% and 71,4% and of the foreign population between 61,5% to 72,5%. The smaller values in the 500 years scenario with respect to the 200 years one is due to the overflow of water from the soil embankment nearby the S.P. 202, that flood an area located in the North-East side of the historical municipality, as shown in the hazard map in Figure 3-50.

3.3.5.4 Exposed road network

Maximum damage to road network has been computed in terms of exposed km for all the reference scenarios, considering only links inside the flooded areas and not the effectively affected network that would have covered a wider area. The estimated damaged roads have been obtained overlapping the flood hazard raster files with the shapefile containing the entire road network in Lodi. Results show a reduction of the exposure between 31,8% to 36,2% for the five reference scenarios, after the construction of the structural defences. No damage curves have been used and, therefore, benefits in terms of avoided damages cannot be quantifiable in monetary terms and considered directly in benefit – cost ratio. This is due to the fact that no damage models have been developed within Flood-IMPAT+ project, for evaluating losses to roads in monetary terms. Several parameters should be taken into account, such as type of road, construction material, length to be effectively considered, connected elements, etc., requiring a detailed approach for each link of the network. Available provincial and regional data are incomplete or not updated, increasing the complexity of collecting the aforementioned information in order to perform a reliable assessment.

Table 3-15 Summary table of exposed road network for reference scenarios

Exposed road network			
T	Without structural defences [km]	With structural defences [km]	Reduction [%]
50	60,1	40,9	31,8
100	66,9	43,2	35,4
120	72,3	46,1	36,2
200	72,6	46,4	36,1
500	79,9	52,1	34,7

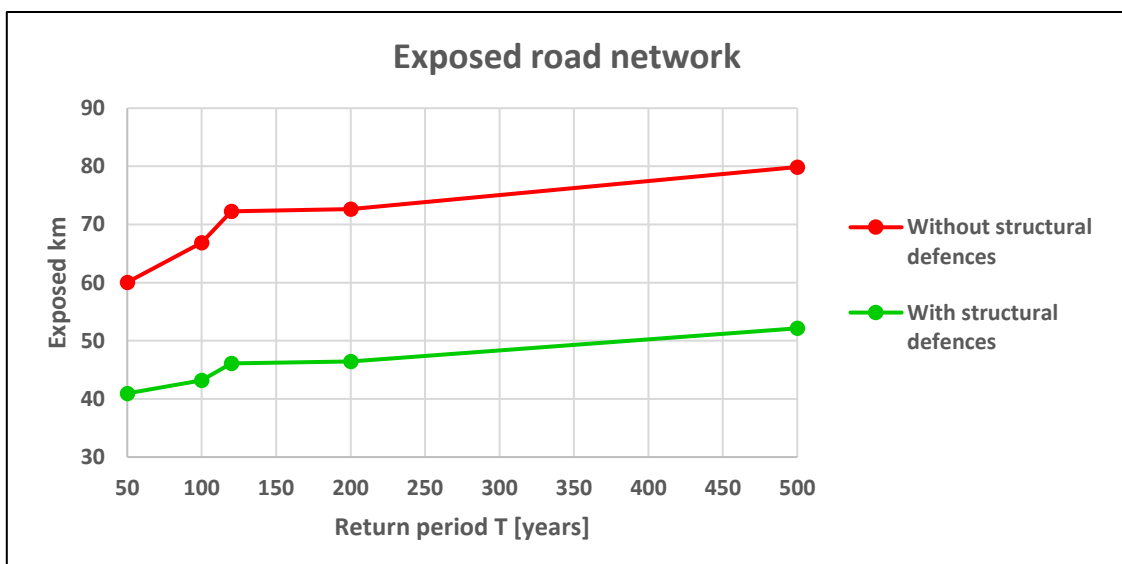


Figure 3-71 Exposed road network with and without structural defences for reference scenarios

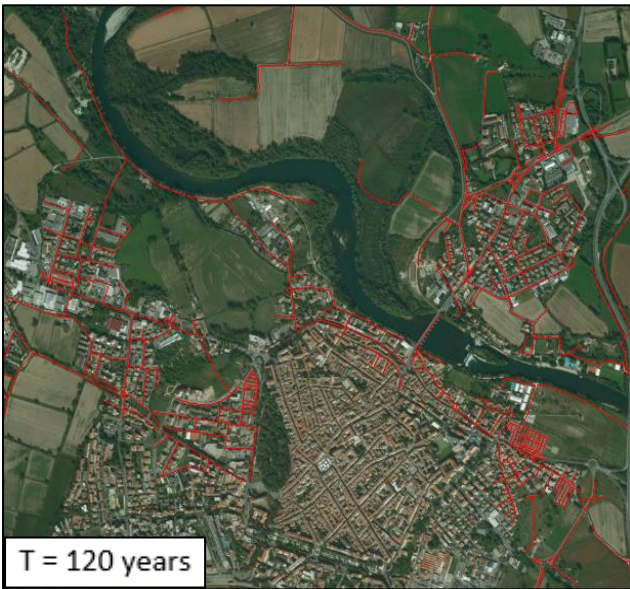
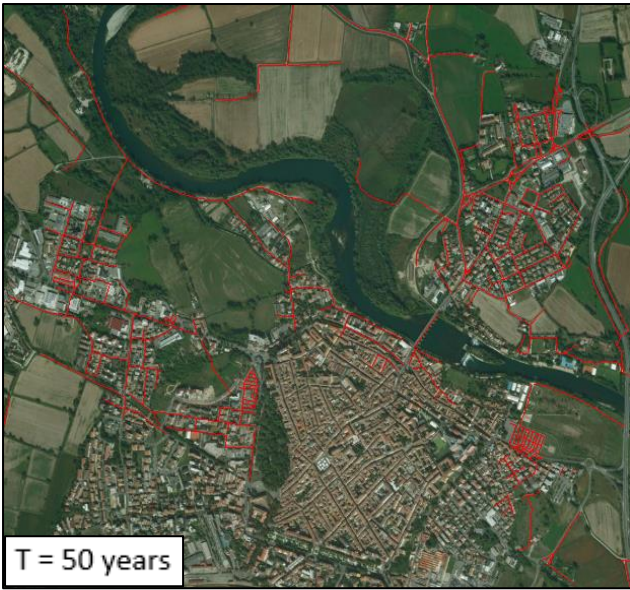


Figure 3-72 Exposed road network (red links) for reference scenarios, without structural defences

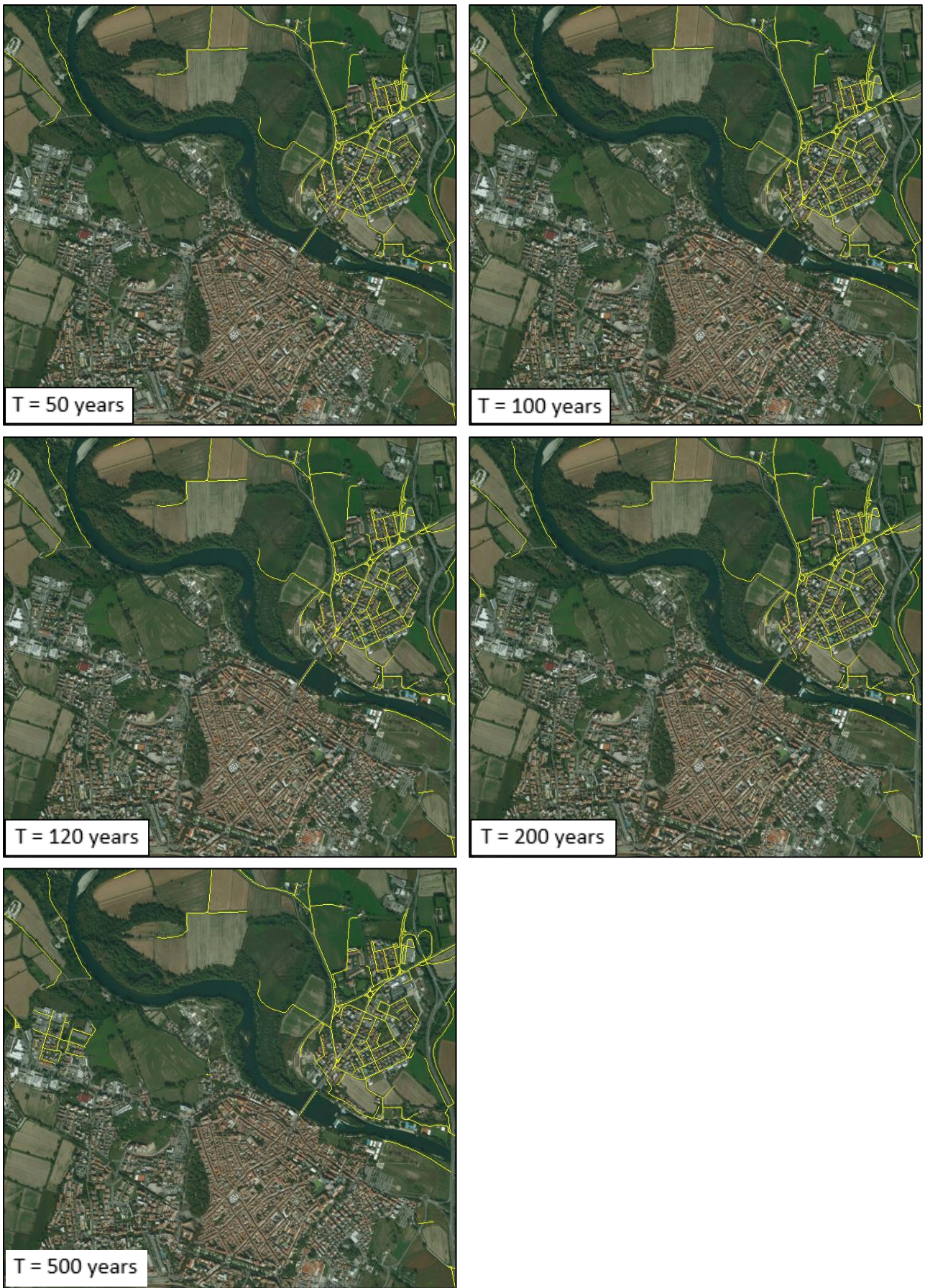


Figure 3-73 Exposed road network (yellow links) for reference scenarios, with structural defences

3.3.5.5 Exposed important facilities

Maximum damages to facilities have been assessed in terms of exposure both in the cases without and with structural defences. As it is possible to see from Table 3-16, facilities have been divided in six categories: commercial services (to which belong hotels, supermarkets and banks), health services, police stations (local police, Carabinieri, Guardia di Finanza), public services (schools, universities, research laboratories, courts), religious places and sport facilities. The last column of the Table 3-16 and Table 3-17 reports the total number of exposed units, while the last column in Table 3-18 represents the reduction of the total number of facilities for each return period event. It has to be remarked that the aforementioned facilities are those located inside the flooded areas of each investigated scenario, identified overlapping the flood hazard raster with the shapefile containing the localisation of all the important structures in the province of Lodi. Indeed, other facilities like town hall and police headquarters, are located in the upper historical part of Lodi and, therefore, in a not flood prone area.

Results show a lower exposure of facilities with the addition of walls and levees, with a reduction between 50% and 55,4%. In regards the direct damage, in order to have monetary values of losses, models for each mentioned category should be required for an assessment. Moreover, in the same category of facility, the kinds of structures, types of contents and service offered must be carefully considered, making necessary a detailed analysis of each unit involved in the flood. Furthermore, not only the direct damages to structure and contents must be taken into account, but also the indirect damages that can affect economy, public order and well-being.

Damages to commercial services could bring to indirect and systemic damages such as commercial chain interruption, loss of jobs (potentially affecting entire families) and social discomfort for residents.

In the scenarios with flood defences, exposure of health services and police stations is completely avoided. However, even in the severe scenarios without structural defences, the hospital is reached by low water levels, being the structure located in a higher area, despite the proximity with the most downstream levee. Health services and police stations are particularly important in case of flood events, being indispensable in the recovery phase and post – event phases operations, such as rescue, organisation and security.

For what concerns schools, universities and research laboratories, in addition to direct damages to structure and contents, indirect damages, such as interruption of the activities and services offered, must be taken into account.

Same reasoning can be done for damages to religious places, that can involve also cultural heritages, and sport facilities, which can induce stop of service offered and social discomfort.

Table 3-16 Summary table of exposed facilities without structural defences

Exposed facilities without structural defences							
T	Commercial services	Health services	Police station	Public services	Religious places	Sport facilities	Total number
50	6	0	3	8	5	24	46
100	9	0	3	9	5	25	51
120	10	1	3	10	5	28	57
200	10	2	3	10	5	28	58
500	10	2	4	10	11	28	65

Table 3-17 Summary table of exposed facilities with structural defences

Exposed facilities with structural defences							
T	Commercial services	Health services	Police station	Public services	Religious places	Sport facilities	Total number
50	3	0	0	1	1	18	23
100	4	0	0	1	1	19	25
120	5	0	0	1	1	20	27
200	5	0	0	1	1	20	27
500	6	0	0	1	2	20	29

Table 3-18 Reduction of exposed facilities with structural defences

Reduction of exposed facilities with structural defences [%]							
T	Commercial services	Health services	Police station	Public services	Religious places	Sport facilities	Total number
50	50.0%	0.0%	100.0%	87.5%	80.0%	25.0%	50.0%
100	55.6%	0.0%	100.0%	88.9%	80.0%	24.0%	51.0%
120	50.0%	100.0%	100.0%	90.0%	80.0%	28.6%	52.6%
200	50.0%	100.0%	100.0%	90.0%	80.0%	28.6%	53.4%
500	40.0%	100.0%	100.0%	90.0%	81.8%	28.6%	55.4%

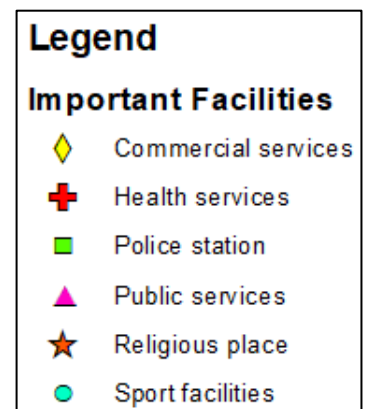
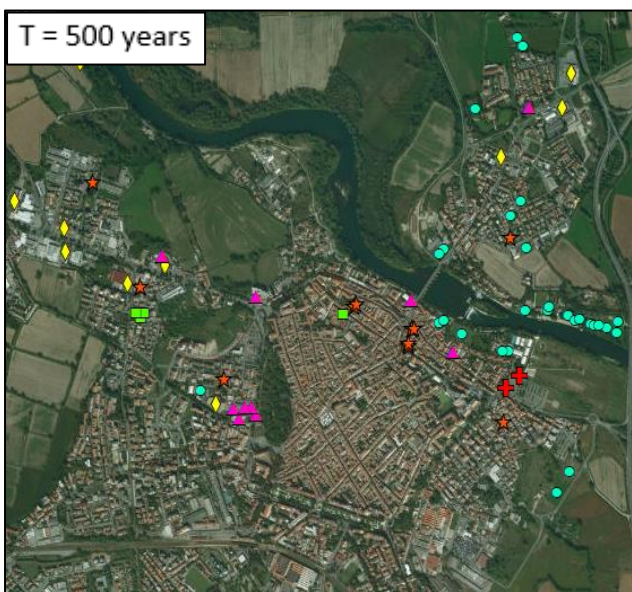
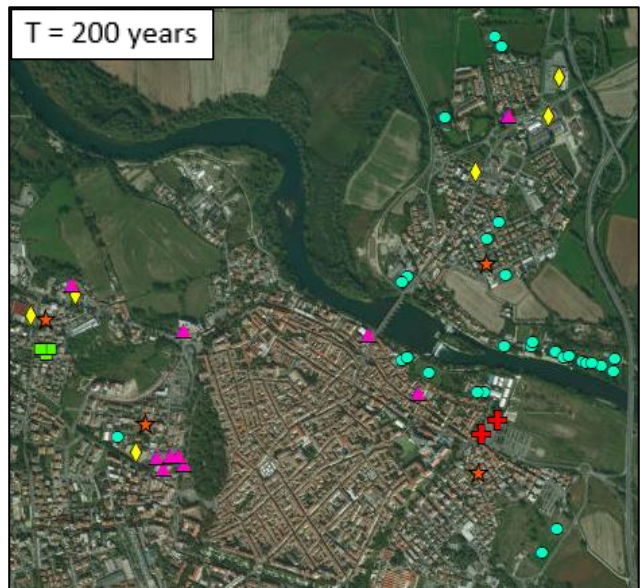
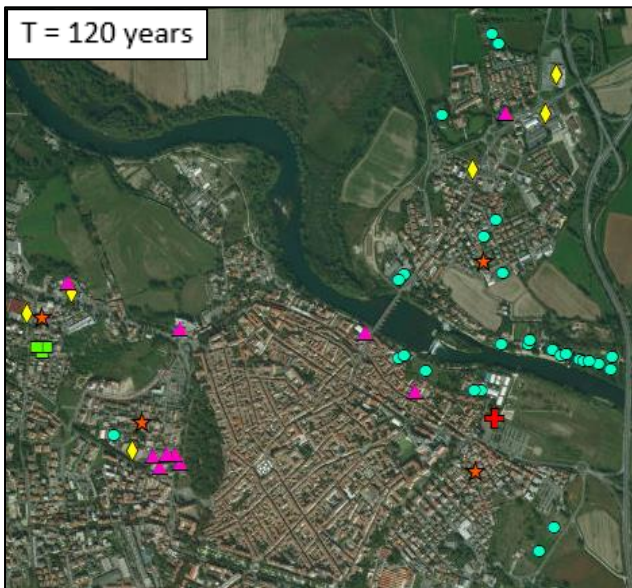
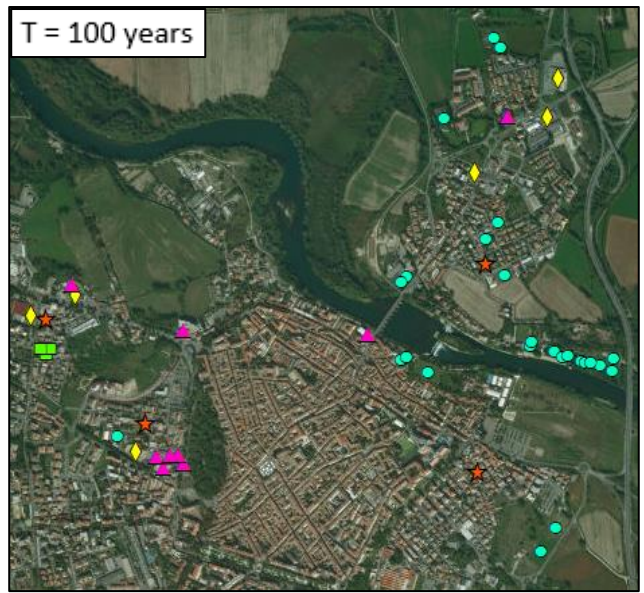
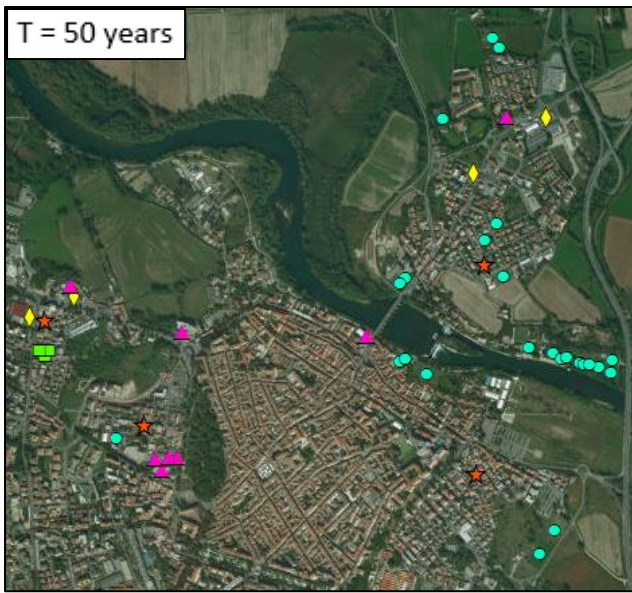


Figure 3-74 Exposed important facilities for reference scenarios, without structural defences

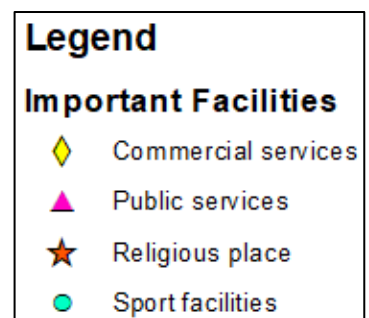
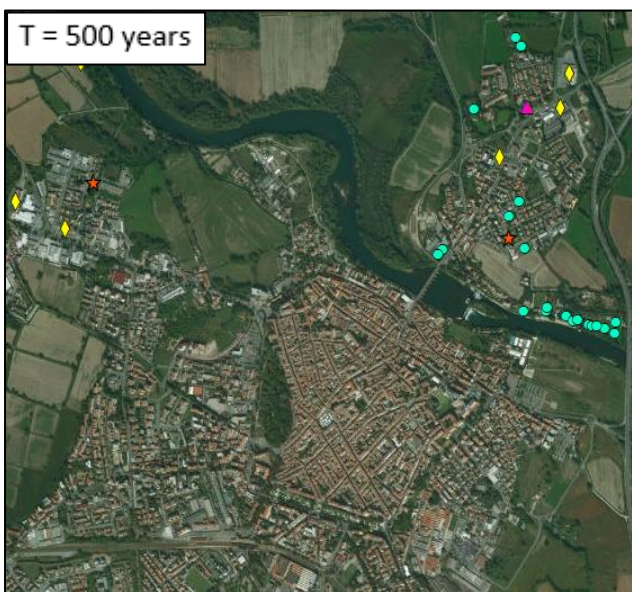
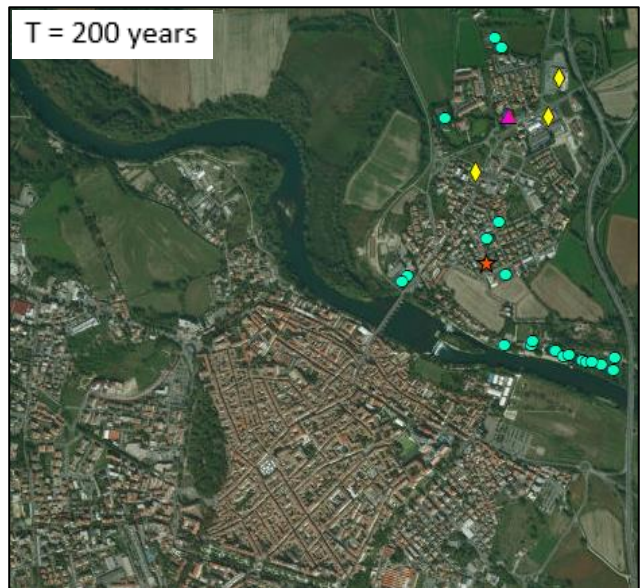
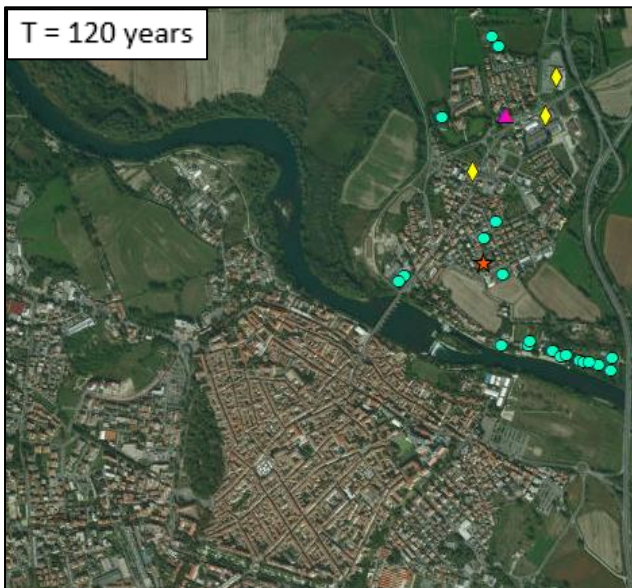
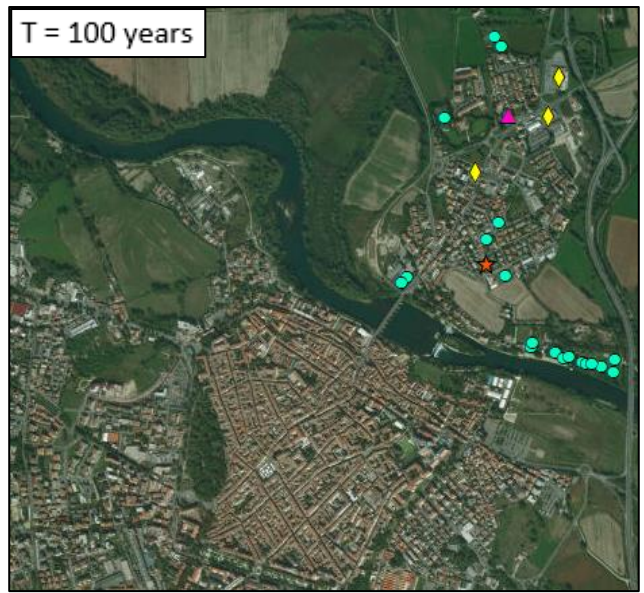
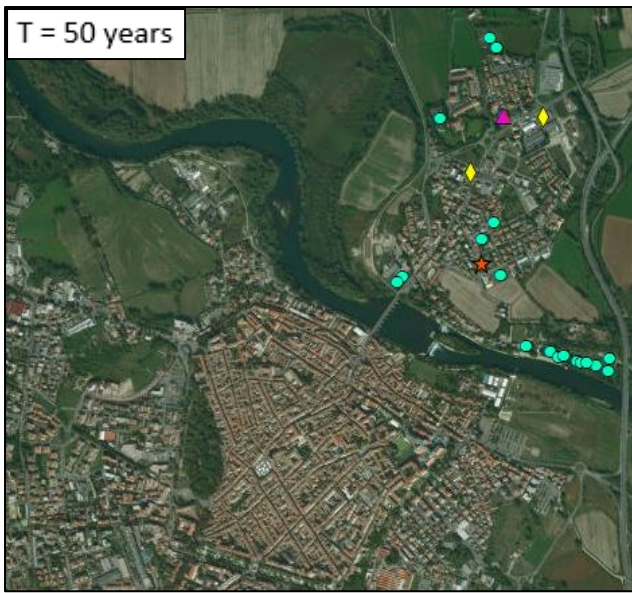


Figure 3-75 Exposed important facilities for reference scenarios, with structural defences

“Page intentionally blank”

3.3.5.6 Exposed cultural heritage

In addition to exposed population, road network and facilities, potential damages to cultural heritage have been assessed in terms of exposure to flood in both the scenarios without and with structural defences. A distinction between industrial architectures, residential architectures and services, religious structures, rural buildings and infrastructures has been done, as shown in the Table 3-19, in order to highlight different cultural items present in Lodi. Results show a reduction of the total number of exposed cultural heritages between 45,8% and 51,4%, after the construction of flood protections. In this case also, only those structures located inside the flooded areas for each reference scenario have been considered, overlapping the flood hazard raster files with the shapefile containing the location of cultural heritage. Direct damages are complex to be quantify, being cultural heritage usually priceless values and very different between them for kind of structure, age and artistic and historical involvement.

Table 3-19 Summary table of exposed cultural heritage without structural defences

Exposed cultural heritage without structural defences						
T	Industrial architecture	Residential architecture and services	Religious architecture	Rural architecture	Infrastructure	Total number
50	3	7	2	11	1	24
100	3	10	3	11	1	28
120	3	10	3	13	1	30
200	3	11	3	14	1	32
500	3	12	7	14	1	37

Table 3-20 Summary table of exposed cultural heritage with structural defences

Exposed cultural heritage with structural defences						
T	Industrial architecture	Residential architecture and services	Religious architecture	Rural architecture	Infrastructure	Total number
50	1	2	1	8	1	13
100	1	4	1	8	1	15
120	1	4	1	8	1	15
200	1	4	1	9	1	16
500	1	6	1	9	1	18

Table 3-21 Reduction of exposed cultural heritage with structural defences

Reduction of exposed cultural heritage with structural defences [%]						
T	Industrial architecture	Residential architecture and services	Religious architecture	Rural architecture	Infrastructure	Total number
50	66.7%	71.4%	50.0%	27.3%	0.0%	45.8%
100	66.7%	60.0%	66.7%	27.3%	0.0%	46.4%
120	66.7%	60.0%	66.7%	38.5%	0.0%	50.0%
200	66.7%	63.6%	66.7%	35.7%	0.0%	50.0%
500	66.7%	50.0%	85.7%	35.7%	0.0%	51.4%

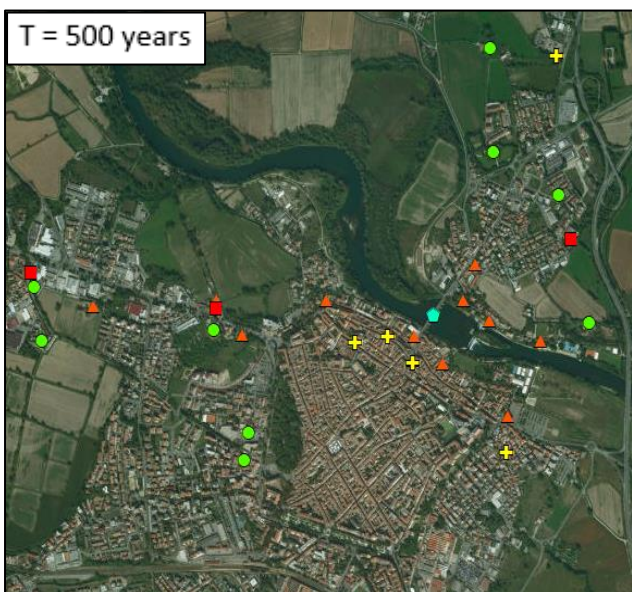
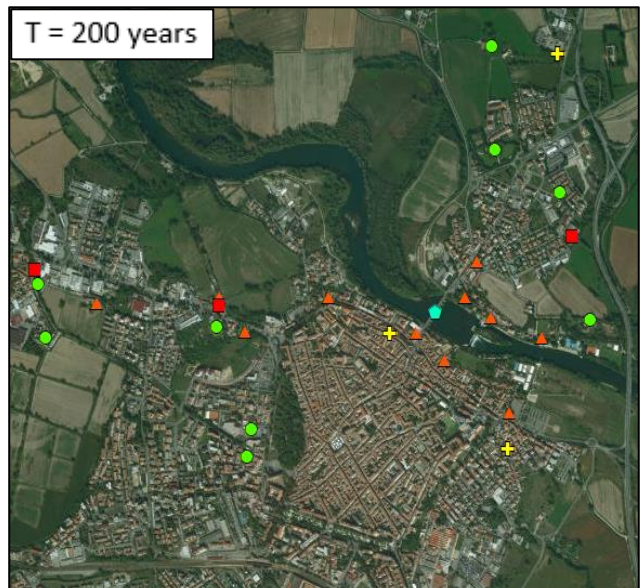
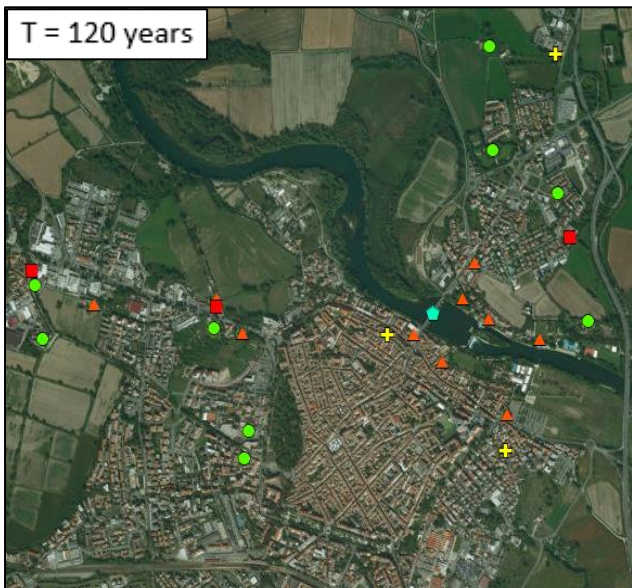
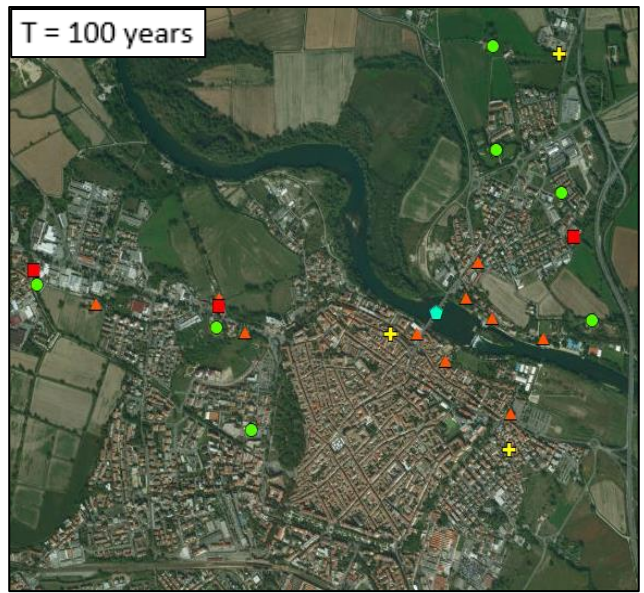
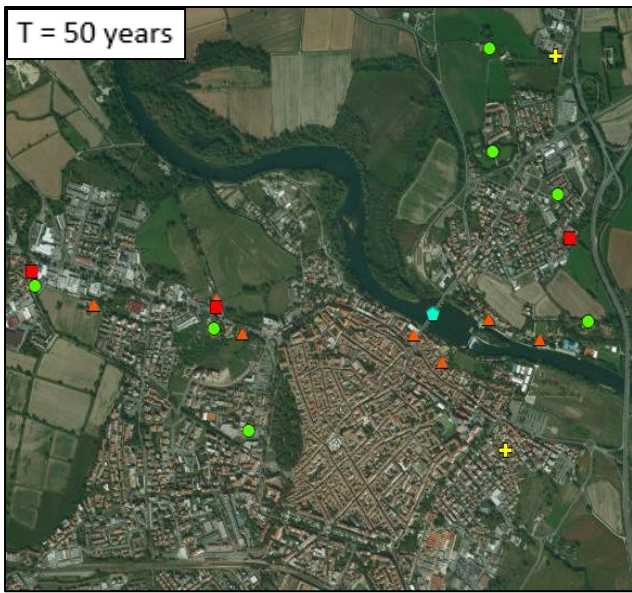


Figure 3-76 Exposed cultural heritage for reference scenarios, without structural defences

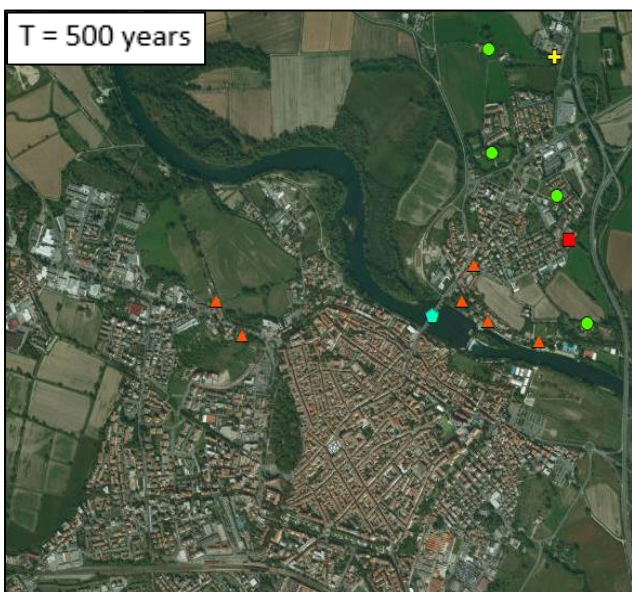
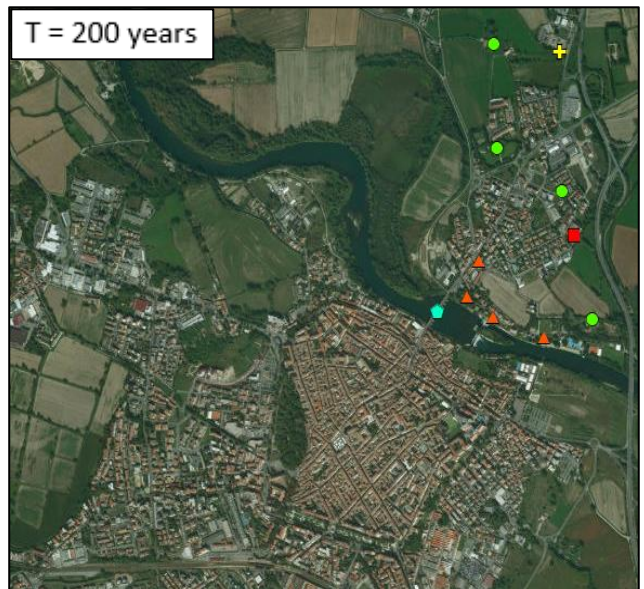
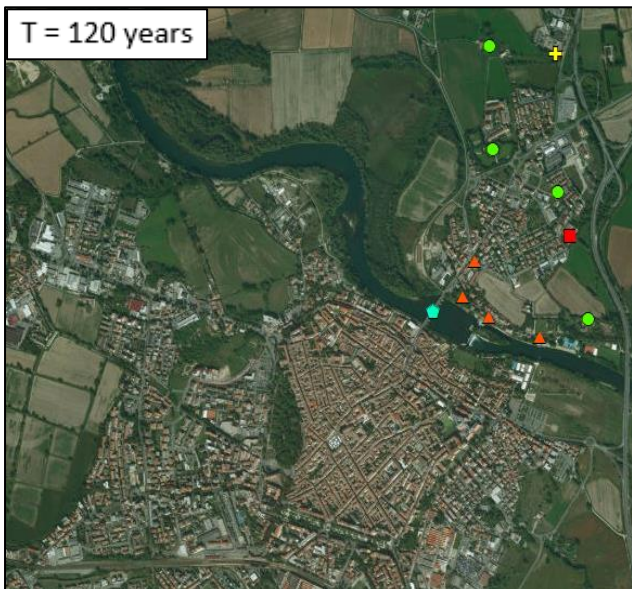
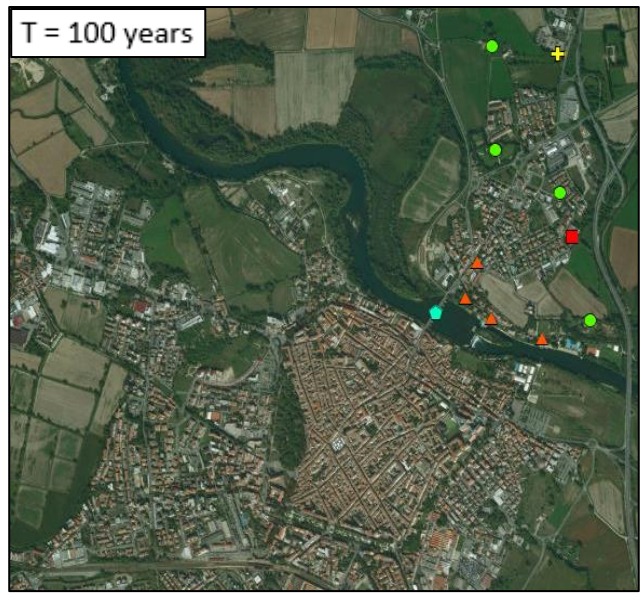
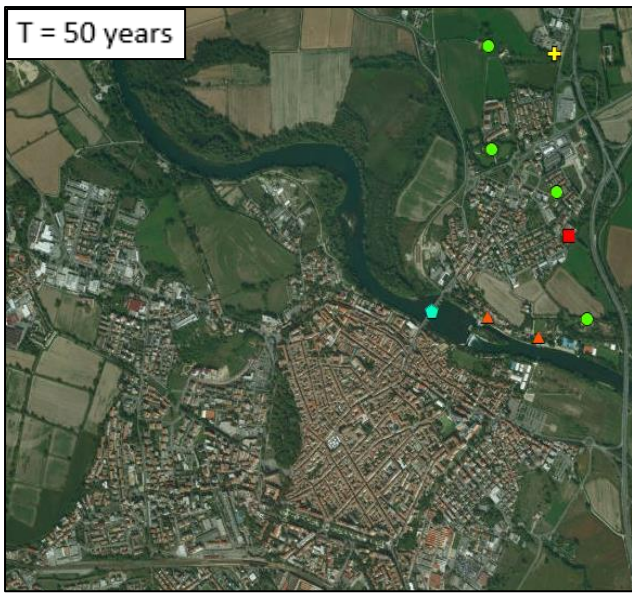


Figure 3-77 Exposed cultural heritage for reference scenarios, with structural defences

3.3.5.7 Other non-quantifiable damages to be considered in MCA

In order to enrich the benefits assessment performed so far, other non-quantifiable values, in terms of exposure reduction, could be considered. For instance, reduction of flooded green areas, lifelines, damaged vehicles and other goods, animals in stables and farms, and many more should be added to the previous benefits assessment. These assets are difficult to be evaluated due to the complexity of data collection and their monetary estimation. Indeed, this analysis would require a micro-scale approach, in which elements should be singularly assessed. Moreover, the presence of experts in each of the aforementioned fields could be required, increasing the complexity of the analysis.

For what concerns lifelines such as water, gas, power supplies and communication system, they represent important resources for the municipality and for the people themselves, ensuring daily functioning of services and activities. Indeed, direct damage to lifelines' function corresponds to an indirect damage to users. Lifelines are inter-connected, having an internal hierarchy among components of the same system. Therefore, in lifelines assessment, physical, functional and organisational vulnerabilities have to be accounted, highlighting the complexity in defining potential damages coming from their exposure to floods. Moreover, most of the lifelines belongs to private companies, making more difficult the collection of information in regards and their localisation.

Potential avoided damages to vehicles reached by the flood should be considered in evaluating benefits coming from the construction of mitigation measures. Indeed, they represents future costs that will be charged to residents but also to insurance companies that will be indirectly involved in case of losses. 32.630 vehicles have been estimated in the municipality of Lodi (ACI, 2017). However, also this analysis would require an assessment of the single element, considering for instance the location of the vehicle (i.e. if located in a basement, probably it will be completely damaged), how many residents are commuters and, therefore, potentially present at the occurrence of the flood and the real value of the goods.

Another bearer of potential damages is the animal breeding sector. According to estimates, 1258 farms and stables are located in the province of Lodi, with 950.329 breeding animals (ISTAT, 2010). Currently, there are no validated models for the monetary evaluation of the potential damage coming from this sector, missing detailed information at a municipal scale.

Other tangible indirect damages could derive from emergency costs in case of flood (i.e. first aid, evacuation, shelter, sandbags), relocation of industries, devaluation of houses and goods, while intangible ones could be represented by health effects, loss of ecological goods, inconvenience of post-flood recovery.

3.3.6 Conclusions of the MCA

In the summary Table 3-22 are reported the results of the performed damage assessments to be considered within a multi-criteria analysis (MCA). In particular, the percentages of damage reduction, with the flood protections in place, for residential buildings and agricultural sector, and the reduction of the maximum direct potential losses for economic activities have been shown for the five investigated scenarios. Moreover, the exposure reduction of number of inhabitants (subdivided in total, vulnerable and foreign), km of road network, number of important facilities and cultural heritage have been also proposed.

Results show a damage reduction between 50% and 53% for residential buildings, while lower values between 8% and 12% for the agricultural sector. The lower percentages of reduction of damage to crops are due to the fact that the hydraulic right of the river Adda, the one on which the structural defences are placed, is mainly characterised by an urban environment. For what concern the exposure of economic activities, a growing trend is observed increasing the severity of the event, due to constantly wider modelled flooded areas. Looking at the values of exposure reduction of inhabitants and road network, the increasing trend is interrupted for the scenario with 500 years of return period, in which part of Lodi is flooded due to the overflow of the soil embankment nearby the S.P. 202. Eventually, the exposure reductions of the important facilities have been estimated between 50% and 55%, slightly greater than the obtained reductions of cultural heritage units between 46% and 51%.

Table 3-22 Summary table of the damage assessment

Involved assets	Unit of measure	% of damage/exposure reduction with the structural defences in place				
		T = 50	T = 100	T = 120	T = 200	T = 500
Residential buildings	Damage in €	51,0 %	50,3 %	52,6 %	52,2 %	51,8 %
Agricultural sector	Damage in €	11,7 %	12,0 %	11,1 %	10,8 %	8,1 %
Economic activities	Exposure in €	48,2 %	51,1 %	66,9 %	67,9 %	76,4 %
Total population	Exposure in inhabitants	60,8 %	62,9 %	69,7 %	69,7 %	66,5 %
Vulnerable population	Exposure in inhabitants	61,2 %	63,9 %	71,4 %	71,4 %	69,6 %
Foreign population	Exposure in inhabitants	65,3 %	68,1 %	72,5 %	72,4 %	61,5 %
Road network	Exposure in km	31,8 %	35,4 %	36,2 %	36,1 %	34,7 %
Important facilities	Exposure in number	50,0 %	51,0 %	52,6 %	53,4 %	55,4 %
Cultural heritage	Exposure in number	45,8 %	46,4 %	50,0 %	50,0 %	51,4 %

3.3.7 Sensitivity analysis

In this chapter, a sensitivity analysis is conducted to determine how the aforementioned results in terms of avoided damages, and therefore in benefit cost ratio, would change in case of modification of some input to the models. First a “levee effect” will be considered and then, separately, the occurrence of floods in May will be simulated.

3.3.7.1 Levee effect

A sensitivity analysis has been performed assuming the “levee effect” due to the presence of the structural defences. Indeed, the construction of flood protections could generate an economic growth of the involved area and a sense of security against inundations perceived by the population. In other words, inhabitants that live behind the structural defences develop the conviction that another severe flood will not create damages but will be contained by the protection. Sometimes, this feeling is accompanied by a lack of resilience from the population, in terms of bad memories of events that occurred in the past. This combination can generate an urbanisation of flood prone areas behind the defence walls and levees. To perform the analysis, a new potential urbanised area is assumed and represented by the red polyline reported in the Figure 3-78, in which also the stretches of structural defences, in the hydraulic right of the river Adda, are drafted in yellow polyline.



Figure 3-78 Representation of the new potential building area (red polygon) and of the structural defences in the hydraulic right (yellow polyline)

The new potential area covers 323.758 m² and it is located between residential zones and few industrial sheds. The hypothesis is that this new area would be filled by other residential blocks, with similar characteristics to the surrounding ones. Therefore, in order to estimate the number of new residential buildings inside the red polyline, four adjacent urban blocks have been analysed. In

details, the area of each zone has been computed, as well as the square meters effectively covered by the belonging houses and structures. Then, estimations of the urban densities have been obtained, dividing the covered square meters with the total area of each zone. Consequently, these four densities have been averaged, giving, as result, an urban density for the new area equal to 23%. Moreover, it has been considered, measuring the sizes of the surrounding residential buildings, that the average area of a construction is equal to 280 m². Eventually, the total number of residential building inside the new urbanisable area has been obtained multiplying the total area (323.758 m²) by the averaged urban density (23%) and then subdivided by the average building size (280 m²), giving, as results, 271 new residential structures. According to the hazard maps for the scenario with T=500 years with structural defences, the new urbanisable area would be flooded with an average depth of 0,31 m.

A further sensitivity analysis has been performed, considering two different typologies of constructions, in terms of type of building structure, presence of basement and finishing levels. As explained in the chapter 2.6, these three parameters involved in the computation of direct damage to residential building, have a great influence in the final amount of potential damage. In particular, buildings made of bricks are more vulnerable than reinforced concrete and wood, the presence of basement implies the total flooding of it with the addition of the damage to the boiler, while high finishing levels leads to higher damages. Therefore, two combinations of construction strategies have been assumed, representing two opposite choices of residential urbanisation:

- Buildings with basement, made of bricks and with high finishing levels;
- Buildings without basement, made of reinforced concrete or wood and with low finishing levels.

It is immediate to notice that the first typology will bring to much higher damages with respect to the second one, making the latter the most rational strategy of construction in a potential flood prone area. However, having regard to the low estimated water depth, being the occurrence of the event rare and having built the structural defences, the first strategy, more vulnerable and so potentially bearer of major damages, could be chosen. Therefore, the estimated total damage to the aforementioned 271 residential buildings has been computed considering the two opposite construction strategy scenarios, by using the INSYDE model.

Table 3-23 Summary table of estimated direct damages of the new residential buildings, considering the “levee effect” scenario

Estimated direct damages to new residential buildings for the scenario T=500 years with structural defences	
Construction strategy	Damage [MLN €]
Buildings with basement, made of bricks, with high finishing levels	12,33
Buildings without basement, made of r.c. or wood, with low finishing levels	1,00

Considering the two opposite conditions of construction parameters, the damage to residential building, to be added to the value obtained in the chapter 3.3.3.1 for T=500 with structural defence, ranges from 3.700,00 € to 45.500,00 € for each building, corresponding respectively to an additional amount between 1 MLN € to 12,33 MLN €.

The 271 new residential buildings would be located in fields currently dedicated to agriculture sector. Therefore, the construction of the new residential area would bring to a reduction of the potential damage to agriculture in November of approximately 13.300,00 €.

Considering the new damages to agriculture sector and the two opposite values of additional damage to residential building, the benefit – cost ratio would decrease. Indeed, the yearly estimated avoided damage to residential buildings would be about € 205.000,00/year for the most vulnerable construction strategy and € 222.000,00/year for the less vulnerable one (the yearly benefits without the new buildings was € 224.700,00/year). In regards to the agricultural sector, the yearly benefits would be slightly greater than the yearly benefits with the current agricultural fields. Therefore, the total benefits would be around € 206.000,00/year for the first building configuration and € 223.500,00/year for the second one, leading to values of benefits – costs ratios respectively of 2,2 and 2,38, slightly lower than the 2,4 obtained without the addition of the new residential area. In the light of these results, even with the construction of 271 new residential buildings, with two different construction strategies, the structural defences would bring more yearly benefits than costs, highlighting the efficacy and usefulness of the flood protections.

“Page intentionally blank”

3.3.7.2 Flood in May as consequence of climate change

Climate change and urban development are key elements contributing to increased flood damage (Poelmans et al., 2011). Recent studies have shown different effects of climate change on flood risk (Löschner et al., 2017) and the Intergovernmental Panel on Climate Change claimed, with low confidence, that climate change has affected the frequency and magnitude of flooding (IPCC, 2014). This sensitivity analysis assumes the possibility of a flood occurrence in May, as consequence of climate change, investigating on the effect of the latter on the potential damages caused by the event.

The computation of damages to agricultural sector has been performed using the AGRIDE-c model and the followed procedure is the same one previously discussed in chapter 3.3.3.2. The choice to consider a flood in May has been assumed after an analysis of the hydrometer levels, from the second half of 1998 until June of 2018, obtained from ARPA Lombardia (*“Agenzia Regionale per la Protezione dell’Ambiente”*). The latter have been converted then in discharge and events with peak greater than 800 m³/s has been analysed only, as highlighted by the yellow line in the Figure 3-79. This graph reports the time expressed in hours on the x axis and the overlapped discharge curves on the y one. It has to be remarked that the values of the time discretization are approximately the cumulative hours of the months of the year, in order to ease the visualization and selection of periods with high frequency of flood occurrence (events with discharge greater than 800 m³/s). As it is possible to notice from the Figure 3-79, May and November are the two months in which more than five events occurred in the last twenty years (included the 2002 flood event) and, therefore, they have been selected for the computation of damages to the agriculture sector. Moreover, May and November coincide with period of the year in which crops show different life phases and, as consequence, different amount of potential losses.

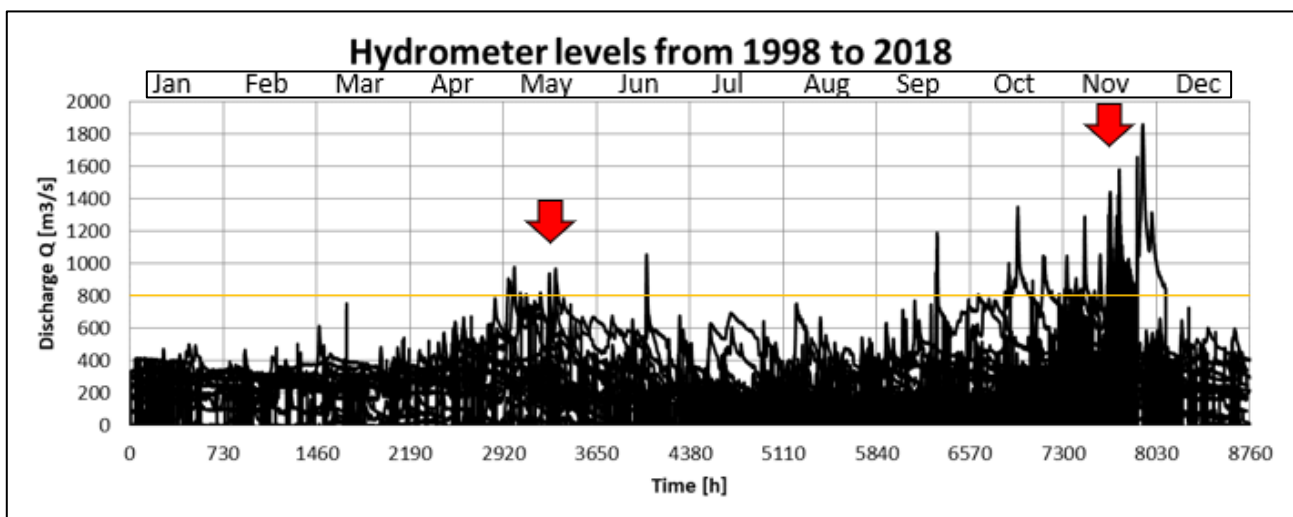


Figure 3-79 Hydrometer levels over the last twenty years

As already done for the computation of damages in November, the duration of the water that inundates the fields has been considered too, in order to define possible combinations of “period of the year and permanence of the water”.

As far as the cultivated phases in May are concerned, total damage (100%) to grain maize occurs if the permanence of the water on the field lasts longer than 10 days, being the crop in the growing phase. Wheat and barley crops are in the flowering stage of their life and their damage trend is similar, in which light to medium damage is obtained from 6 to 12 days, while total damage is reached after 13 days. Low to medium damage is observed in grassland fields if the flood has a duration between 9 and 12 days, after which total damage is achieved. It has to be remembered that grassland has a low weight in the total damage to agriculture fields. For what concerns the soy crops, total damage is reached when the permanence of water lasts longer than 10 days, while light (20 – 40 %) and medium (40 – 60 %) damage is observed respectively after 3 and 7 days (Dutta et al., 2003).

Table 3-24 Damage to crops in May: no damage (green), slight damage (yellow), medium damage (orange), total damage (red)

	Permanence of the water [days]																			
	1	2	3	4	5	6	7	8	9	10	11	12	13	14	15	16	17	18	19	20
Grain Maize	Green	Green	Green	Green	Green	Green	Green	Green	Green	Green	Red	Red	Red	Red	Red	Red	Red	Red	Red	Red
Wheat crop	Green	Green	Green	Green	Green	Yellow	Yellow	Yellow	Yellow	Orange	Orange	Orange	Red							
Barley crop	Green	Green	Green	Green	Green	Yellow	Yellow	Yellow	Yellow	Orange	Orange	Orange	Red							
Grassland	Green	Green	Green	Green	Green	Green	Green	Green	Yellow	Yellow	Orange	Orange	Red							
Soy	Green	Green	Yellow	Yellow	Yellow	Yellow	Orange	Orange	Orange	Orange	Red	Red	Red	Red	Red	Red	Red	Red	Red	Red

Eventually, considering Table 3-24, two different combinations “period of the year – permanence of the water” have been identified, in order to consider the most favourable and the worst of cases:

- May – 3 days;
- May – 15 days.

For each assumed combination, maps without and with flood protections will be presented in two consequent pages, in order to ease the comparison between them and highlight the efficiency of the structural defences. Moreover, a trend curve of the damage and a summary table with the percentages of damage reduction for different T will be reported after the graphical representations.

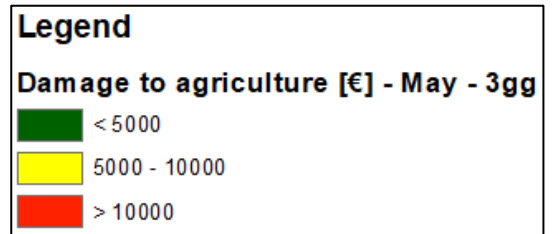
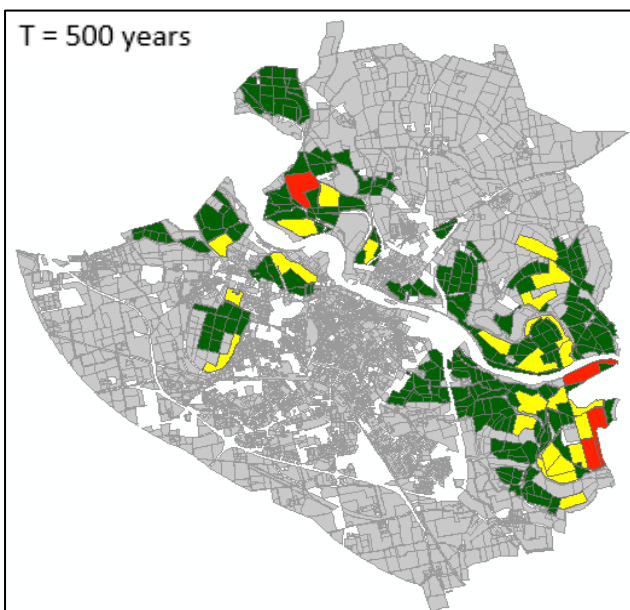
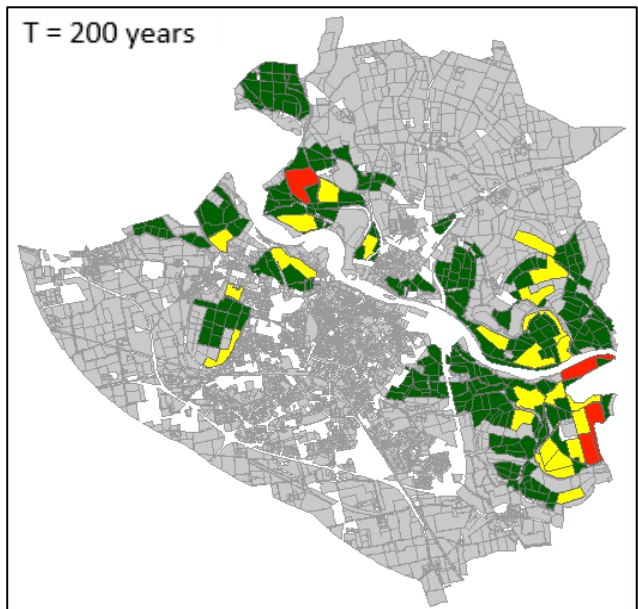
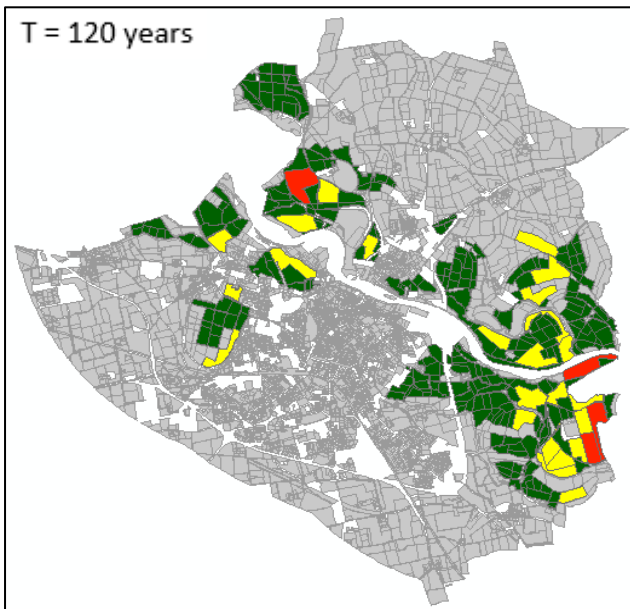
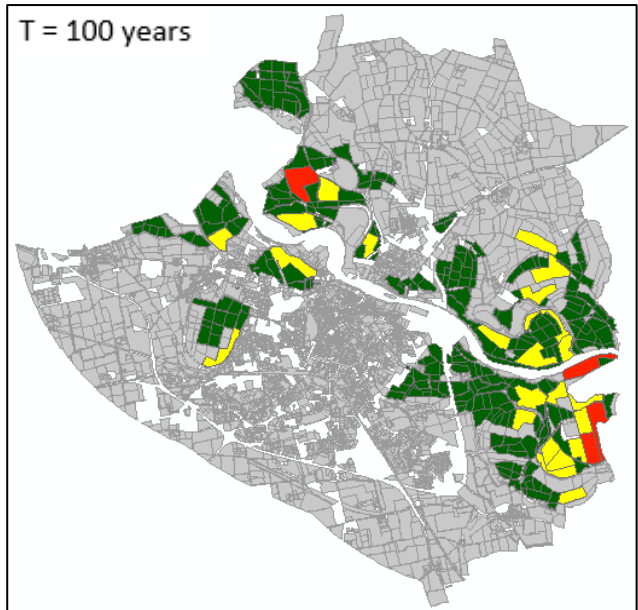
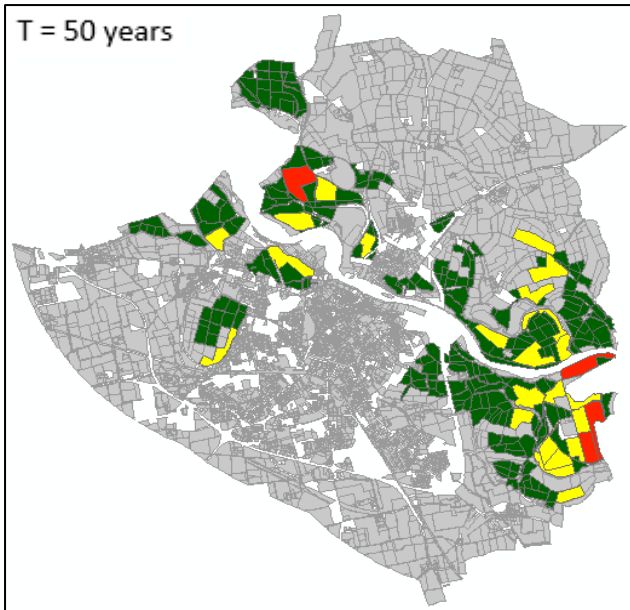


Figure 3-80 Damage to agriculture with the combination May - 3 days, without structural defences

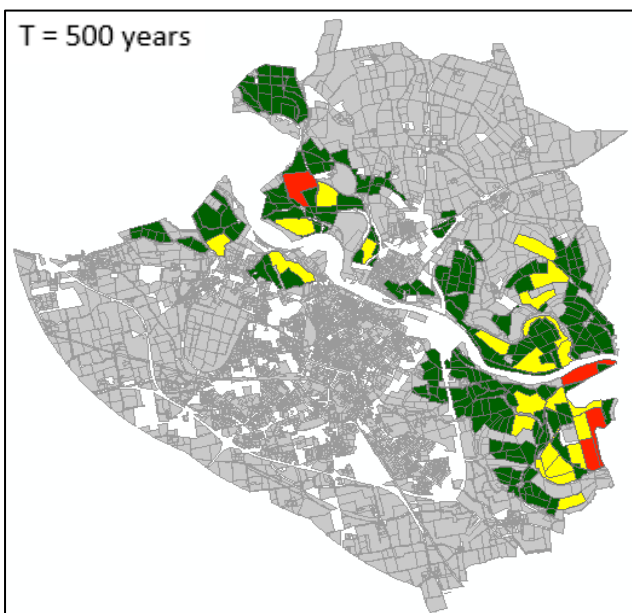
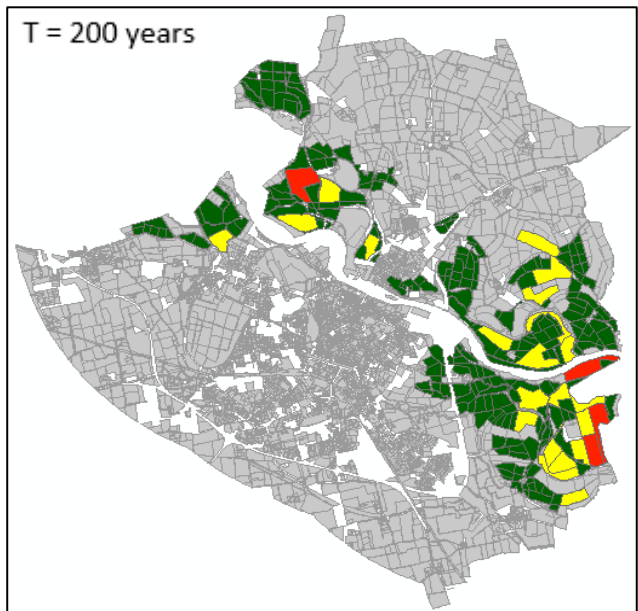
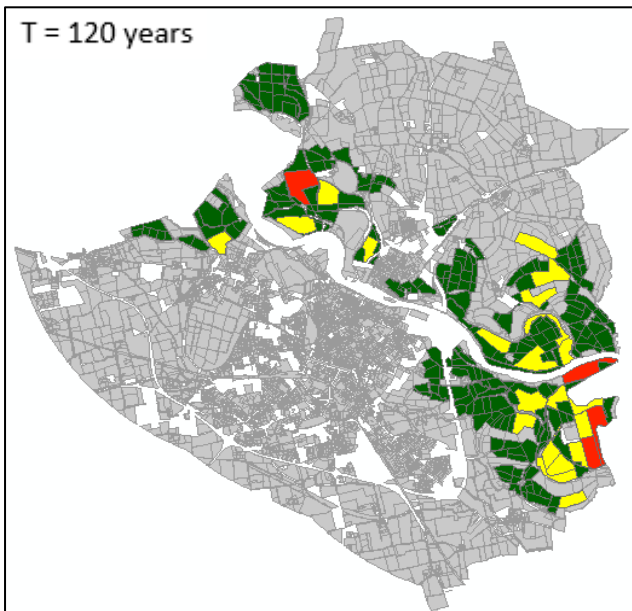
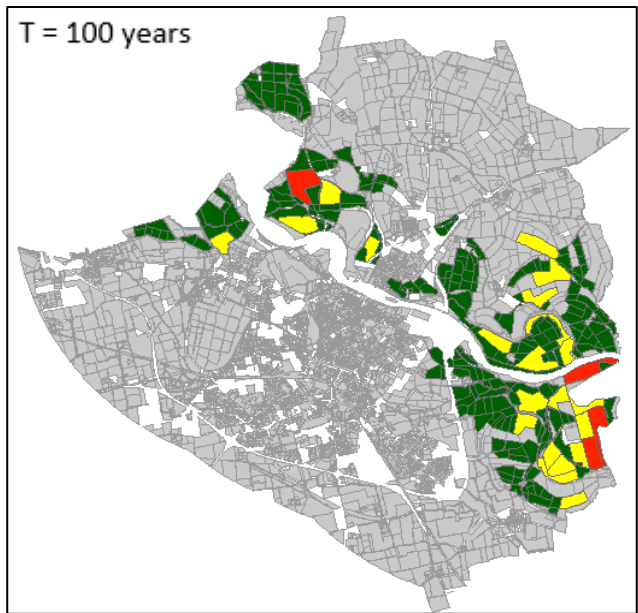
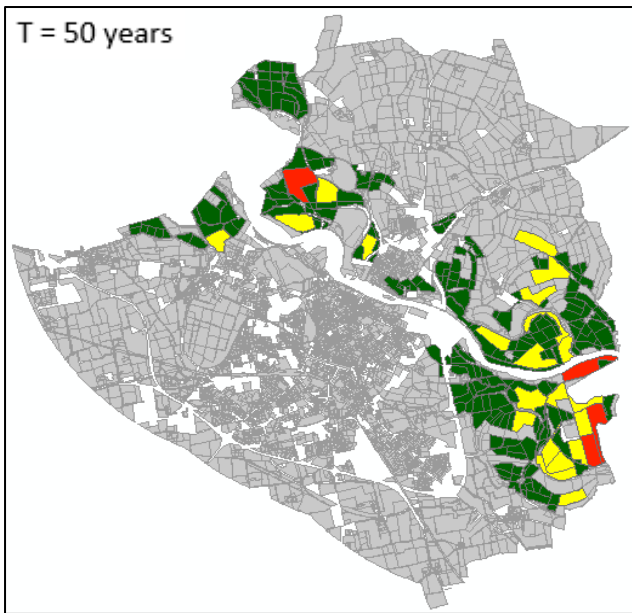


Figure 3-81 Damage to agriculture with the combination May - 3 days with structural defences

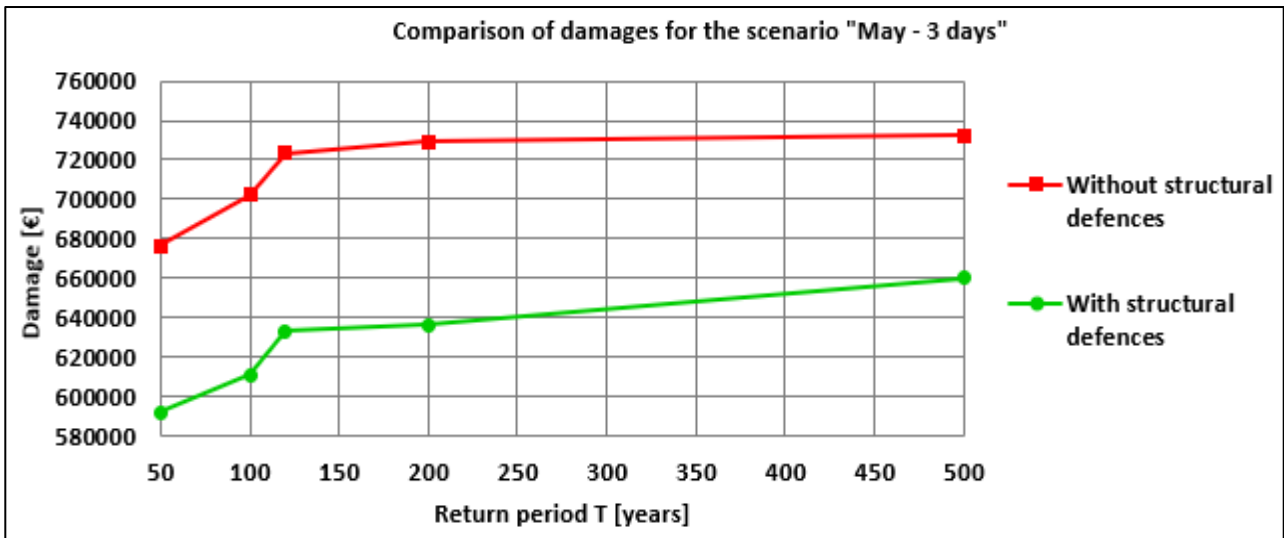


Figure 3-82 Comparison of damage trend curves for the scenarios “May – 3 days”

Table 3-25 Summary results of the damages with and without structural defences and damage reduction for the combination “May – 3 days of water permanence”

T	Damage without structural defences [€]	Damages with structural defences [€]	Damage reduction with structural defences [%]
50	676.400,00	591.800,00	12,5 %
100	702.100,00	611.300,00	12,9 %
120	723.600,00	633.300,00	12,5 %
200	729.100,00	636.400,00	12,7 %
500	732.200,00	660.400,00	9,8 %

Results for the five reference scenarios reports higher damages with respect to the November case, due to the different life stage of the considered crops in May, as previously mentioned. With the addition of the structural defences, estimated reduction of damages between 12,5% and 12,9% have been obtained for scenario with T=50, 100, 120 and 200 years. The growing trend of the curves, represented in Figure 3-82, are due mainly to the increase of the flooded area, involving therefore more agricultural particles, and of the water level on the fields. In regards the 500 years of return period, the smaller estimated reduction of damages (9,8%) is a consequence of the flooded area in the north-east side of Lodi, as represented in the hazard map for T=500 years in Figure 3-50.

“Page intentionally blank”

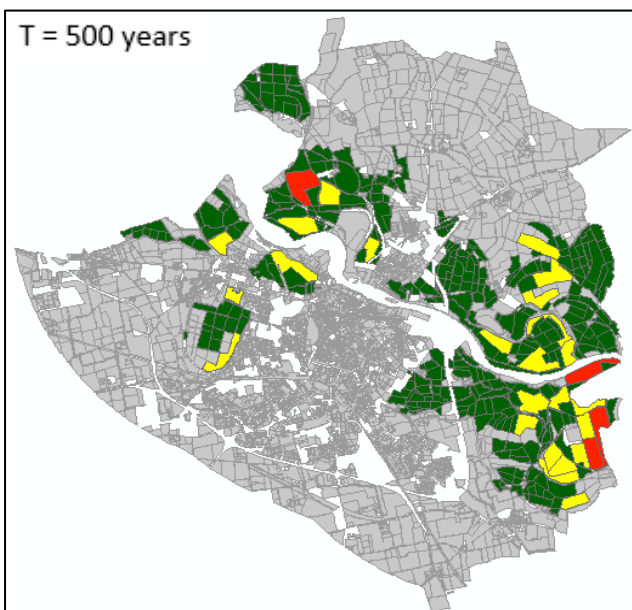
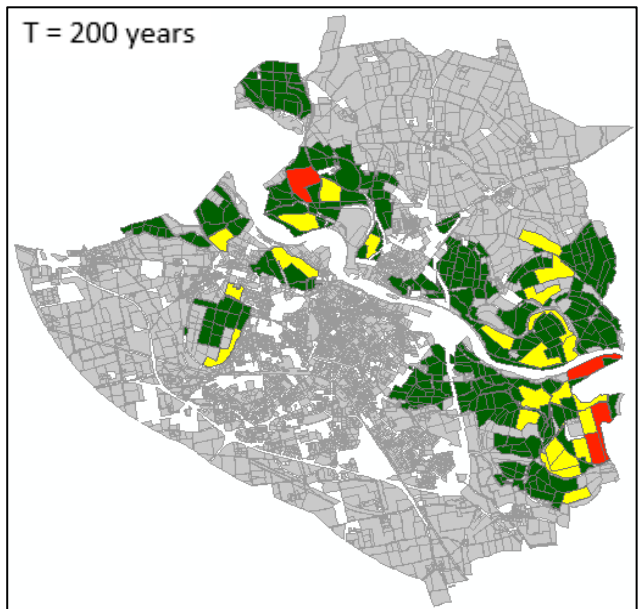
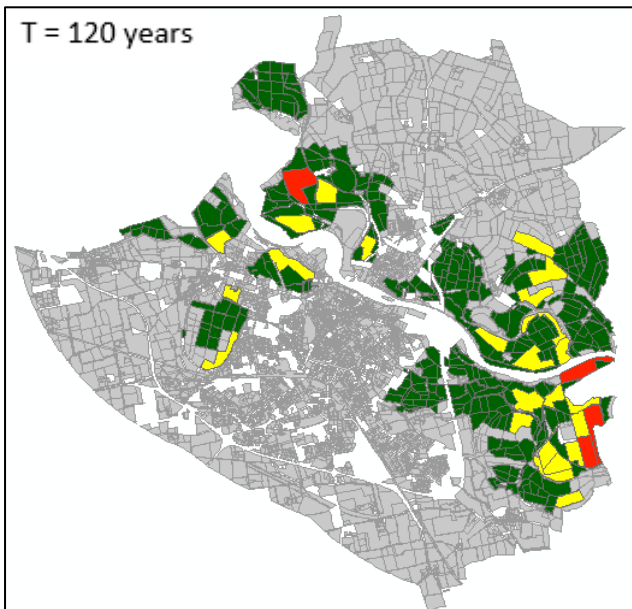
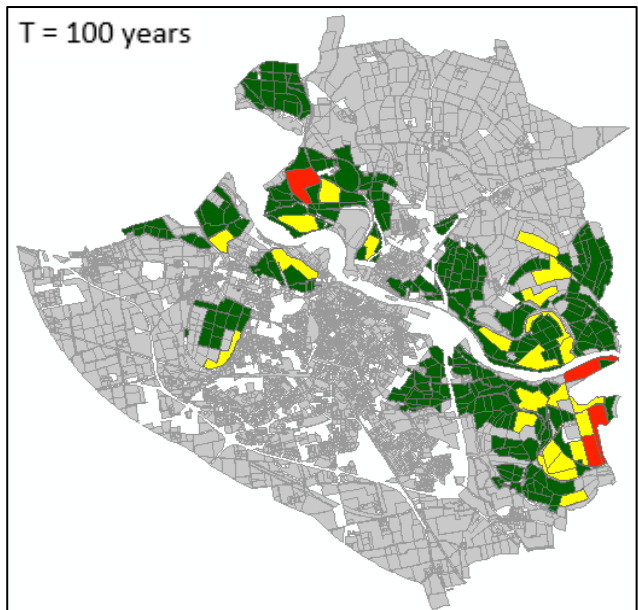
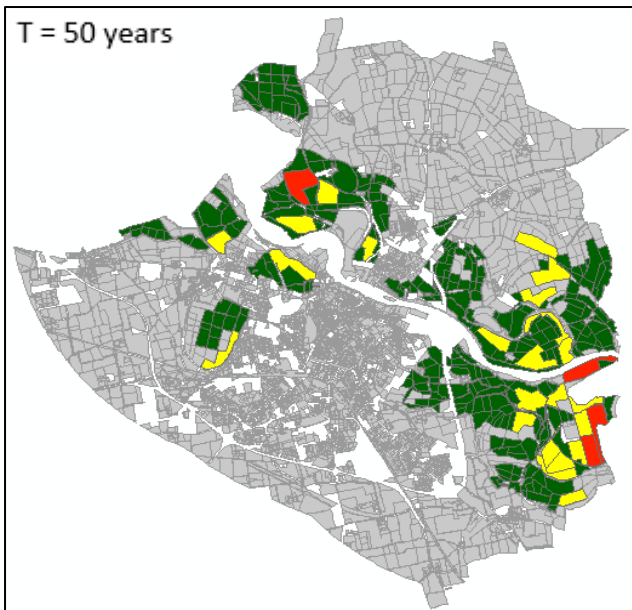


Figure 3-83 Damage to agriculture with combination the May - 15 days, without structural defences

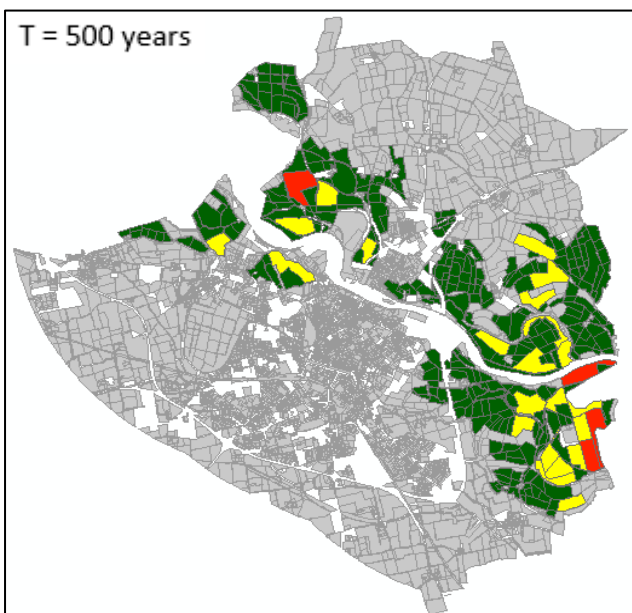
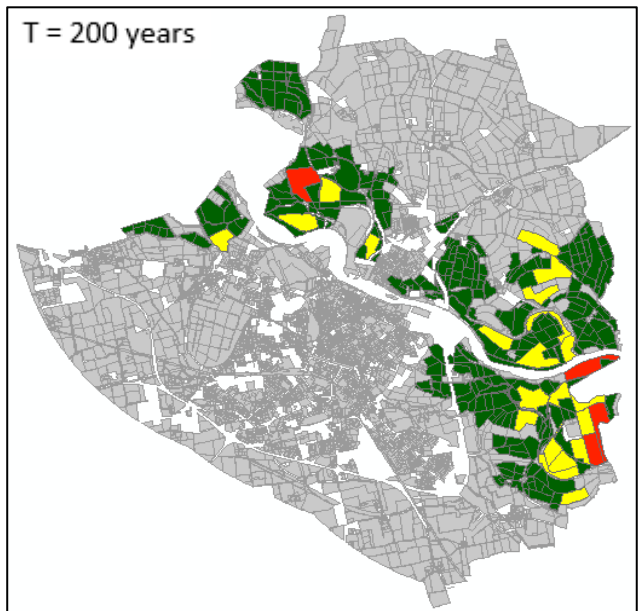
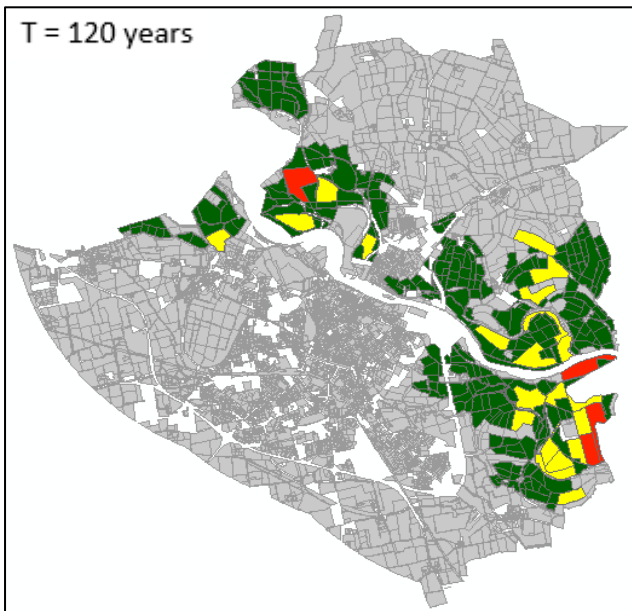
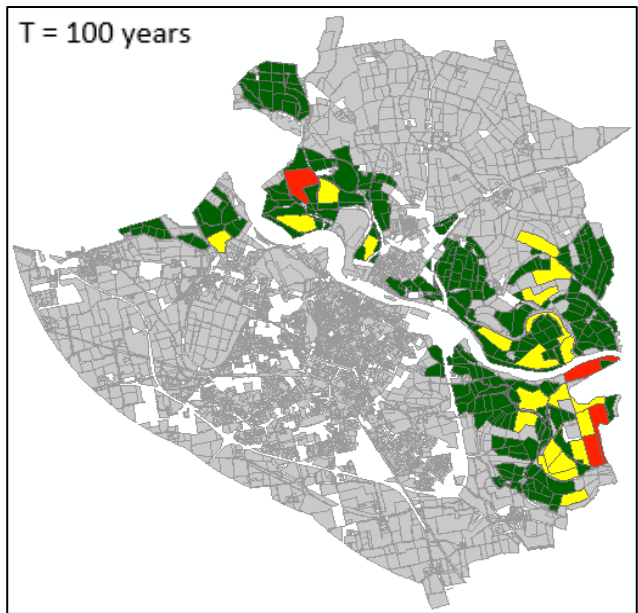
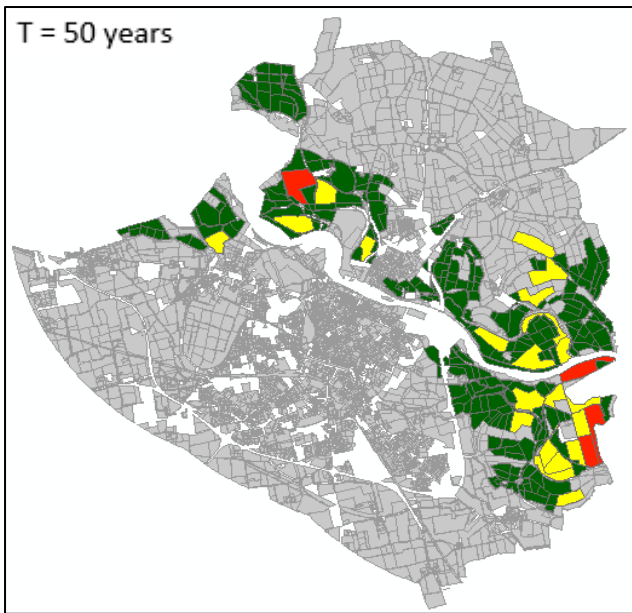


Figure 3-84 Damage to agriculture with combination the May - 15 days with structural defences

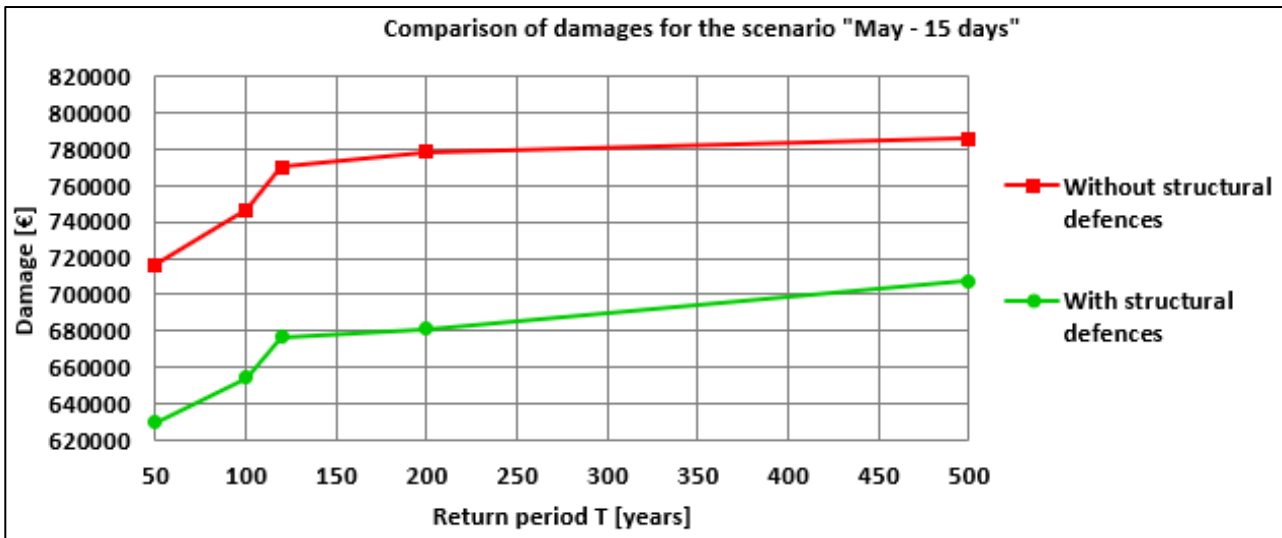


Figure 3-85 Comparison of damage trend curves for the scenarios “May – 15 days”

Table 3-26 Summary results of the damages with and without structural defences and damage reduction for the combination “May – 15 days of water permanence”

T	Damage without structural defences [€]	Damages with structural defences [€]	Damage reduction with structural defences [%]
50	716.400,00	629.700,00	12,1 %
100	746.700,00	654.300,00	12,4 %
120	770.400,00	676.500,00	12,2 %
200	778.500,00	681.100,00	12,5 %
500	786.000,00	707.400,00	10,0 %

Results of the combination “May – 15 days” are in agreement with the ones obtained for scenario “May – 3 days”. Indeed, the trend of the curves reported in the Figure 3-85 are very similar to the ones in Figure 3-82, as well as the estimated reduction of damages after the construction of the structural defences, between 12,1% and 12,5%. A lower reduction for the scenario T=500 years has been obtained also in this combination. Total damages without and with flood protections are slightly higher than the combination “May – 3 days”, due to the greater permanence of water on the fields. Comparing these last results with the simulated scenarios in November, same trend of the curves but a different magnitude is observed, considering that after 15 days all the types of crops achieved the 100% of damages, highlighting a strong influence of the permanence of the flood on agricultural sector.

In the following, the computation of the benefits in terms of avoided damages and the results of the B/C ratio will be proposed, using the same procedure explained in chapter 3.3.4.

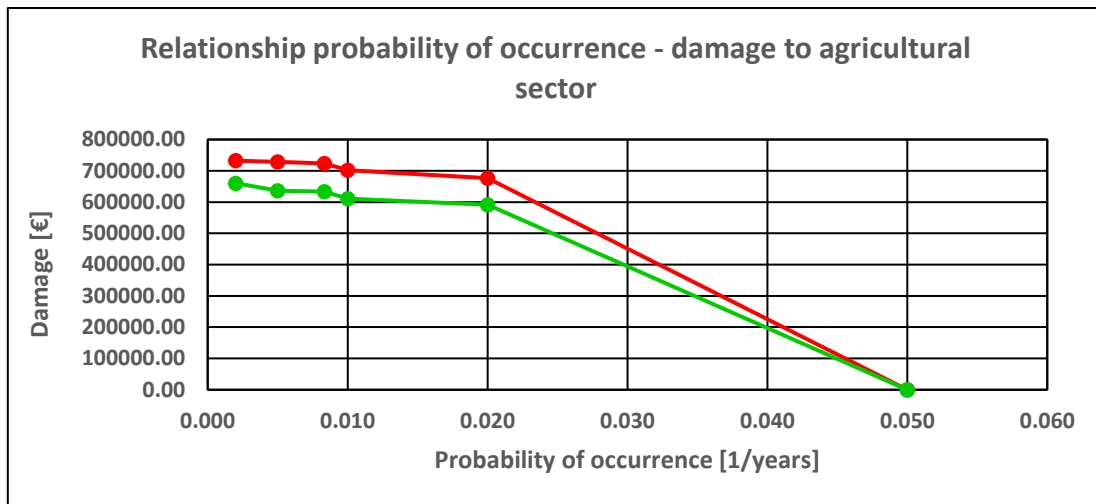


Figure 3-86 Relationship probability of occurrence – damage to agricultural sector for the combination “May – 3 days”

As it has been made in chapter 3.3.4, the area between the red and green curves of the Figure 3-86 has been computed, giving as yearly estimated benefits to agricultural sector around € 2.900,00, that added up to the yearly estimated benefits to residential buildings of € 223.300,00, results in total yearly benefits of € 226.200,00. Remembering that the total amount of cost per year is estimated around € 93.648,00, the obtained B/C ratio is about 2,416.

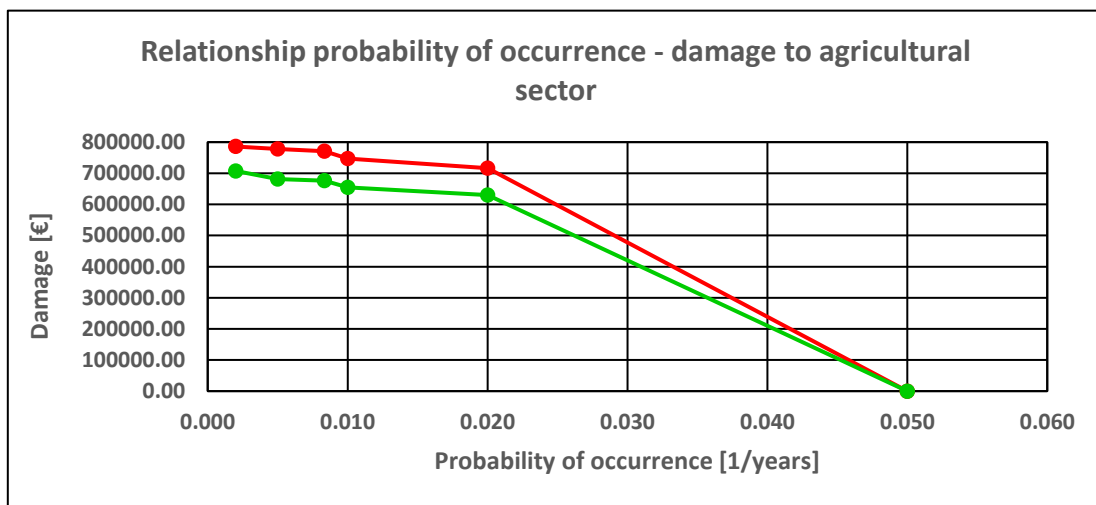


Figure 3-87 Relationship probability of occurrence – damage to agricultural sector for the combination “May – 15 days”

According to the scenario “May – 15 days”, the yearly estimated benefits to agricultural sector € 3.000,00. Therefore, the total yearly benefit is estimated to be around € 226.300,00 that, subdivided by the yearly cost of the structure and maintenance equal to € 93.648,00, gives a B/C ratio of 2.417. It is worth to notice that, in this case, the CBA is not so meaningful because the flood impact on the agricultural sector is much smaller than the one to residential buildings (two order of magnitude smaller), being the analysed area mainly characterised by built environment.

Beyond the increased damages to agricultural activities in May, also the exposure variability of activities with seasonal and cyclical production, such as food, storage and manufacturing companies, should be taken into consideration in this analysis.

4 Conclusions

According to several studies, every year riverine floods affect a large number of people living in floodplains, with severe damages on the built environment and natural ecosystem, affecting social and economic assets. The increasing number of inhabitants in flood prone areas highlights the important role of the hydraulic risk management to assess and mitigate the impact of future floods. In order to face the flood risk, the European Union has implemented the Directive 2007/60/EC, or Floods Directive, that is the reference for flood risk assessment and management in Europe, defining and selecting mitigation actions on the basis of reliable and inclusive cost-benefit analysis (CBA).

In this context, the thesis has been developed within the research project Flood-IMPAT+, that is conducted by the Politecnico di Milano in collaboration with several stakeholders. The project aims at improving the quality of existing flood hazard maps and at developing models for the quantification of damages to be accounted for while producing the risk maps required by the Floods Directive. The province of Lodi, hit by a severe flood in 2002, has been selected as case study for the research project.

The main objective of the thesis is to assess the effectiveness of the structural mitigation measures built on the hydraulic right of the Adda river, after the November 2002 event, with modelling tools developed by the project. The quantifiable damages have been estimated by appropriate models, for following consideration in a CBA; non-quantifiable losses have been estimated in terms of exposure to flood, as an additional assessment to be included in a more comprehensive MCA. In particular, a simplified version of the INSYDE model has been used for assessing damages to residential buildings, while the AGRIDE-c model has been implemented for estimating losses to the agricultural sector. The hazard parameters required by the damage models have been obtained from ten flood hazard maps produced by a two-dimensional river model, that has been preliminarily calibrated with reference to the 2002 event.

The urban flood modelling has been performed using the calculation code "Parflood", developed by the Università degli Studi di Parma. The model solves the Shallow-Water Equations thanks to a numerical scheme that employs a mixture of the finite-volume (in space) and finite-difference (in time) scheme. The code is run using a specific hardware that drastically reduces the computational times compared to those for other academic software for two-dimensional modelling. The reduced computational time represents a significant advantage, as it allows to perform more hydraulic simulations in less time and, therefore, to improve the quality of the model calibration. The latter would lead to more accurate flood hazard representations and risk maps. The two-dimensional unsteady modelling has been performed with a bathymetry file with high resolution (1 meter) that, if needed, has been locally manipulated on the basis of surveys on site. Buildings have been treated as impervious blocks, disregarding the indoor water storage. The interactions with the subsurface systems and with minor moving obstacles such as cars, garbage bins and bus stops, have been also neglected. The development of models able to consider these elements, if a slight additional computational time effort is required, will certainly enrich the quality of the flood model outputs.

The model calibration has been performed modifying the upstream and downstream boundary conditions, as well as the roughness coefficient of urban settlements, agricultural areas and forests. The calibration has been carried out comparing the obtained flooded area and water levels with the observed values taken from past studies. A comparison between simulated and observed water velocities would improve the result of the model calibration but, due to the absence of recorded velocity measures of the 2002 flood event, this hazard parameter has not been considered within this process. With reference to the aforementioned event, calibrating the boundary conditions and the roughness, a maximum difference of 6 cm has been reached with the observed data of the hydrometer at the Napoleone Bonaparte bridge. Furthermore, the average error with reference to more than 120 depth data taken from the damage compensation forms compiled by citizens and reconstructions from photos of the event was around 14 cm, leading to a more than satisfactory result.

Ten hazard maps with a high resolution (1 m) have been produced, considering five different return periods ($T=50, 100, 120, 200$ and 500 years) for two conditions: before the construction of the new banks and with the designed structures in place (only for the right side of the river). The use of more than one annual probability of exceedance has allowed a more reliable computation of the benefit-cost ratio (B/C) within the cost-benefit analysis. The obtained maps with structural defences show a reduction of the flooded area for all the investigated scenarios, highlighting the protective effect of the mitigation measures. Being the flood protections designed with the reference of an event with $T=200$ years (plus the safety margin), the hazard map reproducing the most severe scenario with structural defences shows that a portion of Lodi would have been flooded, due to the overflow of the soil embankments nearby the state road S.P. 202. A future development of this study can be related to the addition of the structural defences on the hydraulic left (flood protections upstream of the Napoleone Bonaparte bridge have been already realised, while downstream of it, the banks are still not in place) in order to complete the flood damage assessment for the Municipality of Lodi.

The considered costs for the realisation of the structural defences (4.394.800,00 €) regard the execution work, security plans, design support activities and additional legal and administrative charges. Moreover, within a CBA, the ordinary maintenance (31.700,00 €/year) and the costs for qualifying courses of the personnel in charge of the montage of the barriers (18.000,00 €/year) have been added to the previously mentioned costs. However, other indirect costs such as impact on daily activities and services, on habitat loss and on the aesthetics have not been considered in this analysis, as well as intangible costs like discomfort and social disruption. Their inclusion in the estimation of the yearly costs of the mitigation measure would bring to a more comprehensive analysis to be included in the CBA.

The quantification of damages to residential buildings has been carried out at the micro-scale with a simplified version of the INSYDE model. This model requires the determination of input parameters related to hazard (water depth outside the building, duration of the flood event and presence of pollutants in the water), to vulnerability (building structure, building type, level of maintenance, finishing level) and to exposure (presence of basement, footprint area, number of floors). Water depths have been taken from the hazard maps, while vulnerability and exposure

values has been obtained from the cadastral database and from the Regione Lombardia Geodatabase, respectively. A more detailed survey and knowledge on vulnerability and exposure elements would improve the quality of the damage assessment to residential buildings and the definition of possible risk mitigation intervention to the single construction. Moreover, only vulnerability parameters related to structural elements has been considered, without including other indirect and systemic damages such as the affected house owners and the loss of the property value. The inclusion of these additional damages should be analysed in further researches because it would bring to a more detailed and accurate estimation of the damage.

Damages to agricultural sector have been computed with a software which implements the AGRIDE-c model. The computation of damages requires the definition of the hazard parameters and an exposure assessment of the crops effectively involved at the occurrence of the flood, making the latter strongly context related. Water depth has been taken from the obtained hazard maps, while the main cultivations in the analysed area (grain maize, wheat, barley, grassland) have been identified according to the cadastral data supplied by the Regional Authority. The inclusion of damages to agricultural sector in CBA and MCA is required, especially when the evaluation of mitigation strategies (i.e. structural defences and river restoration actions) involve floodplains devoted to agricultural activities. Moreover, an understanding of the damage mechanisms to agriculture represents a powerful tool in order to orient farmers' behaviour toward more resilient practices, by supporting them in the identification of damage alleviation and coping strategies (Molinari et al., 2018). In this thesis, damages to crops in November have been evaluated only, but future researches should be focused on a better understanding of damage mechanisms and the extension of this model to assess damages to other components of the farm (i.e. livestock, storage material, machineries). Moreover, the indirect systemic impact on the activities of the company should be taken into consideration in order to have a more comprehensive total damage estimation.

The collection and the share of ex-post damage data regarding residential buildings and agricultural activities, in a unique and consistent manner, should be encouraged, leading to an improvement of the models' calibrations and validations. The creation of a common database (such as the European Union spatial data infrastructure, proposed by the EU INSPIRE Directive) containing the aforementioned elements, will ease the identification of required data and results and would be useful for future land use plans, insurance premium definition and emergency management interventions.

The quantifiable damages to residential buildings and agricultural activities have been evaluated in the two different geometry configurations: before the design of the flood protections and in the condition with the structures in place. The benefits (i.e. avoided damage) arisen from the construction of the mitigation measure, have been compared with the cost of the structural defences (assuming a functional duration of the measure of 100 years) and evaluated in a benefit-cost ratio (B/C), resulting in a value equal to 2,4. Moreover, since the real functional duration of the structures is unknown, it has been verified the minimum functional duration of the flood protection such as the B/C would give positive values (i.e. estimated arisen yearly benefits greater than yearly costs), resulting in 25 years. It has to be remarked that the discount rate involved into the

formulation of the B/C has been neglected, assuming that the actual costs will remain unchanged in the future, considering the very low inflation variation in the last decade.

Despite the obtained positive results of the B/C considering only avoided damages to residential buildings and agricultural activities, it has been tried to take into account damages to other assets. In particular, the exposure in monetary terms (representing the maximum potential direct damage and not the real suffered damage) of economic activities have been computed regarding losses to contents and breakage of systems connected to the structure. However, the lack of validated models or damage curves developed within the project Flood-IMPAT+, limits the inclusion of this expected damages into monetarily evaluations of mitigation measures. As regard secondary damages related to economic activities, a proxy variable has been developed in order to assess the potential systemic and indirect damages to the municipal and provincial economy that physical direct losses suffered by the companies could trigger in cascade effect. Indeed, since the lack of tools in order to quantify direct damage to economic activities, also the provoked indirect and systemic damage assessment would be a complex task. Other potential benefits could arise from the exposure reduction of inhabitants, important facilities and services, cultural heritage and natural environment and the respective avoided systemic damages. Further researches for a more accurate flood risk assessment to economic activities and other assets should be encouraged, whose results would represent an important step forward for a more comprehensive MCA and a better evaluation of the mitigation measures effectiveness.

A sensitivity analysis of the result of the CBA has been performed assuming a different month of occurrence of the flood, as potential impact of the climate change, and, separately, a levee effect scenario for the 500 years of return period. Considering inundations in May, damages to agricultural activities have been computed again, because in this period of the year, crops are in a different life stages with respect to the ones in November. The same ten investigated scenarios have been simulated and higher damages have been obtained. These new damage results have been considered into the BCA, leading to insignificant changes in final value of B/C. This is due to the fact that estimated damages to the agricultural sector are two orders of magnitude lower than those for the residential buildings, as the Municipality of Lodi is mainly characterised by an urban environment. For the levee effect scenario, a new residential development has been assumed in an area that (in the model for the return period of 500 years) is flooded due to the overflow of the soil embankment nearby the S.P. 202. Despite the obtained higher damages for the two different construction strategies (buildings made of bricks, with basement and high finishing levels, and buildings in r.c. or wood, without basement and low finishing levels), the yearly benefits still exceed the costs of the structures, proving the effectiveness of the flood protections even in this aggravated scenario.

In this thesis, several MCA approaches have been presented, highlighting advantages and disadvantages of the different methods. However, none of these procedures have been applied to the case study due to the absence of decision makers in the risk assessment, who have to define the criteria of analyses and the weight to assign to the latter. As support of further research works, this thesis has provided part of the required material for a more comprehensive assessment of the

mitigation measure, reporting several exposure maps of important activities and assets in Lodi. It has to be remarked that MCAs are multidisciplinary methods, involving the assessment and the limitations of several different disciplines and models.

The effectiveness evaluation of the structural defences in Lodi, employing the models developed within Flood-IMPAT+, was in end successful. Notwithstanding the assumptions made on the different implemented models and methodologies, the entire procedure proposed in this thesis can be applied to other geographical contexts, at least in river basins belonging to the Po plain area to evaluate different types of mitigation strategies. Particular attention should be paid in selecting the correct hazard, vulnerability and exposure parameters required by the INSUDE and AGRIDE-c damage models, whose further improvement and validation may guarantee their applicability in a wider number of contexts.

BIBLIOGRAPHY

- AdbPo (Autorità di bacino del fiume Po) – *Studio di fattibilità della sistemazione idraulica*. 2003
- AdbPo (Autorità di bacino del fiume Po) – *Profili di piena dei corsi d'acqua del reticolo principale. Piano per la valutazione e la gestione del rischio di alluvioni. Art. 7 della Direttiva 2007/60/CE e del D. lgs. N. 49 del 23.02.2010*
- Agosti A., Crippa J. – *Flood Hazard Modelling for the City of Lodi*. Politecnico di Milano, 2017.
- Alcrudo, F. – *Mathematical modeling techniques for flood propagation in urban areas*. *Buscar*, 1–34.
- Arrighi C., Oumeraci H., Castelli F. – *Hydrodynamics of pedestrians' instability in floodwaters*. *Hydrol. Earth Syst. Sci. Discuss.*, doi:10.5194/hess-2016 – 261, 2016.
- Ballesteros-Cànovas J.A., Sanchez-Silva M., Bodoque J.M., Diez-Herrero A. – *An Integrated Approach to Flood Risk Management: A Case Study of Navaluega (Central Spain)*. *Water Resour Manage (2013)* 27: 3051 – 3069
- Bazin P., Mignot E., Paquier A. – *Computing flooding of crossroads with obstacles using a 2D numerical model*. *Journal of Hydraulic Research*, 55:1, 72 – 84, DOI: 10.1080/00221686.2016.1217947
- Beckers A., Dewals B., Erpicum S., Dujardin S., Detrembleur S., Teller J., Piroton M., Archambeau P. – *Contribution of land use changes to future flood damage along the river Meuse in the Walloon region*. *Nat. Hazards Earth Syst. Sci.*, 13, 2301 – 2318, 2013
- Botzen W.J.W., Monteiro E., Estrada F., Pesaro G., Menoni S. – *Economic Assessment of Mitigation Damage of Flood Events: Cost-Benefit Analysis of Flood-Proofing Commercial Buildings in Umbria, Italy*. *The Geneva Papers*, 2017, 42, (585-608)
- Brinkhuis-Jak M. & Holterman S.R., Kok M., Jonkman S.N. – *Cost benefit analysis and flood damage mitigation in the Netherlands (n.a.)*
- Brouwer R., van Ek R. – *Integrated ecological, economic and social impact assessment of alternative flood control policies in the Netherlands*. *Science direct. Ecological Economics* 50 (2004) 1 – 21
- Chow, V. Te. – *Open Channel Hydraulics*, 1959. <https://doi.org/10.1016/B978-0-7506-6857-6.X5000-0>
- Collenteur R. A., de Moel H., Jongman B., Di Baldassarre G. – *The failed-levee effect: Do societies learn from flood disasters?* *Nat Hazard (2015)* 76:373 – 388
- Comune di Lodi – *Il rischio idraulico. Piano di Emergenza Comunale edizione 2011. Piano Stralcio del Rischio Idraulico*
- Cunge J.A. – *Of data and models*. *Journal of Hydroinformatics*, 5(2), 2003. 75 – 98.
- DLgs 49/2010 – *Attuazione della direttiva 2007/60/CE relativa alla valutazione e alla gestione dei rischi di alluvioni. (10G0071)*.
- Dottori F., Di Baldassarre G., Todini E. – *Detailed data is welcome, but with a pinch of salt: Accuracy, precision, and uncertainty in flood inundation modelling*. *Water Resources Research*, Vol. 49, 6079 – 6085, doi: 10.1002/wrcr.20406, 2013

Dottori F., Figueireo R., Martina M. L. V., Molinari D. and Scorzini A. R. – *INSYDE: a synthetic, probabilistic flood damage based on explicit cost analysis*. *Nat. Hazard Earth Syst. Sci.*, 16, 2577 – 2591, 2016.

Dung N. V., Merz B., Bardossy A., Thang T. D., Apel H. – *Multi-objective automatic calibration of hydrodynamic models utilizing inundation maps and gauge data*. *Hydrol. Earth Syst. Sci.*, 15, 1339 – 1354, 2011.

EU – *DIRECTIVE 2007/60/EC OF THE EUROPEAN PARLIAMENT AND OF THE COUNCIL of 23 October 2007 on the assessment and management of flood risks*. *Official Journal of the European Union*

FLOODsite – *Evaluating flood damages: guidance and recommendations on principles and methods*. *FLOODsite Project Deliverable D9.1*

Galliani M., Ballio F., Molinari D., Scorzini A. R., Gallazzi A. – *On the development of usable multi-variate damage models for residential buildings*. *Poster at EGU – European Geoscience Union General Assembly, Vienna 2019*. <https://meetingorganizer.copernicus.org/EGU2019/EGU2019-9320.pdf>

Hutton N.S., Tobin G.A., Montz B.E. – *The levee effect revisited: Processes and policies enabling development in Yuba Country, California*. *J Flood Risk Management*. 2018;e12469. <https://doi.org/10.1111/jfr3.12469>

IDEA (Improving Damage assessment to Enhance cost-benefit Analysis) – *Deliverable D.4: Cost-benefit analysis of mitigation measures to pilot firms/infrastructure in Italy*. *ECHO-SUB-2014-694469*. 2004

ISPRA (Istituto Superiore per la Protezione e la Ricerca Ambientale) – *Dissesto idrogeologico in Italia: pericolosità e indicatori di rischio*. *Sintesi Edizione 2018*

ISTAT (Istituto Nazionale di Statistica) – *Censimento della popolazione e delle abitazioni, 2011*. <https://www.istat.it/it/censimenti-permanenti/censimenti-precedenti/popolazione-e-abitazioni/popolazione-2011>

Legates, D. R., McCabe Jr., G. J. – *Evaluating the use of “goodness of fit” measures in hydrologic and hydroclimatic model validation*. *WATER RESOURCES RESEARCH, VOL. 35, NO. 1, PAGES 233 –241. JANUARY 1999*.

Mechler R. – *Reviewing estimated of the economic efficiency of disaster risk management: opportunities and limitations of using risk-based cost-benefits analysis*. *Nat Hazard (2016) 81: 2121 – 2147*

Menoni S., Margottini C. – *Inside Risk: A Strategy for Sustainable Risk Mitigation*. *Springer-VerlagItalia*. 2011

Meyer V., Becker N., Markantonis V., Schwarze R., van den Bergh J.C.J.M., Bouwer L.M., Bubeck P., Ciavola P., Genovese E., Green C., Hallegatte S., Kreibich H., Lequeux Q., Logar I., Papyrakis E., Pfuerscheller C., Poussin J., Przulski V., Thielen A.H., Viavattene C. – *Review article: assessing the costs of natural hazards – state of the art and knowledge gaps*. *Nat. Hazards Earth Syst. Sci.* 13, 1351 – 1373, 2013

Meyer V., Priest S., Kuhlicke C. – *Economic evaluation of structural and non-structural flood risk management measures: examples from the Mulde River*. *Nat Hazard (2012) 62: 301 – 324*

- Meyer V., Scheuer S., Haase D. – *A multicriteria approach for flood risk mapping exemplified at the Mulde river, Germany. Nat Hazard (2009) 48: 17 – 39*
- Molinari D., Menoni S., Aronica G.T., Ballio F., Berni F., Pandolfo C., Stelluti M., Minucci G. – *Ex post damage assessment: an Italian experience. Nat. Hazard Earth Syst. Sci., 14, 901 – 916, 2014*
- Molinari D., Minucci G., Mendoza M. T., Simonelli T. – *Implementing the European “Floods Directive”: the Case of the Po River Basin. Water Resour Manage (2016) 30: 1739 – 1756*
- Molinari D., Scorzini A.R., Gallazzi A., Ballio F. (2019) – *AGRIDE-c: a conceptual model for the estimation of flood damage to crops: development and implementation*
- Molinari D., Ballio F., Radice A., Minucci G., Mendoza M. T., Galliani M., Pesaro G. – *Flood-IMPAT+: an Integrated Meso & micro scale Procedure to Assess Territorial flood risk. 2016*
- Mustafa A., Bruwier M., Archambeau P., Erpicum S., Piroton M., Dewals B., Teller J. – *Effects of spatial planning on future flood risk in urban environments. Journal of Environmental Management 225 (2018) 193 – 204*
- Mysiak J., Gambaro M. – *Il bacino del fiume Adda – Scheda Tecnica. Water2Adapt. Resilience enhancement and water demand management for climate change adaptation. 2011.*
- Natale, L. – *Delimitazione delle aree inondabili ad assegnati tempi di ritorno - Fiume Adda, 2003.*
- Pesaro G. – *Cost benefit analyses: an introduction applied to flood mitigation. Politecnico di Milano. Slides presentation. 2015.*
- Poljanšek K., Marin Ferrer M., De Groeve T., Clark I. – (Eds.), 2017. *Science for disaster risk management 2017: knowing better and losing less. EUR 28034 EN, Publications Office of the European Union, Luxembourg, 2017, ISBN 978-92-79-60679-3, doi:10.2788/842809, JRC102482.*
- Radice A. – *Urban flood modelling slides. Politecnico di Milano, 2017.*
- Risk and Policy Analysts Ltd (RPA) – *Evaluating a multi-criteria analysis (MCA) methodology for application to flood management and coastal defence appraisal. Joint Defra/EA Flood and Coastal Erosion Risk Management R&D Programme. R&D Project Record FD2013/PR1. 2004.*
- Rossetti S., Cella O. W., Lodigiani V. – *Studio idrologico-Idraulico del tratto di F. Adda inserito nel territorio comunale di Lodi. Milano, 2010.*
- Rossetti S., Cella O. W., Lodigiani V. – *Relazione Tecnica Generale. Milano, 2010.*
- Science on the Net – *Climate change in Italy: what do we really know. <http://www.scienceonthenet.eu> (2013)*
- Scorzini A. R., Radice A., Molinari D. – *A New Tool to Estimate Inundation Depths by Spatial Interpolation (RAPIDE): Design, Application and Impact on Quantitative Assessment of Flood Damages. Water 2018, 10, 1805; doi:10.3390/w10121805*
- Shreve C.M., Kelman I. – *Does mitigation save? Reviewing cost-benefit analyses of disaster risk reduction. International Journal of Disaster Risk Reduction 10 (2014) 213-235*
- UNIPR (Università degli Studi di Parma) – *Linee guida sull'utilizzo del codice di calcolo “Parflood” (2018).*
- Xia J., Falconer R. A., Wang Y., Xiao X. – *New criterion for the stability of a human body in floodwaters. 2014. Journal of Hydraulic Research, 52:1, 93-104*

LIST OF ABBREVIATIONS

A: Area;
AAD: Average Absolute of Differences;
ACI: Automobile Club d'Italia;
AdbPo: Autorità di bacino del fiume Po / District basin authority of the river Po;
AD: Average of Differences;
AGRIDE-c: AGRiculture DamagE model for Crops;
AIPO: Agenzia Interregionale per il fiume Po;
ARPA: Agenzia Regionale per la Protezione dell'Ambiente;
ATECO: ATtività ECONomica;
BA: Basement Area;
BC / B.C.: Boundary Condition;
BS: Building Structure;
B/C: Benefit Cost ratio;
CBA: Cost Benefit Analysis;
CISIS: Centro Interregionale per i Sistemi informatici, geografici e statistici;
D: Damage;
DASU: Dipartimento di Architettura e Studi Urbani;
DEP: depth;
DICA: Dipartimento di Ingegneria Civile e Ambientale;
DRR: Disaster Risk Reduction;
DSM: Digital Surface Model;
du: duration;
 $d_{basement}$: damage to basement;
 d_{boiler} : damage to boiler;
 d_p : depth at the peak;
 $d_{pavement}$: damage to pavement;
 d_{storey} : damage to storey;
EC: European Commission;
EEA: European Economic Area;
EU: European Union;
E: Efficiency;
FEMA: Federal Emergency Management Agency;
FHRC: Flood Hazard Research Centre
FL: Finishing Level;
GIS: Geographic Information System;
GNSS: Global Navigation Satellite System;
GPS: Global Positioning System;
GP: Gross Profit;
gg: days;
h: hours;
ha: hectare;
IDEA: Improving Damage assessment to Enhance cost-benefit Analysis;
IMPAT: Integrated Meso-scale Procedure to Assess Territorial;
INSYDE: In-depth Synthetic Model for Flood Damage Estimation;
IPCC: Intergovernmental Panel on Climate Change;
ISPRA: Istituto Superiore per la Protezione e la Ricerca Ambientale;

ISTAT: Istituto nazionale di statistica;
IT: Information Technology;
I.C.: initial condition;
IRR: Internal Rate of Return;
LM: Level of Maintenance;
MATLAB: Matrix Laboratory;
MAXDEP: Maximum Depth;
MAXVEL: Maximum Velocity;
MAXWSE: Maximum Water Surface Elevation;
MCA: Multi Criteria Analysis;
MLN: Milion
m a.s.l.: meters above sea level;
NRTK: Network Real Time Kinematic;
NPV: Net Present Value;
n.a.: not available;
PVR: Present Value Ratio;
Q: discharge;
Q_x: discharge along the x direction;
Q_p: peak discharge;
Q_y: discharge along the y direction;
RPA: Risk and Policy Analysts;
RV: Replacement Value;
sec / [s]: seconds;
SIARL: Sistema Informativo Agricoltura Regione Lombardia;
Sim: simulation;
SpinGNSS: Servizio di Posizionamento Interregionale GNSS;
SWE: Shallow Water Equations;
S.P.: Strada Provinciale
T: return period;
t: time;
TEV: Total Economic Value;
t_p: time at the peak;
txt: text;
UNIPR: Università degli Studi di Parma;
USACE: United States Army Corps of Engineers;
UTM: Universe Transverse of Mercator;
VAT: Value Added Tax;
WGS: World Geodetic System;
WSE: Water Surface Elevation;

APPENDIX

Water depth	Strategy	Flood duration [days]												
		<5	5	6	7	8	9	10	11	>11				
≤ 130 cm	Bare field	Jan	c					36%						
		Feb	c					36%						
		Mar	c					36%						
	Initial phase	Apr	c											
		May	c											
		Jun	c	36%	63%	90%	117%	144%	171%	198%	225%			
	Growing	Jul	c	36%	90%	144%	198%							
		Aug	c	36%	90%	144%	198%							
		Sep	c											
	Maturation	Oct	c											
		Nov	c											
		Dec	c											
≥ 130 cm	Bare field	Jan	c											
		Feb	c											
		Mar	c											
	Initial phase	Apr	c											
		May	c											
		Jun	c	36%	63%	90%	117%	144%	171%	198%	225%			
	Growing	Jul	c	36%	90%	144%	198%							
		Aug	c	36%	90%	144%	198%							
		Sep	c											
	Maturation	Oct	c											
		Nov	c											
		Dec	c											

Relative damage to maize crops (in case of minimum tillage) for the different combinations: times of occurrence of the flood (i.e. month), flood intensities (i.e. water depth and flood duration) and damage alleviation strategies ("c"=continuation, "r"=reseeding, "a"=abandoning)

Water depth	Strategy	Flood duration [days]														
		<5	5	6	7	8	9	10	11	12	13	14	15	16	>16	
< 60 cm	c	114%	164%	193%	223%	253%	282%	312%	342%	371%	401%	430%	460%	490%	-	
	f	213%	470%	-	-	-	-	-	-	-	-	-	-	-	-	
3-leaf	a	-	-	114%	-	-	-	-	-	-	-	-	-	-		
Jan	f	168%	-	-	-	-	-	-	-	-	-	-	-	-		
Feb	f	168%	-	-	-	-	-	-	-	-	-	-	-	-		
Tillering	a	-	-	-	-	-	-	-	-	-	-	-	-	-		
Stem el.	a	-	-	-	-	-	-	-	-	-	-	-	-	-		
Mar	f	114%	164%	193%	223%	253%	282%	312%	342%	371%	401%	430%	460%	490%		
Apr	f	114%	164%	208%	251%	295%	338%	382%	426%	470%	-	-	-	-		
May	f	114%	164%	208%	251%	295%	338%	382%	426%	470%	-	-	-	-		
Flowering	a	-	-	-	-	-	-	-	-	-	-	-	-	-		
Jun	f	114%	-	-	-	-	-	-	-	-	-	-	-	-		
Jul	f	114%	-	-	-	-	-	-	-	-	-	-	-	-		
Maturity	a	-	-	-	-	-	-	-	-	-	-	-	-	-		
Aug	f	114%	-	-	-	-	-	-	-	-	-	-	-	-		
Bare field	a	-	-	-	-	-	-	-	-	-	-	-	-	-		
Sep	f	114%	-	-	-	-	-	-	-	-	-	-	-	-		
Oct	f	114%	-	-	-	-	-	-	-	-	-	-	-	-		
Germin.	a	-	-	-	-	-	-	-	-	-	-	-	-	-		
Nov	f	168%	324%	-	-	-	-	-	-	-	-	-	-	-		
3-leaf	a	-	-	-	-	-	-	-	-	-	-	-	-	-		
Dec	f	114%	213%	470%	-	-	-	-	-	-	-	-	-	-		
	a	-	-	-	-	-	-	-	-	-	-	-	-	-		

Water depth	Strategy	Flood duration [days]														
		<5	5	6	7	8	9	10	11	12	13	14	15	16	>16	
≥ 60 cm	c	114%	164%	193%	223%	253%	282%	312%	342%	371%	401%	430%	460%	490%	-	
	f	213%	470%	-	-	-	-	-	-	-	-	-	-	-	-	
3-leaf	a	-	-	114%	-	-	-	-	-	-	-	-	-	-		
Jan	f	168%	-	-	-	-	-	-	-	-	-	-	-	-		
Feb	f	168%	-	-	-	-	-	-	-	-	-	-	-	-		
Tillering	a	-	-	-	-	-	-	-	-	-	-	-	-	-		
Stem el.	a	-	-	-	-	-	-	-	-	-	-	-	-	-		
Mar	f	114%	164%	193%	223%	253%	282%	312%	342%	371%	401%	430%	460%	490%		
Apr	f	114%	164%	208%	251%	295%	338%	382%	426%	470%	-	-	-	-		
May	f	114%	164%	208%	251%	295%	338%	382%	426%	470%	-	-	-	-		
Flowering	a	-	-	-	-	-	-	-	-	-	-	-	-	-		
Jun	f	114%	-	-	-	-	-	-	-	-	-	-	-	-		
Jul	f	114%	-	-	-	-	-	-	-	-	-	-	-	-		
Maturity	a	-	-	-	-	-	-	-	-	-	-	-	-	-		
Aug	f	114%	-	-	-	-	-	-	-	-	-	-	-	-		
Bare field	a	-	-	-	-	-	-	-	-	-	-	-	-	-		
Sep	f	114%	-	-	-	-	-	-	-	-	-	-	-	-		
Oct	f	114%	-	-	-	-	-	-	-	-	-	-	-	-		
Germin.	a	-	-	-	-	-	-	-	-	-	-	-	-	-		
Nov	f	168%	324%	-	-	-	-	-	-	-	-	-	-	-		
3-leaf	a	-	-	-	-	-	-	-	-	-	-	-	-	-		
Dec	f	114%	213%	470%	-	-	-	-	-	-	-	-	-	-		
	a	-	-	-	-	-	-	-	-	-	-	-	-	-		

Relative damage to wheat crops (in case of conventional tillage) for different combinations of times of flood occurrence (i.e. month), flood intensities (i.e. water depth and flood duration) and damage alleviation strategies ("c"=continuation; "r"=reseeding; "a"=abandoning)

Water depth < 60 cm	Strategy	Flood duration [days]														
		<5	5	6	7	8	9	10	11	12	13	14	15	16	>16	
3-leaf	Jan	c	59%	109%	240%	-	-	-	-	-	-	-	-	-	-	-
	f	-	-	-	-	-	-	-	-	-	-	-	-	-	-	-
Tillering	Feb	c	-	-	59%	-	-	-	-	-	-	-	-	-	-	-
	f	-	-	-	-	-	-	-	-	-	-	-	-	-	-	-
Stem el.	Mar	c	59%	84%	99%	114%	129%	144%	159%	175%	190%	205%	220%	235%	250%	-
	f	-	-	-	-	-	-	-	-	-	-	-	-	-	-	-
Flowering	Apr	c	59%	84%	106%	128%	151%	173%	195%	218%	240%	-	-	-	-	-
	f	-	-	-	-	-	-	-	-	-	-	-	-	-	-	-
Maturity	May	c	59%	84%	106%	128%	151%	173%	195%	218%	240%	-	-	-	-	-
	f	-	-	-	-	-	-	-	-	-	-	-	-	-	-	-
Bare field	Jun	c	-	-	-	-	-	-	-	-	-	-	-	-	-	-
	f	-	-	-	-	-	-	-	-	-	-	-	-	-	-	-
Germin.	Nov	c	-	-	-	-	-	-	-	-	-	-	-	-	-	-
	f	-	-	-	-	-	-	-	-	-	-	-	-	-	-	-
3-leaf	Dec	c	59%	109%	240%	-	-	-	-	-	-	-	-	-	-	-
	f	-	-	-	-	-	-	-	-	-	-	-	-	-	-	-

Water depth ≥ 60 cm	Strategy	Flood duration [days]														
		<5	5	6	7	8	9	10	11	12	13	14	15	16	>16	
3-leaf	Jan	c	59%	109%	240%	-	-	-	-	-	-	-	-	-	-	-
	f	-	-	-	-	-	-	-	-	-	-	-	-	-	-	-
Tillering	Feb	c	-	-	59%	-	-	-	-	-	-	-	-	-	-	-
	f	-	-	-	-	-	-	-	-	-	-	-	-	-	-	-
Stem el.	Mar	c	59%	84%	99%	114%	129%	144%	159%	175%	190%	205%	220%	235%	250%	-
	f	-	-	-	-	-	-	-	-	-	-	-	-	-	-	-
Flowering	Apr	c	59%	84%	106%	128%	151%	173%	195%	218%	240%	-	-	-	-	-
	f	-	-	-	-	-	-	-	-	-	-	-	-	-	-	-
Maturity	May	c	59%	84%	106%	128%	151%	173%	195%	218%	240%	-	-	-	-	-
	f	-	-	-	-	-	-	-	-	-	-	-	-	-	-	-
Bare field	Jun	c	-	-	-	-	-	-	-	-	-	-	-	-	-	-
	f	-	-	-	-	-	-	-	-	-	-	-	-	-	-	-
Germin.	Nov	c	-	-	-	-	-	-	-	-	-	-	-	-	-	-
	f	-	-	-	-	-	-	-	-	-	-	-	-	-	-	-
3-leaf	Dec	c	59%	109%	240%	-	-	-	-	-	-	-	-	-	-	-
	f	-	-	-	-	-	-	-	-	-	-	-	-	-	-	-

Relative damage to wheat crops (in case of minimum tillage) for different combinations of times of flood occurrence (i.e. month), flood intensities (i.e. water depth and flood duration) and damage alleviation strategies (‘c’=continuation; ‘r’=reseeding; ‘a’=abandoning)

Water depth < 60 cm	Strategy	Flood duration (days)														
		<5	5	6	7	8	9	10	11	12	13	14	15	16	>16	
3-leaf	c	371%	619%	1261%							546%					
	f										898%					
Tillering	c	371%	371%	371%	371%	371%	371%	618%	791%	964%	1137%	1310%				
	f							546%								
Stem el.	c	371%	495%	569%	643%	717%	791%	866%	940%	1014%	1088%	1162%	1236%	1310%		
	f														946%	
Flowering	c	371%	495%	605%	713%	823%	932%	1041%	1151%	1261%						
	f														998%	
Matur.	c															
	f														371%	
Bare field	c															
	f														371%	
Germin.	c															
	f														546%	
3-leaf	c	371%	619%	1261%												
	f														813%	
Dec	c															
	f														546%	
															898%	

Water depth ≥ 60 cm	Strategy	Flood duration (days)														
		<5	5	6	7	8	9	10	11	12	13	14	15	16	>16	
3-leaf	c	371%	619%	1261%							546%					
	f										898%					
Tillering	c	371%	371%	371%	371%	371%	371%	618%	791%	964%	1137%	1310%				
	f							546%								
Stem el.	c	371%	495%	569%	643%	717%	791%	866%	940%	1014%	1088%	1162%	1236%	1310%		
	f														946%	
Flowering	c	371%	495%	605%	713%	823%	932%	1041%	1151%	1261%						
	f														998%	
Matur.	c															
	f														371%	
Bare field	c															
	f														371%	
Germin.	c															
	f														546%	
3-leaf	c	371%	619%	1261%												
	f														813%	
Dec	c															
	f														546%	
															898%	

Relative damage to barley crops (in case of conventional tillage) for different combinations of times of occurrence of the flood (i.e. month), flood intensities (i.e. water depth and flood duration) and damage alleviation strategies ("c"=continuation; "r"=reseeding; "a"=abandoning)

Water depth	Strategy	Flood duration [days]															
		<5	5	6	7	8	9	10	11	12	13	14	15	16	>16		
< 60 cm	3-leaf	c	91%	151%	307%												
	f																
Tillering	Feb	c			91%												
	f									151%	193%	235%	277%	319%			
Stem el.	Mar	c	91%	121%	139%	157%	175%	193%	211%	229%	247%	265%	283%	301%	319%		
	f																
Flowering	Apr	c	91%	121%	147%	174%	201%	227%	254%	280%	307%						
	f																
Matur.	Jun	c															
	f																
3-leaf	Jan	c	91%	151%	307%												
	f																
Germin.	Nov	c															
	f																
3-leaf	Dec	c	91%	151%	307%												
	f																

Water depth	Strategy	Flood duration [days]															
		<5	5	6	7	8	9	10	11	12	13	14	15	16	>16		
≥ 60 cm	3-leaf	c	91%	151%	307%												
	f																
Tillering	Feb	c			91%												
	f									151%	193%	235%	277%	319%			
Stem el.	Mar	c	91%	121%	139%	157%	175%	193%	211%	229%	247%	265%	283%	301%	319%		
	f																
Flowering	Apr	c	91%	121%	147%	174%	201%	227%	254%	280%	307%						
	f																
Matur.	Jun	c															
	f																
3-leaf	Jan	c	91%	151%	307%												
	f																
Germin.	Nov	c															
	f																
3-leaf	Dec	c	91%	151%	307%												
	f																

Relative damage to barley crops (in case of minimum tillage) for different combinations of times of flood occurrence (i.e. month), flood intensities (i.e. water depth and flood duration) and damage alleviation strategies ("c"=continuation; "r"=reseeding; "a"=abandoning)

		Strategy	Flood duration [days]										
			<5	7	9	11	13	15	17	19	21	23	>25
Vegetative rest	Jan	c	60%			67%	82%	96%	110%	124%	139%	153%	-
		r	-			-*							71%
	Feb	c	60%			67%	82%	96%	110%	124%	139%	153%	-
		r	-			-*							71%
	Mar	c	60%			67%	82%	96%	110%	124%	139%	153%	-
		r	-			-*							71%
Spring grow	Apr	c	45%		71%	93%	107%	-					
		r	-		-*			148%					
	May	c	45%		71%	93%	107%	-					
		r	-		-*			148%					
Summer growing	Jun	c	4%	24%	34%	-							
		r	-	-*			88%						
	Jul	c	4%	24%	34%	-							
		r	-	-*			88%						
	Aug	c	4%	24%	34%	-							
		r	-	-*			88%						
Aut. grow.	Sep	c	4%	15%	23%	31%	36%	-					
		r	-	-*				88%					
	Oct	c	4%	15%	23%	31%	36%	-					
		r	-	-*				88%					
Veget. rest	Nov	c	60%			67%	82%	96%	110%	124%	139%	153%	-
		r	-			-*							71%
	Dec	c	60%			67%	82%	96%	110%	124%	139%	153%	-
		r	-			-*							71%

- Strategy not possible
-* Reseeding is considered only in case of a 100% physical damage

Relative damage to grassland for different combinations of times of flood occurrence (i.e. month), flood intensities (flood duration) and damage alleviation strategies ("c"-continuation; "r"-reseeding). Results refer to a flood occurring before harvest has been made (under the hypothesis of 15 days remaining to mowing)